IntechOpen

Recent Studies in Perturbation Theory

Edited by Dimo I. Uzunov

RECENT STUDIES IN PERTURBATION THEORY

Edited by **Dimo I. Uzunov**

Recent Studies in Perturbation Theory
http://dx.doi.org/10.5772/65624
Edited by Dimo I. Uzunov

Contributors

Francisco Bulnes, Emmanouil Thrapsaniotis, Jing Huang, Takashi Yanagisawa, Keldibay Alymkulov, Dilmurat Abdillajanovich Tursunov, Baojian Hong, Alexander V. Glushkov, Olga Khetselius, Andrey Svinarenko, Vasily Buyadzhi, Valentin Ternovsky, George Prepelitsa, Petr Bashkarev

First published in Croatia, 2017 by INTECH d.o.o.
eBook (PDF) Published by IN TECH d.o.o.
Place and year of publication of eBook (PDF): Rijeka, 2019.
IntechOpen is the global imprint of IN TECH d.o.o.
Printed in Croatia

Legal deposit, Croatia: National and University Library in Zagreb

Additional hard and PDF copies can be obtained from orders@intechopen.com

Recent Studies in Perturbation Theory
Edited by Dimo I. Uzunov

p. cm.

Print ISBN 978-953-51-3261-5

Online ISBN 978-953-51-3262-2

eBook (PDF) ISBN 978-953-51-4789-3

Meet the editor

Dimo I. Uzunov was born in 1950, Zlatograd, Bulgaria. He graduated from the Physics Faculty of St. Kliment Ohridski University of Sofia in 1974. He majored in condensed matter physics, with emphasis on theory of condensed matter. He received his PhD degree in Physics in 1981 and the degree of Doctor of Physical Sciences in 1988 from the G. Nadjakov Institute of Solid State Physics at the Bulgarian Academy of Sciences (Sofia). He is a professor of Physics and the head of a research group at the G. Nadjakov Institute of Solid State Physics of the Bulgarian Academy of Sciences (Sofia). His research interests include condensed matter theory, statistical physics, field theory, phase transitions and critical phenomena, superconductivity, BEK and superfluidity, and magnetism.

Contents

Preface

There is nothing better than the exact solution of mathematical problems, for example, equations or integrals. There are a huge number of such relatively simple cases but the number of complex problems, which have only approximate solutions, is bigger, even tends to infinity. The approximate solutions are looked for either by analytical methods or by numerical analysis. A powerful and widely applicable analytical approach to the obtaining of reliable approximate solutions is the perturbation method, namely, the development of a perturbation theory of the selected problem. This general approach is well combined with numerical calculations and computer simulations.

The perturbation theories look alike and can easily be recognized through their main features. Their results are represented by infinite series expansions around an exact solution of a simpler problem. The latter is usually a result of a suitable reduction of the initial problem when the mathematical part, which is responsible for the lack of exact solution, is ignored. The ignored part is called “perturbation part." Under the supposition that the perturbation term has a small effect on the final result, the solution of the entire problem is represented as an infinite series in powers of some expansion parameter, which is a small factor in the ignored term. The first term in this expansion is usually labeled by the subscript “0" (zero-order term) and represents the solution of the exactly solved reduced task, whereas the other terms are in powers of the expansion parameter.

The perturbation series are infinite, but in the self-consistent theories, the magnitude of the terms in nonzero power decreases with the increase of the expansion parameter powers, and the final sum of the perturbation terms is smaller than the zero-order term. In this much desired case, the perturbation leads to a relatively small correction to the result for the exactly solvable part of the problem. This usually happens under some conditions that depend on the features of the specific task and are to be deduced within the development of the theory. In case of a number of relevant problems, both in mathematics and natural sciences, the perturbation contributions are larger than the zero-order solution. This circumstance requires a more specific interpretation of the final results.

In other important cases, the perturbation series are divergent for some parameters of the theory. This situation is frequent in research problems in natural sciences, in particular, in physics. Significant efforts to extract useful information from asymptotic perturbation series are the daily concern of many theoretical physicists working on the most important physics problems, particularly in the field of quantum field theory and in the theory of phase transitions, where the interparticle interactions are relatively strong. Namely, the interaction terms in the Hamiltonian of a physical system are usually chosen as the perturbation part of perturbation expansions in quantum field theory and statistical physics, where the perturbation methods are widely used on the basis of the so-called Green's function approach. In modern theory of strongly interacting systems, the perturbation expansions are combined with ideas of scaling and renormalization, and thus these expansions are in the basis of the so-called renormalization group. The latter is a powerful tool of investigation of the effect of strong interactions in field theories.

Once introduced and highly developed in physics, perturbation methods of study are also spread in chemistry—mainly in quantum chemistry, in physical chemistry, in chemical physics, and in biophysics. In the last three–four decades, new interdisciplinary research fields appeared, for example, sociophysics and econophysics, where perturbation theories together with numerical analysis and computer simulations will undoubtedly be very important.

The book contains seven chapters, written by noted experts and young researchers who present their recent studies of both pure mathematical problems of perturbation theories and application of perturbation methods to the study of important topics in physics, for example, renormalization group theory and applications to basic models in theoretical physics (Y. Takashi), the quantum gravity and its detection and measurement (F. Bulnes), atom-photon interactions (E. G. Thrapsaniotis), treatment of spectra and radiation characteristics by relativistic perturbation theory (A. V. Glushkov et al.), and Green's function approach and some applications (Jing Huang). The pure mathematical issues are related to the problem of generalization of the boundary layer function method for bisingularly perturbed differential equations (K. Alymkulov and D. A. Torsunov) and to the development of new homotopy asymptotic methods and their applications (Baojian Hong).

Dimo I. Uzunov
Professor of Physics
Bulgarian Academy of Sciences
Sofia, Bulgaria

Chapter 1

Perturbed Differential Equations with Singular Points

Keldibay Alymkulov and
Dilmurat Adbillajanovich Tursunov

Additional information is available at the end of the chapter

http://dx.doi.org/10.5772/67856

Dedicated to academician of National Academy Sciences Kyrgyz Republic
and Corresponding member of RAS Imanaliev Murzabek

Abstract

Here, we generalize the boundary layer functions method (or composite asymptotic expansion) for bisingular perturbed differential equations (BPDE that is perturbed differential equations with singular point). We will construct a uniform valid asymptotic solution of the singularly perturbed first-order equation with a turning point, for BPDE of the Airy type and for BPDE of the second-order with a regularly singular point, and for the boundary value problem of Cole equation with a weak singularity.A uniform valid expansion of solution of Lighthill model equation by the method of uniformization and the explicit solution—this one by the generalization method of the boundary layer function—is constructed. Furthermore, we construct a uniformly convergent solution of the Lagerstrom model equation by the method of fictitious parameter.

Keywords: turning point, singularly perturbed, bisingularly perturbed, Cauchy problem, Dirichlet problem, Lagerstrom model equation, Lighthill model equation, Cole equation, generalization boundary layer functions

1. Preliminary

1.1. Symbols O, o, ~. Asymptotic expansions of functions

Let a function $f(x)$ and $\varphi(x)$ be defined in a neighborhood of $x = 0$.

Definition 1. If $\lim_{x\to 0}\frac{f(x)}{\varphi(x)} = M$, then write $f(x) = O(\varphi(x)), \quad x \to 0$, and M is constant.

If $\lim_{x\to 0}\frac{f(x)}{\varphi(x)} = 0$, then write $f(x) = o(\varphi(x)), \quad x \to 0$.

If $\lim_{x\to 0}\frac{f(x)}{\varphi(x)} = 1$, then write $f(x) \sim \varphi(x), \quad x \to 0$.

Definition 2. The sequence $\{\delta_n(\varepsilon)\}$, where $\delta_n(\varepsilon)$ defined in some neighborhood of zero, is called the asymptotic sequence in $\varepsilon \to 0$, if

$$\lim_{\varepsilon\to 0}\frac{\delta_{n+1}(\varepsilon)}{\delta_n(\varepsilon)} = 0, \quad \forall n = 1, 2, \dots$$

For example.

$$\{\varepsilon^n\}, \ \left\{\left(1/\ln(1/\varepsilon)\right)^n\right\}, \ \left\{\left(\varepsilon\ln(1/\varepsilon)\right)^n\right\}.$$

Note 1. Everywhere below ε denotes a small parameter.

Definition 3. We say that $f(x)$ function can be expanded in an asymptotic series by the asymptotic sequence $\{\varphi_n(x)\}, \ x \to 0$, if there exists a sequence of numbers $\{f_n\}$ and has the relation

$$f(x) = \sum_{k=0}^{n} f_k\varphi_k(x) + O(\varphi_{n+1}(x)), \quad x \to 0,$$

and write

$$f(x)\tilde{}\sum_{k=0}^{\infty} f_k\varphi_k(x), \quad x \to 0.$$

1.2. The asymptotic expansion of infinitely differentiable functions

Theorem (Taylor (1715) and Maclaurin (1742)). If the function $f(x) \in C^\infty$ in some neighborhood of $x = 0$, then it can be expanded in an asymptotic series for the asymptotic sequence $\{x^n\}$, i.e.,

$f(x) \sim \sum_{n=1}^{\infty} f_n x^n$, where $f_n = f^{(n)}(0)/n!$.

Thus, the concept of an asymptotic expansion was given for the first time by Taylor and Maclaurin,although an explicit definition was given by Poincaré in 1886.

1.3. The asymptotic expansion of the solution of the ordinary differential equation

Consider the Cauchy problem for a normal ordinary differential equation

$$y'(x) = f(x, y, \varepsilon), \quad y(0) = 0. \tag{1}$$

The function $f(x, y, \varepsilon)$ is infinitely differentiable on the variables x, y, ε in some neighborhood $O(0, 0, 0)$. It is correct next.

Theorem 1. The solution $y = y(x, \varepsilon)$ of problem (1) exists and unique in some neighborhood point $O(0, 0, 0)$ and $y(x, \varepsilon) \in C^\infty$, for small x, ε.

Corollary. The solution of problem (1) can be expanded in an asymptotic series by the small parameter $\boldsymbol{\varepsilon}$, i.e.,

$$y(x, \varepsilon) = \sum_{k=1}^{\infty} \varepsilon^k y_k(x). \tag{2}$$

Here and below, the equality is understood in an asymptotic sense.

Note 2. Theorem 1 for the case when $f(x, y, \varepsilon)$ is analytical was given in [1] by Duboshin.

Note 3. This theorem 1 is not true if $f(x, y, \varepsilon)$ is not smooth at ε. For example, the solution of a singularly perturbed equation

$$\varepsilon y'(x) = -y(x), \quad y(0) = a$$

function $y(x) = ae^{-x/\varepsilon}$ and is not expanded in an asymptotic series in powers of ε, because here $f(x, y, \varepsilon) = -y(x)/\varepsilon$ and f have a pole of the first order with respect to ε.

Note 4. The series 2 is a uniform asymptotic expansion of the function $y(x)$ in a neighborhood of $x = 0$.

For example. Series

$$y(x, \varepsilon) = 1 + \varepsilon x^{-1} \ + (\varepsilon x^{-1})^2 + \ldots + (\varepsilon x^{-1})^n + \ldots$$

It is not uniform valid asymptotic series on the interval [0, 1], but it is a uniform valid asymptotic expansion of the segment $[\varepsilon^\alpha, 1]$, where $0 < \alpha < 1$.

1.4. Singularly perturbed ordinary differential equations

We divide such equations into three types:

(I) Singular perturbations of ordinary differential equations such as the Prandtl-Tikhonov [2–56], i.e., perturbed equations that contain a small parameter at the highest derivative, i.e., equations of the form

$$y'(x) = f(x, y, \varepsilon), \quad y(0) = 0, \qquad \varepsilon z'(x) = g(x, y, \varepsilon), \quad z(0) = 0,$$

where $f,\ g$ are infinitely differentiable in the variables x, y, ε in the neighborhood of $O(0, 0, 0)$. It is obvious that unperturbed equation ($\varepsilon = 0$)

$$y_0{}'(x) = f(x, y, 0), \quad 0 = g(x, y, 0)$$

is a first order.

Definition 4. Singularly perturbed equation will be called bisingulary perturbed if the corresponding unperturbed differential equation has a singular point, or this one is an unbounded solution in the considering domain.

For example

1. Equation $\varepsilon y'(x) = -y(x)$ is a singularly perturbed ordinary differential equation.
2. Equation Vander Pol

$$\varepsilon y''(x) + (1 - y^2(x))y'(x) + y(x) = 0.$$

It is a bisingularly perturbed ordinary differential equation with singular points, if $y(x) = \pm 1$.

3. $\varepsilon y'(x) - xy(x) = 1$, $x \in [0, 1]$ is a bisingularly perturbed equation, because the unperturbed equation has an unbounded solution $y_0(x) = -x^{-1}$.

4. $\varepsilon y''(x) - xy(x) = 1$, $x \in [0, 1]$ is a bisingularly perturbed equation also.

(II) Singularly perturbed differential equations such as the Lighthill's type [57–69], in which the order of the corresponding unperturbed equation is not reduced, but has a singular point in the considering domain.

For example, a Lighthill model equation

$$(x + \varepsilon y(x))y'(x) + p(x)y(x) = r(x), \quad y(1) = a$$

where $x \in [0, 1]$, $p(x)$, $r(x) \in C^\infty[0, 1]$. For unperturbed equation

$$xy_0'(x) + p(x)y_0(x) = r(x),$$

point $x = 0$ is a regular singular point.

(III) A singularly perturbed equation with a small parameter is considered on an infinite interval. For example, the Lagerstrom equation [70–81]

$$y''(x) + nx^{-1}y'(x) + y(x)y'(x) = \beta(y'(x))^2,$$
$$y(\varepsilon) = 0, y(\infty) = 1.$$

where $0 < \beta$ is a given number and n is the dimension space.

Remark. The division into such classes is conditional, because singularly perturbed equation of Van der Pol in the neighborhood of points $y = \pm 1$ leads to an equation of Lighthill type [2, 3].

1.5. Methods of construction of asymptotic expansions of solutions of singularly perturbed differential equations

1. The method of matching of outer and inner expansions [13, 19, 28, 29, 37, 49] is the most common method for constructing asymptotic expansions of solutions of singularly perturbed differential equations. Justification for this method is given by Il'in [22]. However, this method is relatively complex for applied scientists.

2. The boundary layer function method (or composite asymptotic expansion)dates back to the work of many mathematicians. For the first time, this method for a singularly perturbed differential equations in partial derivatives is developed by Vishik and Lyusternik [52] and for nonlinear integral-differential equations (thus for the ordinary differential equations) Imanaliev [24], O'Malley (1971) [38], and Hoppenstedt (1971) [42].

   It should be noted that, for the first time, the uniform valid asymptotic expansion of the solution of Eq. (5) is constructed by Vasil'eva (1960) [50] after Wasow [69] and Sibuya in 1963 [68] by the method of matching.

This method is constructive and understandable for the applied scientists.

3. The method of Lomov or regularization method [33] is applied for the construction of uniformly valid solutions of a singularly perturbed equation and will apply Fredholm ideas.
4. The method WKB or Liouville-Green method is used for the second-order differential equations.
5. The method of multiple scales.
6. The averaging method is applicable to the construction of solutions of a singularly perturbed equation on a large but finite interval.

Here, we consider a bisingularly perturbed differential equations and types of equations of Lighthill and Lagerstrom.

Here, we generalize the boundary layer function method for bisingular perturbed equations. We will construct a uniform asymptotic solution of the Lighthill model equation by the method of uniformization and construct the explicit solution of this one by the generalized method of the boundary layer functions.

Furthermore, we construct a uniformly convergent solution of the Lagerstrom model equation by the method of fictitious parameter.

2. Bisingularly perturbed ordinary differential equations

2.1. Singularly perturbed of the first-order equation with a turning point

Consider the Cauchy problem [5]

$$\varepsilon y'(x) + xy(x) = f(x), \quad 0 < x \le 1, \quad y(0) = a, \tag{3}$$

where $f(x) \in C^{\infty}[0,1]$, $f(x)=\sum_{k=0}^{\infty} f_k x^k$, $f_k = f^{(k)}(0)/k!$, $f_0 \neq 0$; a is the constant

Explicit solution of the problem (3) has the form: $y(x) = ae^{-x^2/2\varepsilon} + \frac{1}{\varepsilon}\int_0^x e^{(s^2-x^2)/2\varepsilon} f(s)ds.$

The corresponding unperturbed equation ($\varepsilon = 0$)

$$-x\tilde{y}(x) + f(x) = 0,$$

has a solution $\tilde{y}(x) = f(x)/x$, which is unbounded at $x = 0$.

If you seek a solution to problem (1) in the form

$$y(x) = y_0(x) + \varepsilon y_1(x) + \varepsilon^2 y_2(x) + \dots, \tag{4}$$

then

$$y_0(x) = \frac{f(x)}{x} \sim f_0 x^{-1}, \quad x \to 0,$$

$$y_1(x) = x^{-1} y_0'(x) \sim f_0 x^{-3}, \quad x \to 0,$$

$$y_2(x) = x^{-1} y_1'(x) \sim 3 f_0 x^{-5}, \quad x \to 0,$$

$$y_3(x) = x^{-1} y_2'(x) \sim 3 \cdot 5 f_0 x^{-5}, \quad x \to 0,$$

$$y_n(x) = x^{-1} y_{n-1}'(x) \sim 3 \cdot 5 \cdot \ldots \cdot (2n-1) f_0 x^{-(2n+1)}, \quad x \to 0,$$

and a series of Eq. (4) is asymptotic in the segment $(\sqrt{\varepsilon}, 1]$, and the point x_0=$\sqrt{\varepsilon} = \mu$ is singular point of the asymptotic series of Eq. (4). Therefore, the solution of problem (3) we will seek in the form

$$y(x) = \mu^{-1}\pi_{-1}(t) + Y_0(x) + \pi_0(t) + \mu\Big(Y_1(x) + \pi_1(t)\Big) + \mu^2\Big(Y_2(x) + \pi_2(t)\Big) + \ldots, \quad \mu \to 0, \tag{5}$$

where $Y_k(x) \in C^{(\infty)}[0, 1]$, $\pi_k(t) \in C^{(\infty)}[0, \mu^{-1}]$, $x = \mu t$ and boundary layer functions $\pi_k(t)$ decreasing by power law as $t \to \infty$, that is,$\pi_k(t) = O(t^{-m})$, $t \to \infty, m \in N$.

Substituting Eq. (5) into Eq. (3), we obtain

$$\begin{aligned}&\pi_{-1}'(t) + \mu^2 Y_0'(x) + \mu\pi_0'(t) + \mu^3 Y_1'(x) + \mu^2\pi_1'(t) + \mu^4 Y_2'(x) + \mu^3\pi_2'(t) + \mu^5 Y_3'(x) + \mu^4\pi_3'(t) + \ldots\\ &+ xY_0(x) + \mu x Y_1(x) + \mu^2 x Y_2(x) + \mu^3 x Y_3(x) + \ldots + t\pi_{-1}(t) + \mu t\pi_0(t) + \mu^2 t\pi_1(t) + \mu^3 t\pi_2(t)\\ &+ \mu^4 t\pi_3(t) + \ldots = f(x).\end{aligned} \tag{6}$$

The initial conditions for the functions $\pi_{k-1}(t)$, $k = 0, 1, \ldots$ we take in the next form

$$\pi_{-1}(0) = 0, \ \pi_0(0) = a - Y_0(0), \ \pi_k(0) = -Y_k(0), \quad k = 1, 2, \ldots$$

From Eq. (6), we have

$$\mu^0: \quad \pi_{-1}'(t) + t\pi_{-1}(t) + xY_0(x) = f(x), \tag{7.-1}$$

$$\mu^1: \quad \pi_0'(t) + t\pi_0(t) + xY_1(x) = 0, \tag{7.0}$$

$$\mu^{k+1}: \quad \pi_k'(t) + t\pi_k(t) + xY_{k+1}(x) + Y_{k-1}'(x) = 0, \quad k = 1, 2, \ldots \tag{7.k}$$

To $Y_0(x)$ function has been smooth, and we define it from the equation

$$xY_0(x) = f(x) - f_0 \Rightarrow Y_0(x) = (f(x) - f_0)/x,$$

and then from Eq. (7.−1), we have obtained the equation

$$\pi'_{-1}(t) + t\pi_{-1}(t) = f_{0.}$$

Therefore

$$\pi_{-1}(t) = f_0 e^{-t^2/2}\int_0^t e^{s^2/2}ds \in C^\infty[0, \mu^{-1}],$$

Obviously, this function bounded and is infinitely differentiable on the segment $[0, \mu^{-1}]$, and

$$\pi_{-1}(t) = -\frac{f_0}{t}(1 + \frac{1}{t^2} + \frac{3}{t^4} + \ldots), \quad t \to \infty.$$

This asymptotic expression can be obtained by integration by parts the integral expression for $\pi_{-1}(t)$.

Eq. (7.0) define $Y_1(x)$ and $\pi_0(t)$. Let $Y_1(x) \equiv 0$, then

$$\pi'_0(t) + t\pi_0(t) = 0, \;\; \pi_0(0) = a - f_{1.}$$

Hence, we find

$$\pi_0(t) = (a - f_1)e^{-t^2/2.}$$

From Eq. (7c) for $k = 1$, we have

$$\pi'_1(t) + t\pi_1(t) + xY_2(x) + Y'_0(x) = 0.$$

Let $xY_2(x) = Y'_0(0) - Y'_0(x)$, then $\pi'_1(t) + t\pi_1(t) = -Y'_0(0)$.

From these, we get

$$Y_2(x) = (Y'_0(0) - Y'_0(x))/x, \quad \pi_1(t) = -f_2 e^{-t^2/2}\int_0^t e^{s^2/2}ds \in C^\infty[0, \mu^{-1}],$$

and

$$\pi_{-1}(t) = \frac{f_2}{t}(1 + \frac{1}{t^2} + \frac{3}{t^4} + \ldots), \quad t \to \infty.$$

From Eq. (7c) for $k = 2$, we have

$$\pi'_2(t) + t\pi_2(t) + xY_3(x) + Y'_1(x) = 0 \text{ or } \pi'_2(t) + t\pi_2(t) + xY_3(x) = 0.$$

Let $Y_3(x) \equiv 0$, then

$$\pi'_{2}(t)+t\pi_2(t)=0,\ \ \pi_2(0)=-Y_2(0)=2f_3.$$

From this, we get

$$\pi_2(t)=2f_3e^{-t^2/2}.$$

Analogously continuing this process, we determine the others of the functions $Y_k(x),\ \pi_k(t)$.

In order to show that the constructed series of [Eq. (5)] is asymptotic series, we consider remainder term $R_m(x)=y(x)-y_m(x)$,

where $y_m(x)=\frac{1}{\mu}\pi_{-1}(t)+Y_0(x)+\pi_0(t)+\mu\Big(Y_1(x)+\pi_1(t)\Big)+\ldots+\mu^m\Big(Y_m(x)+\pi_m(t)\Big)$.

For the remainder term $R_m(x)$, we obtain a problem:

$$\varepsilon R'_m(x)+xR_m(x)=-\mu^{m+2}Y'_m(x),\quad 0<x\leq 1,\ \ R_m(0)=0. \tag{8}$$

We note that if m is odd, then $Y'_m(x)\equiv 0$.

The problem (8) has a unique solution

$$R_m(x)=-\mu^m e^{-x^2/2\varepsilon}\int_0^x Y'_m(s)e^{s^2/2\varepsilon}ds,$$

and from this, we have $R_m(x)=O(\mu^m),\ \mu\to 0,\ x\in[0,1]$.

2.2. Bisingularly perturbed in a homogenous differential equation of the Airy type

Consider the boundary value problem for the second-order ordinary in a homogenous differential equation with a turning point

$$\varepsilon y''(x)-xy(x)=f(x),\quad x\in(0,1), \tag{9}$$

$$y(0)=0,\quad y(1)=0. \tag{10}$$

where $f(x)=\sum_{k=0}^{\infty}f_kx^k,\quad x\to 0,\quad f_k=f^{(k)}(0)/k!,\quad f_0\neq 0.$

Note 5. It is the general case of this one was considered in Ref. [8, 45–47].

Without loss of generality, we consider the homogeneous boundary conditions, since $y(0)=a,\ y(1)=b,\ \ a^2+b^2\neq 0,$ using transformation

$$y(x)=a+(b-a)x+z(x),$$

can lead to conditions (10).

If the asymptotic solution of the problems (9)–(10) we seek in the form

$$y(x) = y_0(x) + \varepsilon y_1(x) + \varepsilon^2 y_2(x) + \ldots, \tag{11}$$

then we have

$$y_0(x) = -\frac{f(x)}{x} \sim f_0 x^{-1}, \quad x \to 0,$$

$$y_1(x) = x^{-1} y''_0(x) \sim 1 \cdot 2 f_0 x^{-4}, \quad x \to 0,$$

$$y_2(x) = x^{-1} y''_1(x) \sim 1 \cdot 2 \cdot 4 \cdot 5 f_0 x^{-7}, \quad x \to 0,$$

$$y_3(x) = x^{-1} y''_2(x) \sim 1 \cdot 2 \cdot 4 \cdot 5 \cdot 7 \cdot 8 f_0 x^{-10}, \quad x \to 0,$$

$$y_n(x) = x^{-1} y''_{n-1}(x) \sim 1 \cdot 2 \cdot 4 \cdot 5 \cdot 7 \cdot 8 \cdot \ldots \cdot (3n-2) \cdot (3n-1) f_0 x^{-(3n+1)},\ 0 < n, \quad x \to 0,$$

and the series (11) is asymptotic in the segment $(\sqrt[3]{\varepsilon}, 1]$. The point $x_0 = \sqrt[3]{\varepsilon} = \mu$ is singular point of asymptotic series (11).

The solution of problems (9) and (10) will be sought in the form

$$y(x) = \mu^{-1}\pi_{-1}(t) + \sum_{k=0}^{\infty} \mu^k \Big(Y_k(x) + \pi_k(t) \Big) + \sum_{k=0}^{\infty} \lambda^k w_k(\eta), \tag{12}$$

where $t = x/\mu$, $\mu = \sqrt[3]{\varepsilon}$, $\eta = (1-x)/\lambda$, $\lambda = \sqrt{\varepsilon}$. Here, $Y_k(x) \in C^\infty[0,1]$, $\pi_k(t) \in C^\infty[0, 1/\mu]$ is boundary layer function in a neighborhood of $t = 0$ and decreases by the power law as $t \to \infty$, and the function $w_k(t) \in C^\infty[0, 1/\lambda]$ is boundary function in a neighborhood of $\eta = 0$ and decreases exponentially as $\eta \to \infty$.

Substituting Eq. (12) in Eq. (9), we get

$$\sum_{k=0}^{\infty} \mu^k (\pi''_{k-1}(t) - t\pi_{k-1}(t)) + \sum_{k=0}^{\infty} \mu^{k+3} Y''_k(x) - x \sum_{k=0}^{\infty} \mu^k Y_k(x) = f(x) \tag{13}$$

$$\sum_{k=0}^{\infty} \lambda^k \Big(w''_k(\eta) - (1 - \lambda\eta) w_k(\eta) \Big) = 0. \tag{14}$$

From Eq. (13), we have

$$\mu^0: \quad \pi''_{-1}(t) - t\pi_{-1}(t) - xY_0(x) = f(x), \tag{15.-1}$$

$$\mu^1: \quad \pi''_0(t) - t\pi_0(t) - xY_1(x) = 0, \tag{15.0}$$

$$\mu^2: \quad \pi''_1(t) - t\pi_1(t) - xY_2(x) = 0, \tag{15.1}$$

$$\mu^3: \quad \pi''_2(t) - t\pi_2(t) + Y''_0(x) - xY_3(x) = 0, \tag{15.2}$$

$$\mu^k: \quad \pi''_{k-1}(t) - t\pi_{k-1}(t) + Y''_{k-3}(x) - xY_k(x) = 0, \quad k > 3, \tag{15.k}$$

Boundary conditions for functions $\pi_{k-1}(t),\ k=0,1,\dots$ we take next form

$$\pi_{-1}(0)=0,\ \pi_k(0)=-Y_k(0),\ \lim_{\mu\to 0}\pi_{k-1}(1/\mu)=0,\quad k=0,1,2,\dots$$

To $Y_0(x)$ function has been smooth; therefore, we define it from the equation

$$-xY_0(x)=f(x)-f_0\Rightarrow Y_0(x)=-(f(x)-f_0)/x,$$

then from Eq. (15.1), we have the equation

$$\pi''_{-1}(t)-t\pi_{-1}(t)=f_{0.}$$

Let us prove an auxiliary lemma.

Lemma 1. Next boundary value problem

$$z''(t)-tz(t)=b,\quad 0<t<1/\mu,\ \text{ here } b \text{ is the constant,} \tag{16}$$

$$z(0)=z^0,\quad z(1/\mu)\to 0,\quad \mu\to 0 \tag{17}$$

will have the unique solution and this one have next form

$$z(t)=z^0\frac{Ai(t)}{Ai(0)}-\pi b\Big(Ai(t)\int_0^t Bi(s)ds+Bi(t)\int_t^{1/\mu}Ai(s)ds-Ai(t)\sqrt{3}\int_0^{1/\mu}Ai(s)ds\Big),$$

and $z(t)\in C^\infty[0,\mu^{-1}]$.

Proof. We verify the boundary conditions:

$$z(0)=z^0-\pi b\Big(Bi(0)\int_0^{1/\mu}Ai(s)ds-Ai(0)\sqrt{3}\int_0^{1/\mu}Ai(s)ds\Big),$$

as $Bi(0)=Ai(0)\sqrt{3}$, so $z(0)=z^0$.

$$z(1/\mu)=z^0\frac{Ai(1/\mu)}{Ai(0)}-\pi b(1-\sqrt{3})Ai(1/\mu)\int_0^{1/\mu}Bi(s)ds,$$

as $Ai(t)\sim t^{-1/4}e^{-\frac{2}{3}t^{3/2}},\quad Bi(t)\sim t^{-1/4}e^{\frac{2}{3}t^{3/2}},\quad t\to\infty$, so $z(1/\mu)=O(\mu),\quad \mu\to 0$.

Now we show that $z(t)$ satisfies Eq. (16). For this, we compute derivatives:

$$z'(t)=z^0\frac{Ai'(t)}{Ai(0)}-\pi b\Big(Ai'(t)\int_0^t Bi(s)ds+Bi'(t)\int_t^{1/\mu}Ai(s)ds-Ai'(t)\sqrt{3}\int_0^{1/\mu}Ai(s)ds\Big)$$

$$z''(t)=z^0\frac{Ai''(t)}{Ai(0)}-\pi b\left(Ai''(t)\int_0^t Bi(s)ds+Bi''(t)\int_t^{1/\mu}Ai(s)ds-\frac{1}{\pi}-Ai''(t)\sqrt{3}\int_0^{1/\mu}Ai(s)ds\right)$$

Substituting the expressions for $z''(t)$ and $z(t)$ in Eq. (17), and given that $Ai''(t) - tAi(t) \equiv 0$ and $Bi''(t) - tBi(t) \equiv 0$, we get: $b \equiv b$.

The uniqueness of $z(t)$ the solution is proved by contradiction. Let $u(t)$also be a solution of problems (16) and (17), $z(t) \neq u(t)$. Considering the function $r(t) = z(t) - u(t)$, for the function $r(t)_,$ we obtain the problem

$$r''(t) - tr(t) = 0, \quad 0 < t < 1/\mu, \quad r(0) = 0, \quad r(1/\mu) \to 0, \quad \mu \to 0.$$

The general solution of the homogeneous equation is

$r(t) = c_1 Ai(t) + c_2 Bi(t); \quad c_{1,2}$ is the constant.

Considering the boundary condition $r(1/\mu) \to 0,\ \mu \to 0_,$ we have $c_2 = 0;\ r(t) = c_1 Ai(t)$. And the second condition $r(0) = 0,\ c_1 = 0$ follows. This implies that $r(t) \equiv 0$.

Therefore, $z(t) \equiv u(t)$. It is obvious that $z(t) \in C^\infty[0, \mu^{-1}]$. Lemma 1 is proved.

This Lemma 1 implies the existence and uniqueness of $\pi_{-1}(t) \in C^\infty[0, \mu^{-1}]$ solution of the problem:

$$\pi''_{-1}(t) - t\pi_{-1}(t) = f_0, \quad 0 < t < 1/\mu, \quad \pi_{-1}(0) = 0, \quad \pi_{-1}(1/\mu) \to 0, \quad \mu \to 0.$$

This function bounded and is infinitely differentiable on the segment $[0, \mu^{-1}]$, and as $t \to \infty$:

$$\pi_{-1}(t) = -\frac{f_0}{t}\left(1 + \frac{1\cdot 2}{t^3} + \frac{1\cdot 2\cdot 4\cdot 5}{t^6} + \dots\right).$$

This asymptotic expression can be obtained by integration by parts the integral expression for $\pi_{-1}(t)$.

From Eq. (15.0), we define $Y_1(x)$ and $\pi_0(t)$. Let $Y_1(x) \equiv 0$, then

$$\pi''_0(t) - t\pi_0(t) = 0, \quad \pi_0(0) = f_1, \quad \pi_0(1/\mu) \to 0, \quad \mu \to 0,$$

And by Lemma 1, we have

$$\pi_0(t) = f_1 Ai(t)/Ai(0).$$

Analogously, from Eq. (15.1), we define $Y_2(x)$ and $\pi_1(t)$. Let $Y_2(x) \equiv 0$, then

$$\pi''_1(t) - t\pi_1(t) = 0, \quad \pi_1(0) = 0, \quad \pi_0(1/\mu) \to 0, \quad \mu \to 0\ .$$

In view of Lemma 1, we have $\pi_1(t) \equiv 0$.

To $Y_3(x)$ function has been smooth; as above, we define it from the equation

$$xY_3(x) = Y''_0(x) - Y''_0(0) \Rightarrow Y_3(x) = (Y''_0(x) - Y''_0(0))/x, \quad (Y''_0(0) = -2f_3),$$

then Eq. (15.2) to $\pi_2(t)$hase the problem

$$\pi''_2(t) - t\pi_2(t) = 2f_3, \quad \pi_2(0) = 0, \quad \pi_2(1/\mu) \to 0, \quad \mu \to 0.$$

By Lemma 1, we can write an explicit solution to this problem, and this solution bounded and is infinitely differentiable on the segment $[0, \mu^{-1}]$, and as $t \to \infty$:

$$\pi_2(t) = -\frac{2f_3}{t}\left(1 + \frac{1\cdot 2}{t^3} + \frac{1\cdot 2\cdot 4\cdot 5}{t^6} + \ldots\right).$$

Analogously continuing this process, we determine the rest of the functions $Y_k(x)$, $\pi_k(t)$.

Now we will define functions $w_k(\eta)$ from the equality (14) by using the boundary conditions $y(1) = 0$ We state problems

$$Lw_0 \equiv w''_0(\eta) - w_0(\eta) = 0, \ \ w_0(0) = Y_0(1), \ \ \lim_{\eta\to\infty} w_0(\eta) = 0 \tag{18.0}$$

$$Lw_k = -\eta w_{k-1}(\eta), \ \ w_{2i}(0) = Y_{3i}(1), \ \ w_{2i-1}(0) = 0, \ \ \lim_{\eta\to\infty} w_k(\eta) = 0, \quad k, i \in N. \tag{18.k}$$

One can easily make sure that all these problems (18.0) and (18.k) have unique solutions such that $w_k(\eta) \in C^\infty[0, \infty)$, $w_k(\eta) = O(e^{-\eta})$ with $\eta \to \infty$.

Thus, all functions $Y_k(x)$, $w_k(\eta)$, and $\pi_k(t)$ in equality (12) are defined, i.e., a formally asymptotic expansion is constructed. Let us justify the constructed expansion. Let

$$y_m(x) = \mu^{-1}\pi_{-1}(t) + \sum_{k=0}^{3m} \mu^k \Big(Y_k(x) + \pi_k(t)\Big) + \sum_{k=0}^{2m} \lambda^k w_k(\eta), \quad r_m(x) = y(x) - y_m(x).$$

Then for the remainder term, we state the following problem:

$$\varepsilon r''_m(x) - x r_m(x) = O(\varepsilon^{m+1/2}), \quad \varepsilon \to 0, \quad x \in (0, 1). \tag{19}$$

$$r_m(0) = O(e^{-1/\sqrt{\varepsilon}}), \quad r_m(1) = O(\varepsilon^{m+1}), \quad \varepsilon \to 0. \tag{20}$$

Let $r_m(x) = (2 - x^2)R_m(x)/2$, and then problems (19) and (20) take the form

$$\varepsilon R''_m(x) - \frac{4x\varepsilon}{2 - x^2} R'_m(x) - \left(\frac{2\varepsilon}{2 - x^2} + x\right) R_m(x) = O(\varepsilon^{m+1/2}), \quad \varepsilon \to 0,$$

$$R_m(0) = O(e^{-1/\sqrt{\varepsilon}}), \quad R_m(1) = O(\varepsilon^{m+1}), \quad \varepsilon \to 0.$$

According to the maximum principle [23, p. 117, 82], we have $R_m(x) = O(\varepsilon^{m-1/2})$, $\varepsilon \to 0, x \in [0, 1]$.

Hence, we get $r_m(x) = O(\varepsilon^{m-1/2}), \quad \varepsilon \to 0, \quad x \in [0, 1]$.

Thus, we have proved.

Theorem 2. Let $f(0) \neq 0$, then the solution to problem (9) and (10) will have next form

$$y(x) = \frac{1}{\sqrt[3]{\varepsilon}}\pi_{-1}\left(\frac{x}{\sqrt[3]{\varepsilon}}\right) + \sum_{k=0}^{\infty}\sqrt[3]{\varepsilon^k}\left(y_k(x) + \pi_k\left(\frac{x}{\sqrt[3]{\varepsilon}}\right)\right) + \sum_{k=0}^{\infty}\sqrt{\varepsilon^k}w_k\left(\frac{1-x}{\sqrt{\varepsilon}}\right).$$

Example. Consider the problem

$$\varepsilon y''(x) - xy(x) = 1 + x, \quad x \in (0, 1), \quad y(0) = 0, \quad y(1) = 0.$$

The asymptotic solution this problem we can represent in the form $y(x) = \mu^{-1}\pi_{-1}(t) + \sum_{k=0}^{3}\mu^k(Y_k(x)+\pi_k(t)) + w_0(\eta) + \lambda w_1(\eta) + \lambda^2 w_2(\eta) + R(x)$.

We have got $Y_0(x) = -(1 + x - 1)/x = -1, \ \ Y_{1,2,3}(x) \equiv 0$,

$$\pi_{-1}(t) = -\pi\left(Ai(t)\int_0^t Bi(s)ds + Bi(t)\int_t^{1/\mu} Ai(s)ds - Ai(t)\sqrt{3}\int_0^{1/\mu} Ai(s)ds\right),$$

$$\pi_0(t) = Ai(t)/Ai(0), \ \ \pi_{1,2,3}(t) \equiv 0, w_0(\eta) = 2e^{-\eta}, \ \ w_k(\eta) = O(e^{-\eta}), \ k = 1, 2.$$

$$\varepsilon R''(x) - xR(x) = O(\varepsilon^{3/2}), 0 < x < 1, R(0) = O(e^{-1/\sqrt{\varepsilon}}), R(1) = O(\boldsymbol{\varepsilon}^2), \boldsymbol{\varepsilon} \to 0.$$

We have

$$y(x) = \varepsilon^{-1/3}\pi_{-1}(t) - 1 + 2e^{-(1-x)/\sqrt{\varepsilon}} + \pi_0(t) + \sqrt{\varepsilon}w_1(\eta) + \varepsilon w_2(\eta) + O(\sqrt{\varepsilon}), \boldsymbol{\varepsilon} \to 0.$$

2.3. Bisingularly perturbed equation of the second order with a regularly singular point

Consider the boundary value problem [6, 7]

$$L_\varepsilon y \equiv \varepsilon y'' + xy' - q(x)y = f(x), \quad x \in [0, 1], \tag{21}$$

$$y(0) = 0, \quad y(1) = 0, \tag{22}$$

where $q(x), f(x) \in C^\infty[0, 1]$.

Here, for simplicity, we consider the case $q(0) = 1, q(x) \geq 1$.

The solution of the unperturbed problem

$$My \equiv xy' - q(x)y = f(x),$$

represented as

$$y_0(x) \equiv xp(x)\int_1^x r(s)s^{-2}ds, \tag{23}$$

where

$$r(x) = p^{-1}(x)f(x), \quad p(x) = \exp\left\{\int_1^x \left(q(x) - 1\right)s^{-1}ds\right\}.$$

Extracting in Eq. (23), the main part of the integral in the sense of Hadamard [34], it can be represented as

$$y_0(x) = a(x) + r_1 xp(x)\ln x, \tag{24}$$

where

$$\begin{aligned} &a(x) = xp(x)\int_1^x \left(r(s) - r_0 - r_1 s\right)s^{-2}ds + r_0 p(x)[x-1], \\ &r_0 = r(0),\ r_1 = r'(0) = p(0)^{-1}[f'(0) - q'(0)f(0)]. \end{aligned} \tag{25}$$

Function $a(x) \in C^\infty[0, 1]$.

Theorem 3. Suppose that the conditions referred to the above with respect to $q(x)$ and $f(x)$. Then the asymptotic behavior of the solution of the problems (21) and (22) can be written as:

$$\sum_{k=0}^{\infty}\mu^k\left(z_k(x) + \pi_k(t)\right), \quad \varepsilon = \mu^2, \ \ x = \mu t, \tag{26}$$

where $z_k(x) \in C^\infty[0, 1],\ \pi_k(t) \in C^\infty[0, \mu^{-1}]$.

Function $z_0(x)$is a solution of equation

$$Mz_0 = f(x) - c_0 xp(x),$$

where$c_0 = p(0)^{-1}[f'(0) - q'(0)f(0)]$.

The coefficients $z_k(x)$of the series (26) will be determined as the solution of equations

$$Mz_k = -z''_{k-1}(x) - c_k xp(x),$$

where $c_k = p(0)^{-1}[-z'''_{k-1}(0) + z''_{k-1}(0)q'(0)]$, with boundary conditions $z_k(1) = 0,\ k \geq 1$.

Functions $\pi_k(t)$ is the solution of the equations

$$L\pi_k \equiv \pi''_k(t) + t\pi'_k(t) - q(\mu t)\pi_k(t) - c_k\mu t p(\mu t)$$

with boundary conditions $\pi_k(0) = -z_k(0),\ \pi_k(\mu^{-1}) = 0.$

Next, we use the following lemma.

Lemma 2. The problem

$$My = f(x) - r_1 x p(x)$$

It has a unique solution $y(x) \in C^\infty[0, 1]$.

The proof of Lemma 2 follows from Eqs. (24) and (25).

Lemma 3. A boundary value problem

$$L_0 v \equiv v'' + tv' - v(t) = 0, \quad v(0) = a, \quad v(1/\mu) = 0,$$

has solution $v(t) = aX(t)$, where

$$X(t) = t\int_t^{\mu^{-1}} s^{-2}\exp\left(\frac{-s^2}{2}\right)ds, \ \ 0 \le X(t) \le 1, \quad X(0) = 1.$$

The proof of Lemma 3 is obvious.

Lemma 4. In order to solve the boundary value problem

$$L_0 W = -\mu t, W(0) = W(\mu^{-1}) = 0,$$

we have the estimate

$$0 \le W(\mu, t) \le e^{-1}\ln\mu^{-1}.$$

Proof. This follows from the fact that the solution of this problem existsuniquely by the maximum principle [23, 82] and will be represented in the form

$$W(\mu, t) = \mu t\int_t^{\mu^{-1}} y^{-2}\exp\left(-\frac{y^2}{2}\right)\int_0^y s^2\exp\left(\frac{s^2}{2}\right)dsdy.$$

Lemma 5. The estimate

$$|\pi_k(\mu, t)| < B_k,$$

where $0 < B_k$is constant.

Proof. Consider the function

$$V_{\pm}(\mu, t) = \gamma_1 W(\mu, t) + \gamma_2 X(t) \pm \pi_k(\mu, t),$$

where γ_1 and γ_2 are positive constants such that

$$\gamma_1 > \max_{[0,\,1]}|p(x)|, \gamma_2 > |z_k(0)|.$$

It is obvious that

$$V_{\pm}(\mu, 0) > 0, \;\; V_{\pm}(\mu, \mu^{-1}) > 0, \;\; L_0 V_{\pm} \equiv V''_{\pm}(t) + tV'_{\pm}(t) - V_{\pm}(t) < 0$$

From the maximum principle, it follows that $|\pi_k(\mu, t)| < \gamma_1 W(\mu, t) + \gamma_2 X(t)$.

Now the proof of the lemma 5 follows from estimates of $W(\mu, t)$ and $X(t)$.

If we introduce the notation

$$Y_n(x, \varepsilon) = \sum_{k=0}^{n} \varepsilon^k \Big(z_k(x) + \pi_k(\mu, t) \Big),$$

where $z_k(x), \;\pi_k(\mu, t)$are constructed above functions, then

$$L_\varepsilon Y_n(x, \varepsilon) = f(x) + \varepsilon^{n+1} z''_n.$$

Let $y(x, \varepsilon)$be the solution of the problems (21) and (22). Then

$$|L_\varepsilon \Big(Y_n(x, \varepsilon) - y(x, \varepsilon) \Big)| < B_n \varepsilon^{n+1}, \quad Y_n(0, \varepsilon) - y(0, \varepsilon) = Y_n(1, \varepsilon) - y(1, \varepsilon) = 0.$$

Therefore, $|Y_n(x, \varepsilon) - y(x, \varepsilon)| < B_n \varepsilon^{n+1}$.

2.4. The bisingular problem of Cole equation with a weak singularity

The following problem is considered [9, 13, 28, 29],

$$\varepsilon y''(x) + \sqrt{x} y'(x) - y(x) = 0, \; 0 < x < 1, \tag{27}$$

$$y(0) = a, \;\; y(1) = b \tag{28}$$

where $x \in [0, 1]; \;\; a, b$ are the given constants.

The unperturbed equation $\sqrt{x} y'(x) - y(x) = 0, \, 0 < x < 1$,

has the general solution

$$y_0(x) = ce^{2\sqrt{x}}, \; c - \text{const}.$$

This is a nonsmooth function in $[0, 1]$.

We seek asymptotic representation of the solution of the problems (27) and (28) in the form:

$$y(x) = \sum_{k=0}^{n} \varepsilon^k y_k(x) + \sum_{k=0}^{3(n+1)} \mu^k \pi_k(t) + R(x, \varepsilon), \tag{29}$$

where $t = x/\mu^2,\ \varepsilon = \mu^3,\ y_k(x) \in C[0, 1],\ \pi_k(t) \in C[0, 1/\mu^2],\ R(x, \varepsilon)$ is the reminder term.

Substituting Eq. (29) into Eq. (27), we have

$$\begin{gathered}\sum_{k=0}^{n} \varepsilon^k (\varepsilon y''_k(x) + \sqrt{x} y'_k(x) - y_k(x)) + \frac{1}{\mu}\left(\pi''_0(t) + \sqrt{t}\pi'_0(t)\right) \\ + \sum_{k=1}^{3(n+1)} \mu^{k-1}\left(\pi''_k(t) + \sqrt{t}\pi'_k(t) - \pi_{k-1}(t)\right) - \mu^{3(n+1)}\pi_{3(n+1)}(t) + \varepsilon R''(x, \varepsilon) + \sqrt{x} R'(x, \varepsilon) \\ -R(x, \varepsilon) - h(x, \varepsilon) + h(x, \varepsilon) = 0\end{gathered} \tag{30}$$

By the method of generalized boundary layer function, we put the term $h(x, \varepsilon) = \sum_{k=0}^{n-1} \varepsilon^k h_k(x)$ into the equation. We choose functions $h_k(x)$ so that $y_k(x) \in C[0, 1]$.

Taking into account the boundary condition (28), from Eq. (30), we obtain

$$\sqrt{x} y'_0(x) - y_0(x) = 0, \quad 0 < x < 1, \quad y_0(1) = b. \tag{31}$$

$$\sqrt{x} y'_k(x) - y_k(x) = h_{k-1}(x) - y''_{k-1}(x), \quad 0 < x < 1, \ k \in N, \quad y_k(1) = 0. \tag{32}$$

The solution of the problems (31) and (32) exists. It is unique and has the form

$$y_0(x) = be^{2(\sqrt{x}-1)}, y_k(x) = e^{2\sqrt{x}} \int_1^x \frac{h_{k-1}(s) - y''_{k-1}(s)}{\sqrt{s}} e^{-2\sqrt{s}} ds, \ \ k \in N.$$

We choose indefinite functions $h_k(x)$ as follows: $y''_{k-1}(x) - h_{k-1}(x) \in C[0, 1]$. We can represent

$$y_0(x) = be^{-2}\left(1 + 2\sqrt{x} + \frac{(2\sqrt{x})^2}{2!} + \frac{(2\sqrt{x})^3}{3!} + \frac{(2\sqrt{x})^4}{4!} + \ldots + \frac{(2\sqrt{x})^n}{n!} + \ldots\right).$$

Let $h_1(x) = be^{-2}\left(2\sqrt{x} + \frac{(2\sqrt{x})^3}{3!}\right)'' = -be^{-2}\left(\frac{1}{2\sqrt{x^3}} - \frac{1}{\sqrt{x}}\right)$.

Then

$$y''_0(x) - h_0(x) \in C[0, 1], \mu^3 h_1(t\mu^2) = -c_1\left(\frac{1}{2\sqrt{t^3}} - \frac{\mu^2}{\sqrt{t}}\right), \ \ c_1 = be^{-2},$$

$$y_1(x) = c_1 e^{2\sqrt{x}} \int_1^x \left(-\frac{1}{2s^2} + \frac{1}{s} + \frac{1}{2s^2} e^{2\sqrt{s}} - \frac{1}{\sqrt{s^3}} e^{2\sqrt{s}}\right) e^{-2\sqrt{s}} ds.$$

We can rewrite $y_1(x)$ in the form:

$$y_1(x) = y_{1,0} + y_{1,1}(2\sqrt{x}) + y_{1,2}(2\sqrt{x})^2 + y_{1,3}(2\sqrt{x})^3 + \ldots,$$

where $y_{1,0} = \left(\frac{3}{2} + \frac{1}{2e^2}\right)c_1,\ y_{1,1} = \left(\frac{1}{6} + \frac{1}{2e^2}\right)c_1,\ y_{1,2} = \left(\frac{-1}{6} + \frac{1}{4e^2}\right)c_1,\ y_{1,3} = \left(\frac{-1}{10} + \frac{1}{12e^2}\right)c_1.$

Analogously, we have obtained

$$h_1(x) = \left(y_{1,1}(2\sqrt{x}) + y_{1,3}(2\sqrt{x})^3\right)'' = -\frac{y_{1,1}}{2\sqrt{x^3}} + \frac{6y_{1,3}}{\sqrt{x}}.$$

Then

$$y''_2(x) - h_2(x) \in C[0,1],\ \mu^6 h_2(t\mu^2) = -\frac{\mu^3 y_{1,1}}{2\sqrt{t^3}} + \frac{\mu^5 y_{1,3}}{\sqrt{t}}.$$

Continuing this process, we have

$$h_{k-1}(x) = -\frac{y_{k-1,1}}{2\sqrt{x^3}} + \frac{6y_{k-1,3}}{\sqrt{x}},\ k = 4, \ldots, n,$$

where $y_{k-1,1},\ y_{k-1,3}$ are corresponding coefficients of the expansion of $y_{k-1,1}(x)$ in powers of $(2\sqrt{x})$.

From Eq. (30), we have the following equations for the boundary functions $\pi_k(t)$:

$$L\pi_0 \equiv \pi''_0(t) + \sqrt{t}\pi'_0(t) = 0, \quad 0 < t < \tilde{\mu}, \quad \pi_0(0) = a - y_0(0),\ \pi_0(\tilde{\mu}) = 0,\ \tilde{\mu} = 1/\mu^2, \tag{33}$$

$$L\pi_{3k+1}(t) = \pi_{3k}(t) + \frac{y_{k,1}}{2\sqrt{t^3}}, \quad 0 < t < \tilde{\mu}, \quad \pi_{3k+1}(0) = 0, \quad \pi_{3k+1}(\tilde{\mu}) = 0, \quad k = 0, 1, \ldots, n \tag{34}$$

$$L\pi_{3k+2}(t) = \pi_{3k+1}(t), \quad 0 < t < \tilde{\mu}, \quad \pi_{3k+2}(0) = 0, \quad \pi_{3k+2}(\tilde{\mu}) = 0, \quad k = 0, 1, \ldots, n \tag{35}$$

$$L\pi_{3k+3} = \pi_{3k+2}(t) - \frac{y_{k,3}}{\sqrt{t}}, \quad 0 < t < \tilde{\mu}, \quad \pi_{3k}(0) = -y_k(0), \quad \pi_{3k}(\tilde{\mu}) = 0, \quad k = 0, 1, \ldots, n\text{–}1 \tag{36}$$

$$L\pi_{3(n+1)}(t) = \pi_{3n+2}(t) - \frac{y_{n,3}}{\sqrt{t}}, \quad 0 < t < \tilde{\mu}, \quad \pi_{3n}(0) = 0, \quad \pi_{3n}(\tilde{\mu}) = 0 \tag{37}$$

The solution of problem (33) is represented in the form

$$\pi_0(t) = (a - be^{-2})A\int_t^{\tilde{\mu}} e^{-\frac{2}{3}s^{3/2}}ds, \quad A = \left(\int_0^{\tilde{\mu}} e^{-\frac{2}{3}s^{3/2}}ds\right)^{-1}.$$

We note that $\pi_0(t)$ will exponentially decrease as $t \to \tilde{\mu}$.

Lemma 6. The general solution of this equation $Lz(t) = 0$ will have $z(t) = c_1 Y(t) + c_2 X(t)$; here $c_1,\ c_2$ are constants, and

$$Y(t) = 1 - X(t),\ \ X(t) = \alpha\int_t^{\tilde{\mu}} e^{-\frac{2}{3}s^{3/2}}ds\ \ (\ \alpha\int_0^{\tilde{\mu}} e^{-\frac{2}{3}s^{3/2}}ds = 1).$$

Two linearly independent solutions and $Y(t) = O(t),\ t \to 0,\ 0 < X(t) \leq 1,$

$$X(t)\ = t^{-\frac{1}{2}}e^{-\frac{2}{3}t^{3/2}}\left(1 - \frac{1}{2}t^{-\frac{3}{2}} + \ldots + \frac{(-1)^n}{2^n}\prod_{k=1}^{n} 1\cdot 4\cdot \ldots \cdot (3k-2)t^{-\frac{3n}{2}} + \ldots\right),\quad t \to \tilde{\mu} \tag{38}$$

Lemma 7. The boundary problem $Lz(t) = 0,\ z(0) = z(\tilde{\mu}) = 0$ will have only trivial solution.

The proofs of Lemmas 6 and 7 are evident.

Theorem 4. The problem

$$Lz(t) = f(t),\ z(0) = 0,\ \ z(\tilde{\mu}) = 0,$$

will have the unique solution and this one has the next form

$$z(t) = \int_0^{\tilde{\mu}} G(t,s)e^{\frac{2}{3}s^{3/2}}f(s)ds,$$

and $G(t,s) = \begin{cases} -Y(t)X(s), & 0 \leq t \leq s, \\ -Y(s)X(t), & s \leq t \leq \tilde{\mu}, \end{cases}$

is the function of Green and$f(t) \in C(0, \tilde{\mu}]$.

Theorem 4 implies the existence and uniqueness of the solution of problem (34)–(37): $|\pi_k(t)| < l = const,\ t \in [0, \tilde{\mu}]$.

Lemma 8. Asymptotical expansions of functions $\pi_k(t),\ t \to \tilde{\mu}\ (k = 1, 2, \ldots)$ will have the next forms

$$\pi_1(t) = -\frac{y_{0,1}}{2t}\left(1 + \frac{4}{5\sqrt{t^3}} + \frac{7}{4t^3} + \frac{42}{11\sqrt{t^9}} + \frac{39}{2t^7} + \ldots\right),$$

$$\pi_2(t) = \frac{y_{0,1}}{\sqrt{t}}\left(1 + \frac{23}{40\sqrt{t^3}} + \frac{173}{2t^3} + \ldots\right), \pi_3(t) = -\frac{23y_{0,1}}{60\sqrt{t^3}} + O\left(\frac{1}{t^3}\right),$$

$$\pi_{3k+1}(t) = t^{-1}\sum_{j=0}^{\infty} l_{3k+1,j}t^{-\frac{3}{2}j}, \pi_{3k+2}(t) = t^{-1/2}\sum_{j=0}^{\infty} l_{3k+2,j}t^{-\frac{3}{2}j}, \pi_{3k}(t) = \sum_{j=1}^{\infty} l_{3k,j}t^{-\frac{3}{2}j}.$$

Proof for Lemma 8.

Firs proof. We can prove this lemma by applying formulas (38) and Theorem 4.

Second proof. We can receive these representations from Eqs. (34)–(37) directly.

Now we will prove the boundedness of the reminder function $R(x, \varepsilon)$. This function will satisfy the next equation:

$$\varepsilon R''(x,\varepsilon) + \sqrt{x}R'(x,\varepsilon) - R(x,\varepsilon) = \mu^{3(n+1)}\pi_{3(n+1)}(t) + \varepsilon^{n+1}(h_n(x) - y''_n(x)),$$
$$R(0,\varepsilon) = 0, \ \ R(1,\varepsilon) = 0.$$

Applying to this problem theorem [23, p.117, 82], we obtained

$$|R(x,\varepsilon)| \le \varepsilon^{n+1} C \max_{\substack{0\le x\le 1\\ 0\le t\le \tilde{\mu}}} |\pi_{3(n+1)}(t) + h_n(x) - y''_n(x)|.$$

Therefore, we have $R(x,\varepsilon) = O(\varepsilon^{n+1}), \ \ \varepsilon \to 0, \ x \in [0,1]$.

We prove next.

Theorem 5. The asymptotical expansion of the solution of the problems (27) and (28) and will have the next form

$$y(x) = \sum_{k=0}^{n} \varepsilon^k y_k(x) + \sum_{k=0}^{3(n+1)} \mu^k \pi_k(t) + O(\varepsilon^{n+1}), \ \ \varepsilon \to 0.$$

3. Singularly perturbed differential equations Lighthill type

3.1. The idea of the method of Poincare

Consider the equation

$$My(x) := y''(x) + y(x) - \varepsilon y^3(x) = 0. \tag{39}$$

Unperturbed equation has solutions $y_0(x) = a_1 \cos x + b_1 \sin x$ (where $a_1, \ b_1$ are arbitrary constants) with period 2π. We are looking for the periodic solution of the equation $y(x,\varepsilon)$ with a period of $\omega(\varepsilon) = \omega(0) = 2\pi$.

Note that the operator M transforms Fourier series $\sum_{k=1}^{\infty} a_k \cos kx$ and $\sum_{k=1}^{\infty} a_k \sin kx$ in itself. Poincare's method reduces the existence of periodic solutions of differential equations to the existence of the solution of an algebraic equation.

We will seek a periodic solution of Eq. (39) with the initial condition

$$y(0) = 1, \ \ y'(0) = 0.$$

If we seek the solution in the form

$$y(x) = y_0(x) + \varepsilon y_1(x) + \varepsilon^2 y_2(x) + \dots$$

with the initial conditions

$$y_0(0) = 1,\ \ y_0'(1) = 0,\ y_k(0) = y_k'(1) = 0,\ \ k = 1, 2, \ldots$$

then for $y_s(x),\ s = 0, 1, \ldots$ we have next equations

$$Ly_0 := y''_0(x) + y_0(x) = 0\ \Rightarrow y_0(x) = \cos x$$

$$Ly_1 = \cos^3 x = \frac{3}{4}\cos x + \frac{1}{4}\cos 3x \Rightarrow y_1(x) = \frac{3}{8}x\sin x - \frac{1}{32}\cos 3x + \frac{1}{32}\cos x,$$

Thus, $y(x) = \cos x + \frac{\varepsilon}{8}\left(3x\sin x - \frac{1}{4}\cos 3x + \frac{1}{4}\cos x\right) + \ldots$it is not a uniform expansion of the $y(x)$ on the segment $[-\infty, \infty]$, since the term $\varepsilon x\sin x$ is present here.

If these secular terms do not appear in Eq. (39), it is necessary to make the substitution

$$x = t(1 + \varepsilon\alpha_1 + \varepsilon^2\alpha_2 + \ldots)$$

where the constant α_k should be selected so as not to have secular terms in t.

Thus, the solution of Eq. (39) must be sought in the form

$$\begin{aligned} &y(t) = y_0(t) + \varepsilon y_1(t) + \varepsilon^2 y_2(t) + \ldots \\ &x = t(1 + \varepsilon\alpha_1 + \varepsilon^2\alpha_2 + \ldots) \end{aligned} \tag{40}$$

Then Eq. (39) has the form

$$z''(t) + (1 + \alpha_1\varepsilon + \alpha_2\varepsilon^2 + \ldots)z(t) = \varepsilon(1 + \alpha_1\varepsilon + \alpha_2\varepsilon^2 + \ldots)z^3(t)$$

where $y(w(\varepsilon)t) = z(t)$.

We will seek the 2π periodic solution of this equation in the form

$$z(t) = z_0(t) + \varepsilon z_1(t) + \varepsilon^2 z_2(t) + \ldots$$

Then

$$Lz_0 := z''_0(t) + z_0(t) = 0\ \Rightarrow z_0(t) = \cos t.$$

$$Lz_1(t) = \alpha_1\cos t + \frac{3}{4}\cos t + \frac{1}{4}\cos 3t.$$

The function Z_1(t) will have the periodical solution we take $\alpha_1 = -3/4$. Then $z_1(t) = -\frac{1}{32}\cos 3t$.

Similarly, from equations

$$\alpha z_n(t) = -\alpha_n\cos t + g(\alpha_1, \alpha_2, \ldots, \alpha_{n-1})\cos t + \sum_{m=1}^{2n+1}\beta_n\cos mt$$

α_n and etc. are uniquely determined.

Theorem 6. Equation (39) has a unique $2\pi/\omega$ periodic solution, and it can be represented in the form (40).

3.2. The idea of the Lighthill method

Lighthill in 1949 [67] reported an important generalization of the method of Poincare.

He considered the model equation [67, 82]:

$$(x + \varepsilon y(x))y'(x) + q(x)y(x) = r(x), \quad y(1) = a \tag{41}$$

where $x \in [0, 1] q(x),\ r(x) \in C^{\infty}[0, 1]$.

Lighthill proposed to seek the solution of Eq. (41) in the form

$$\begin{aligned} y(\xi) &= y_0(\xi) + \varepsilon y_1(\xi) + \varepsilon^2 y_2(\xi) + \dots \\ x &= \xi + \varepsilon x_1(\xi) + \varepsilon^2 x_2(\xi) + \dots \end{aligned} \tag{42}$$

It is obvious that Eq. (42) has generalized the Poincare ideas (see, the transformation Eq. (40)).

At first, we consider the example

$$(x + \varepsilon y(x))y'(x) + y(x) = 0, \quad y(1) = b. \tag{43}$$

It has exact solution

$$y(x) = (\sqrt{x^2 + 2b\varepsilon + \varepsilon^2 b^2} - x)/\varepsilon. \tag{44}$$

It is obvious that for $b > 0$, the solution (43) exists on the interval $[0, 1]$ and

$$y(0) = \sqrt{2b + \varepsilon b^2}/\sqrt{\varepsilon}.$$

The solution of Eq. (43) is obtained by the method of small parameter that can be obtained from Eq. (44). For this purpose, we write Eq. (44) in the form

$$y(x) = \frac{x}{\varepsilon}\left(-1 + \sqrt{1 + 2b\frac{\varepsilon}{x} + b^2\left(\frac{\varepsilon}{x}\right)^2}\right)$$

and considering $x^2 > 2\varepsilon b$, this expression can be expanded in powers of ε, and then we have

$$y(x) = \frac{b}{x} + \frac{b^2}{2x}\frac{\varepsilon}{x^2}(x^2 - 1) + \dots + O\left(\frac{1}{x}\left(\frac{\varepsilon}{x^2}\right)^n\right) + \dots \tag{45}$$

The series (45) is uniformly convergent asymptotic series only on the segment $[\varepsilon^{\alpha}, 1],\ 0 < \alpha < 1/2$.

First, we write Eq. (43) in the form

$$(x + \varepsilon y(\xi))y'(\xi) + y(\xi)x'(\xi) = 0 \tag{46}$$

Substituting Eq. (42) into Eq. (46):

$$(\xi + \varepsilon(y_0(\xi) + x_1(\xi)) + \ldots + \varepsilon^n(y_{n-1}(\xi) + x_n(\xi)) + \ldots)(y_0'(\xi) + \varepsilon y_1'(\xi) + \ldots +$$
$$+\varepsilon^n y_n'(\xi) + \ldots) + (y_0(\xi) + \varepsilon y_1'(\xi) + \ldots \varepsilon^n y_n'(\xi) + \ldots)(1 + \varepsilon x_1'(\xi) + \ldots + \varepsilon^n x_n'(\xi) + \ldots) = 0$$

and equating coefficients of the same powers ε,we have

$$\xi y_0'(\xi) + y_0(\xi) = 0 \tag{47}$$

$$\xi y_n'(\xi) + y_n(\xi) + \sum_{i=0}^{n-1}\Big((y_i(\xi) + x_{i+1}(\xi))y_{n-1-i}'(\xi) + y_i(\xi)x_{n-i}'(\xi)\Big) = 0, \quad y_n(1) = 0, \; n = 1, 2, \ldots \tag{48}$$

From Eq. (47), we have

$$y_0(\xi) = b\xi^{-1}.$$

Using Eq. (47), Eq. (48) for $n = 1$ can be written as

$$\xi y_1'(\xi) + y_1(\xi) = (\xi x_1'(\xi) - x_1(\xi) + y_0(\xi))y_0'(\xi) = 0, \quad y_1(1) = 0. \tag{49}$$

If we put $x_1(\xi) = 0$ in Eq. (49), we obtain

$$\xi y_1'(\xi) + y_1(\xi) = -b^2\xi^{-3}, \quad y_1(1) = 0.$$

Hence, solving this equation, we have

$$y_1(\xi) = b^2(2\xi)^{-1} - b^2(2\xi^3)^{-1}.$$

Since differentiation increased singularity of nonsmooth function, we select $x_1(\xi)$ so that the expression in the right side of Eq. (49) is equal to zero, i.e.,

$$\xi x_1'(\xi) - x_1(\xi) + y_0(\xi) = 0, \quad x_1(1) = 0.$$

Hence, we have

$$x_1(\xi) = 2^{-1}b\xi - (2\xi)^{-1}b.$$

Then Eq. (49) takes the form

$$\xi y_1'(\xi) + y_1(\xi) = 0, \quad y_1(1) = 0.$$

Hence, we obtain $y_1(\xi) = 0$.

Now Eq. (48) for $n = 2$ takes the form

$$\xi y_2'(\xi) + y_2(\xi) = (\xi x_2'(\xi) - x_2(\xi))y_0'(\xi) = 0, \quad y_2(1) = 0.$$

Let $x_2(\xi) = 0$, and then $y_1(\xi) = 0$. Further also choose $x_i(\xi) = y_i(\xi) = 0$ $(i = 3, 4, \ldots)$, as they also satisfy the initial conditions. Thus, we have found that

$$y(\xi) = b\xi^{-1} \tag{50}$$

$$x(\xi) = \xi + \frac{b}{2}\left(\xi - \frac{1}{\xi}\right)\varepsilon. \tag{51}$$

Putting in Eq. (51) $x = 0$, we have

$$\eta = \sqrt{b\varepsilon/(2 + b\varepsilon)}. \tag{52}$$

For $b > 0$, the point $x = 0$ is achieved. Moreover, the except in variable ξ from Eq. (50) and to Eq. (51) setting ξ, we obtain the exact solution (44).

Now we will present the main idea of the Lighthill method to Eq. (41) under conditions:$q(x)$, $r(x) \in C^\infty[0, 1]$ and $q_0 = q(0) > 0$. We will write it in the form of

$$(x(\xi) + \varepsilon y(\xi))y'(\xi) = [r(x(\xi)) - q(x(\xi))y(\xi)]x'(\xi), \quad y(1) = y^0. \tag{53}$$

It is obvious that we have one equation for two unknown functions, $y(\xi)$, $x(\xi)$. Now we substitute the series (42) to Eq. (53):

$$\begin{aligned}&\left(\xi + \sum_{k=0}^{\infty}\varepsilon^k(y_k(\xi) + x_k(\xi))\right)\sum_{k=0}^{\infty}\varepsilon^k y_k'(\xi) = \\ &= \left(\sum_{j=0}^{\infty} r_j(\xi)\left(\sum_{k=0}^{\infty} x_k(\xi)\varepsilon^k\right)^j - \sum_{j=0}^{\infty} q_j(\xi)\left(\sum_{k=0}^{\infty} x_k(\xi)\varepsilon^k\right)^j\right)\left(1 + \sum_{k=0}^{\infty} x_k'(\xi)\varepsilon^k\right),\end{aligned}$$

where $q_j = q_j(\xi) = \frac{1}{j!}q^{(j)}(\xi)$, $r_j = r_j(\xi) = \frac{1}{j!}r^{(j)}(\xi)$.

Hence, equating the coefficients of equal powers has ε

$$Lu_0 \equiv \xi y_0'(\xi) + q(\xi)y_0(\xi) = r(\xi), \quad y_0(1) = y^0, \tag{54}$$

$$Ly_1 = [\xi y_0' x_1' - y_0' x_1 - y_0 y_0'] + (r_1 - q_1 y_0)x_1, \quad y_1(1) = 0, \tag{55}$$

$$\begin{aligned}Ly_2 = {} & [\xi y_0' x_2' - (y_0 + x_1)y_1' - (y_1 + x_2)y_0' + ((r_1 - q_1 y_0)x_1 - q y_1)x_1'] + \\ & + \{r_1 x_2 + r_2 x_1^2 - q_1 x_1 y_1 - (q_1 x_2 + q_2 x_1^2)y_0\}, \quad y_2(1) = 0,\end{aligned} \tag{56}$$

…

$$\begin{aligned}Ly_n = {} & [y_0' x_n' - y_0' x_n + f_n(y_0, \ldots, y_{n-1}, x_1, \ldots, x_{n-1}, y_0', \ldots, y_{n-1}', x_1', \ldots, x_{n-1}')] + \\ & + \{g_n(y_0, \ldots, y_{n-1}, x_1, \ldots, x_{n-1})\}, \quad y_n(1) = 0; \; \ldots\end{aligned} \tag{57}$$

where $q = q_0$, $r = r_0$,

$$f_n = -(y_0 + x_1)y'_{n-1} - (y_1 + x_2)y'_{n-2} - \dots - (y_{n-2} + x_{n-1})y'_1 - y_{n-1}y'_0 +$$
$$+(r_1x_1 - qy_1 - q_1x_1y_0)x'_{n-1} + (r_1x_2 + r_2x_1^2 - qy_2 - q_1x_1y_1 - (q_1x_2 + q_2x_1^2)y_0)x'_{n-2} + \dots$$
$$+(r_1x_{n-1} + 2r_2x_1x_{n-2} + 2r_2x_2x_{n-3} + \dots + r_{n-1}x_1^{n-1} - q_1y_1x_{n-2} - (q_1x_{n-1} + 2q_2x_1x_{n-2} + \dots$$
$$+q_{n-1}x_1^{n-1})y'_0)x'_1,$$

$$g_n = r_1x_n + 2r_2x_1x_{n-1} + \dots + r_nx_1^n - q_1x_1y_{n-1} - (q_1x_2 + q_2x_1^2)y_{n-2} - \dots$$
$$-(q_1x_n + 2q_2x_1x_{n-1} + \dots + q_nx_1^n)y_0.$$

In these equations, the coefficient $r(\xi) - q(\xi)y_0(\xi)$ of the derivative $x'_n(\xi)$ $(n = 1, 2, \dots)$was replaced by Eq. (54) on $\xi y'_0(\xi)$.

From Eq. (57) for n = 1,2,…, it follows that if we want to define functions $x_n(\xi)$ $(n = 1, 2, \dots)$ from this differential equations, then we must assume that

$$\xi y'_0(\xi) = r(\xi) - q(\xi)y_0(\xi) \neq 0, \quad \xi \in (0, 1]. \tag{58}$$

And this condition cannot be avoided by applying the Lighthill method to Eq. (41). Condition (58) first appeared in [69], justifying Lighthill method, then in the works Habets [66] and Sibuya, Takahashi [68]. Comstock [65] on the example shows that the condition (58) is not necessary for the existence of solutions on the interval $[0, 1]$. Further assume that the condition (58) holds. Note that the right-handside of Eq. (57) is linear with respect to $x_n(\xi)$, and f_n function depends from $y'_0, \dots, y'_{n-1}, x'_1, \dots, x'_{n-1}$ only.

The solution of Eq. (54) can be written as

$$y_0(\xi) = \xi^{-q_0}g(\xi)(y^0 + \int_1^\xi s^{q_0-1}r(s)g^{-1}(s)ds) := \xi^{-q_0}w(\xi), \tag{59}$$

where $g(\xi) = \exp\left(\int_1^\xi \Big(q_0 - q(s)\Big)s^{-1}ds\right)$.

Let

$$w_0 = y^0 - \int_0^1 s^{q_0-1}r(s)g^{-1}(s)ds \neq 0 \Leftrightarrow w_0 = w(0) \neq 0.$$

Hence, we have

$$y_0(\xi) \sim \xi^{-q_0}w_0, \quad \xi \to 0. \tag{60}$$

Since the differentiation of $y_0(\xi)$ increased of its singularity at the point $\xi = 0$, it is better to choose such that the first brace in Eq. (55) is equal to zero, i.e.,

$$\xi x'_1 = x_1 + y_0, \quad x(1) = 0.$$

Hence, using Eq. (60), we obtain

$$x_1(\xi) = \xi + \xi \int_1^{\xi} s^{-2} y_0(s) ds \sim -\frac{w_0}{1+q_0} \xi^{-q_0}. \tag{61}$$

Then Eq. (55) takes the form

$$Ly_1 = (r_1 - q_1 y_0) x_1 \sim \tilde{a}_1 \xi^{-2q_0},$$

where $\tilde{a}_1$=const. Hence, we have

$$y_1(\xi) \sim a_1 \ \ \xi^{-2q_0} (a_1 = const), \xi \to 0. \tag{62}$$

Now equating to zero the expression in the first brace in the right-hand side of Eq. (56), we have

$$\xi x_2' - x_2 = y_1 + ((y_0 + x_1) y_1' - ((r_1 - q_1 y_0) x_1 - q y_1) x_1')(y_0')^{-1} \sim \tilde{b}_2 \xi^{-2q_0}, \ \tilde{b}_2 = \text{const}.$$

From this, we get

$$x_2(\xi) \tilde{} b_2 \xi^{-2q_0}, \ \ b_2 = const, \ \ \xi \to 0. \tag{63}$$

Now Eq. (56) takes the form

$$Ly_2 = g_2(y_0, y_1, x_1, x_2) \sim \tilde{a}_2 \xi^{-3q_0}, \ \ \tilde{a}_2 = const, \ \ \xi \to 0$$

Solving this equation, we have

$$y_2(\xi) \sim a_2 \xi^{-3q_0}, \ \ a_2 = \text{const}, \ \ \xi \to 0 \tag{64}$$

Next, the method of induction, it is easy to show that

$$x_j(\xi) \sim b_j \xi^{-jq_0}, \ \ \ y_j(\xi) \sim a_j \xi^{-(j+1)q_0}, \ \ j = 1, 2, \ldots. \tag{65}$$

Thus, the series (42) has the asymptotic

$$y(\xi) \sim \xi^{-q_0} (w_0 + a_1 \varepsilon \xi^{-q_0} + \ldots + a_n (\varepsilon \xi^{-q_0})^n + \ldots), \ \ \xi \to 0, \tag{66}$$

$$x \sim \xi - \frac{w_0}{1+q_0} \xi^{-q_0} \varepsilon + b_2 (\varepsilon \xi^{-q_0})^2 + \ldots + b_n (\varepsilon \xi^{-q_0})^n + \ldots \tag{67}$$

From Eq. (67), it follows that the point $x = 0$ corresponds to the root of the equation

$$\eta + \varepsilon x_1(\eta) + \varepsilon^2 x_2(\eta) + \ldots = 0 \tag{68}$$

Moreover, this equation should have a positive root and if the solution of Eq. (41) exists on the interval $(0, 1]$. Solving Eq. (68), we obtain

$$\eta \sim (w_0\varepsilon/1 + q_0)^{1/(1+q_0)}, \quad \varepsilon \to 0. \tag{69}$$

And, under the condition$w_0 > 0$, η_0 will be positive. It is obvious that on the interval $[\xi_0, 1]$ series (42) or (66) and (67) remains asymptotic. Substituting Eq. (69) into Eq. (66), we have

$$y(0) \sim w_0 \left(\frac{w_0 \varepsilon}{1 + q_0} \right)^{-q_0/(1+q_0)}, \quad \varepsilon \to 0.$$

If $w_0 < 0$ the point $x = 0$ does not have the positive root of Eq. (68), so that the solution of Eq. (41) goes to infinity, before reaching the point $x = 0$.

We have the

Theorem 7. Suppose that the conditions (1) $q(x),\ r(x) \in C^\infty[0, 1]$; (2) $q_0 > 0$; (3) $w_0 > 0$; (4) $\xi y_0' \neq 0,\ \xi \in [0, 1]$. Then the solution of problem (41) exists on the interval $[0, 1]$, and it can be represented in the asymptotic series (42), (66) and (67).

Theorem 7 proved by Wasow [69], Sibuya and Takahashi [68] in the case where $q(x),\ r(x)$ are analytic functions on $[0, 1]$; proved by Habets [66] in the case $q(x),\ r(x) \in C^2[0, 1]$. Moreover, instead of the condition (3) Wasow impose a stronger condition: $a >> 1$.

In the proof of Theorem 7, we will not stop because it is held by Majorant method.

From the foregoing, it follows that Wasow condition $y_0'(\xi) \neq 0,\ \xi \in (0, 1]$ is essential in the Lighthill method.

Comment 2. Prytula and later Martin [65] proposed the following variant of the Lighthill method. At first direct expansion determined using by the method of small parameter

$$y(x) = y_0(x) + \varepsilon y_1(x) + \varepsilon^2 y_2(x) + \dots \tag{70}$$

and further at second they will make transformation

$$x = \xi + \varepsilon x_1(\xi) + \varepsilon^2 x_2(\xi) + \dots \tag{71}$$

Here unknowns $x_j(\xi)$ are determined from the condition that function $y_j(\xi)$ was less singular function $y_{j-1}(\xi)$. We show that using the method Prytula or Martin, also cannot avoid Wasow conditions. Really, substituting Eq. (71) into Eq. (70) and expanding in a Taylor series in powers of ε, we have

$$y(\xi) = y_0(\xi) + \varepsilon\{y_1(\xi) + y_0'(\xi)x_1(\xi)\} + O(\varepsilon^2).$$

Hence, to obtain a uniform representation of the solution to the second order by ε, we must to put to zero the expression in the curly brackets, i.e., $x_1(\xi) = -y_1(\xi)/y_0'(\xi)$. Therefore, $y(\xi) = y_0(\xi) + O(\varepsilon^2)$. Hence, it is clear that we must make the condition of Wasow: $y_0'(\xi) \neq 0$ in the method of Prytula or Martin also.

3.3. Uniformization method for a Lighthill model equation

We will consider the problem (41) again [3, 58–60], i.e.,

$$(x+\varepsilon y(x))y'(x)=r(x)-q(x)y(x),\quad y(1)=a, \tag{72}$$

Theorem 8. Suppose that the problem (72) has a parametric representation of the solution $y=y(\xi),\ x=x(\xi)$, where $\xi\in[\eta,1],\ \eta=\eta(\varepsilon)>0$, then the problem (72) is equivalent to the problem

$$\begin{cases}\xi y'(\xi)=r(x(\xi))-q(x(\xi))y(\xi),\ \ y(1)=y^0,\\ \xi x'(\xi)=x(\xi)+\varepsilon y(\xi),\ \ x(1)=1,\quad \xi\in[\eta,1],\end{cases} \tag{73}$$

where $\eta=\eta(\varepsilon)$ is the root equation $x(\eta)=0$ and if the root $\eta=\eta(\varepsilon)>0$ and $x(\xi)+\varepsilon y(\xi)\neq 0$ on the interval $[\eta,1]$.

Proof. Sufficiency. Let the solution of the problem (72) exists and $x(\xi),\ \ y(\xi)$ are a parametric representation of the solution of the problem (72). Then introducing the variable-parameter ξ, we obtain the problem (73).

Necessity. Let it fulfill the conditions of Theorem 8. Then dividing the first equation by second one, we get Eq. (72). Theorem 8 is proved.

Equation (73) on the proposal of the Temple [43], we will call uniformizing equation for the problem (72).

We have the following

Theorem 9. Suppose that the first three conditions of Theorem 8. i.e.,(1) $q(x),\ r(x)\in C^\infty[0,1]$; (2) $q_0>0$; (3) $w_0>0$. Then the solution of problem (72) is represented in the form of an asymptotic series (42) and its solution can be obtained from uniformizing equation (73).

The proof of this theorem is completely analogous to the proof of Theorem 8, even more easily.

Only it remains to show that under the conditions of Theorem 9 we can get an explicit solution $y=y(x,\varepsilon)$. Really, since

$$\widetilde{x}\,\xi-\frac{w_0}{1+q_0}\xi^{-q_0}\varepsilon,\ \xi\to 0.$$

Let

$$F(x,\xi,\varepsilon)=x-\xi+\frac{w_0}{1+q_0}\xi^{-q_0}\varepsilon+O\Big((\varepsilon\xi^{-q_0})^2\Big),\ \ \xi\to 0,\eta=\sqrt[q0+1]{\frac{w_0}{1+q_0}}\varepsilon,\ \varepsilon\to 0.$$

then

$$\frac{\partial F(x,\xi,\varepsilon)}{\partial\xi}|_{\xi=\eta(\varepsilon)}=-1-q_0+O\Big(\varepsilon^{1/(1+q_0)}\Big)\neq 0,\ \ \xi\in[\eta,1].$$

Therefore, by the implicit function theorem, we can express $\xi:\ \xi=\varphi(x,\varepsilon)$.

Then when we put it in first equality (42), we obtain an explicit solution $y = y(x, \varepsilon)$.

Comment 3. Explicit asymptotic solution that this problem obtained in Section 3.4.

Example 43. Uniformized equation is

$$\begin{cases} \xi y'(\xi) = -y(\xi), \quad y(1) = b, \\ \xi x'(\xi) = x(\xi) + \varepsilon y(\xi), \ \ x(1) = 1, \quad \xi \in [\eta, 1], \end{cases}$$

It is easy to integrate this system, and we obtain

$$y(\xi) = b\xi^{-1}\, , x(\xi) = (1 + 2^{-1}b\varepsilon)\xi - (2\xi)^{-1}b\varepsilon,$$

Hence, excluding variable ξ, we have an exact solution (44).

Example 2 [37, 43])

$$(x + \varepsilon y(x))y'(x) + (2 + x)y(x) = 0, \ \ y(1) = e^{-1}.$$

Uniformized equation is

$$\begin{cases} \xi x'(\xi) = x + \varepsilon y(\xi), \quad x(1) = 1, \\ \xi y'(\xi) = -(2 + x(\xi))y(\xi), \ \ y(1) = e^{-1}, \quad \xi \in [\eta, 1], \end{cases} \tag{74}$$

Let

$$\begin{cases} x(\xi) = x_0(\xi) + \varepsilon x_1(\xi) + O(\varepsilon^2), \\ y(\xi) = y_0(\xi) + \varepsilon y_1(\xi) + O(\varepsilon^2), \end{cases} \tag{75}$$

Substituting Eq. (75) into Eq. (74), we have

$$x_0(\xi) = \xi, \ x_1(\xi) = \xi \int_1^{\xi} e^{-s}s^{-4}ds, \ \ y_0(\xi) = e^{-\xi}\xi^{-2}, \ \ y_1(\xi) = -e^{-\xi}\xi^{-2}\int_1^{\xi} e^{-s}s^{-4}ds,$$

Hence if $\xi \to 0$, we obtain

$$x_0(\xi) = \xi, \quad x_1(\xi) = -\frac{1}{3}\xi^{-2} + \ldots, \quad y_0(\xi) = \xi^{-2} + \ldots, \quad y_1(\xi) = -\frac{1}{6}\xi^{-4} + \ldots$$

From the equation $x(\eta) = 0$, we find $\eta: \ \ \eta \tilde{\ } \sqrt[3]{\varepsilon/3}$.

We prove that $x(\xi) + \varepsilon y(\xi) \neq 0$ on the interval $[\eta, 1]$.

Really,

$$x(\xi) + \varepsilon y(\xi) \tilde{\ } \xi + \varepsilon\xi^{-2} \neq 0, \ \ \xi \in [\eta, 1].$$

3.4. It is construction explicit form of the solution of the model Lighthill equation

We will consider the problem [57], i.e., (41) again

$$(x+\varepsilon y(x))y'(x)+q(x)y(x)=r(x),\ \ y(1)=b \tag{76}$$

where b is given constant, $x\in[0,1]$, $y'(x)=dy/dx$. Given functions are subjected to the conditions U: $q(x), r(x)\in C^{(\infty)}[0,1]$.

Here, we consider the case $q_0=-1$; this is done to provide a detailed illustration of the idea of the application of the method. We search for the solution of problem (76) in the form

$$y(x)=\mu^{-1}\pi_{-1}(t)+\sum_{k=0}^{\infty}\Big(\pi_k(t)+u_k(x)\Big)\mu^k, \tag{77}$$

where $t=x/\mu$, $\varepsilon=\mu^2, u_k(x)\in C^{(\infty)}[0,1]$ and $\pi_k(t)\in C^{(\infty)}[0,\mu_0]$, $\mu_0=1/\mu$.

Note that $\pi_k(t)=\pi_k(t,\mu)$, i.e., $\pi_k(t)$ depends also on μ, but this dependence is not indicated.

The initial conditions for the functions $\pi_j(t)$ are taken as

$$\pi_{-1}(1/\mu)=b\mu, \quad b=u^0-\sum_{k=0}^{\infty}\mu^k u_k(1), \quad \pi_k(\mu_0)=0, \quad k=0,1,\dots \tag{78}$$

Substituting Eq. (77) into Eq. (76), we obtain to determine the functions $\pi_k(t)$, $k=-1,0,1,\dots,$ $u_n(x)$, $n=0,1,\dots,$

we have the following equations:

$$\Big(t+\pi_{-1}(t)\Big)\pi'_{-1}(t)=q(\mu\ t)\pi_{-1}(t), \quad \pi_{-1}(\mu_0)=b\mu, \tag{79.-1}$$

$$Lu_0(x):=xu'_0(x)-q(x)u_0(x)=r(x), \quad u_0(x)\in C^{(\infty)}[0,1] \tag{80.0}$$

$$D\pi_0(t):=\Big(t+\pi_{-1}(t)\Big)\pi'_0(t)+\Big(\pi'_{-1}(t)-q(\mu\ t)\Big)\pi_0(t)=-u_0(t\mu)\pi'_{-1}(t), \quad \pi_0(\mu_0)=0 \tag{79.0}$$

$$Lu_1(x)=0, \quad u_1(x)\in C^{(\infty)}[0,1], \tag{80.1}$$

$$D\pi_1(t)=-u_0(t\mu)\pi'_0(t)+\pi_0(t)\pi'_0(t)-u_1(t\mu)\pi'_{-1}(t), \quad \pi_1(\mu_0)=0 \tag{79.1}$$

$$Lu_2(x):=-u_0(x)u'_0(x), \quad u_2(x)\in C^{(\infty)}[0,1] \tag{80.2}$$

$$D\pi_2(t):=-u_0(t\mu)\pi'_{-1}(t)-\pi_0(t)\pi'_1(t)-u_1(t\mu)\pi'_0(t)-\pi_1(t)\pi'_0(t)-u_2(t\mu)\pi'_{-1}(t),\ \pi_2(\mu_0)=0 \tag{79.2}$$

$$Lu_3(x):=-u_0(x)u'_1(x)-u'_0(x)u_1(x), \quad u_3(x)\in C^{(\infty)}[0,1], \tag{80.3}$$

$$D\pi_3(t)=\sum_{\substack{i+j=2\\ i\geq 0,\, j\geq -2}} u_i(\mu\ t)\pi_i^{j\prime}(t)+\sum_{\substack{i+j=2\\ i,j\geq 0}}\pi_i(t)\pi_i^{j\prime}(t), \quad \pi_3(\mu_0)=0, \tag{79.3}$$

We solve these problems successively. We write problem (79.−1) as

$$tz'(t) - q(\mu t)z(t) = -z(t)z'(t), \quad z(\mu_0) = b\mu,$$

where

$$z = \pi_{-1}(t), \quad \mu_0 = \mu^{-1}.$$

The fundamental solution of the homogeneous equation corresponding to this equation is of the form

$$z^0(t) = \exp\left\{\int_{\mu_0}^{t} q(\mu s)\frac{ds}{s}\right\} = \exp\left\{\int_{\mu_0}^{t}\Big(q(\mu s)+1\Big)\frac{ds}{s} - \int_{\mu_0}^{t}\frac{ds}{s}\right\} = \frac{p(t,\mu)}{\mu t},$$

where

$$p(t,\mu) = \exp\left\{\int_{\mu_0}^{t}\Big(q(\mu s)+1\Big)\frac{ds}{s}\right\}.$$

Using the expression for $z^0(t)$, the solution of the inhomogeneous equation for $z(t)$ can be written as

$$z(t) = \frac{p(t,\mu)}{\mu t}\left[z(\mu_0) + \mu\int_{\mu_0}^{t} p^{-1}(s,\mu)z(s)z'(s)ds\right],$$

Or $tz(t) = p(t,\mu)b - p(t,\mu)\int_{\mu_0}^{t} p^{-1}(s,\mu)z(s)z'(s)ds.$

After integrating by parts, we reduce the last expression to the following equation:

$$tz(t) = p(t,\mu)b - \frac{z^2(t)}{2} + p(t,\mu)\frac{b^2\mu^2}{2} + \frac{p(t,\mu)}{2}\int_{\mu_0}^{t}\frac{1+q(\mu s)}{s}p^{-1}(s,\mu)z^2(s)ds$$

or

$$z^2(t) + 2tz(t) - p(t,\mu)b_0 = p(t,\mu)\int_{\mu_0}^{t}\phi(s,\mu)p^{-1}(s,\mu)z^2(s)ds := p(t,\mu)T(t,z^2) \tag{81}$$

where $\varphi(s,\mu) = (1+q(\mu s))/s, \ \ b_0 = 2b + b^2\mu^2.$

Let $b_0 > 0$. Let us introduce the notation $z_0(t) = -t + \sqrt{t^2 + b_0 p(t,\mu)}$. This function satisfies the inequality $0 < z_0(t) \le Mt^{-1}$ $(t > 0)$ and is a strictly decreasing bounded function on the closed interval $[0, \mu_0]$. Here and elsewhere, all constants independent of the small parameter μ are denoted by M. Let S_μ be the set of functions $z(t)$ satisfying the condition

$\|z - z_0\| \le M\mu,$ where $\|z\| = \max\limits_{0\le t\le \mu_0}|z(t)|,$

Theorem 10. *If* $b_0 > 0$, *then there exists a unique constraint of the solution of problem* (79.-1) *from the set* S_μ.

Proof. Equation (81) is equivalent to the equation $z = F[t, z]$, where

$$F[t, z] = -t + \sqrt{t^2 + bp(t, \mu) + p(t, \mu)T(t, z^2)}.$$

Suppose that $\|\varphi(t, \mu)\| \leq M\mu, \quad 0 < m \leq p(t, \mu) \leq M, \quad \|p^{-1}(t)\| \leq M$. First, let us estimate $T(t, z^2)$ on the set S_μ. We have

$$|T(t, z^2)| \leq \int_t^{\mu_0} |\varphi(s, \mu)||p^{-1}(s, \mu)||z(s)|^2 ds \leq M\mu \int_t^{\mu_0} |z(s)|^2 ds \leq M\mu \int_0^{\mu_0} |z(s)|^2 ds \leq$$
$$\leq M\mu \int_0^1 |z(s)|^2 ds + M\mu \int_1^{\mu_0} |z(s)|^2 ds \leq M\mu.$$

Here, we have used the triangle inequality

$$|z(t)| \leq |z(t) - z_0(t)| + |z_0(t)|,$$

as well as the inequality

$$|z_0(t)| \leq Mt^{-1} \quad (t > 0).$$

The Fréchet derivative of the operator $F(t, z)$ with respect to z at the point $z_0(t)$ is a linear operator:

$$F'_z(t, z_0)h = -p(t, \mu) \int_t^{\mu_0} \varphi(s, \mu)p^{-1}(s, \mu)z_0(s)h(s) \frac{ds}{\sqrt{t^2 + p(t, \mu)\left(b + T(t, z^2)\right)}},$$

where $h(t)$ is a continuous function on the closed interval $[0, \mu_0]$. Note that, in view of $T(t, z_0^2) = O(\mu)$, the denominator of this expression is strictly positive on the closed interval $[0, \mu_0]$. For $F'_z(t, z_0)$, we can obtain the estimate $\|F_z(t, z_0)\| \leq M\mu \ln \mu^{-1}$ in the same way as the estimate for $T(t, z^2)$. Hence, in turn, it follows from the Lagrange inequality that the operator is a contraction operator in the set S_μ. Therefore, by the fixed-point principle, Eq. (81) has a unique solution from the class S_μ. The theorem is proved.

Corollary. *The following inequalities hold*:

1. $z(t) = \pi_{-1}(t) \geq M > 0$ *for all* $t \in [0, \mu_0]$;

2. $\pi_{-1}(t) \leq Mt^{-1} \quad (t > 0)$.

The other function $\pi_j(t), \; u_j(x), \; j = 0, 1, 2, \ldots$ is determined from the inhomogeneous linear equations; therefore, the following lemmas are needed.

Lemma 9. *For any function* $f(x) \in C^{(\infty)}[0, 1]$, *the equation* $L\xi = f(x)$ *has a unique bounded solution* $\xi(x) \in C^{(\infty)}[0, 1]$ *expressible as*

$$\xi(x) = Q(x)\int_0^x Q^{-1}(s)f(s)\frac{ds}{x}, Q(x) = \exp\left\{\int_1^x \left(q(s)+1\right)\frac{ds}{s}\right\}.$$

Proof. The proof follows from the fact that the general solution of the equation under consideration is expressed as

$$\xi(x) = Q(x)x^{-1}[\xi(1) + \int_1^x Q^{-1}(s)f(s)ds].$$

If we choose

$$\xi(1) = \int_0^1 Q^{-1}(s)f(s)ds.$$

then we obtain the required result.

This lemma implies that all the functions $u_k(x),\ k = 0, 1, \ldots$ are uniquely determined and belong to the class $C^\infty[0, 1]$.

Lemma 10. *The problem*

$$\left(t + \pi_{-1}(t)\right)\eta'(t) + \left(\pi'_{-1}(t) - q(\mu t)\right)\eta(t) = k(t), \quad \eta(\mu_0) = 0, \tag{82}$$

where the function $k(t)$ belongs to $C^\infty[0, 1]$ is continuous and bounded, and if $|k(t)| \leq Mt^{-2},\ \ t \to \infty$, has a unique uniformly bounded solution$\eta(t) = \eta(t, \mu)$ on the closed interval $t \in [0, \mu_0]$for a small μ.

Proof. The fundamental solution of the homogeneous equation (82) is of the form

$$\Phi(t) = \frac{(1+\mu^2 b)g(t,\mu)}{\mu\left(t + \pi_{-1}(t)\right)}, \quad g(t,\mu) = \exp\left\{-\int_t^{\mu_0}\left(1 + q(\mu s)\right)\frac{ds}{s + \pi_{-1}(s)}\right\}.$$

Obviously, $\|g(t, \mu)\| \leq M$ and $g^{-1}(t, \mu) \leq M$ for $t \in [0, \mu_0]$and μaresmall. The solution of problem (82) can be expressed as

$$\eta(t) = \frac{g(t,\mu)}{t + \pi_{-1}(t)}\int_{\mu_0}^t g^{-1}(s,\mu)k(s)ds. \tag{83}$$

The estimate of the integral term in Eq. (83) shows that it is bounded by the constant M. Hence, it also follows that $|\eta(t)| \leq Mt^{-1}$ $(t > 0)$. The solution of problem (79.0) is defined by the integral Eq. (83), where

$$k(t) = -u_0(t\mu)\pi_{-1}(t) = -u_0(t\mu)q(\mu t)\frac{\pi_{-1}(t)}{t + \pi_{-1}(t)},$$

satisfies the assumptions of the lemma. Therefore, the function $\pi_0(t)$ is bounded on $[0, \mu_0]$. The boundedness of the other functions $\pi_k(t),\ k = 1, 2, \ldots$ is proved in a similar way, because the right-hand sides of the equations defining these functions satisfy the assumptions of Lemma 10. The estimate of the asymptotic behavior of the series (77) is also carried out using Lemma 10.

Let us introduce the notation

$$y(x) = \mu^{-1}\pi_{-1}(t) + \sum_{k=0}^{n}\mu^{k}\Big(\pi_k(t) + u_k(x)\Big) + \mu^{n+1}R_{n+1}(x,\mu). \tag{84}$$

The following statement holds.

Theorem 11. *Let* $b_0 > 0$ (*for this, it suffices that the condition* $b_0 := b - y_0(1) > 0$*holds*). *Then the solution of problem* (76) *exists on the closed interval* $[0,1]$*and its asymptotics can be expressed as Eq.* (84) and$|R_{n+1}(x,\mu)| \le M$ *for all* $x \in [0,1]$.

Example. Consider the equation

$$\Big(x + \varepsilon\, y(x)\Big)y'(x) + y(x) = 1, \quad y(1) = b,$$

This equation is integrated exactly

$$y(x) = \varepsilon^{-1}\left[-x + \sqrt{x^2 + 2b_0\varepsilon + \varepsilon^2\Big(y^{(0)}\Big)^2 + 2\varepsilon x}\right],$$

where $b_0 = b - 1$. If $b_0 > 0$, then the solution of problem (1) exists on the closed interval $[0,1]$, which is confirmed by Theorem 11. The equation for $\pi_{-1}(t)$ is of the form

$$\Big(t + \pi_{-1}(t)\Big)\pi'_{-1}(t) + \pi_{-1}(t) = 0, \quad \pi_{-1}(\mu_0) = b\mu.$$

The solution of this problem can be expressed as

$$\pi_{-1}(t) = -t + \sqrt{t^2 + 2b + b^2\mu^2}.$$

The equation for $u0(x)$ has the solution $y_0(x) = 1 \in C^\infty[0,1]$. Further,

$$\pi_0(t) = \frac{-\pi_{-1}(t) + b\mu}{t + \pi_{-1}(t)}, \quad u_k(x) = 0, \quad k = 1, 2, \ldots,$$

where $b = b_0$. The asymptotics of the solutions of problem (76) can be expressed as

$y(x) = \mu^{-1}\pi_{-1}(x/\mu) + 1 + \pi_0(x/\mu) + o(\mu)$ for all $x \in [0,1], \quad \mu \to 0.$

4. Lagerstrom model problem

The problem [32]

$$v''(r) + \frac{k}{r}v'(r) + v(r)v'(r) = \beta[v'(r)]^2, \;\; v(\varepsilon) = 0, \;\; v(\infty) = 1, \tag{85}$$

where $0 < \beta$ is constant, $k \in N$.

It has been proposed as a model for Lagerstrom Navier-Stokes equations at low Reynolds numbers. It can be interpreted as a problem of distribution of a stationary temperature $v(r)$.

The first two terms in Eq. (1) is $(k + 1)$ dimensional Laplacian depending only on the radius, and the other two members—some nonlinear heat loss.

It turns out that not only the asymptotic solution but also convergent solutions of Eq. (1) can be easily constructed by a fictitious parameter [70]. The basic idea of this method is as follows. The initial problem is entered fictitious parameter $\lambda \in [0, 1]$ with the following properties:

1. $\lambda = 0$, the solution of the equation satisfies all initial and boundary conditions;

2. The solution of the problem can be expanded in integral powers of the parameter λ for all $\lambda \in [0, 1]$.

It is convenient in Eq. (85) to make setting $r = \varepsilon x, \; v = 1 - u$, then

$$u''(x) + (kx^{-1} + \varepsilon)u'(x) - \lambda\varepsilon u(x)u'(x) = [u'(x)]^2, \;\; u(1) = 1, \;\; u(\infty) = 0. \tag{86}$$

We have the following

Theorem 12. For small $\varepsilon > 0$, the solution of problem (86) can be represented in the form of absolutely and uniformly convergent series

$$u(x) = u_0(x, \varepsilon) + v_k(\varepsilon)u_1(x, \varepsilon) + \ldots + v_k^n(\varepsilon)u_n(x, \varepsilon) + \ldots,$$

for the sufficiently small parameter ε, where

$$v_1(\varepsilon) \sim \left(\ln\frac{1}{\varepsilon}\right)^{-1}, \quad v_2 \sim \varepsilon\ln\frac{1}{\varepsilon}, \quad v_k \sim \frac{k-1}{k-2}\,\varepsilon(j > 2) \;\; ; u_k(x, \varepsilon) = O(1), \forall x \in [1, \infty)$$

Note that the function $u_n(x, \varepsilon)$ also depends on k, but for simplicity, this dependence is not specified.

Proof. We introduce Eq. (86) parameter λ, i.e., consider the problem

$$u''(x) + (kx^{-1} + \varepsilon)u'(x) - \beta[u'(x)]^2 = \lambda\varepsilon u(x)u'(x), \;\; u(1) = 1, \;\; u(\infty) = 0 \tag{87}$$

Here, we will prove this Theorem 12 in the case $\beta = 0$ only for simplicity.

Setting $\lambda = 0$ in Eq. (87), we have

$$u''_0 + (x^{-1}k + \varepsilon)u'_0 = 0, \quad u_0(1) = 1, \quad u_0(\infty) = 0. \tag{88}$$

It has a unique solution

$$u_0 = X(x, \varepsilon) := 1 - X_1(X, \varepsilon), \quad X_1 = C_0 \int_1^x s^{-k} e^{-\varepsilon s} ds, \quad C_0^{-1} = \int_1^\infty s^{-k} e^{-\varepsilon s} ds.$$

Therefore, Eq. (88) with zero boundary conditions is the Green's function

$$K(x, s, \varepsilon) = \begin{cases} C_0^{-1} X_1(x, \varepsilon) X(s, \varepsilon), & 1 \le x \le s, \\ C_0^{-1} X_1(s, \varepsilon) X(x, \varepsilon), & s < x < \infty. \end{cases}$$

Hence, the problem (87) is reduced to the system of integral equations

$$\begin{aligned} u(x) &= X(x, \varepsilon) + \lambda\varepsilon \int_1^\infty G(x, s, \varepsilon) u(s) u'(s) ds, \\ u'(x) &= X'(x, \varepsilon) + \lambda\varepsilon \int_1^\infty G_x(x, s, \varepsilon) u(s) u'(s) ds, \end{aligned} \tag{89}$$

where

$$G(x, s, \varepsilon) = \begin{cases} X_1(x, \varepsilon) X(s, \varepsilon) / X'(s, \varepsilon), & 1 \le x \le s, \\ X_1(s, \varepsilon) X(x, \varepsilon) / X'(s, \varepsilon), & s < x < \infty. \end{cases}$$

In Eq. (89), we make the substitution $u = X(x, \varepsilon)\varphi(x), \quad u' = X'(x, \varepsilon)\psi(x)$, and then we have

$$\begin{aligned} \varphi(x) &= 1 + \lambda\varepsilon \int_1^\infty Q_1(x, s, \varepsilon)\varphi(s)\psi(s) ds := 1 + \lambda\varepsilon Q_1(\varphi\psi), \\ \psi(x) &= 1 + \lambda\varepsilon \int_1^\infty Q_2(x, s, \varepsilon)\varphi(s)\psi(s) ds := 1 + \lambda\varepsilon Q_2(\lambda\psi), \end{aligned} \tag{90}$$

where

$$\begin{aligned} Q_1 &= X^{-1}(x, \varepsilon) G(x, s, \varepsilon) X(s, \varepsilon) X'(s, \varepsilon), \\ Q_2 &= X_x^{-1}(x, \varepsilon) G_x(x, s, \varepsilon) X(s, \varepsilon) X'(s, \varepsilon). \end{aligned}$$

To prove the theorem, we need next

Lemma 11. The following estimate holds

$$\int_1^\infty |Q_j(x, s, \varepsilon)| ds \le \int_1^\infty X(s, \varepsilon) ds \qquad (j = 1, 2) \tag{91}$$

Given that, we have $0 \le X_1(x, \varepsilon) \le 1, \quad |X'(x, \varepsilon)| = X'(x, \varepsilon), \quad X'(x, \varepsilon) \le 0, \quad x \in [1, \infty)$, we have

$$\begin{aligned} &\int_1^\infty |Q_1(x, s, \varepsilon)| ds \le \int_1^x \frac{X_1(s, \varepsilon)}{X'_1(s, \varepsilon)} |X'(s, \varepsilon)| X(s, \varepsilon) ds + \\ &+ \int_x^\infty X^{-1}(x, \varepsilon) \frac{X^2(s, \varepsilon)|X'(s, \varepsilon)|}{X'_1(s, \varepsilon)} ds \le \int_1^x X(s, \varepsilon) ds + \int_x^\infty X(s, \varepsilon) ds = \int_1^\infty X(s, \varepsilon) ds. \end{aligned}$$

Inequality Eq. (91) for $j = 2$ is proved similarly.

Further, by integrating by parts, we have

$$\int_1^\infty X(s,\varepsilon)ds = -1 + C_0\int_1^\infty s^{-k+1}e^{-\varepsilon s}ds \le \int_1^\infty s^{-k+1}e^{-\varepsilon s}ds/\int_1^\infty s^{-k}e^{-\varepsilon s}ds := \frac{v_k(\varepsilon)}{\varepsilon}.$$

Consequently,

$$\varepsilon\int_1^\infty X(x,\varepsilon)ds \le v_k(\varepsilon). \tag{92}$$

It is from integral expressing of $v_k(\varepsilon)$ we can obtain the asymptotic behavior such as indicated in the theorem.

With the solution of Eq. (90), we can expand in series

$$\begin{aligned}\varphi(x) &= 1 + \varphi_1(x,\varepsilon)\lambda + \varphi_2(x,\varepsilon)\lambda^2 + \dots,\\ \Psi(x) &= 1 + \Psi_1(x,\varepsilon)\lambda + \Psi_2(x,\varepsilon)\lambda^2 + \dots.\end{aligned}$$

The coefficients of this series are uniquely determined from the equations $\varphi_0 = \Psi_0 = 1, \quad \varphi_1 = \varepsilon Q_1(1), \quad \Psi_1 = Q_2(1),$
$\varphi_n = \varepsilon Q_1(\varphi_{n-1}) + \varepsilon Q_1(\Psi_{n-1}) + \varepsilon Q_1(\varphi_1\Psi_{n-2}) + \dots + \varepsilon Q_1(\varphi_{n-2}\Psi_1),$
$\Psi_n = \varepsilon Q_2(\varphi_{n-1}) + \varepsilon Q_2(\Psi_{n-1}) + \varepsilon Q_2(\varphi_1\Psi_{n-2}) + \dots + \varepsilon Q_2(\varphi_{n-2}\Psi_1), \quad (n = 2, 3, \dots).$

Let $z = \sup\limits_{1\le x<\infty}\{|\varphi(x)|, |\Psi(x)|\}$, then by using Eq. (92) we have a Majorant equation: $z = 1 + \lambda v_k(\varepsilon)z^2$. The solution of this equation can be expanded in powers λ the under condition $8v_k(\varepsilon) \le 1$ for all $\lambda \in [0,1]$.

If we call $u_n(x,\varepsilon) = \frac{X(x,\varepsilon)\varphi_n(x,\varepsilon)}{v_k^n(\varepsilon)}$, we get the proof of the theorem.

Author details

Keldibay Alymkulov* and Dilmurat Adbillajanovich Tursunov

*Address all correspondence to: keldibay@mail.ru

Institute of the Fundamental and Applied Researches, Osh State University, Osh, Kyrgyzstan

References

[1] Duboshin, G.N. Celestial Mechanics: Analytical and Qualitative Methods. Moscow, Nauka. 1964. [In Russian].

[2] Alymkulov, K. To the theory relaxation oscillation solution of Van der Pole equation. Izvestia AN KyrgSSR. 1985. No. 2, pp. 14-17. [In Russian]

[3] Alymkulov, K. Perturbed differential equations with singularly points and same bifurcations problems. Ilim, Bishkek, 1992. 138 p. [In Russian]

[4] Alymkulov, K., Zulpukarov, A.Z. Uniformly asymptotic of the solution of the boundary value problem for singularly perturbed equation of the second order with weakly singularity. DAN Russian. 2004, Vol. 398, No. 5. pp. 1-4. [In Russian]

[5] Alymkulov, K., Asylbekov, T. Generalization of the boundary Leary function for construction of asymptotic solution singularly perturbed equation with turning point. Vestnik KNU. Bishkek. 2011. pp. 43-45. [In Russian]

[6] Alymkulov, K., Asylbekov, T.D., Dolbeeva, S.F. Generalization of the boundary function method for solving boundary-value problems for bisingularly perturbed second-order differential equations. Math. Notes. 2013, Vol. 94. No. 3-4, pp. 451-454.

[7] Alymkulov, K. Method of boundary layer function to solve the boundary value problem for a singularly perturbed differential equation of the order two with a turning point. Universal J. Appl. Math. 2014, Vol. 2, No. 3, pp. 119-124.

[8] Alymkulov, K., Tursunov, D.A. A method for constructing asymptotic expansions of bisingularly perturbed problems. Russian Math. 2016, Vol. 60, No. 12, pp. 1-8.

[9] Alymkulov, K., Tursunov, D.A., Azimov, B.A. Generalized method of boundary layer function for bisingularly perturbed differential Cole equation. FJMS. Pushpa Publishing House, Allahabad, India, 2017, Vol. 101, No. 3, pp. 507-516.

[10] Steinrück, H. Asymptotic Methods in Fluid Mechanics: Survey and Recent Advances. Springer-Verlag, Wien, 2010.

[11] Carrier, G.P. Boundary layer problems in applied mathematics. Comm. Appl. Math. 1954, Vol. 7, pp. 11-17.

[12] Chang, K., Howes, F.A. Nonlinear Singular Perturbation Phenomena: Theory and Applications. Springer-verlag, Berlin, 1984.

[13] Cole, J.D. Perturbation Methods in Applied Mathematics. Blaisdell Publishing Company, New York, 1968.

[14] Cousteix, J., Mauss, J. Asymptotic Analysis and Boundary Layers. Springer-Verlag, Berlin Heidelberg, 2007.

[15] Eckhaus, W. Asymptotic Analysis of Singular Perturbations. North Holland, Amsterdam, 287 p, 1979.

[16] Fruchard, A., Schafke, R. Composite Asymptotic Expansions. Lecture Notes in Mathematics. Vol. 2066. Springer, Berlin, Heidelberg, 2013.

[17] Georgescu, A. Asymptotic Treatment of Differential Equations. Chapman & Hall, New York, 1995.

[18] Hastings, S.P., Mcleod, J.B. Classical Methods in Ordinary Differential Equations, with Applications to Boundary Value Problems, AMS, Providence, Rhode Island, 2012.

[19] Hinch, E.J. Perturbation Methods. Cambridge University Press, Cambridge, England, 1981.

[20] Holmes, M.H. Introduction to Perturbation Methods. Springer-Verlag, New York, 1995.

[21] Hsieh, P-F., Sibuya, Y. Basic Theory of Ordinary Differential Equations. Springer, New York, 1999.

[22] Il'in, A.M. Matching of Asymptotic Expansions of Solutions of Boundary Value Problems. AMS, Providence, Rhode Island, 1992.

[23] Il'in, A.M., Danilin, A.R. Asymptotic Methods in Analysis. Fizmatlit, Moscow, 2009. [In Russian].

[24] Imanaliev, M., Asymptotic Methods in the Theory of Singularly Perturbed Integrodifferential Systems. Ilim, Bishkek, 1972. [In Russian].

[25] de Jager, E.M., Jiang, F. The Theory of Singular Perturbations, North-Holland Series in Applied Mathematics and Mechanics. Vol. 42, North-Holland Publication, Amsterdam, 1996.

[26] John, N.C. Singular Perturbation in the Physical Sciences. AMS, University of California, Berkeley, CA, 2015.

[27] Johnson, R.S. Singular Perturbation Theory. Springer, New York, 2004.

[28] Kevorkian, J., Cole, J.D. Perturbation Methods in Applied Mathematics. Springer-Verlag, New York, 1981.

[29] Kevorkian, J., Cole, J.D. Multiple Scale and Singular Perturbations Method. Springer, New York, 1996.

[30] Kreiss, H.-O., Parter, S.V. Remarks on singular perturbation with turning points. SIAM J. Math. Anal. 1974, Vol. 5, pp. 230-51.

[31] Kuzmina, R.P. Asymptotic Methods for Ordinary Differential Equations. Springer, New York, 2000.

[32] Lagerstrom, P.A. Matched Asymptotic Expansions. Ideas and Techniques. Springer-Verlag, New York, 1988.

[33] Lomov, S.A. Introduction to the General Theory of Singular Perturbations. AMS, Providence, Rhode Island, 1992.

[34] Mischenko, E.F., Rozov, N.Ch. Differential Equations with Small Parameters and Relaxation Oscillations. Plenum Press, New York, London, 1980.

[35] Murdock, J.A. Perturbations: Theory and Methods (Classics in Applied Mathematics). John Willey & Sons, New York, 1991.

[36] Nagumo, M. Collected Paper. Springer-Verlag, Tokyo, 1993

[37] Nayfeh, A.H. Perturbation Methods. John Wiley & Sons , Chichester, New York, 2008.

[38] O'Malley, R.E., Jr. Introduction to Singular Perturbation. Academic Press, New York, 1974.

[39] O'Malley, R.E. Singular Perturbation Methods for Ordinary Differential Equations. Springer, New York, 1991.

[40] Sirovich, L. Techniques of Asymptotic Analysis. Springer-Verlag, New York, 1971.

[41] Skinner, L.A. Singular Perturbation Theory. Springer, New York, 2011.

[42] Smit, D.R. Singularl-Perturbation Theory: An Introduction with Applications. Cambridge University Press, Cambridge, 1985.

[43] Temple, G. Linearization and delinearization. Proc. Inter. Congr. Math., Edinburgh, pp. 233-247, 1958.

[44] Trenogin, V.A. The development and applications of the asymptotic method of Lyusternik and Vishik. Uspekhi Mat. Nauk. 1970, Vol. 25, No. 4, pp. 123-156 [Russian Math. Surveys 25 (4), 119-156 (1970)].

[45] Tursunov, D.A. Asymptotic expansion for a solution of an ordinary second-order differential equation with three turning points, Tr. IMM UrO RAN, 2016, Vol. 22, No. 1, pp. 271-281. [In Russian]

[46] Tursunov, D.A. Asymptotic expansion of the solution of a singularly perturbed ordinary second-order differential equation with two turning points. Tomsk State University Journal of Mathematics and Mechanics. 2012, Vol. 21, No. 1, pp. 34-40. [In Russian]

[47] Tursunov, D.A. The asymptotic solution of the bisingular Robin problem, Sib. Èlektron. Mat. Izv., 2017, Vol. 14, pp. 10-21. [In Russian]

[48] Verhulst, F. Methods and Applications of Singular Perturbations. Boundary Layers and Multiple Timescale Dynamics. Springer, New York, 2005.

[49] Van Dyke, M. Perturbation Methods in Fluid Dynamics. Academic Press, New York, 1964.

[50] Vasil'eva, A.B., Butuzov, V.F. Asymptotic Expansions of the Solutions of Singular Perturbed Equations. Nauka, Moscow, 1973. [In Russian].

[51] Vasil'eva, A.B., Butuzov, V.F., Kalachev, L.V. The Boundary Function Method for Singular Perturbed Problems. SIAM, Cambridge University Press, Cambridge, 1987.

[52] Visik, M.I., Lyusternik, L.A. Regular degeneration and boundary layer for linear differential equations with small parameter. Uspehi Mat. Nauk. 1957, Vol. 5, No. 77, pp. 3-122.

[53] Wasow, W.A. Linear Turning Point Theory. Springer, Berlin, 1985.

[54] Wasow, W. Asymptotic Expansions for Ordinary Differential Equations. Dover Publication Inc., New York, 1987.

[55] Watts, A.M. A singular perturbation problem with a turning point. Bull. Australian Math. Soc. 1971, Vol. 5, pp. 61-73.

[56] Zauderer, E. Partial Differential Equations of Applied Mathematics. John Willey & Sons, Inc., New York, 1989.

[57] Alymkulov, K., Khalmatov, A.A. A boundary function method for solving the model Lighthill equation with a regular singular point. Math. Notes. 2012. Vol. 92, No. 6, pp. 117-121.

[58] Alymkulov, K. The method of small parameter and justification of Lighthill method. Izvestia AN KyrgSSR. 1979, No. 6, pp. 8-11. [In Russian]

[59] Alymkulov, K. The method of uniformization and justification of Lighthill method. Izvestia AN KyrgSSR. 1981, No. 1. pp. 35-38. [In Russian]

[60] Alymkulov, K. Development the method and justification of Lighthill method. Izvestia AN KyrgSSR. 1985, No. 1. pp. 13-17. [In Russian]

[61] Alymkulov, K. Generation of a periodic solution from a loop of a saddle-point separatrix in singularly perturbed systems, DAN SSSR, 1987, Vol. 295, No. 5, pp. 1033-1036. [In Russian]

[62] Alymkulov, K., Zheentaeva, Zh.K. Method of structural Matching the Solution to the Lighthill model equation with a regular singular point. Doklady Math. Sci. 2004, Vol. 398, No. 6, pp. 1-4. [In Russian]

[63] Alymkulov, K. Analog of the method of boundary layer function for the solution of the Lighthill's model equation with the regular singular point. Am. J. Math. Stat. 2013, Vol. 3, No. 1, pp. 53-61.

[64] Alymkulov, K., Matanova, K.B., Khalmatov, A.A. About new statement and about new method of Cauchy problem for singular perturbed differential equation of the type of Lighthill. Int. J. Sci. Innovative Math. Res. (IJSIMR). 2015, Vol. 3, pp. 54 -64.

[65] Comstok, C. The Poincare-Lighthill perturbation technique and its generalizations. SIAM Review. 1972, Vol. 14, No. 3, pp. 433-443.

[66] Habets, P. On the method of strained coordinates. Lect. Notes Math. 1976, Vol. 564, No. 1, pp. 152-162.

[67] Lighthill, M.J. A technique for rendering approximate solution to physical problems uniformly valid. Phil. Mag. 1949, Vol. 40, No. 7, pp. 1179-1201.

[68] Sibuya, Y., Takahasi, K.J. On the differential equation. Func. Eqs. 1955. Vol. 9, No. 1-3, pp. 71-81.

[69] Wasow, W.A. On the convergence of an approximation method of M.J. Lighthill. J. Rat. Mech. Anal. 1955, Vol. 40, pp. 751-767.

[70] Alymkulov, K., Tolubaev, J. Solution of the Lagerstrom model problem. Math. Note 1994. Vol. 56, No. 4, pp. 3-8.

[71] Alynkulov, K., Omuraliev, M.K. Method of structural matching and its application to Lagerstrom's model equation. Int. J. Inn. Sci. Math. 2015, Vol. 3, pp. 81-88.

[72] Bush, W.B. On the Lagerstrom mathematical model for viscous flow at low Reynolds number. SIAM J. Appl. Math. 1971, Vol. 20, pp. 279-187.

[73] Cohen, D.S., Fokas, A., Lagerstrom, P.A. Proof of some asymptotic results for a model equation for low Reynolds number flow. SIAM J. Apll. Math. 1978, Vol. 35, No. 1, pp. 187-207.

[74] Hunter, C., Tajdari, M., Boyer, S.D. On the Lagerstrom model of slow incompressible viscous flow numbers. SIAM. J.Appl. Math. 1990, Vol. 50, No. 1, pp.48-63.

[75] Popović, N., Szmolyan, P.A. Geometric analysis of the Lagerstrom model problem. J. Differ. Equ. May 20, 2004, Vol. 199, No. 2, pp. 290-325.

[76] Popović, N., Szmolyan, P.A. Rigorous asymptotic expansions for Lagerstrom's model equation a geometric approach. Nonlinear Anal. Theory Methods Appl. 2004, Vol. 59, No. 4, pp. 531-565.

[77] Rosenblat, S., Shepherd, J. On the asymptotic solution Lagerstom model equation, SIAM J. Appl. Math. 1975, Vol. 29, No. 1, pp. 110-120.

[78] Sachdev, P.L. Nonlinear Ordinary Differential Equations and their Applications, Marcel Dekker, New York, 1991.

[79] Tam, K.K. On the Lagerstrom model for flow at low Reynolds numbers. J. Math. Anal. Appl. 1975, Vol. 49, No. 2, pp. 286-294.

[80] Teruhiko, K. An asymptotic approach on Lagerstrom mathematical model for viscous flow at Reynolds numbers. Bull. Univ. Osaka Prefect. Ser. A. 1988, Vol. 36, No. 2, pp. 83-97.

[81] Tsien, H.S. The Poincare-Lighthill-Kuo Method. Advances in Applied Mechanics. Academic Press Inc., New York. 1956, Vol. 4, pp. 281-350.

[82] Protter, M.H., Weinberger, H.F. Maximum Principles in Differential Equations. Prentice Hall, Englewood Cliffs, New Jersey, 1967.

Chapter 2

Homotopy Asymptotic Method and Its Application

Baojian Hong

Additional information is available at the end of the chapter

http://dx.doi.org/10.5772/67876

Abstract

As we all know, perturbation theory is closely related to methods used in the numerical analysis fields. In this chapter, we focus on introducing two homotopy asymptotic methods and their applications. In order to search for analytical approximate solutions of two types of typical nonlinear partial differential equations by using the famous homotopy analysis method (HAM) and the homotopy perturbation method (HPM), we consider these two systems including the generalized perturbed Kortewerg-de Vries-Burgers equation and the generalized perturbed nonlinear Schrödinger equation (GPNLS). The approximate solution with arbitrary degree of accuracy for these two equations is researched, and the efficiency, accuracy and convergence of the approximate solution are also discussed.

Keywords: homotopy analysis method, homotopy perturbation method, generalized KdV-Burgers equation, generalized perturbed nonlinear Schrödinger equation, approximate solutions, Fourier transformation

1. Introduction

In the past decades, due to the numerous applications of nonlinear partial differential equations (NPDEs) in the areas of nonlinear science [1, 2], many important phenomena can be described successfully using the NPDEs models, such as engineering and physics, dielectric polarization, fluid dynamics, optical fibers and quantitative finance and so on [3–5]. Searching for analytical exact solutions of these NPDEs plays an important and a significant role in all aspects of this subject. Many authors presented various powerful methods to deal with this problem, such as inverse scattering transformation method, Hirota bilinear method, homogeneous balance method, Bäcklund transformation, Darboux transformation, the generalized Jacobi elliptic function expansion method, the mapping deformation method and so on [6–10]. But once people noticed the complexity of nonlinear terms of NPDEs, they could not find the exact analytic solutions for many of them, especially with disturbed terms. Researchers had to develop some approximate and numerical methods for nonlinear theory; a great deal of efforts has been proposed for these problems, such as the multiple-scale method, the variational iteration method, the indirect matching method, the renormalization method, the Adomian decomposition method (ADM), the generalized differential transform method and so forth [11–13], among them the perturbation method [14], including the regular perturbation method, the singular perturbation method and the homotopy perturbation method (HPM) and so on.

Perturbation theory is widely used in numerical analysis as we all know. The earliest perturbation theory was built to deal with the unsolvable mathematical problems in the calculation of the motions of planets in the solar system [15]. The gradually increasing accuracy of astronomical observations led to incremental demands in the accuracy of solutions to Newton's gravitational equations, which extended and generalized the methods of perturbation theory. In the nineteenth century, Charles-Eugène Delaunay discovered the problem of small denominators which appeared in the nth term of the perturbative expansion when he was studying the perturbative expansion for the Earth-Moon-Sun system [16]. These well-developed perturbation methods were adopted and adapted to solve new problems arising during the development of Quantum Mechanics in the twentieth century. In the middle of the twentieth century, Richard Feynman realized that the perturbative expansion could be given a dramatic and beautiful graphical representation in terms of what are now called Feynman diagrams [17]. In the late twentieth century, because the broad questions about perturbation theory were found in the quantum physics community, including the difficulty of the nth term of the perturbative expansion and the demonstration of the convergent about the perturbative expansion, people had to pay more attention to the area of non-perturbative analysis, and much of the theoretical work goes under the name of quantum groups and non-commutative geometry [18]. As we all know, the solutions of the famous Korteweg-de Vries (KdV) equation cannot be reached by perturbation theory, even if the perturbations were carried out. Now, we can divide the perturbation theory to regular and singular perturbation theory; singular perturbation theory concerns those problems which depend on a parameter (here called ε) and whose solutions at a limiting value have a non-uniform behavior when the parameter tends to a pre-specified value. For regular perturbation problems, the solutions converge to the solutions of the limit problem as the parameter tends to the limit value. Both of these two methods are frequently used in physics and engineering today. There is no guarantee that perturbative methods lead to a convergent solution. In fact, the asymptotic series of the solution is the norm. In order to obtain the perturbative solution, we involve two distinct steps in general. The first is to assume that there is a convergent power asymptotic series about the parameter ε expressing the solution; then, the coefficients of the nth power of ε exist and can be computed via finite computation. The second step is to prove that the formal asymptotic series converges for ε small enough or to at least find a summation rule for the formal asymptotic series, thus providing a real solution to the problem.

The homotopy analysis method (HAM) was firstly proposed in 1992 by Liao [19], which yields a rapid convergence in most of the situations [20]. It also showed a high accuracy to solutions of the nonlinear differential systems. After this, many types of nonlinear problems were solved with HAM by others, such as nonlinear Schrödinger equation, fractional KdV-

Burgers-Kuramoto equation, a generalized Hirota-Satsuma coupled KdV equation, discrete KdV equation and so on [21–24]. With this basic idea of HAM (as $\hbar = -1$ and $H(x, t) = 1$), Jihuan He proposed the homotopy perturbation method(HPM) [25] which has been widely used to handle the nonlinear problems arising in the engineering and mathematical physics [26, 27].

In this chapter, we extend the applications of HAM and HPM with the aid of Fourier transformation to solve the generalized perturbed KdV-Burgers equation with power-law nonlinearity and a class of disturbed nonlinear Schrödinger equations in nonlinear optics. Many useful results are researched.

1.1. The homotopy analysis method (HAM)

Let us consider the following nonlinear equation

$$N[u(x, t)] = 0, \tag{1}$$

where N is a nonlinear operator, $u(x, t)$ is an unknown function and $x$and t denote spatial and temporal independent variables, respectively.

With the basic idea of the traditional homotopy method, we construct the following zero-order deformation equation

$$(1 - q)L[\phi(x, t; q) - u_0(x, t)] = q\hbar H(x, t)N[\phi(x, t; q)] \tag{2}$$

where $\hbar \neq 0$ is a non-zero auxiliary parameter, $q \in [0, 1]$ is the embedding parameter, $H(x, t)$ is an auxiliary function, L is an auxiliary linear operator, $\tilde{u}_0(x, t)$ is an initial guess of $u(x, t)$ and $\phi(x, t; q)$ is an unknown function. Obviously, when $q = 0$ and $q = 1$, it holds

$$\phi(x, t; 0) = u_0(x, t), \phi(x, t; 1) = u(x, t). \tag{3}$$

Thus, as q increases from 0 to 1, the solution $\phi(x, t; q)$ varies from the initial guess $u_0(x, t)$ to the solution $u(x, t)$. Expanding $\phi(x, t; q)$ in Taylor series with respect to q, we have

$$\begin{aligned} \phi(x, t; q) &= u_0 + \sum_{m=1}^{\infty} u_m q^m \\ &= u_0 + qu_1 + q^2u_2 + \cdots; u_0 = \tilde{u}_0(x, t), u_m = u_m(x, t). \end{aligned} \tag{4}$$

where

$$u_m(x, t) = \frac{1}{m!}\frac{\partial^m}{\partial q^m}\phi(x, t; q)|_{q = 0}. \tag{5}$$

If the auxiliary linear operator, the initial guess, the auxiliary parameter and the auxiliary function are so properly chosen such that they are smooth enough, the Taylor's series (4) with respect to q converges at $q = 1$, and we have

$$u = \phi(x, t; 1) = \sum_{m=0}^{\infty} u_m, \tag{6}$$

which must be one of the solutions of the original nonlinear equation, as proved by Liao. As $\hbar = -1$ and $H(x, t) = 1$, Eq. (2) becomes

$$(1-q)L[\phi(x, t; q) - u_0(x, t)] + qN[\phi(x, t; q)] = 0. \tag{7}$$

Eq. (7) is used mostly in the HPM, whereas the solution is obtained directly, without using Taylor's series. As $H(x, t) = 1$, Eq. (2) becomes

$$(1-q)L[\phi(x, t; q) - u_0(x, t)] = q\hbar N[\phi(x, t; q)], \tag{8}$$

which is used in the HAM when it is not introduced in the set of base functions. According to definition (5), the governing equation can be deduced from Eq. (2). Define the vector

$$\vec{u}_m(x, t) = \{u_0, u_1, u_2, \cdots, u_m\}. \tag{9}$$

Differentiating Eq. (2) m times with respect to the embedding parameter q and then setting $q = 0$ and finally dividing them by $m!$, we have the so-called mth-order deformation equation

$$L[u_m(x, t) - \chi_m u_{m-1}(x, t)] = \hbar H(x, t) R_{m-1}(\vec{u}_{m-1}, x, t), \tag{10}$$

where

$$R_{m-1}(\vec{u}_{m-1}, x, t) = \frac{1}{(m-1)!} \frac{\partial^{m-1}}{\partial q^{m-1}} N[\phi(x, t; q)]|_{q=0}. \tag{11}$$

And

$$\chi_m = \begin{cases} 0, x \le 1 \\ 1, x \ge 2 \end{cases}. \tag{12}$$

It should be emphasized that $u_m(x, t)$ for $m \ge 1$ is governed by the linear Eq. (10) with the linear boundary conditions that come from the original problem, which can be easily solved by symbolic computation software such as Mathematica and Matlab.

1.2. The homotopy perturbation method

To illustrate the basic concept of the homotopy perturbation method, consider the following nonlinear system of differential equations with boundary conditions

$$\begin{cases} A(u) = f(r), r \in \Omega, & (13.1) \\ B(u, \frac{\partial u}{\partial n}) = 0, r \in \Gamma = \partial\Omega & (13.2) \end{cases}, \tag{13}$$

where B is a boundary operator and Γ is the boundary of the domain Ω, $f(r)$ is a known analytical function. The differential operator A can be divided into two parts, L and N, in general, where L is a linear and N is a nonlinear operator. Eq. (13) can be rewritten as follows:

$$L(u) + N(u) = f(r). \tag{14}$$

We construct the following homotopy mapping $H(\phi, q){:}\Omega \times [0, 1] \rightarrow R$, which satisfies

$$H(\phi, q) = (1 - q)[L(v) - L(\tilde{u}_0)] + q[A(v) - f(r)] = 0, q \in [0, 1], r \in \Omega, \tag{15}$$

where $\tilde{u}_0$is an initial approximation of Eq. (13), and is the embedding parameter; we have the following power series presentation for ϕ,

$$\phi = \sum_{i=0}^{\infty} u_i(x, t)q^i = u_0 + qu_1 + q^2u_2 + \cdots. \tag{16}$$

The approximate solution can be obtained by setting $q = 1$, that is

$$u = \lim_{q\rightarrow 1}\phi = u_0 + u_1 + u_2 + \cdots. \tag{17}$$

If we let $u_0(x, t) = \tilde{u}_0(x, t)$,notice the analytic properties of f, L, $\tilde{u}_0$ and mapping (15), we know that the series of (17) is convergence in most cases when $q \in [0, 1]$ [28]. We obtain the solution of Eq. (13).

To study the convergence of the method, let us state the following theorem.

Theorem (Sufficient Condition of Convergence).

Suppose that X and Y are Banach spaces and $N : X \rightarrow Y$ is a contract nonlinear mapping that is

$$\forall u, u* \in X : \|N(u) - N(u*)\| \le \gamma\|u - u*\|, 0 < \gamma < 1. \tag{18}$$

Then, according to Banach's fixed point theorem, N has a unique fixed point u, that is $N(u) = u$. Assume that the sequence generated by homotopy perturbation method can be written as

$$U_n = N(U_{n-1}), U_n = \sum_{i=0}^{n} u_i, u_i \in X, n = 1, 2, 3, \cdots, \tag{19}$$

and suppose that

$$U_0 = u_0 \in B_r(u), B_r(u) = \{u* \in X| \|u* - u\| < \gamma\} \tag{20}$$

$$\text{then, we have (i) } U_n \in B_r(u), \text{(ii)} \lim_{n\rightarrow\infty} U_n = u. \tag{21}$$

Proof. (i) By inductive approach, for $n = 1$, we have

$\|U_1 - u\| = \|N(U_0) - N(u)\| \le \gamma \|U_0 - u\|$ and then

$$\|U_n - u\| = \|N(U_{n-1}) - N(u)\| \le \gamma^n \|U_0 - u\| \le \gamma^n r \Rightarrow U_n \in B_r(u)$$

(ii) Because of $0 < \gamma < 1$, we have $\lim\limits_{n\to\infty} \|U_n - u\| = 0$ that is $\lim\limits_{n\to\infty} U_n = u$.

2. Application to the generalized perturbed KdV-Burgers equation

Consider the following generalized perturbed KdV-Burgers equation

$$u_t + \alpha u^p u_x + \beta u^{2p} u_x + \gamma u_{xx} + \delta u_{xxx} = f(t, x, u). \tag{22}$$

where $\alpha, \beta, \gamma, \delta, p$ are arbitrary constants, and $f = f(t, x, u)$ is a disturbed term, which is a sufficiently smooth function in a corresponding domain.

This equation with $p \ge 1$ is a model for long-wave propagation in nonlinear media with dispersion and dissipation. Eq. (22) arises in a variety of physical contexts which include a number of equations, and many valuable results about Eq. (22) have been studied by many authors in [29–31]. In fact, if one takes different value of $\alpha, \beta, \gamma, \delta, p$ and f, Eq.(22) represents a large number of equations, such as KdV equation, MKdV equation, CKdV equation, Burgers equation, KdV-Burgers equation and the equations as the following forms.

Fitzhugh-Nagumo equation [32]:

$$u_t - u_{xx} = f = u(u - \alpha)(1 - u), \tag{23}$$

Burgers-Huxley equation [33]

$$u_t + \alpha u^\delta u_x - \lambda u_{xx} = f = \beta u(1 - u^\delta)(\eta u^\delta - \gamma) \tag{24}$$

Burgers-Fisher equation [34]

$$u_t + \alpha u^\delta u_x - u_{xx} = f = \beta u(1 - u^\delta) \tag{25}$$

It's significant for us to handle Eq. (22).

2.1. The generalized KdV-Burgers equation

If we let $f = 0$ in Eq. (22), we can obtain the famous generalized KdV-Burgers equation with nonlinear terms of any order [35, 36].

$$u_t + \alpha u^p u_x + \beta u^{2p} u_x + \gamma u_{xx} + \delta u_{xxx} = 0. \tag{26}$$

Eq. (26) is solved on the infinite line $-\infty < x < \infty$ together with the initial condition $u(x, 0) = f(x), \ -\infty < x < \infty$ by using the HAM. We first introduce the traveling wave transform

http://dx.doi.org/10.5772/67876

$$\xi = x + ct + \xi_0. \tag{27}$$

where c are constants to be determined later and $\xi_0 \in C$ are arbitrary constants. Secondly, we make the following transformation:

$$u(\xi) = v^{1/p}(\xi). \tag{28}$$

Eq. (26) is reduced to the following form:

$$\begin{aligned} &p(p+1)(2p+1)\delta v(\xi)v''(\xi) + (p+1)(2p+1)\delta(1-p)v'^2(\xi) \\ &+p(p+1)(2p+1)\gamma v(\xi)v'(\xi) + cp^2(p+1)(2p+1)v^2(\xi) \\ &+p^2(2p+1)\alpha v^3(\xi) + p^2(p+1)\beta v^4(\xi) = 0 \end{aligned} \tag{29}$$

where the derivatives are performed with respect to the coordinate ξ. We can conclude that Eq. (26) has the following solution, by using the deformation mapping method:

$$\tilde{u}_0 = \left\{ -\frac{c(1+p)}{2\alpha} + \frac{d(1+p)\gamma}{p\alpha}\sqrt{\frac{c^2p^2}{4d^2\gamma^2}}\tanh(d\sqrt{\frac{c^2p^2}{4d^2\gamma^2}}(x+ct+\xi_0)) \right\}^{\frac{1}{p}}. \tag{30}$$

2.2. The approximate solutions by using HAM

To solve Eq. (22) by means of HAM, we choose the initial approximation

$$u_0(x,t) = \tilde{u}_0(x,t)\Big|_{t=0} = g(x), \tag{31}$$

where $\tilde{u}_0(x,t)$ is an arbitrary exact solution of Eq. (23).

According to Eq. (1), we define the nonlinear operator

$$N[\phi] = \phi_t + \alpha\phi^p\phi_x + \beta\phi^{2p}\phi_x + \gamma\phi_{xx} + \delta\phi_{xxx} - f(\phi), \phi = \phi(x,t;q). \tag{32}$$

It is reasonable to express the solution $u(x,t)$ by set of base functions $g_n(x)t^n, n \geq 0$, under the rule of solution expression; it is straightforward to choose $H(x,t) = 1$ and the linear operator

$$L[\phi(x,t;q)] = \frac{\partial\phi(x,t;q)}{\partial t} \tag{33}$$

with the property

$$L[c(x)] = 0. \tag{34}$$

From Eqs. (10, 11 and 32), we have

$$\begin{aligned} R_{m-1}(\vec{u}_{m-1},x,t) = u_{m-1,t} + \gamma u_{m-1,xx} + \delta u_{m-1,xxx} + \alpha D_{m-1}(\phi^p\phi_x) \\ + \beta D_{m-1}(\phi^{2p}\phi_x) - F(u_0,u_1,\cdots,u_{m-1}), \end{aligned} \tag{35}$$

where

$$D_{m-1}(\phi^n\phi_x)=\sum_{k_1=0}^{n}\sum_{k_2=0}^{k_1}\sum_{k_3=0}^{k_2}\cdots\sum_{k_{m-1}=0}^{k_{m-2}}\sum_{i=0}^{m-1}C_n^{k_1}C_{k_1}^{k_2}C_{k_2}^{k_3}\cdots C_{k_{m-2}}^{k_{m-1}}u_0^{n-k_1}u_1^{k_1-k_2}\cdots u_{m-1}^{k_{m-1}}u_{i\xi} \tag{36}$$

and $n\geq k_1\geq k_2\geq\cdots\geq k_{m-1}\geq 0\in N$, with

$$\begin{aligned}&\sum_{j=1}^{m-1}k_j+i=m-1,\, i=0,\cdots,m-1\\ &F(u_0,u_1,\cdots,u_{m-1})=\frac{1}{(n-1)!}\frac{\partial^{(m-1)}}{\partial q^{m-1}}f(x,t,u)\bigg|_{q=0}.\end{aligned} \tag{37}$$

Now, the solution of the mth-order deformation in Eq. (10) with initial condition $u_m(x,t)=0$ for $m\geq 1$ becomes

$$u_m=\chi_m u_{m-1}+L^{-1}[\hbar R_{m-1}(\vec{u}_{m-1},x,t)], \tag{38}$$

Thus, from Eqs. (31, 35 and 38), we can successively obtain

$$u_0=\tilde{u}_0(x,0)=g(x), \tag{39}$$

$$u_1=-\hbar t[\tilde{u}_{0t}+f(u_0)],\, \tilde{u}_{0t}=\frac{\partial}{\partial t}\tilde{u}_0(x,t)|_{t=0}, \tag{40}$$

$$u_2=(1+\hbar)u_1+\hbar(\alpha u_0^p u_{1,x}+\beta u_0^{2p}u_{1,x}+\gamma u_{1,xx}+\delta u_{1,xxx}-f_u(u_0)u_1)t \tag{41}$$

$$\vdots$$

$$u_m=(1+\hbar)u_{m-1}+\hbar[\gamma u_{1,xx}+\delta u_{1,xxx}+\alpha D_{m-1}(\phi^p\phi_x)+\beta D_{m-1}(\phi^{2p}\phi_x)-F(u_0,u_1,\cdots,u_{m-1})]t \tag{42}$$

$$\vdots$$

We obtain the mth-order approximate solution and exact solution of Eq. (22) as follows

$$u_{m,appr}=\sum_{k=0}^{m}u_k,\, u_{exact}=\phi(x,t;1)=\lim_{m\to\infty}\sum_{k=0}^{m}u_k \tag{43}$$

if we choose

$$\tilde{u}_0(x,0)=\left\{-\frac{c(1+p)}{2\alpha}+\frac{d(1+p)\gamma}{p\alpha}\sqrt{\frac{c^2p^2}{4d^2\gamma^2}}\tanh\left(d\sqrt{\frac{c^2p^2}{4d^2\gamma^2}}x\right)\right\}^{\frac{1}{p}}. \tag{44}$$

From Eqs. (39–44), we can obtain the corresponding approximate solution of Eq. (22).

2.3. Example

In the following, three examples are presented to illustrate the effectiveness of the HAM. We first plot the so-called $\hbar$ curves of $u''_{appr}(0,0)$ and $u'''_{appr}(0,0)$ to discover the valid region of $\hbar$, which corresponds to the line segment nearly parallel to the horizontal axis. The simulate comparison between the initial exact solution, exact solution and the fourth order of approximation solution is given.

Now, we consider the small perturbation term $f = \varepsilon\tilde{f}$ in Eq. (22).

Example 1. Consider the CKdV equation with small disturbed term

$$u_t + 6uu_x - 6u^2u_x + u_{xxx} = \varepsilon u^2, 0 < \varepsilon \ll 1 \tag{45}$$

with the initial exact solution

$$\tilde{u}_0(x,t) = \frac{1}{2} - \frac{1}{2}\tanh[\frac{1}{2}(x-t)]. \tag{46}$$

From Section 2.2, we have

$$u_0 = \frac{1}{2} - \frac{1}{2}\tanh\left(\frac{1}{2}x\right), \tilde{u}_{0t} = \frac{1}{4}\mathrm{sech}^2\left(\frac{1}{2}x\right), \tag{47}$$

$$u_1 = -\hbar\left\{\frac{1}{4}\mathrm{sech}^2\left(\frac{1}{2}x\right) + \varepsilon\left[\frac{1}{2} - \frac{1}{2}\tanh\left(\frac{1}{2}x\right)\right]^2\right\}t \tag{48}$$

$$\begin{aligned}
u_2 = &-(1+\hbar)\hbar t\left\{\frac{1}{4}\mathrm{sech}^2\left(\frac{1}{2}x\right) + \varepsilon\left[\frac{1}{2} - \frac{1}{2}\tanh\left(\frac{1}{2}x\right)\right]^2\right\}\\
&- \hbar^2t^2\left\{6\left[\frac{1}{2} - \frac{1}{2}\tanh\left(\frac{1}{2}x\right)\right]\left\{\frac{1}{4}\mathrm{sech}^2\left(\frac{1}{2}x\right) + \varepsilon\left[\frac{1}{2} - \frac{1}{2}\tanh\left(\frac{1}{2}x\right)\right]^2\right\}_x\right.\\
&+ 6\hbar^2t^2\left[\frac{1}{2} - \frac{1}{2}\tanh\left(\frac{1}{2}x\right)\right]2\left\{\frac{1}{4}\mathrm{sech}^2\left(\frac{1}{2}x\right) + \varepsilon\left[\frac{1}{2} - \frac{1}{2}\tanh\left(\frac{1}{2}x\right)\right]^2\right\}_x\\
&- \hbar^2t^2\left\{\frac{1}{4}\mathrm{sech}^2\left(\frac{1}{2}x\right) + \varepsilon\left[\frac{1}{2} - \frac{1}{2}\tanh\left(\frac{1}{2}x\right)\right]^2\right\}_{xxx}\\
&+ 2\varepsilon\hbar^2t^2\left[\frac{1}{2} - \frac{1}{2}\tanh\left(\frac{1}{2}x\right)\right]\left\{\frac{1}{4}\mathrm{sech}^2\left(\frac{1}{2}x\right) + \varepsilon\left[\frac{1}{2} - \frac{1}{2}\tanh\left(\frac{1}{2}x\right)\right]^2\right\}\\
= &\frac{\hbar t}{32}\left[\cosh\left(\frac{x}{2}\right) - \sinh\left(\frac{x}{2}\right)\right]\sec h^5\left(\frac{x}{2}\right)\left\{\hbar(5t-3-3\varepsilon) - 3 - 3\varepsilon\right.\\
&+ 2\hbar t\varepsilon(1+\varepsilon) + 2\cosh(x)\left[2\varepsilon - 2 - 2\hbar(1+\varepsilon) + \hbar t\left(2\varepsilon^2 + 7\varepsilon - 3\right)\right]\\
&+ \left[\hbar\left(t - \varepsilon - 1 + 2t\varepsilon^2\right) - \varepsilon - 1\right]\cosh(2x) - 2\sinh\left(\frac{x}{2}\right)[1 - \varepsilon + \hbar - \varepsilon\hbar\\
&\left.+ \hbar t\left(2 - 3\varepsilon + 2\varepsilon^2\right) + (1-\varepsilon)\cosh x + \hbar\left(1 - t - \varepsilon + 2t\varepsilon^2\right)\cosh x)]\right\}\\
&\cdots
\end{aligned} \tag{49}$$

$$
\begin{aligned}
u_{appr} = {} & \frac{1}{2} - \frac{1}{2}\tanh\left(\frac{1}{2}x\right) - \hbar\left\{\frac{1}{4}\operatorname{sech}^2\left(\frac{1}{2}x\right) + -\varepsilon\left[\frac{1}{2} - \frac{1}{2}\tanh\left(\frac{1}{2}x\right)\right]^2\right\}t \\
& + \frac{\hbar t}{32}\left[\cosh\left(\frac{x}{2}\right) - \sinh\left(\frac{x}{2}\right)\right]\sec h^5\left(\frac{x}{2}\right)\Big\{\hbar(5t - 3 - 3\varepsilon) - 3 - 3\varepsilon + \\
& 2\hbar t\varepsilon(1+\varepsilon) + 2\cosh(x)\left[2\varepsilon - 2 - 2\hbar(1+\varepsilon) + \hbar t\left(2\varepsilon^2 + 7\varepsilon - 3\right)\right] \\
& + \left[\hbar\left(t - \varepsilon - 1 + 2t\varepsilon^2\right) - \varepsilon - 1\right]\cosh(2x) - 2\sinh\left(\frac{x}{2}\right)\left[1 - \varepsilon + \hbar - \varepsilon\hbar\right. \\
& \left. + \hbar t\left(2 - 3\varepsilon + 2\varepsilon^2\right) + (1-\varepsilon)\cosh x + \hbar\left(1 - t - \varepsilon + 2t\varepsilon^2\right)\cosh x\right)\Big]\Big\} + \cdots
\end{aligned}
\tag{50}
$$

The $\hbar$ curves of $u''_{appr}(0,0)$ and $u'''_{appr}(0,0)$ in Eq. (45) are shown in **Figure 1(a)**, and the comparison between the initial exact solution and the fourth order of approximation solution is shown in **Figure 1(b)**.

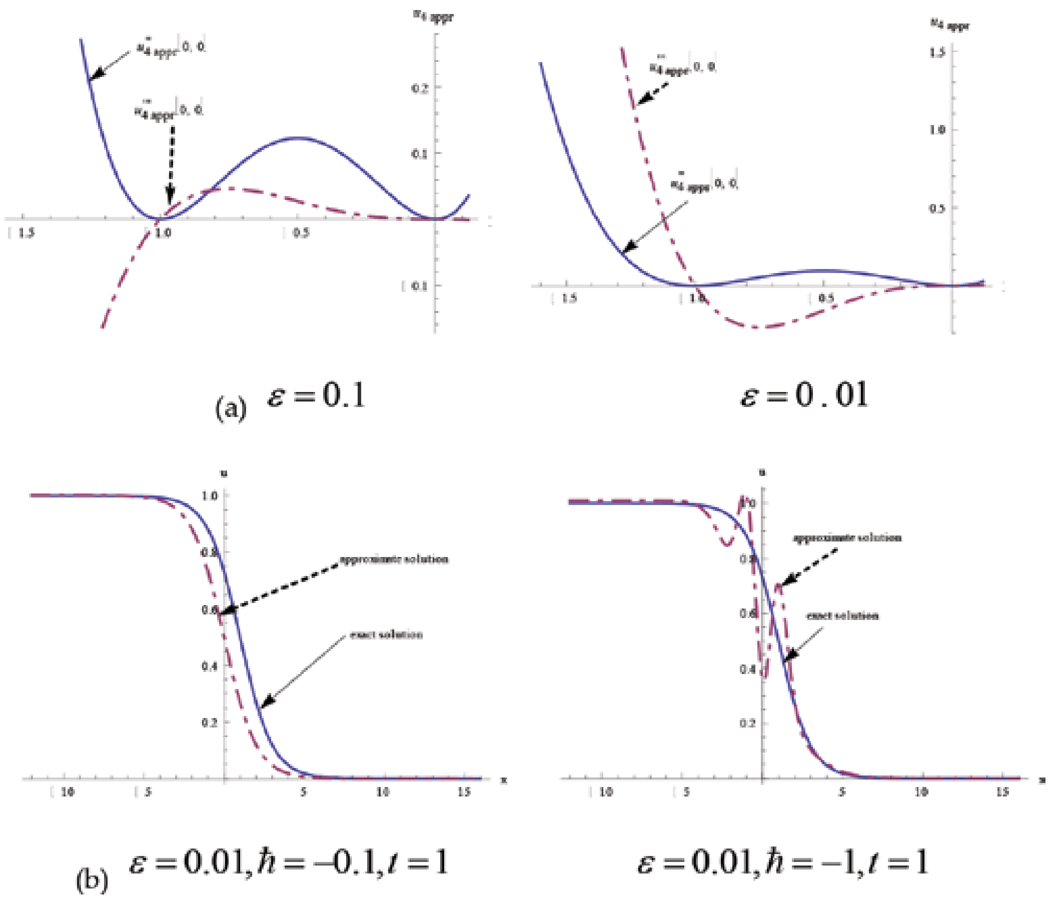

Figure 1. (a) The $\hbar$ curves of $u''_{appr}(0,0)$ and $u'''_{appr}(0,0)$at the fourth order of approximation. (b) The initial exact solution and the fourth order of approximation solution.

Example 2. Consider the KdV-Burgers equation with small disturbed term

$$u_t + 6uu_x + u_{xx} - u_{xxx} = \varepsilon \sin u \tag{51}$$

with the initial exact solution

$$\tilde{u}_0(x,t) = \frac{1}{50}\left\{1 - \coth[-\frac{1}{10}(x - \frac{6}{25}t)]\right\}^2 \tag{52}$$

From Section 2.2, we have

$$u_0 = \frac{1}{50}[1 - \coth(-\frac{1}{10}x)]^2, \tilde{u}_{0t} = \frac{3}{3125}\mathrm{csch}^2(\frac{1}{10}x)[1 + \coth(\frac{1}{10}x)] \tag{53}$$

$$u_1 = -\hbar\varepsilon \sin\left\{\frac{1}{50}[1 - \coth(\frac{-1}{10}x)]^2\right\}t - \frac{3\hbar t}{3125}\mathrm{csch}^2(\frac{1}{10}x)[1 + \coth(\frac{1}{10}x)] \tag{54}$$

$$u_2 = (1+\hbar)u_1 + \hbar t(6u_0u_{1,x} + u_{1,xx} - u_{1,xxx} - \varepsilon u_1 \cos u_0) \tag{55}$$

$$\begin{aligned} u_{appr} = &\frac{1}{50}\left[1 - \coth\left(-\frac{1}{10}x\right)\right]^2 - \hbar\varepsilon \sin\left\{\frac{1}{50}\left[1 - \coth\left(-\frac{1}{10}x\right)\right]^2\right\}t \\ &- \frac{3}{3125}\hbar t\mathrm{csch}^2\left(\frac{1}{10}x\right)\left[1 + \coth\left(\frac{1}{10}x\right)\right] + u_2 + \cdots \end{aligned} \tag{56}$$

The $\hbar$ curves of $u''_{appr}(0,0)$ and $u'''_{appr}(0,0)$ in Eq. (51) are shown in **Figure 2(a)**; the comparison between the initial exact solution and the fourth order of approximation solution is shown in **Figure 2(b)**.

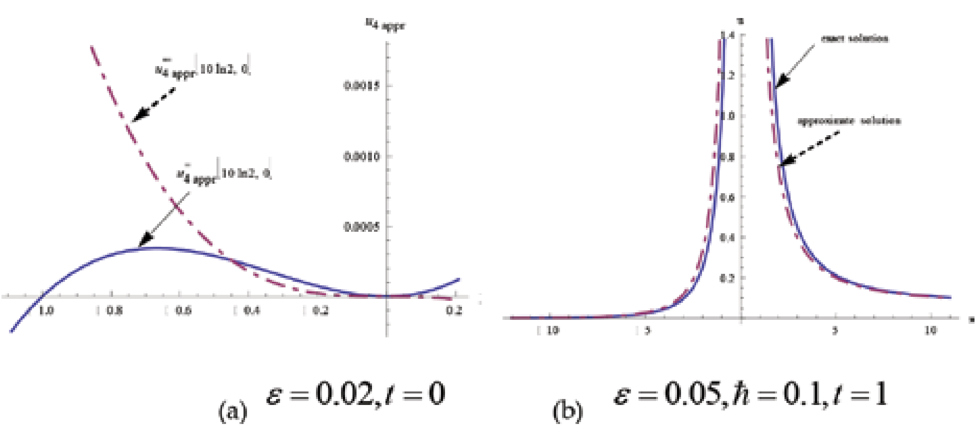

Figure 2. (a) The $\hbar$ curves of $u''_{appr}(10\ln 2, 0)$ and $u'''_{appr}(10\ln 2, 0)$ at the fourth order of approximation. (b) The initial exact solution and the fourth order of approximation solution.

Example 3. Consider the Burgers-Fisher equation

$$u_t + u^2 u_x - u_{xx} = \varepsilon u(1 - u^2) \tag{57}$$

with the exact solution and the initial exact solution

$$u_{1_{exact}} = \sqrt{\frac{1}{2} - \frac{1}{2}\tanh\left[\frac{1}{3}x - \frac{1+9\varepsilon}{9}t + \xi_0\right]} \tag{58}$$

$$u_{2_{exact}} = \sqrt{\frac{1}{2} - \frac{1}{2}\coth\left[\frac{1}{3}x - \frac{1+9\varepsilon}{9}t + \xi_0\right]} \tag{59}$$

$$\tilde{u}_0(x, t) = \sqrt{\frac{1}{2} - \frac{1}{2}\tanh\left[\frac{1}{3}x - \frac{1}{9}t + \xi_0\right]} \tag{60}$$

From Section 2.2, we have

$$u_0 = \sqrt{\frac{1}{2} - \frac{1}{2}\tanh\left(\frac{1}{3}x\right)}, \qquad \tilde{u}_{0t} = \mathrm{sech}^2\left(\frac{1}{3}x\right)/18\sqrt{2 - 2\tanh\left(\frac{1}{3}x\right)} \tag{61}$$

$$u_1 = -\frac{\hbar t\,\mathrm{sech}^2\left(\frac{1}{3}x\right)}{18\sqrt{2 - 2\tanh\left(\frac{1}{3}x\right)}} - \hbar t\varepsilon\sqrt{\frac{1}{2} - \frac{1}{2}\tanh\left(\frac{1}{3}x\right)}\left(\frac{1}{2} + \frac{1}{2}\tanh\left(\frac{1}{3}x\right)\right) \tag{62}$$

$$u_2 = (1 + \hbar)u_1 + \hbar t(\alpha u_0 u_{1,x} - u_{1,xx} - \varepsilon u_1 + 3\varepsilon u_0^2 u_1) \tag{63}$$

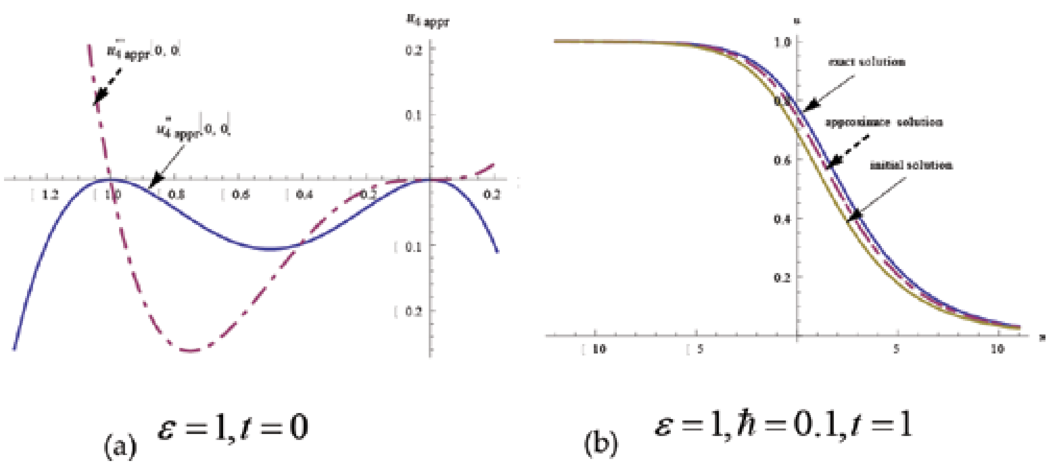

Figure 3. (a) The $\hbar$ curves of $u''_{appr}(0, 0)$ and $u'''_{appr}(0, 0)$ at the fourth order of approximation. (b) The exact solution, initial exact solution and the fourth order of approximation solution.

$$u_{appr} = \sqrt{\frac{1}{2} - \frac{1}{2}\tanh\left(\frac{1}{3}x\right)} - \frac{\hbar t \operatorname{sech}^2\left(\frac{1}{3}x\right)}{18\sqrt{2 - 2\tanh\left(\frac{1}{3}x\right)}} - \hbar t\varepsilon\sqrt{\frac{1}{2} - \frac{1}{2}\tanh\left(\frac{1}{3}x\right)}\left(\frac{1}{2} + \frac{1}{2}\tanh\left(\frac{1}{3}x\right)\right) + u_2 + \cdots \tag{64}$$

The $\hbar$ curves of $u''_{appr}(0,0)$ and $u'''_{appr}(0,0)$ in Eq. (57) are shown in **Figure 3(a)**, the comparison between the initial exact solution and the fourth order of approximation solution is shown in **Figure 3(b)**.

3. Application to the generalized perturbed NLS equation

In this section, we will use the HPM and Fourier's transformation to search for the solution of the generalized perturbed nonlinear Schrödinger equation (GPNLS)

$$i\frac{\partial u}{\partial z} + \frac{1}{2}\beta(z)\frac{\partial^2 u}{\partial t^2} + \delta(z)u|u|^2 - i\alpha(z)u = \beta(z)f(u,z,t). \tag{65}$$

If we let $t \to x, z \to t$,Eq. (65) turns to the following form

$$i\frac{\partial u}{\partial t} + \frac{1}{2}\beta(t)\frac{\partial^2 u}{\partial x^2} + \delta(t)u|u|^2 - i\alpha(t)u = \beta(t)f(u,t,x). \tag{66}$$

where disturbed term f is a sufficiently smooth function in a corresponding domain. $\alpha(t)$ represents the heat-insulating amplification or loss. $\beta(t)$ and $\delta(t)$ are the slowly increasing dispersion coefficient and nonlinear coefficient, respectively. The transmission of soliton in the real communication system of optical soliton is described by Eq. (66) with $f = 0$ [37–39].

$$i\frac{\partial u}{\partial t} + \frac{1}{2}\beta(t)\frac{\partial^2 u}{\partial x^2} + \delta(t)u|u|^2 - i\alpha(t)u = 0. \tag{67}$$

We make the transformation

$$u = A(t)\varphi(\xi)e^{i\eta}, \xi = k_1x + c_1(t), \eta = k_2x + c_2(t) \tag{68}$$

With the following consistency conditions,

$$A(t) = ce^{\int_0^t \alpha(\tau)d\tau}, c_1(t) = -k_1k_2\int_0^t \beta(\tau)d\tau, c_2(t) = \frac{1}{2}(a_2k_1^2 - k_2^2)\int_0^t \beta(\tau)d\tau, \delta(t) = \frac{-a_4k_1^2}{c^2}\beta(t)e^{-2\int_0^t \alpha(\tau)d\tau} \tag{69}$$

where k_1, k_2, a_2, a_4, c are arbitrary non-zero constants.

If we let $f(u,t,x) = \frac{1}{2}k_1^2 f(\varphi)e^{i\eta}$, substituting Eq. (68) into Eq. (67), we have

$$\varphi''_{\xi\xi} - a_2\varphi - 2a_4\varphi^3 = f(\varphi). \tag{70}$$

By using the general mapping deformation method [10, 40], we can obtain the following solutions of the corresponding undisturbed Eq. (70) when $f = 0$.

$$\tilde{\varphi}_0 = cn[k_1 x - k_1 k_2 \int_0^t \beta(\tau)d\tau]. \tag{71}$$

In order to obtain the solution of Eq. (70), we introduce the following homotopic mapping $H(\varphi, p)$: $R \times I \to R$,

$$H(\varphi,p) = L\varphi - L\tilde{\varphi}_0 + q\left(L\tilde{\varphi}_0 - 2a_4\varphi^3 - f(\varphi)\right). \tag{72}$$

where $R = (-\infty, +\infty), I = [0,1], \tilde{\varphi}_0$ is an initial approximate solution to Eq. (70), and the linear operator L is expressed as

$$L(u) = \varphi''_{\xi\xi} - a_2\varphi. \tag{73}$$

Obviously, from mapping Eq. (72), $H(\varphi,1) = 0$ is the same as Eq. (70). Thus, the solution of Eq. (70) is the same as the solution of $H(\varphi,q)$ as $q \to 1$.

3.1. Approximate solution

In order to obtain the solution of Eq. (70), set

$$\varphi = \sum_{i=0}^{\infty}\varphi_i(\xi)q^i = \varphi_0 + q\varphi_1 + q^2\varphi_2 + \cdots \tag{74}$$

If we let $\varphi_0 = \tilde{\varphi}_0$,notice the analytical properties of $f, \tilde{\varphi}_0$, and mapping Eq. (72), we can deduce that the series of Eq. (74) are uniform convergence when $q \in [0,1]$. Substituting expression (74) into $H(u,q) = 0$ and expanding nonlinear terms into the power series in powers of q, we compare the coefficients of the same power of q on both sides of the equation and we have

$$q^0 : L\varphi_0 = L\tilde{\varphi}_0, \tag{75}$$

$$q^1 : L\varphi_1 = f(\varphi_0), \tag{76}$$

$$q^2 : L\varphi_2 = 6a_4\varphi_0^2\varphi_1 + f_\varphi(\varphi_0)\varphi_1, \tag{77}$$

$$\cdots$$

$$\begin{aligned} q^n : L\varphi_n = F(\varphi_0,\varphi_1,\cdots,\varphi_{n-1}) + 2a_4\sum_{k_1=0}^{3}\sum_{k_2=0}^{k_1}\sum_{k_3=0}^{k_2}\cdots \\ \sum_{k_{n-1}=0}^{k_{n-2}} C_3^{k_1}C_{k_1}^{k_2}C_{k_2}^{k_3}\cdots C_{k_{n-2}}^{k_{n-1}}\varphi_0^{3-k_1}\varphi_1^{k_1-k_2}\varphi_2^{k_2-k_3}\cdots\varphi_{n-2}^{k_{n-2}-k_{n-1}}\varphi_{n-1}^{k_{n-1}} \end{aligned}. \tag{78}$$

$$\cdots$$

where $3 \geq k_1 \geq k_2 \geq \cdots \geq k_{n-1} \geq 0 \in N$, $\sum_{j=1}^{n-1} k_j = n-1, n \in N^+$ and $F(\varphi_0, \varphi_1, \cdots, \varphi_{n-1}) = \frac{1}{(n-1)!}\frac{\partial^{(n-1)}}{\partial p^{n-1}}$ $f(\varphi_0, \varphi_1, \cdots, \varphi_{n-1})|_{p=0}$.

From Eq. (75) we have $\varphi_0(\xi) = \tilde{\varphi}_0(\xi)$. If we select $\varphi_1|_{\xi=0} = 0$, by using Fourier transformation and from Eq. (76), we have

$$\varphi_1 = \frac{1}{\sqrt{a_2}}\int_0^{\xi} f(\varphi_0)(e^{\sqrt{a_2}(\xi-\tau)} - e^{-\sqrt{a_2}(\xi-\tau)})d\tau, \quad a_2 \neq 0, \quad f(\varphi_0) = f(\varphi_0(\tau)). \tag{79}$$

If we select $\varphi_2|_{\xi=0} = 0$, from Eq. (77) we have

$$\varphi_2 = \frac{1}{\sqrt{a_2}}\int_0^{\xi}[6a_4\varphi_0^2\varphi_1 + f_{\varphi}(\varphi_0)\varphi_1](e^{\sqrt{a_2}(\xi-\tau)} - e^{-\sqrt{a_2}(\xi-\tau)})d\tau. \tag{80}$$

where $a_2 \neq 0, \varphi_0 = \varphi_0(\tau), \varphi_1 = \varphi_1(\tau)$.

We obtain the first- and second-order approximate solutions $u_{1\mathrm{hom}}(x,t)$ and $u_{2\mathrm{hom}}(x,t)$ of the Eq. (70) as follows:

$$\varphi_{1\mathrm{hom}}(x,t) = \tilde{\varphi}_0 + \frac{1}{\sqrt{2m^2-1}}\int_0^{\xi} f(\varphi_0)(e^{\sqrt{2m^2-1}(\xi-\tau)} - e^{-\sqrt{2m^2-1}(\xi-\tau)})d\tau \tag{81}$$

$$u_{1\mathrm{hom}}(x,t) = ce^{\int_0^t \alpha(\tau)d\tau + i[k_2x + \frac{1}{2}\int_0^t((2m^2-1)k_1^2 - k_2^2)\beta(\tau)d\tau]}\varphi_{1\mathrm{hom}}(x,t) \tag{82}$$

$$\begin{aligned}\varphi_{2\mathrm{hom}}(x,t) = \tilde{\varphi}_0 &+ \frac{1}{\sqrt{2m^2-1}}\int_0^{\xi} f(\varphi_0)(e^{\sqrt{2m^2-1}(\xi-\tau)} - e^{-\sqrt{2m^2-1}(\xi-\tau)})d\tau \\ &+ \frac{1}{\sqrt{2m^2-1}}\int_0^{\xi}[-6m^2\varphi_0^2\varphi_1 + f_{\varphi}(\varphi_0)\varphi_1](e^{\sqrt{2m^2-1}(\xi-\tau)} - e^{-\sqrt{2m^2-1}(\xi-\tau)})d\tau\end{aligned} \tag{83}$$

$$u_{2\mathrm{hom}}(x,t) = ce^{\int_0^t \alpha(\tau)d\tau + i[k_2x + \frac{1}{2}\int_0^t((2m^2-1)k_1^2 - k_2^2)\beta(\tau)d\tau]}\varphi_{2\mathrm{hom}}(x,t) \tag{84}$$

With the same process, we can also obtain the N-order approximate solution

$$\begin{aligned}\varphi_{n\mathrm{hom}}(x,t) = \tilde{\varphi}_0 &+ \frac{1}{\sqrt{2m^2-1}}\int_0^{\xi} f(\varphi_0)(e^{\sqrt{a_2}(\xi-\tau)} - e^{-\sqrt{a_2}(\xi-\tau)})d\tau \\ &+ \frac{1}{\sqrt{2m^2-1}}\int_0^{\xi}[-6m^2\varphi_0^2\varphi_1 + f_{\varphi}(\varphi_0)\varphi_1](e^{\sqrt{2m^2-1}(\xi-\tau)} - e^{-\sqrt{2m^2-1}(\xi-\tau)})d\tau \\ &+ \cdots + \frac{1}{\sqrt{2m^2-1}}\int_0^{\xi}(e^{\sqrt{2m^2-1}(\xi-\tau)} - e^{-\sqrt{2m^2-1}(\xi-\tau)})[F(\varphi_0, \varphi_1, \cdots, \varphi_{n-1}) - 2m^2 \\ &\sum_{k_1=0}^{3}\sum_{k_2=0}^{k_1}\sum_{k_3=0}^{k_2}\cdots\sum_{k_{n-1}=0}^{k_{n-2}} C_3^{k_1}C_{k_1}^{k_2}C_{k_2}^{k_3}\cdots C_{k_{n-2}}^{k_{n-1}}\varphi_0^{3-k_1}\varphi_1^{k_1-k_2}\varphi_2^{k_2-k_3}\cdots\varphi_{n-2}^{k_{n-2}-k_{n-1}}\varphi_{n-1}^{k_{n-1}}]d\tau\end{aligned} \tag{85}$$

$$u_{n\mathrm{hom}}(x,t) = ce^{\int_0^t \alpha(\tau)d\tau + i[k_2x + \frac{1}{2}\int_0^t((2m^2-1)k_1^2 - k_2^2)\beta(\tau)d\tau]}\varphi_{n\mathrm{hom}}(x,t) \tag{86}$$

where $3 \geq k_1 \geq k_2 \geq \cdots \geq k_{n-1} \geq 0 \in N$, $\sum_{j=1}^{n-1} k_j = n-1$, $n \in N^+$ and

$$F(\varphi_0, \varphi_1, \cdots, \varphi_{n-1}) = \frac{1}{(n-1)!} \frac{\partial^{(n-1)}}{\partial p^{n-1}} f(\varphi_0, \varphi_1, \cdots, \varphi_{n-1}) \bigg|_{p=0} \tag{87}$$

3.2. Comparison of accuracy

In order to explain the accuracy of the expressions of the approximate solution represented by Eq. (86), we consider the small perturbation term

$$i\frac{\partial u}{\partial t} + \frac{1}{2}\beta(t)\frac{\partial^2 u}{\partial x^2} + \delta(t)u|u|^2 - i\alpha(t)u = \frac{1}{2}\varepsilon k_1^2 \beta(t) e^{i\eta} \sin^n \varphi, \tag{88}$$

where $n \in N^+$, $\varphi = e^{-\int_0^t \alpha(\tau)d\tau - i(k_2 x + \frac{1}{2}(a_2 k_1^2 - k_2^2)\int_0^t \beta(\tau)d\tau)} u/c$, $0 < \varepsilon \ll 1$.

From the discussion of Section 3.1, we obtain the second-order approximate Jacobi-like elliptic function solution of Eq. (88) as follows

$$\begin{aligned}\varphi_{2\text{hom}}(x,t) = {} & cn[k_1 x - k_1 k_2 \int_0^t \beta(\tau)d\tau] + \frac{\varepsilon}{\sqrt{2m^2-1}} \int_0^\xi \sin^n(\varphi_0)(e^{\sqrt{2m^2-1}(\xi-\tau)} \\ & - e^{-\sqrt{2m^2-1}(\xi-\tau)})d\tau + \frac{1}{\sqrt{2m^2-1}} \int_0^\xi [-6m^2\varphi_0^2\varphi_1 + \varepsilon n \sin^{n-1}(\varphi_0) \\ & \cos(\varphi_0)\varphi_1](e^{\sqrt{2m^2-1}(\xi-\tau)} - e^{-\sqrt{2m^2-1}(\xi-\tau)})d\tau\end{aligned} \tag{89}$$

$$u_{2\text{hom}}(x,t) = ce^{\int_0^t \alpha(\tau)d\tau + i[k_2 x + \frac{1}{2}\int_0^t ((2m^2-1)k_1^2 - k_2^2)\beta(\tau)d\tau]} \varphi_{2\text{hom}}(x,t). \tag{90}$$

Set $\varphi_{exa}(x,t) = \sum_{i=0}^\infty \varphi_i(x,t)$ to be an exact solution of Eq. (88), notice that

$$\begin{aligned}L(\varphi_{exa} - \varphi_{2\text{hom}}) = {} & f(\varphi) + 2a_4{\varphi_{exa}}^3 - [2a_4{\varphi_0}^3 + f(\varphi_0) + 6a_4\varphi_0^2\varphi_1 \\ & + f_\varphi(\varphi_0)\varphi_1] = \varepsilon \sin^n\left(\sum_{i=0}^\infty \varphi_i\right) + 2a_4\left(\sum_{i=0}^\infty \varphi_i\right)^3 - [2a_4{\varphi_0}^3 + \varepsilon \sin^n(\varphi_0), \\ & + 6a_4\varphi_0^2\varphi_1 + \varepsilon n \sin^{n-1}(\varphi_0)\cos(\varphi_0)\varphi_1] = O(\varepsilon^2)\end{aligned} \tag{91}$$

where $0 < \varepsilon \ll 1$, selecting arbitrary constants such that $\varphi_{exa}(0) = \varphi_{2\text{hom}}(0)$, from the fixed point theorem [41], we have $\varphi_{exa} - \varphi_{2\text{hom}} = O(\varepsilon^2)$, then

$$\begin{aligned}|u_{exa} - u_{2\text{hom}}| & = |A(t)e^{i\eta}[\varphi_{exa} - \varphi_{2\text{hom}}]| \\ & = \left| \frac{\varepsilon^2 A n \sin^{n-1}(\varphi_0)\cos(\varphi_0)}{\sqrt{2m^2-1}} \int_0^\xi \sin^n(\varphi_0)(e^{\sqrt{a_2}(\xi-\tau)} - e^{-\sqrt{a_2}(\xi-\tau)})d\tau \right| = O(\varepsilon^2).\end{aligned} \tag{92}$$

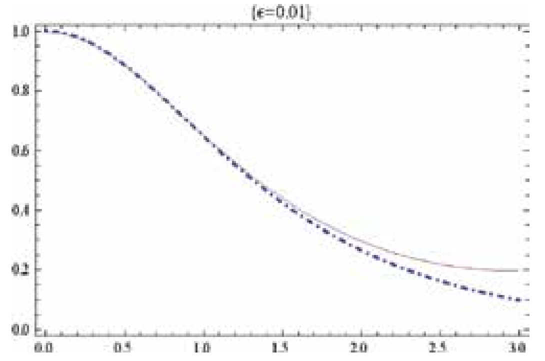

Figure 4. A comparison between the curves of solutions $|u_{1\text{hom}}(\xi)|$ (solid line) and $|u_0(\xi)|$ (dashed line) with $\varepsilon = 0.01$.

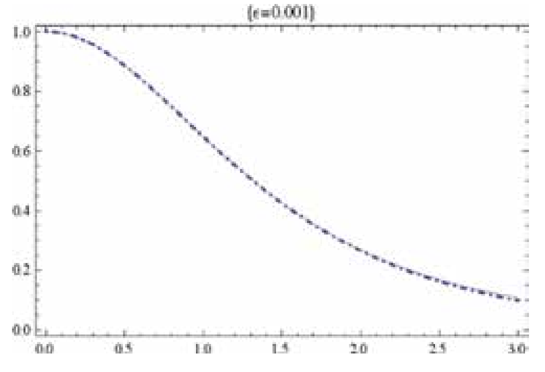

Figure 5. A comparison between the curves of solutions $|u_{1\text{hom}}(\xi)|$ (solid line) and $|u_0(\xi)|$ (dashed line) with $\varepsilon = 0.001$.

Therefore, from the above result, we know that the approximate solution,$u_{2\text{hom}}$, obtained by asymptotic method and possesses better accuracy.

Set $A(t) = 1, k_1 = k_2 = 1, \beta(t) = 1, m \to 1, n = 1, \xi \in [0, 3]$ and $\varepsilon = 0.01, 0.001$ for Eq. (90), and then, we will have the curves of solutions $|u_{1\text{hom}}(\xi)|$ and $|u_0(\xi)|$ and be able to compare them; see **Figures 4** and **5**. From **Figures 4** and **5**, it is easy to see that as $0 < \varepsilon \ll 1$ is a small parameter, and the solutions $|u_{1\text{hom}}(\xi)|$ and $|u_0(\xi)|$ are very close to each other. This behavior is coincident with that of the approximate solution of the weakly disturbed evolution in Eq. (88).

4. Conclusions

We research the generalized perturbed KdV-Burgers equation and GPNLS equation by using the HAM and HPM; these two powerful straightforward methods are much more simple and efficient than some other asymptotic methods such as perturbation method and Adomian decomposition method and so on. The Jacobi elliptic function and solitary wave approximate solution with arbitrary degree of accuracy for the disturbed equation are researched, which shows that these two methods have wide applications in science and engineering and also can be used in the soliton equation with complex variables, but it is still worth to research whether or not these two methods can be used in the system with high dimension and high order.

Acknowledgements

The work is supported by the Scientific Research Foundation of Nanjing Institute of Technology (Grant No. ZKJ201513,2016YB22).

Author details

Baojian Hong

Address all correspondence to: hbj@njit.edu.cn

Department of Mathematical and Physical Science, Nanjing Institute of Technology, Nanjing, China

References

[1] C.H. Gu. Soliton Theory and its applications. Berlin and Heidelberg: Springer-Verlag and GmbH & Co. KG; 1995.

[2] M. Dalir and M. Bashour. Applications of fractional calculus. Applied Mathematical Sciences, 4, 2010, 1021–1032.

[3] J.M. Tu, S.F. Tian, M.J. Xu, P-Li. Ma, T.T. Zhang. On periodic wave solutions with asymptotic behaviors to a(3+1)-dimensional generalized B-type Kadomtsev–Petviashvili equation in fluid dynamics. Computers & Mathematics with Applications, 72(9), 2016, 2486–2504.

[4] M. Sílvio. Duarte Queirós, Celia Anteneodo. Complexity in quantitative finance and economics. Chaos, Solitons & Fractals, 88, 2016, 1–2.

[5] A.H. Kara, Anjan Biswas, Milivoj Belic. Conservation laws for optical solitons in birefringent fibers and magneto-optic waveguides. Optik-International Journal for Light and Electron Optics, 127(24), 2016, 11662–11673.

[6] M.J. Ablowitz, P.A. Clarkson. Solitons. Nonlinear evolution equations and inverse scattering. New York: Cambridge University Press; 1991.

[7] H.Z. Liu, X.P. Xin, Z.G. Wang, X.Q. Liu. Bäcklund transformation classification, integrability and exact solutions to the generalized Burgers'–KdV equation. Communications in Nonlinear Science and Numerical Simulation, 44, 2017, 11–18.

[8] A. Babaaghaie, K. Maleknejad. Numerical solutions of nonlinear two-dimensional partial Volterra integro-differential equations by Haar wavelet. Journal of Computational and Applied Mathematics, 317, 2017, 643–651.

[9] D. Andrei. Polyanin, Alexei Zhuro. Parametrically defined nonlinear differential equations, differential–algebraic equations, and implicit ODEs: transformations, general solutions, and integration methods. Applied Mathematics Letters, 64, 2017, 59–66.

[10] B.J. Hong. New Jacobi elliptic functions solutions for the variable-coefficient mKdV equation. Applied Mathematics and Computation, 215(8), 2009, 2908–2913.

[11] V.A. Galaktionov, E. Mitidieri, S.I. Pohozaev. Variational approach to complicated similarity solutions of higher-order nonlinear PDEs. II. Nonlinear Analysis: Real World Applications, 12, 2011, 2435–2466.

[12] Q.K. Wu. The indirect matching solution for a class of shock problems. Acta Physica Sinica, 54(6), 2005, 2510–2513. (in Chinese)

[13] L.N. Song, W.G. Wang. A new improved Adomian decomposition method and its application to fractional differential equations. Applied Mathematical Modelling, 37(3), 2013, 1590–1598.

[14] Ali H. Nayfeh. Perturbation methods. Wiley VCH; 1973.

[15] V.R. Bond, M.C. Allman. Book review: modern astrodynamics: fundamentals and perturbation methods. Princeton University Press; 1996. Irish Astronomical Journal, 24, 1997, 202.

[16] P.A. Gavin. Physicists' pantheon: great physicists – the life and times of leading physicists from Galileo to Hawking, by William H. Cropper. Oxford University Press; 2001. ISBN 0195137485. Endeavour, 28(1), 2004, 5.

[17] N.N. Bogolyubov, A.A. Logunov, D.V. Shirkov. Dispersion relations and perturbation theory. Soviet Physics Jetp USSR, 37(10), 1959, 574–581.

[18] J.J. Sakurai, S.F. Tuan, R.G. Newton. Modern quantum mechanics. American Journal of Physics, 39(7), 2006, 668.

[19] S.J. Liao. The proposed homotopy analysis technique for the solution of nonlinear problems. PhD thesis, Shanghai Jiao Tong University, 1992.

[20] S.J. Liao, Beyond Perturbati on: introduction to the homotopy analysis method. New York: CRC Press; 2004.

[21] Y.Y. Wu, S.J. Liao. Solving the one-loop soliton solution of the Vakhnenko equation by means of the homotopy analysis method. Chaos, Solitons & Fraction. 23(5), 2004, 1733–1740.

[22] Y. Bouremel. Explicit series solution for the Glauert-jet problem by means of the homotopy analysis method. International Journal of Nonlinear Sciences & Numerical Simulation. 12(5), 2007, 714–724.

[23] L. Song, H. Zhang. Application of homotopy analysis method to fractional KdV–Burgers–Kuramoto equation. Physics Letters A, 367(1–2), 2007, 88–94.

[24] S. Abbasbandy. The application of homotopy analysis method to solve a generalized Hirota–Satsuma coupled KdV equation. Physics Letters A, 361(6), 2007, 478–483.

[25] J.H. He. Homotopy perturbation technique. Computer Methods in Applied Mechanics and Engineering, 178(3–4), 1999, 257–262.

[26] D.D. Ganji. The application of He's homotopy perturbation method to nonlinear equations arising in heat transfer. Physics Letters A, 355, 2006, 337–341.

[27] A.M. Siddiqui, R. Mahmood, Q.K. Ghori. Homotopy perturbation method for thin film flow of a fourth grade fluid down a vertical cylinder. Physics Letters A, 352, 2006, 404–410.

[28] Jafar Biazar, Hossein Aminikhah. Study of convergence of homotopy perturbation method for systems of partial differential equations. Computers and Mathematics with Applications, 58, 2009, 2221–2230.

[29] B. Li, Y. Chen, H.Q. Zhang. Explicit exact solutions for compound KdV-type and compound KdV Burgers-type equations with nonlinear terms of any ord. Chaos, Solitons & Fractals, 15, 2003, 647–654.

[30] W.G. Zhang, Q.S. Chang, B.G. Jiang. Explicit exact solitary-wave solutions for compound KdV-type and compound KdV-Burgers-type equations with nonlinear terms of any order. Chaos, Solitons & Fractals, 13, 2002, 311–319.

[31] B.F. Feng, Takuji Kawahara. Stationary travelling-wave solutions of an unstable KdV-Burgers equation. Physica D, 137, 2000, 228–236.

[32] S. Abbasbandy. Soliton solutions for the Fitzhugh-Nagumo equation with the homotopy analysis method. Applied Mathematical Modelling, 32, 2008, 2706–2714.

[33] A. Molabahrami, F. Khani. The homotopy analysis method to solve the Burgers-Huxley equation. Nonlinear Analysis: Real World Applications, 10, 2009, 589–600.

[34] A.M. Wazwaz. The tanh method for generalized forms of nonlinear heat conduction and Burgers-Fisher equations. Applied Mathematics and Computation, 169, 2005, 321–338.

[35] J. Wang. Some new and general solutions to the compound KdV-Burgers system with nonlinear terms of any order. Applied Mathematics and Computation, 217, 2010, 1652–1657.

[36] M.M. Hassan. Exact solitary wave solutions for a generalized KdV-Burgers equation. Chaos, Solitons & Fractals. 19, 2004, 1201–1206.

[37] V. Serkin, A. Hasegawa. Novel soliton solutions of the nonlinear Schrödinger equation model. Physical Review Letters, 85, 2000, 4502–4505.

[38] R.Y. Hao, L. Li, Z. Li, et al. A new approach to exact soliton solutions and soliton interaction for the nonlinear Schrödinger equation with variable coefficients. Optics Communications, 236, 2004, 79–86.

[39] Y. Chen, B. Li. An extended sub-equation rational expansion method with symbolic computation and solutions of the nonlinear Schrödinger equation model. Nonlinear Analysis: Hybrid Systems, 2, 2008, 242–255.

[40] B.J. Hong, D.C. Lu. New exact solutions for the generalized variable-coefficient Gardner equation with forcing term. Applied Mathematics and Computation, 219, 2012, 2732–2738.

[41] L. Barbu, G. Morosanu. Singularly perturbed boundary-value problems. Basel: Birkhauserm Verlag AG; 2007.

Chapter 3

Green Function

Jing Huang

Additional information is available at the end of the chapter

http://dx.doi.org/10.5772/68028

Abstract

Both the scalar Green function and the dyadic Green function of an electromagnetic field and the transform from the scalar to dyadic Green function are introduced. The Green function of a transmission line and the propagators are also presented in this chapter.

Keywords: Green function, boundary condition, scatter, propagator, convergence

1. Introduction

In 1828, Green introduced a function, which he called a potential, for calculating the distribution of a charge on a surface bounding a region in Rn in the presence of external electromagnetic forces. The Green function has been an interesting topic in modern physics and engineering, especially for the electromagnetic theory in various source distributions (charge, current, and magnetic current), various construct conductors, and dielectric. Even though most problems can be solved without the use of Green functions, the symbolic simplicity with which they could be used to express relationships makes the formulations of many problems simpler and more compact. Moreover, it is easier to conceptualize many problems; especially the dyadic Green function is generalized to layered media of planar, cylindrical, and spherical configurations.

2. Definition of Green function

2.1. Mathematics definition

For the linear operator, there are: $\hat{L}x = f(t)$, $t > 0$;

$$x(t)|_{t=0} = y_0; \cdots x^{(n)}(t)|_{t=0} = y_n \tag{1}$$

Rewriting Eq. (1) as:

$$\hat{L}x = \int f(t')\delta(t-t')dt' \tag{2}$$

Defining the Green function as:

$$\hat{L}G(t,t') = \delta(t-t') \tag{3}$$

So, the solution of Eq. (1) is:

$$x(t) = \int f(t')G(t,t')dt' \tag{4}$$

We give several types of Green functions [1]

$\hat{L} = -(\frac{d^2}{dt^2} + 2\gamma\frac{d}{dt} + \omega_0^2)$	$G(t,t') = \frac{1}{2\pi}\int_{-\infty}^{+\infty} \frac{\exp[-i(t-t')k]}{k^2 + 2i\gamma k - \omega_0^2} dk$
$\hat{L} = -[f_0(t)\frac{d^2}{dt^2} + f_1(t)\frac{d}{dt} + f_2(t))$	$G(t,t') = -\frac{\Psi_1(t)\Psi_2(t') - \Psi_2(t)\Psi_1(t')}{f_0(t')[\Psi_1(t')\dot{\Psi}_2(t') - \dot{\Psi}_1(t')\Psi_2(t')]}$
$\hat{L} = -\frac{d}{dt}[(1-t^2)\frac{d}{dt}]$	$G(t,t') = \frac{1}{2} + \sum_{n=1}^{\infty} \frac{1}{n(n+1)} \cdot \frac{2n+1}{2} P_n(t)P_n(t')$

3. The scalar Green function

3.1. The scalar Green function of an electromagnetic field

The Green function of a wave equation is the solution of the wave equation for a point source [2]. And when the solution to the wave equation due to a point source is known, the solution due to a general source can be obtained by the principle of linear superposition (see **Figure 1**).

This is merely a result of the linearity of the wave equation, and that a general source is just a linear superposition of point sources. For example, to obtain the solution to the scalar wave equation in V in **Figure 1**

$$(\nabla^2 + k^2)\varphi(\mathbf{r}) = s(\mathbf{r}) \tag{5}$$

we first seek the Green function in the same V, which is the solution to the following equation:

$$(\nabla^2 + k^2)g(\mathbf{r},\mathbf{r}') = \delta(\mathbf{r}-\mathbf{r}') \tag{6}$$

Given $g(\mathbf{r},\mathbf{r}')$, $\phi(\mathbf{r})$ can be found easily from the principle of linear superposition, since $g(\mathbf{r},\mathbf{r}')$ is the solution to Eq. (5) with a point source on the right-hand side. To see this more clearly, note that an arbitrary source $s(\mathbf{r})$ is just

http://dx.doi.org/10.5772/68028

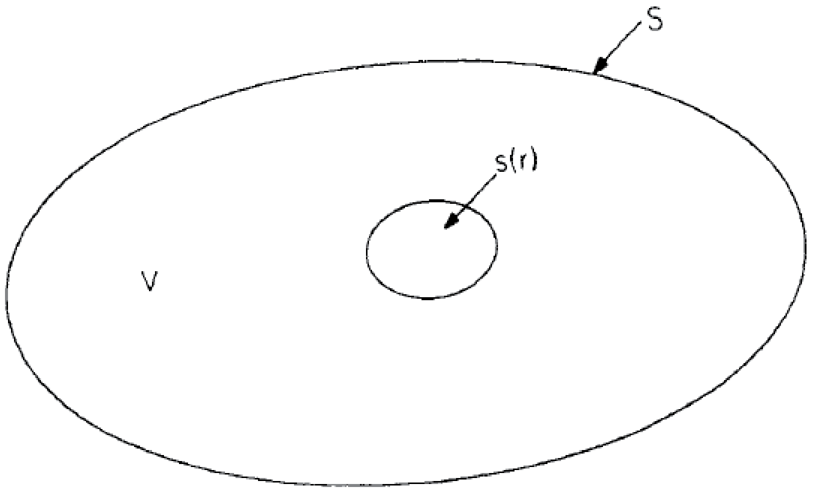

Figure 1. The radiation of a source s(r) in a volume V.

$$s(\mathbf{r}) = \int d\mathbf{r}' s(\mathbf{r}')\delta(\mathbf{r} - \mathbf{r}') \tag{7}$$

which is actually a linear superposition of point sources in mathematical terms. Consequently, the solution to Eq. (5) is just

$$\varphi(\mathbf{r}) = -\int_V d\mathbf{r}' g(\mathbf{r}, \mathbf{r}') s(\mathbf{r}') \tag{8}$$

which is an integral linear superposition of the solution of Eq. (6). Moreover, it can be seen that **g(r, r′)** $\equiv$ **g(r′, r**,) from reciprocity irrespective of the shape of V.

To find the solution of Eq. (6) for an unbounded, homogeneous medium, one solves it in spherical coordinates with the origin at **r**'. By so doing, Eq. (6) becomes

$$(\nabla^2 + k^2) g(\mathbf{r}) = \delta(x)\delta(y)\delta(z) \tag{9}$$

But due to the spherical symmetry of a point source, $g(\mathbf{r})$ must also be spherically symmetric. Then, for $\mathbf{r} \neq 0$, adopt the proper coordinate origin (the vector **r** is replaced by the scalar r), the homogeneous, spherically symmetric solution to Eq. (9) is given by

$$g(r) = c_1 \frac{e^{ikr}}{r} + c_2 \frac{e^{-ikr}}{r} \tag{10}$$

Since sources are absent at infinity, physical grounds then imply that only an outgoing solution can exist; hence,

$$g(r) = c \frac{e^{ikr}}{r} \tag{11}$$

The constant c is found by matching the singularities at the origin on both sides of Eq. (9). To do this, we substitute Eq. (11) into Eq. (9) and integrate Eq. (9) over a small volume about the origin to yield

$$\int_{\Delta V} dV \nabla \cdot \nabla \frac{ce^{ik\mathbf{r}}}{r} + \int_{\Delta V} dV k^2 \frac{ce^{ikr}}{r} = -1 \tag{12}$$

Note that the second integral vanishes when $\Delta V \to 0$ because $dV = 4\pi r2dr$. Moreover, the first integral in Eq. (12) can be converted into a surface integral using Gauss theorem to obtain

$$\lim_{r\to 0} 4\pi r^2 \frac{d}{dr} c \frac{e^{ikr}}{r} = -1 \tag{13}$$

or $c = 1/(4\pi)$.

The solution to Eq. (6) must depend only on $\mathbf{r} - \mathbf{r}'$. Therefore, in general,

$$g(\mathbf{r}, \mathbf{r}') = g(\mathbf{r} - \mathbf{r}') = \frac{e^{ik(\mathbf{r}-\mathbf{r}')}}{4\pi(\mathbf{r} - \mathbf{r}')} \tag{14}$$

implying that $g(\mathbf{r}, \mathbf{r}')$ is translationally invariant for unbounded, homogeneous media. Consequently, the solution to Eq. (5), from Eq. (9), is then

$$\varphi(\mathbf{r}) = -\int_V d\mathbf{r}' \frac{e^{ik(\mathbf{r}-\mathbf{r}')}}{4\pi(\mathbf{r} - \mathbf{r}')} s(\mathbf{r}') \tag{15}$$

Once $\varphi(\mathbf{r})$ and $\hat{n} \cdot \nabla\varphi(\mathbf{r})$ are known on S, then $\varphi(\mathbf{r}')$ away from S could be found

$$\varphi(\mathbf{r}') = \oint_S dS\hat{n} \cdot [g(\mathbf{r}, \mathbf{r}')\nabla\varphi(\mathbf{r}) - \varphi(\mathbf{r})\nabla g(\mathbf{r}, \mathbf{r}')] \tag{16}$$

3.2. The scalar Green functions of one-dimensional transmission lines

We consider a transmission line excited by a distributed current source, $K(x)$, as sketched in **Figure 2**. The line may be finite or infinite, and it may be terminated at either end with impedance or by another line [3]. For a harmonically oscillating current source $K(x)$, the voltage and the current on the line satisfy the following pair of equations:

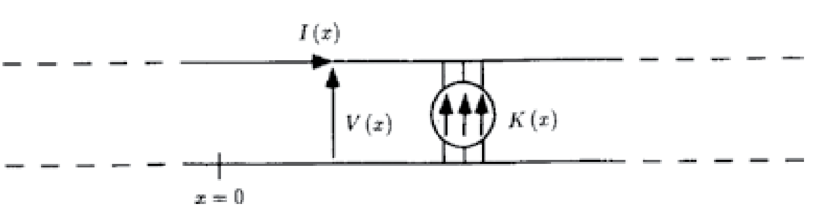

Figure 2. Transmission line excited by a distributed current source, $K(x)$.

http://dx.doi.org/10.5772/68028

$$\frac{\mathrm{d}V(x)}{dx} = i\omega LI(x) \tag{17}$$

$$\frac{dI(x)}{dx} = i\omega CV(x) + K(x) \tag{18}$$

L and C denote, respectively, the distributed inductance and capacitance of the line.

By eliminating $I(x)$ between Eq. (17) and Eq. (18), there is

$$\frac{d^2V(x)}{dx^2} + k^2V(x) = i\omega LK(x) \tag{19}$$

where $k = \omega\sqrt{LC}$ denotes the propagation constant of the line. Eq. (19) has been designated as an inhomogeneous one-dimensional scalar wave equation.

The Green function pertaining to a one-dimensional scalar wave equation of the form of Eq. (19), denoted by $g(x, x')$, is a solution of the Eq. (9). The solution for $g(x, x')$ is not completely determined unless there are two boundary conditions which the function must satisfy at the extremities of the spatial domain in which the function is defined. The boundary conditions which must be satisfied by $g(x, x')$ are the same as those dictated by the original function which we intend to determine, namely, $V(x)$ in the present case. For this reason, the Green functions are classified according to the boundary conditions, which they must obey. Some of the typical ones (for the transmission line) are illustrated in **Figure 3**.

In general, the subscript 0 designates infinite domain so that we have outgoing waves at $x \to \pm\infty$, often called the radiation condition. Subscript 1 means that one of the boundary conditions satisfies the so-called Dirichlet condition, while the other satisfies the radiation condition. When one of the boundary conditions satisfies the so-called Neumann condition, we use subscript 2. Subscript 3 is reserved for the mixed type. Actually, we should have used a double subscript for two distinct boundary conditions. For example, case (b) of **Figure 3** should be denoted by $g01$, indicating that one radiation condition and one Dirichlet condition are involved. With such an understanding, the simplified notation should be acceptable.

In case (d), a superscript becomes necessary because we have two sets of line voltage and current ($V1$, $I1$) and ($V2$, $I2$) in this problem, and the Green function also has different forms in the two regions. The first superscript denotes the region where this function is defined, and the second superscript denotes the region where the source is located.

Let the domain of **x** corresponds to ($x1$, $x2$). The function $g(x, x')$ in Eq. (9) can represent any of the three types, $g0$, $g1$, and $g2$, illustrated in **Figures 3a–c**, respectively. The treatment of case (d) is slightly different, and it will be formulated later.

(a) By multiplying Eq. (19) by $g(x, x')$ and Eq. (9) by $V(x)$ and taking the difference of the two resultant equations, we obtain

$$\int_{x_1}^{x_2}[V(x)\frac{d^2g_0(x,x')}{dx^2} - g_0(x,x')\frac{d^2V(x,x')}{dx^2}]dx = -\int_{x_1}^{x_2} V(x)\delta(x-x')dx - i\omega L\int_{x_1}^{x_2} K(x)g_0(x,x')dx \tag{20}$$

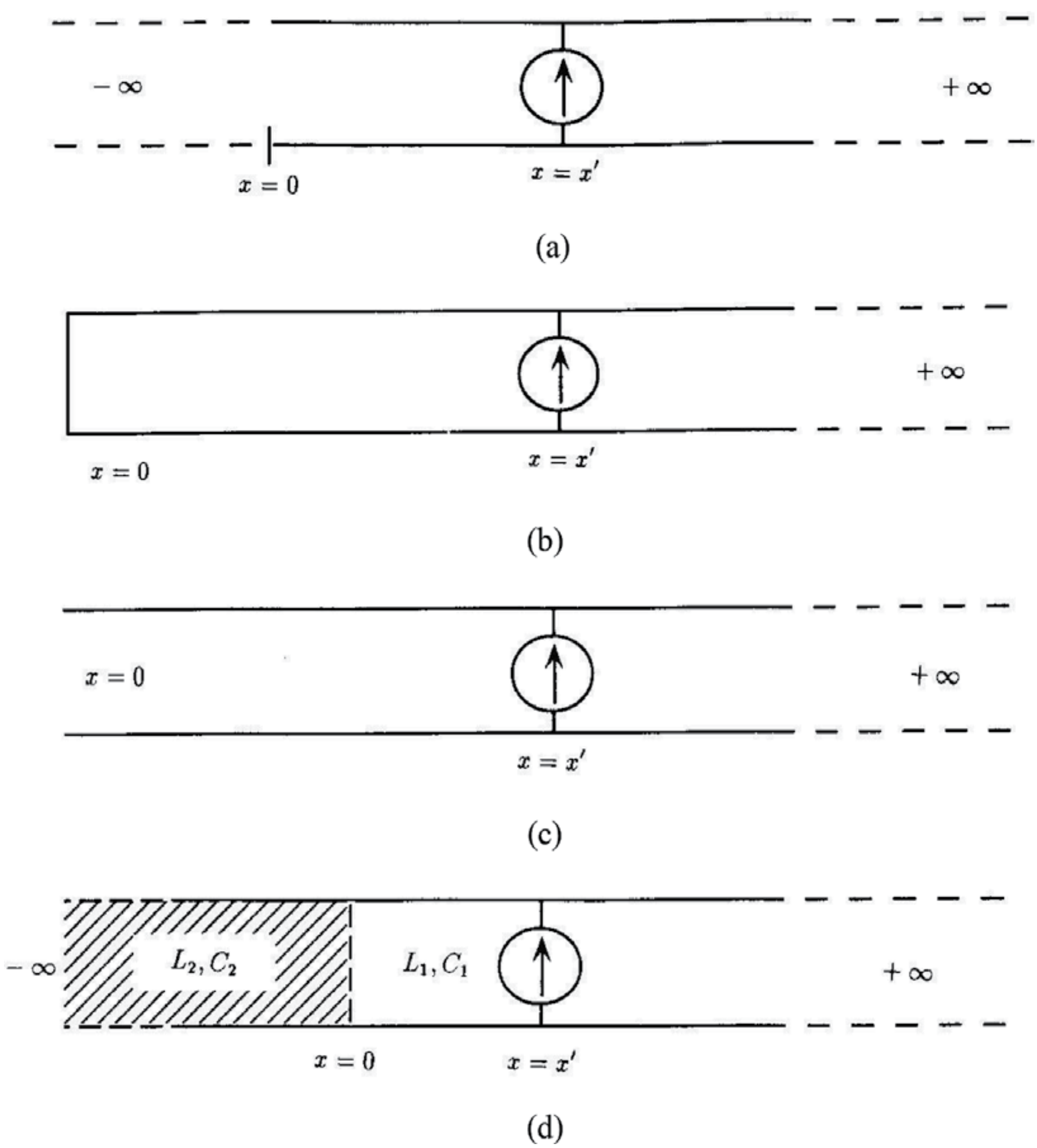

Figure 3. Classification of Green functions according to the boundary conditions.

The first term at the right-hand side of the above equation is simply V(xl), and the term at the left-hand side can be simplified by integration by parts, which gives

$$V(x') = -i\omega L \int_{x_1}^{x_2} g_0(x, x') K(x) dx \tag{21}$$

If we use the unprimed variable x to denote the position of a field point, as usually is the case, Eq. (21) can be changed to [4]

http://dx.doi.org/10.5772/68028

$$V(x) = -i\omega L \int_{x_1}^{x_2} g(x', x)K(x')dx' \\ = -i\omega L \int_{x_1}^{x_2} g_0(x, x')K(x')dx' \tag{22}$$

The last identity is due to the symmetrical property of the Green function. The shifting of the primed and unprimed variables is often practiced in our work. For this reason, it is important to point out that $g(x', x)$, by definition, satisfies the Eq. (9).

The general solutions for Eq. (9) in the two regions (see **Figure 3a**) are

$$g_0(x, x') = \begin{cases} i/(2k)e^{ik(x-x')}, x \geq x' \\ i/(2k)e^{-ik(x-x')}, x \leq x' \end{cases} \tag{23}$$

The choice of the above functions is done with the proper satisfaction of boundary conditions at infinity. At $x = x'$, the function must be continuous, and its derivative is discontinuous.

They are: $[g_0(x, x')]_{x'-0}^{x'+0} = 0$, and $\left[\frac{dg_0(x, x')}{dx}\right]_{x'-0}^{x'+0} = -1$

The physical interpretation of these two conditions is that the voltage at x' is continuous, but the difference of the line currents at x' must be equal to the source current.

(b) The choice of this type of function is done with the proper satisfaction of boundary conditions. At $x = x'$, the function must be continuous, its derivative is discontinuous, and a Dirichlet condition is satisfied at $x = 0$.

$$g_1(x, x') = \begin{cases} \iota/(2\kappa)\left[e^{\iota\kappa(x-x')} - e^{\iota\kappa(x+x')}\right], x \geq x' \\ \iota/(2\kappa)\left[e^{-\iota\kappa(x-x')} - e^{\iota\kappa(x+x')}\right], 0 \leq x \leq x' \end{cases} \tag{24}$$

In view of Eq. (24), it can be interpreted as consisting of an incident and a scattered wave; that is

$$g_1(x, x') = g_0(x, x') + g_{1s}(x, x') \tag{25}$$

where $g_{1s}(x, x') = \frac{-i}{2k} e^{ik(x+x')}$.

Such a notion is not only physically useful, but mathematically it offers a shortcut to finding a composite Green function. It is called as the shortcut method or the method of scattering superposition.

(c) Similarly, the method of scattering superposition suggests that we can start with

$$g_2(x, x') = g_0(x, x') + Ae^{ikx} \tag{26}$$

To satisfy the Neumann condition at $x = 0$, we require

$$\left[\frac{dg_0(x,x')}{dx} + ikAe^{ikx}\right]_{x=0} = 0 \tag{27}$$

Hence

$$A = \frac{i}{2k}e^{ikx'} \tag{28}$$

$$g_2(x,x') = i/(2k)\begin{cases} e^{ik(x-x')} + e^{ik(x+x')}, & x \geq x' \\ e^{-ik(x-x')} + e^{ik(x+x')}, & 0 \leq x \leq x' \end{cases} \tag{29}$$

(d) In this case, we have two differential equations to start with

$$\frac{d^2V_1(x)}{dx^2} + k_1^2V_1(x) = i\omega L_1K_1(x), x \geq 0 \tag{30}$$

$$\frac{d^2V_2(x)}{dx^2} + k_2^2V_2(x) = 0, x \leq 0 \tag{31}$$

It is assumed that the current source is located in region 1 (see **Figure 3d**). We introduce two Green functions of the third kind, denoted by g(11) (x, x') and g(21) (x, x'). g(21), the first number of the superscript corresponds to the region where the function is defined. The second number corresponds to the region where the source is located; then

$$\frac{d^2g^{(11)}(x,x')}{dx^2} + k_1^2g^{(11)}(x,x') = -\delta(x-x'), x \geq 0 \tag{32}$$

$$\frac{d^2g^{(21)}(x,x')}{dx^2} + k_2^2g^{(21)}(x,x') = 0, x \leq 0 \tag{33}$$

At the junction corresponding to x = 0, g(11) and g(21) satisfy the boundary condition that

$$g^{(11)}(x,x')_{x=0} = g^{(21)}(x,x')_{x=0} \tag{34}$$

$$\frac{1}{L_1}\frac{dg^{(11)}(x,x')}{dx}\bigg|_{x=0} = \frac{1}{L_2}\frac{dg^{(21)}(x,x')}{dx}\bigg|_{x=0} \tag{35}$$

The last condition corresponds to the physical requirement that the current at the junction must be continuous. Again, by means of the method of scattering superposition, there are

$$\begin{aligned} g^{(11)}(x,x') &= g_0(x,x') + g_s^{(11)}(x,x') \\ &= \frac{i}{2k_1}\begin{cases} e^{ik_1(x-x')} + \mathrm{R}e^{ik_1(x-x')}, & x \geq x' \\ e^{-ik_1(x-x')} + \mathrm{R}e^{ik_1(x+x')}, & 0 \leq x \leq x' \end{cases} \end{aligned} \tag{36}$$

$$g^{(21)}(x,x') = \frac{i}{2k_1}Te^{-i(k_2x-k_1x')}, x \geq 0 \tag{37}$$

The characteristic impedance of the lines, respectively, is

http://dx.doi.org/10.5772/68028

$$z_1 = \left(\frac{L_1}{C_1}\right)^{1/2}, z_2 = \left(\frac{L_2}{C_2}\right)^{1/2} \tag{38}$$

By the boundary condition, there are

$$R = \frac{z_2 - z_1}{z_2 + z_1}, T = \frac{2z_2}{z_2 + z_1} \tag{39}$$

Example: Green function solution of nonlinear Schrodinger equation in the time domain [5].

The nonlinear Schrodinger equation including nonresonant and resonant nonlinear items is:

$$\begin{aligned}\frac{\partial A}{\partial z} + \frac{i}{2}\beta_2\frac{\partial^2 A}{\partial t^2} - \frac{1}{6}\beta_3\frac{\partial^3 A}{\partial t^3} &= -\frac{a}{2}A + i\frac{3k_0}{8nA_{\text{eff}}}\chi_{NR}^{(3)}|A|^2A \\ &+ \frac{ik_0 g(\omega_0)[1 - if(\omega_0)]}{2nA_{\text{eff}}}A\int_{-\infty}^{t}\chi_R^{(3)}(t-\tau)|A(\tau)|^2 d\tau\end{aligned} \tag{40}$$

Where A is the field, β_2 and β_3 are the second and third order dispersion, respectively. $A(z)$ is the fiber absorption profile. $k_0 = \omega_0/c$, ω_0 is the center frequency. A_{eff} is the effective core area. n is the refractive index.

$$f(\omega_1 + \omega_2 + \omega_3) = \frac{2(\omega_1 + \omega_2 + \omega_3)(1 - |\Gamma|)}{-2(\omega_1 + \omega_2 + \omega_3)^2 - 2|\Gamma| + |\Gamma|^2} \tag{41}$$

$$g(\omega_1 + \omega_2 + \omega_3) = [-2(\omega_1 + \omega_2 + \omega_3)^2 - 2|\Gamma| + |\Gamma|^2] \tag{42}$$

where $g(\omega_1 + \omega_2 + \omega_3)$ is the Raman gain and $f(\omega_1 + \omega_2 + \omega_3)$ is the Raman nongain coefficient. Γ is the attenuation coefficient.

The original nonlinear part is divided into the nonresonant and resonant susceptibility items $\chi_{NR}^{(3)}$ and $\chi_R^{(3)}$. The solution has the form:

$$A(z,t) = \varphi(t)e^{-iEz} \tag{43}$$

Then, there is:

$$\frac{1}{2}\beta_2\frac{\partial^2\phi}{\partial t^2} + \frac{i}{6}\beta_3\frac{\partial^3\phi}{\partial t^3} - \frac{3k_0}{8nA_{\text{eff}}}\chi_{NR}^{(3)}|\phi|^2\phi - \frac{k_0 g(\omega_s)[1 - if(\omega_s)]}{2nA_{\text{eff}}}\phi\int_{-\infty}^{+\infty}\chi_N^{(3)}(t-\tau)|\phi(\tau)|d\tau = E\phi \tag{44}$$

Let:

$$\hat{H}_0(t) = \frac{1}{2}\beta_2\frac{\partial^2}{\partial t^2} + \frac{i}{6}\beta_3\frac{\partial^3}{\partial t^3} \tag{45}$$

$$\hat{V}(t) = \frac{-3k_0}{8nA_{\text{eff}}}\chi_{NR}^{(3)}|\phi| - \frac{k_0 g(\omega_s)[1 - if(\omega_s)]}{2nA_{\text{eff}}}\int_{-\infty}^{+\infty}\chi_R^{(3)}(t-\tau)|\phi(\tau)|^2 d\tau \tag{46}$$

and taking the operator $\hat{V}(t)$as a perturbation item, the eigenequation $-\sum_{n=2}^{k}\frac{i^n}{n!}\beta_n\frac{\partial^n\phi}{\partial T^n}=E\phi$ is

$$\frac{1}{2}\beta_2\frac{\partial^2\phi}{\partial T^2}+\frac{i}{6}\beta_3\frac{\partial^3\phi}{\partial T^3}=E\phi \tag{47}$$

Assuming $E = 1$, we get the corresponding characteristic equation:

$$-\frac{1}{2}\beta_2 r^2+\frac{\beta_3}{6}r^3=E \tag{48}$$

Its characteristic roots are r_1,r_2,r_3. The solution can be represented as:

$$\phi=c_1\phi_1+c_2\phi_2+c_3\phi_3 \tag{49}$$

where $\varphi_m=\exp(ir_m t),\ \ m=1,2,3$, and c_1,c_2,c_3 are determined by the initial pulse. The Green function of Eq. (47) is:

$$(E-\hat{H}_0(t))G_0(t,t')=\delta(t-t') \tag{50}$$

Constructing the Green function as:

$$G_0(t,t')=\begin{cases}a_1\phi_1+a_2\phi_2+a_3\phi_3,\ t>t'\\ b_1\phi_1+b_2\phi_2+b_3\phi_3,\ t<t'\end{cases} \tag{51}$$

At the point $t = t'$, there are:

$$a_1\phi_1(t')+a_2\phi_2(t')+a_3\phi_3(t')=b_1\phi_1(t')+b_2\phi_2(t')+b_3\phi_3(t') \tag{52}$$

$$a_1\phi'_1(t')+a_2\phi'_2(t')+a_3\phi'_3(t')=b_1\phi'_1(t')+b_2\phi'_2(t')+b_3\phi'_3(t') \tag{53}$$

$$a_1\phi''_1(t')+a_2\phi''_2(t')+a_3\phi''_3(t')-b_1\phi''_1(t')-b_2\phi''_2(t')-b_3\phi''_3(t')=-6i/\beta_3 \tag{54}$$

It is reasonable to let $b_1 = b_2 = b_3 = 0$, then:

$$a_1=\frac{\phi_2\dot{\phi}_3-\dot{\phi}_2\phi_3}{W(t')},a_2=\frac{\phi_3\dot{\phi}_1-\dot{\phi}_3\phi_1}{W(t')},a_3=\frac{\phi_1\dot{\phi}_2-\dot{\phi}_1\phi_2}{W(t')} \tag{55}$$

$$W(t')=\begin{vmatrix}\phi_1 & \phi_2 & \phi_3\\ \phi_1^{(1)} & \phi_2^{(1)} & \phi_3^{(1)}\\ \phi_1^{(2)} & \phi_2^{(2)} & \phi_3^{(2)}\end{vmatrix} \tag{56}$$

Finally, the solution of Eq. (44) can be written with the eigenfunction and Green function:

http://dx.doi.org/10.5772/68028

$$\begin{aligned}
\phi(t) &= \phi(t) + \int G_0(t,t')V(t')\phi(t')dt' \\
&= \varphi(t) + \int G_0(t,t',E)V(t')\varphi(t')dt' + \int dt' G_0(t,t',E)V(t')\int G_0(t',t'',E)V(t'')\phi(t'')dt'' \\
&= \varphi(t) + \int G_0(t,t',E)V(t')\varphi(t')dt' + \int dt' G_0(t,t',E)V(t')\int G_0(t',t'',E)V(t'')\varphi(t'')dt'' + \cdots \\
&\quad + \underbrace{\int dt' G_0(t,t')V(t')\int G_0(t',t'')V(t'')dt'' \cdots}_{\text{times } l}\int G_0(t^l,t^{l+1})V(t^{l+1})\phi(t^{l+1})dt^{l+1}
\end{aligned} \tag{57}$$

The accuracy can be estimated by the last term of Eq. (57).

4. The dyadic Green function

4.1. The dyadic Green function for the electromagnetic field in a homogeneous isotropic medium

The Green function for the scalar wave equation could be used to find the dyadic Green function for the vector wave equation in a homogeneous, isotropic medium [3]. First, notice that the vector wave equation in a homogeneous, isotropic medium is

$$\nabla\times\nabla\times\mathbf{E}(\mathbf{r}) - k^2\mathbf{E}(\mathbf{r}) = i\omega\mu\mathbf{J}(\mathbf{r}) \tag{58}$$

Then, by using the fact that $\nabla\times\nabla\times\mathbf{E}(\mathbf{r}) = -\nabla^2\mathbf{E} + \nabla\nabla\cdot\mathbf{E}$ and that $\nabla\cdot\mathbf{E} = \rho/\varepsilon = \nabla\cdot\mathbf{J}/i\omega\varepsilon$, which follows from the continuity equation, we can rewrite Eq. (58) as

$$\nabla^2\mathbf{E}(\mathbf{r}) - k^2\mathbf{E}(\mathbf{r}) = -i\omega\mu\left[\hat{\mathbf{I}} + \frac{\nabla\nabla}{k^2}\right]\cdot\mathbf{J}(\mathbf{r}) \tag{59}$$

where $\hat{\mathbf{I}}$ is an identity operator. In Cartesian coordinates, there are actually three scalar wave equations embedded in the above vector equation, each of which can be solved easily in the manner of Eq. (4). Consequently,

$$\mathbf{E}(\mathbf{r}) = -i\omega\mu\int_V d\mathbf{r}' g(\mathbf{r}'-\mathbf{r})\left[\hat{\mathbf{I}} + \frac{\nabla'\nabla'}{k^2}\right]\cdot\mathbf{J}(\mathbf{r}) \tag{60}$$

where $g(\mathbf{r}'-\mathbf{r})$is the unbounded medium scalar Green function. Moreover, by using the vector identities $\nabla gf = f\nabla g + g\nabla f$and $\nabla\cdot g\mathbf{F} = g\nabla\cdot\mathbf{F} + (\nabla g)\cdot\mathbf{F}$, it can be shown that

$$\int_V d\mathbf{r}' g(\mathbf{r}'-\mathbf{r})\nabla' f(\mathbf{r}') = -\int_V d\mathbf{r}'\nabla' g(\mathbf{r}'-\mathbf{r})f(\mathbf{r}') \tag{61}$$

and

$$\int_V d\mathbf{r}'[\nabla' g(\mathbf{r}' - \mathbf{r})]\nabla' \cdot \mathbf{J}(\mathbf{r}') = -\int_V d\mathbf{r}'\mathbf{J}(\mathbf{r}') \cdot \nabla'\nabla' g(\mathbf{r}' - \mathbf{r}) \tag{62}$$

Hence, Eq. (60) can be rewritten as

$$\mathbf{E}(\mathbf{r}) = i\omega\mu\int_V d\mathbf{r}'\mathbf{J}(\mathbf{r}') \cdot \left[\hat{\mathbf{I}} + \frac{\nabla'\nabla'}{k^2}\right] g(\mathbf{r}' - \mathbf{r}) \tag{63}$$

It can also be derived using scalar and vector potentials.

Alternatively, Eq. (63) can be written as

$$\mathbf{E}(\mathbf{r}) = i\omega\mu\int_V d\mathbf{r}'\mathbf{J}(\mathbf{r}') \cdot \hat{\mathbf{G}}_e(\mathbf{r}', \mathbf{r}) \tag{64}$$

where

$$\hat{\mathbf{G}}_e(\mathbf{r}) = \left[\bar{\mathbf{I}} + \frac{\nabla'\nabla'}{k^2}\right] g(\mathbf{r}' - \mathbf{r}) \tag{65}$$

is a dyad known as the dyadic Green function for the electric field in an unbounded, homogeneous medium. (A dyad is a 3 × 3 matrix that transforms a vector to a vector. It is also a second rank tensor). Even though Eq. (64) is established for an unbounded, homogeneous medium, such a general relationship also exists in a bounded, homogeneous medium. It could easily be shown from reciprocity that

$$\begin{aligned}\left\langle \mathbf{J}_1(\mathbf{r}), \hat{\mathbf{G}}_e(\mathbf{r}, \mathbf{r}'), \mathbf{J}_2(\mathbf{r}') \right\rangle &= \left\langle \mathbf{J}_2(\mathbf{r}), \hat{\mathbf{G}}_e(\mathbf{r}, \mathbf{r}'), \mathbf{J}_1(\mathbf{r}') \right\rangle \\ &= \left\langle \mathbf{J}_1(\mathbf{r}), \hat{\mathbf{G}}_e^t(\mathbf{r}, \mathbf{r}'), \mathbf{J}_2(\mathbf{r}') \right\rangle\end{aligned} \tag{66}$$

where

$$\left\langle \mathbf{J}_i(\mathbf{r}), \hat{\mathbf{G}}_e(\mathbf{r}, \mathbf{r}'), \mathbf{J}_j(\mathbf{r}') \right\rangle = \int_V\int_V dr' dr \mathbf{J}_i(\mathbf{r}') \cdot \hat{\mathbf{G}}_e(\mathbf{r}', \mathbf{r}) \cdot \mathbf{J}_j(\mathbf{r}) \tag{66a}$$

is the relation between Ji and the electric field produced by $\mathbf{J}_j$. Notice that the above equation implies [6]

$$\hat{\mathbf{G}}_e^t(\mathbf{r}', \mathbf{r}) = \hat{\mathbf{G}}_e(\mathbf{r}, \mathbf{r}') \tag{66b}$$

Then, by taking transpose of Eq. (66b), Eq. (64) becomes

$$\mathbf{E}(\mathbf{r}) = i\omega\mu\int_V d\mathbf{r}'\hat{\mathbf{G}}_e(\mathbf{r}, \mathbf{r}') \cdot \mathbf{J}(\mathbf{r}') \tag{67}$$

Alternatively, the dyadic Green function for an unbounded, homogeneous medium can also be written as

http://dx.doi.org/10.5772/68028

$$\hat{\mathbf{G}}_e(\mathbf{r},\mathbf{r}') = \frac{1}{k^2}\left[\nabla\times\nabla\times\hat{\mathbf{I}}g(\mathbf{r}-\mathbf{r}') - \hat{\mathbf{I}}\delta(\mathbf{r}-\mathbf{r}')\right] \tag{68}$$

By substituting Eq. (67) back into Eq. (58) and writing

$$\mathbf{J}(\mathbf{r}) = \int d\mathbf{r}'\hat{\mathbf{I}}\delta(\mathbf{r}-\mathbf{r}')\cdot\mathbf{J}(\mathbf{r}') \tag{69}$$

we can show quite easily that

$$\nabla\times\nabla\times\hat{\mathbf{G}}_e(\mathbf{r},\mathbf{r}') - k^2\hat{\mathbf{G}}_e(\mathbf{r},\mathbf{r}') = \hat{\mathbf{I}}\delta(\mathbf{r}-\mathbf{r}') \tag{70}$$

Equation (64) or (67), due to the $\nabla\nabla$ operator inside the integration operating on $g(\mathbf{r}'-\mathbf{r})$, has a singularity of $1/|\mathbf{r}'-\mathbf{r}|^3$ when $\mathbf{r}'\to\mathbf{r}$. Consequently, it has to be redefined in this case for it does not converge uniformly, specifically, when $\mathbf{r}$ is also in the source region occupied by **J(r)**. Hence, at this point, the evaluation of Eq. (67) in a source region is undefined.

And as the vector analog of Eq. (16)

$$\mathbf{E}(\mathbf{r}') = \oint_S dS\left[\mathbf{n}\times\mathbf{E}(\mathbf{r})\cdot\nabla\times\hat{\mathbf{G}}_e(\mathbf{r},\mathbf{r}') + i\omega\mu\mathbf{n}\times\mathbf{H}(\mathbf{r})\cdot\hat{\mathbf{G}}_e(\mathbf{r},\mathbf{r}')\right] \tag{71}$$

4.2. The boundary condition

The dyadic Green function is introduced mainly to formulate various canonical electromagnetic problems in a systematic manner to avoid treatments of many special cases which can be treated as one general problem [3, 7, 8]. Some typical problems are illustrated in **Figure 4** where (a) shows a current source in the presence of a conducting sphere located in air, (b) shows a conducting cylinder with an aperture which is excited by some source inside the cylinder, (c) shows a rectangular waveguide with a current source placed inside the guide, and (d) shows two semi-infinite isotropic media in contact, such as air and "flat" earth with a current source placed in one of the regions.

Unless specified otherwise, we assume that for problems involving only one medium such as (a), (b), and (c) the medium is air, then the wave number k is equal to $\omega(\mu_0\varepsilon_0)^{1/2} = 2\pi/\lambda$. The electromagnetic fields in these cases are solutions of the wave Eq. (62) and

$$\nabla\times\nabla\times\mathbf{H}(\mathbf{r}) - k^2\mathbf{H}(\mathbf{r}) = \nabla\times\mathbf{J}(\mathbf{r}) \tag{72}$$

The fields must satisfy the boundary conditions required by these problems.

In general, using the notations $\hat{\mathbf{G}}_e$ and $\hat{\mathbf{G}}_m$ to denote, respectively, the electric and the magnetic dyadic Green functions; they are solutions of the dyadic differential equations

$$\nabla\times\nabla\times\hat{\mathbf{G}}_e(\mathbf{r},\mathbf{r}') - k^2\hat{\mathbf{G}}_e(\mathbf{r},\mathbf{r}') = \hat{\mathbf{I}}\delta(\mathbf{r}-\mathbf{r}') \tag{73}$$

$$\nabla\times\nabla\times\hat{\mathbf{G}}_m(\mathbf{r},\mathbf{r}') - k^2\hat{\mathbf{G}}_m(\mathbf{r},\mathbf{r}') = \nabla\times\left[\hat{\mathbf{I}}\delta(\mathbf{r}-\mathbf{r}')\right] \tag{74}$$

is the same as Eq. (70), and there is

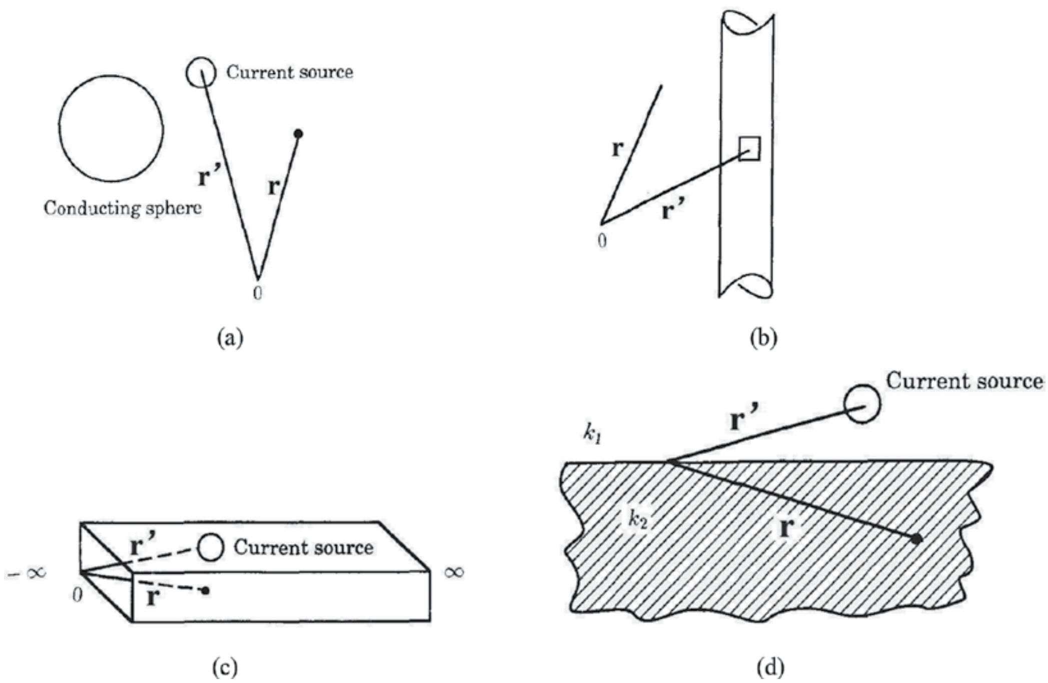

Figure 4. Some typical boundary value problems.

$$\hat{\mathbf{G}}_m = \nabla \times \hat{\mathbf{G}}_e \tag{75}$$

(a) and (b): Electric dyadic Green function (the first kind, using the subscript 1 denotes $\hat{\mathbf{G}}_{e1}$, $\hat{\mathbf{G}}_{m1}$, and the subscript "0" represents the free-space condition that the environment does not have any scattering object) is required to satisfy the dyadic Dirichlet condition on *Sd*, namely,

$$\mathbf{n} \times \hat{\mathbf{G}}_{e1} = 0, \mathbf{n} \times \hat{\mathbf{G}}_{\mathrm{m}1} = 0 \tag{76}$$

So, for (a)

$$\mathbf{E}(\mathbf{r}') = \int d\mathbf{r}\mathbf{J}(\mathbf{r}) \cdot \hat{\mathbf{G}}_e(\mathbf{r}, \mathbf{r}') \tag{77}$$

and for (b)

$$\mathbf{E}(\mathbf{r}') = \oint_{S_A} dS\mathbf{n} \times \mathbf{E}(\mathbf{r}) \cdot \nabla \times \hat{\mathbf{G}}_e(\mathbf{r}, \mathbf{r}') \tag{78}$$

(c) the electric dyadic Green function is required to satisfy the dyadic boundary condition on *Sd*, namely,

$$\mathbf{n} \times \nabla \times \hat{\mathbf{G}}_{e2} = 0 \; \mathbf{n} \times \nabla \times \hat{\mathbf{G}}_{m2} = 0 \tag{79}$$

$$\mathbf{H}(\mathbf{r}') = \int d\mathbf{r}\mathbf{J}(\mathbf{r}) \cdot \nabla \times \hat{\mathbf{G}}_e(\mathbf{r}, \mathbf{r}') \tag{80}$$

(d) For problems involving two isotropic media such as the configuration shown in **Figure 4d**, there are two sets of fields [9]. The wave numbers in these two regions are denoted by $k_1 = \omega(\mu_1 \varepsilon_1)^{1/2}$ and $k_2 = \omega(\mu_2 \varepsilon_2)^{1/2}$. There are four functions for the dyadic Green function of the electric type and another four functions for the magnetic type, denoted, respectively, by $\hat{\mathbf{G}}_e^{11}$ $\hat{\mathbf{G}}_e^{12}$ $\hat{\mathbf{G}}_e^{21}$and $\hat{\mathbf{G}}_e^{22}$, and $\hat{\mathbf{G}}_m^{11}$ $\hat{\mathbf{G}}_m^{12}$ $\hat{\mathbf{G}}_m^{21}$ and $\hat{\mathbf{G}}_m^{22}$. The superscript notation in $\hat{\mathbf{G}}_e^{11}$ means that both the field point and the source point are located in region 1. For $\hat{\mathbf{G}}_e^{21}$, it means that the field point is located in region 1 and the source point is located in region 2. A current source is located in region 1 only, and the two sets of wave equations are

$$\nabla \times \nabla \times \mathbf{E}_1(\mathbf{r}) - k^2 \mathbf{E}_1(\mathbf{r}) = i\omega\mu_1 \mathbf{J}_1(\mathbf{r}) \tag{81}$$

$$\nabla \times \nabla \times \mathbf{H}_1(\mathbf{r}) - k^2 \mathbf{H}_1(\mathbf{r}) = \nabla \times \mathbf{J}_1(\mathbf{r}) \tag{82}$$

and

$$\nabla \times \nabla \times \mathbf{E}_2(\mathbf{r}) - k^2 \mathbf{E}_2(\mathbf{r}) = 0 \tag{83}$$

$$\nabla \times \nabla \times \mathbf{H}_2(\mathbf{r}) - k^2 \mathbf{H}_2(\mathbf{r}) = 0 \tag{84}$$

There are

$$\nabla \times \nabla \times \hat{\mathbf{G}}_e^{11}(\mathbf{r}, \mathbf{r}') - k_1^2 \hat{\mathbf{G}}_e^{11}(\mathbf{r}, \mathbf{r}') = \hat{\mathbf{I}}\delta(\mathbf{r} - \mathbf{r}') \tag{85}$$

$$\nabla \times \nabla \times \hat{\mathbf{G}}_e^{21}(\mathbf{r}, \mathbf{r}') - k_2^2 \hat{\mathbf{G}}_e^{21}(\mathbf{r}, \mathbf{r}') = 0 \tag{86}$$

At the interface, the electromagnetic field and the corresponding dyadic Green function satisfy the following boundary conditions

$$\mathbf{n} \times [\hat{\mathbf{G}}_e^{11} - \hat{\mathbf{G}}_e^{21}] = 0 \tag{87}$$

$$\mathbf{n} \times [\nabla \times \hat{\mathbf{G}}_e^{11}/\mu_1 - \nabla \times \hat{\mathbf{G}}_e^{21}/\mu_2] = 0 \tag{88}$$

The electric fields are

$$\mathbf{E}_1(\mathbf{r}') = i\omega\mu_1 \int d\mathbf{r}\mathbf{J}(\mathbf{r}) \cdot \hat{\mathbf{G}}_e^{11}(\mathbf{r}, \mathbf{r}') \tag{89}$$

$$\mathbf{E}_2(\mathbf{r}') = i\omega\mu_2 \int d\mathbf{r}\mathbf{J}(\mathbf{r}) \cdot \hat{\mathbf{G}}_e^{21}(\mathbf{r}, \mathbf{r}') \tag{90}$$

5. Vector wave functions, L, M, and N

The vector wave functions are the building blocks of the eigenfunction expansions of various kinds of dyadic Green functions. These functions were first introduced by Hansen [10–12] in formulating certain electromagnetic problems.Three kinds of vector wave functions, denoted by **L, M**, and **N**, are solutions of the homogeneous vector Helmholtz equation. To derive the eigenfunction expansion of the magnetic dyadic Green functions that are solenoidal and satisfy with the vector wave equation, the **L** functions are not needed. If we try to find eigenfunction expansion of the electric dyadic Green functions then the **L** functions are also needed.

A vector wave function, by definition, is an eigenfunction or a characteristic function, which is a solution of the homogeneous vector wave equation $\nabla\times\nabla\times\mathbf{F}-\kappa^2\mathbf{F}=0$.

There are two independent sets of vector wave functions, which can be constructed using the characteristic function pertaining to a scalar wave equation as the generating function. One kind of vector wave function, called the Cartesian or rectilinear vector wave function, is formed if we let

$$\mathbf{F}=\nabla\times(\Psi_1\mathbf{c}) \tag{91}$$

where ψ_1 denotes a characteristic function, which satisfies the scalar wave equation

$$\nabla^2\Psi+\kappa^2\Psi=0 \tag{92}$$

And **c** denotes a constant vector, such as **x, y**, or **z**. For convenience, we shall designate **c** as the piloting vector and Ψ as the generating function. Another kind, designated as the spherical vector wavefunction, will be introduced later, whereby the piloting vector is identified as the spherical radial vector **R**.

Actually, substituting Eq. (91) into Eq. (92), it is

$$\nabla\times[\mathbf{c}(\nabla^2\Psi_1+\kappa^2\Psi_1)]=0 \tag{93}$$

The set of functions so obtained

$$\mathbf{M}_1=\nabla\times(\Psi_1\mathbf{c}) \tag{94}$$

$$\mathbf{N}_2=\frac{1}{\kappa}\nabla\times\nabla\times(\Psi_2\mathbf{c}) \tag{95}$$

$$\mathbf{L}_3=\nabla(\Psi_3) \tag{96}$$

Ψ_2,Ψ_3 denote the characteristic functions which also satisfy (92) but may be different from the function used to define **M**1.

In the following, the expressions for the dyadic Green functions of a rectangular waveguide will be derived asserting to the vector wave functions. The method and the general procedure would apply equally well to other bodies (cylindrical waveguide, circular cylinder in free space, and inhomogeneous media and moving medium).

Figure 5 shows the orientation of the guide with respect to the rectangular coordinate system, and we will choose the unit vector **z** to represent the piloting vector **c**.

The scalar wave function

$$\Psi=(A\cos k_x x+B\sin k_x x)(C\cos k_y y+D\sin k_y y)e^{ihz} \tag{97}$$

where $k_x^2+k_y^2+h^2=\kappa^2$.

http://dx.doi.org/10.5772/68028

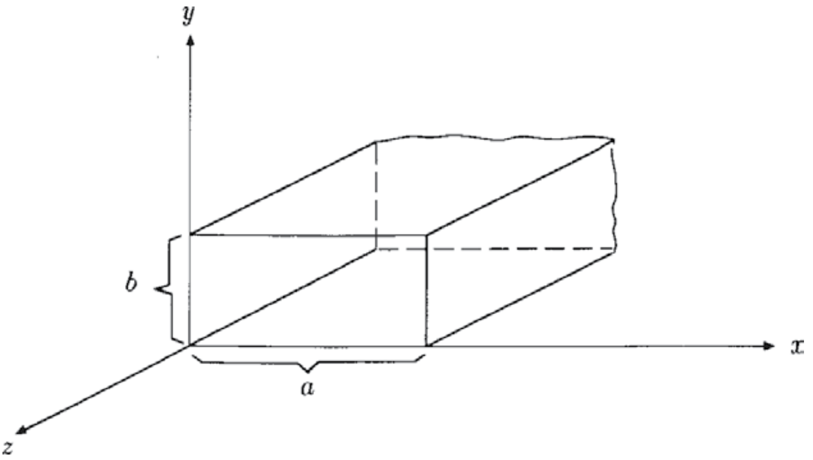

Figure 5. A rectangular waveguide.

the constants k_x and k_y should have the following characteristic values

$$k_x = \frac{m\pi}{a}, m = 0, 1, \cdots \tag{98}$$

$$k_y = \frac{n\pi}{b}, n = 0, 1, \cdots \tag{99}$$

The complete expression and the notation for the set of functions **M**, which satisfy the vector Dirichlet condition are

$$\begin{aligned} \mathbf{M}_{emn}(h) &= \nabla \times [\Psi_{emn}\mathbf{z}] \\ &= (-k_y C_x S_y \mathbf{x} + k_x C_y S_x \mathbf{y})e^{ihz} \end{aligned} \tag{100}$$

where $S_x = \sin k_x x, C_x = \cos k_x x,\ S_y = \sin k_y y, C_y = \cos k_y y$. The subscript "$e$" attached to **M**$emn$ is an abbreviation for the word "even," and "o" for "odd."

In a similar manner

$$\mathbf{N}_{omn} = \frac{1}{\kappa}(ihk_x C_x S_y \mathbf{x} + ihk_y C_y S_x \mathbf{y} + (k_x^2 + k_y^2) S_x S_y \mathbf{z})e^{ihz} \tag{101}$$

It is obvious that **M**emn represents the electric field of the $TEmn$ mode, while **N**omn represents that of the $TMmn$ mode.

In summary, the vector wave functions, which can be used to represent the electromagnetic field inside a rectangular waveguide, are of the form

$$\mathbf{M}_{e(o)mn} = \nabla \times [\Psi_{e(o)mn}\mathbf{z}] \tag{102}$$

$$\mathbf{N}_{e(o)mn} = \frac{1}{\kappa}\nabla \times \nabla \times [\Psi_{e(o)mn}\mathbf{z}] \tag{103}$$

Then

$$\hat{\mathbf{G}}_{m2}(\mathbf{R},\mathbf{R}') = \int_{-\infty}^{+\infty} dh \sum_{m,n} \frac{(2-\delta_0)\kappa}{\pi ab(k_x^2+k_y^2)} \cdot [a(h)\mathbf{N}_{emn}(h)\mathbf{M}'_{emn}(-h) + b(h)\mathbf{M}_{omn}(h)\mathbf{N}'_{omn}(-h)] \quad (104)$$

where $a(h) = b(h) = \frac{1}{\kappa^2 - k^2}$, $h = \pm(k^2 - k_x^2 - k_y^2)^{1/2}$and $\delta_0 = \begin{cases} 1, m = 0 or n = 0 \\ 0, m \neq 0, \ n \neq 0 \end{cases}.$

M', N', m', n', h' denote another set of values, which may be distinct or the same as **M, N**, m, n, h.

6. Retarded and advanced Green functions

Green function is also utilized to solve the Schrödinger equation in quantum mechanics. Being completely equivalent to the Landauer scattering approach, the GF technique has the advantage that it calculates relevant transport quantities (e.g., transmission function) using effective numerical techniques. Besides, the Green function formalism is well adopted for atomic and molecular discrete-level systems and can be easily extended to include inelastic and many-body effects [13, 14].

(A) The definitions of propagators

The time-dependent Schrödinger equation is:

$$i\hbar \frac{\partial|\Psi(t)\rangle}{\partial t} = \hat{H}|\Psi(t)\rangle \quad (105)$$

The solution of this equation at time t can be written in terms of the solution at time t':

$$|\Psi(t)\rangle = \hat{U}(t,t')|\Psi(t')\rangle \quad (106)$$

where $\hat{U}(t,t')$ is called the time-evolution operator.

For the case of a time-independent Hermitian Hamiltonian $\hat{H}$, so that the eigenstates $|\Psi_n(t)\rangle = e^{-iE_n t/\hbar}|\Psi_n\rangle$ with energies E_n are found from the stationary Schrödinger equation

$$\hat{H}|\Psi_n\rangle = E_n|\Psi_n\rangle \quad (107)$$

The eigenfunctions $|\Psi_n\rangle$are orthogonal and normalized, for discrete energy levels 1:

$$\langle\Psi_m|\Psi_n\rangle = \delta_{mn} \quad (108)$$

and form a complete set of states ($\hat{I}$ is the unity operator)

$$\sum_n \langle\Psi_n|\Psi_n\rangle = 1 \quad (109)$$

The time-evolution operator for a time-independent Hamiltonian can be written as

http://dx.doi.org/10.5772/68028

$$\hat{U}(t-t') = e^{-i(t-t')\hat{H}/\hbar} \tag{110}$$

This formal solution is difficult to use directly in most cases, but one can obtain the useful eigenstate representation from it. From the identity $\hat{U} = \hat{U}\hat{I}$ and (107), (109), (110) it follows that

$$\hat{U}(t-t') = \sum_n e^{i/\hbar E_n(t-t')}|\Psi_n\rangle\langle\Psi_n| \tag{111}$$

which demonstrates the superposition principle. The wave function at time t is

$$|\Psi(t)\rangle = \hat{U}(t,t')|\Psi(t')\rangle = \sum_n e^{-i/\hbar E_n(t-t')}\langle\Psi_n|\Psi(t')|\Psi_n\rangle \tag{112}$$

where $\langle\Psi_n|\Psi(t')\rangle$ are the coefficients of the expansion of the initial function $|\Psi(t')\rangle$on the basis of eigenstates.

It is equivalent and more convenient to introduce two Green operators, also called propagators, retarded $\hat{G}^R(t,t')$ and advanced $\hat{G}^A(t,t')$:

$$\hat{G}^R(t,t') = -\frac{i}{\hbar}\theta(t-t')\hat{U}(t,t') = -\frac{i}{\hbar}\theta(t-t')e^{-i(t-t')\hat{H}/\hbar} \tag{113}$$

$$\hat{G}^A(t,t') = \frac{i}{\hbar}\theta(t'-t)\hat{U}(t,t') = \frac{i}{\hbar}\theta(t'-t)e^{-i(t-t')\hat{H}/\hbar} \tag{114}$$

so that at $t > t'$ one has

$$|\Psi(t)\rangle = i\hbar\hat{G}^R(t-t')|\Psi(t')\rangle \tag{115}$$

while at $t < t'$ it follows

$$|\Psi(t)\rangle = i\hbar\hat{G}^A(t-t')|\Psi(t')\rangle \tag{116}$$

The operators $\hat{G}^R(t,t')$ at $t > t'$and $\hat{G}^A(t,t')$ at $t < t'$ are the solutions of the equation

$$\left[i\hbar\frac{\partial}{\partial t} - \hat{H}\right]\hat{G}^{R(A)}(t,t') = \hat{I}\delta(t-t') \tag{117}$$

with the boundary conditions $\hat{G}^R(t,t') = 0$ at $t < t'$, $\hat{G}^A(t,t') = 0$ at $t > t'$. Indeed, at $t > t'$ Eq. (118) satisfies the Schrödinger equation Eq. (105) due to Eq. (117). And integrating Eq. (117) from $t = t' - \eta$ to $t = t' + \eta$ where η is an infinitesimally small positive number $\eta = 0^+$, one gets

$$\hat{G}^R(t+\eta,t') = \frac{1}{i\hbar}\hat{I} \tag{118}$$

giving correct boundary condition at $t = t'$. Thus, if the retarded Green operator $\hat{G}^R(t,t')$ is known, the time-dependent wave function at any initial condition is found (and makes many other useful things, as we will see below).

For a time-independent Hamiltonian, the Green function is a function of the time difference $\tau = t - t'$, and one can consider the Fourier transform

$$\hat{G}^{R(A)}(E) = \int_{-\infty}^{+\infty} \hat{G}^{R(A)}(\tau) e^{iE\tau/\hbar} d\tau \tag{119}$$

This transform, however, can not be performed in all cases, because $\hat{G}^{R(A)}(E)$ includes oscillating terms $e^{iE\tau/\hbar}$. To avoid this problem we define the retarded Fourier transform

$$\hat{G}^{R}(E) = \lim_{\eta \to 0+} \int_{-\infty}^{+\infty} \hat{G}^{R}(\tau) e^{i(E+i\eta)\tau/\hbar} d\tau \tag{120}$$

and the advanced one

$$\hat{G}^{A}(E) = \lim_{\eta \to 0+} \int_{-\infty}^{+\infty} \hat{G}^{A}(\tau) e^{i(E-i\eta)\tau/\hbar} d\tau \tag{121}$$

where the limit $\eta \to 0$ is assumed in the end of calculation. With this addition, the integrals are convergent. This definition is equivalent to the definition of a retarded (advanced) function as a function of complex energy variable at the upper (lower) part of the complex plain.

Applying this transform to Eq. (117), the retarded Green operator is

$$\hat{G}^{R}(E) = [(E + i\eta)\hat{I} - \hat{H}]^{-1} \tag{122}$$

The advanced operator $\hat{G}^{A}(E)$ is related to the retarded one through

$$\hat{G}^{A}(E) = \hat{G}^{R+}(E) \tag{123}$$

Using the completeness property $\sum_n |\Psi_n\rangle\langle\Psi_n| = 1$, there is

$$\hat{G}^{R}(E) = \sum_n \frac{|\Psi_n\rangle\langle\Psi_n|}{(E + i\eta)\hat{I} - \hat{H}} \tag{124}$$

and

$$\hat{G}^{R}(E) = \sum_n \frac{|\Psi_n\rangle\langle\Psi_n|}{E - E_n + i\eta} \tag{125}$$

Apply the ordinary inverse Fourier transform to $\hat{G}^{R}(E)$, the retarded function becomes

$$\hat{G}^{R}(\tau) = \int_{-\infty}^{+\infty} \hat{G}^{R}(E) e^{-iE\tau/\hbar} \frac{dE}{2\pi\hbar} = -\frac{i}{\hbar}\theta(\tau) \sum_n e^{-iE_n\tau/\hbar} |\Psi_n\rangle\langle\Psi_n| \tag{126}$$

http://dx.doi.org/10.5772/68028

Indeed, a simple pole in the complex E plain is at $E = E_n - i\eta$, the residue in this point determines the integral at $\tau > 0$ when the integration contour is closed through the lower half-plane, while at $\tau < 0$ the integration should be closed through the upper half-plane and the integral is zero.

The formalism of retarded Green functions is quite general and can be applied to quantum systems in an arbitrary representation. For example, in the coordinate system Eq. (124) is

$$\hat{G}^R(\mathbf{r}, \mathbf{r}', E) = \frac{\sum_n \langle \mathbf{r}|\Psi_n\rangle\langle\Psi_n|\mathbf{r}'\rangle}{E - E_n + i\eta} = \sum_n \frac{\Psi_n(\mathbf{r})\Psi_n^*(\mathbf{r})}{E - E_n + i\eta} \tag{127}$$

(B) Path integral representation of the propagator

In the path integral representation, each path is assigned an amplitude $e^{i\int dtL}$, L is the Lagrangian function. The propagator is the sum of all the amplitudes associated with the paths connecting *xa* and *xb* (**Figure 6**). Such a summation is an infinite-dimensional integral.

The propagator satisfies

$$iG(x_b, t_b, x_a, t_a) = \int dx iG(x_b, t_b, x, t) iG(x, t, x_a, t_a) \tag{128}$$

Let us divide the time interval [*ta, tb*] into N equal segments, each of length $\Delta t = (t_b - t_a)/N$.

$$\begin{aligned} iG(x_b, t_b, x_a, t_a) &= \int dx_1 \cdots dx_N \prod_{j=1}^{N} iG(x_j, t_j, x_{j-1}, t_{j-1}) \\ &= A^N \int \prod_j dx_j \exp\left[i \sum \Delta t L(t_j, \frac{x_j + x_{j-1}}{2}, \frac{x_j - x_{j-1}}{2}) \right] \\ &= \int D(x) e^{i\int dtL(t,x,\dot{x})} \end{aligned} \tag{129}$$

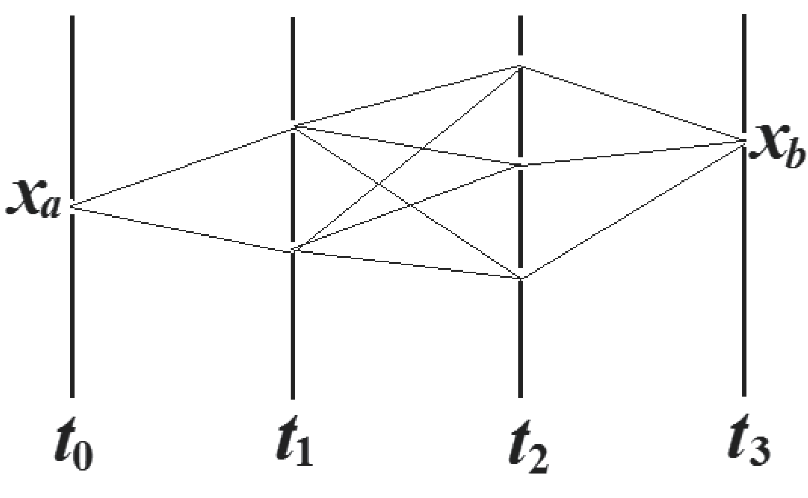

Figure 6. The total amplitude is the sum of all amplitudes associated with thee paths connecting *xa* and *xb*.

where $\ln[iG(x_j, t_j, x_{j-1}, t_{j-1})] = i\Delta t L(t_j, \frac{x_j+x_{j-1}}{2}, \frac{x_j-x_{j-1}}{2})$.

Example: LC circuit-based metamaterials

In this section, we will use the relationship of current and voltage in the LC circuit to build the propagator of the LC circuit field coupled to an atom.

Figure 7 shows the LC-circuit.The following are valid:

$$I = -\frac{dq}{dt} \tag{130}$$

$$V = \frac{q}{C} = L\frac{dI}{dt} \tag{131}$$

Thus:

$$C\frac{d^2x}{dt^2} = -\frac{x}{L} \tag{132}$$

where $x = LI$, I is the current, V is the voltage, q is the charge quantity, L and C are the inductance and capacitance, respectively. Eq. (132) is equal to a harmonic, and the Lagrangian operator is:

$$L_0(x,\dot{x}) = \frac{1}{2g}(\dot{\varepsilon}^2 - \Omega_{LC}^2\varepsilon^2) \tag{133}$$

The Lagrangian operator describing the bipole is:

$$L_0(x,\dot{x}) = \frac{m}{2}\dot{x}^2 - \frac{m\Omega_0^2}{2}x^2 \tag{134}$$

where x is the coordinate of the bipole, ε is the LC field, m is the mass of an electron, and e is the unit of charge. $g = \frac{1}{c}$, and $\Omega_{LC} = \frac{1}{\sqrt{LC}}$. Defining their action items as:

$$S_{LC} = \int dt \left[\frac{1}{2g}(\dot{\varepsilon}^2 - \Omega_{LC}^2\varepsilon^2)\right] \tag{135}$$

And

$$S_0 = \int dt \left[\frac{m}{2}(\dot{x}^2 - \Omega_0^2 x^2)\right] \tag{136}$$

Taking the coupling effect $(ex\varepsilon)$ into account, the Green function of the coupled system is:

$$G(\mathbf{x}, \boldsymbol{\varepsilon}) = \int DxD\varepsilon e^{iS_{LC}+iS_0+i\int dt[ex\varepsilon]} \tag{137}$$

Where $\mathbf{x}$ represents the series coordinates $x1,x2,\ldots$,and so on and $\boldsymbol{\varepsilon}$ represents $\varepsilon1,\varepsilon2,\ldots.$, and so on.

http://dx.doi.org/10.5772/68028

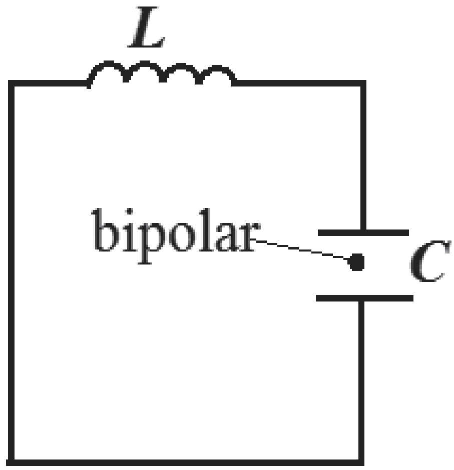

Figure 7. The coupled system, including an LC field and a bipole.

7. The recent applications of the Green function method

7.1. Convergence

In the Green function, the high oscillation of Bessel/Hankel functions in the integrands results in quite time-consuming integrations along the Sommerfeld integration paths (SIP) which ensures that the integrands can satisfy the radiation condition in the direction normal to the interface of a medium. To facilitate the evaluation, the method of moments (MoM) [15], the steepest descent path (SDP) method, and the discrete complex image method (DCIM) [16, 17] are very important methods.

The technique for locating the modes is quite necessary for accurately calculating the spatial Green functions of a layered medium. The path tracking algorithm can obtain all the modes for the configuration shown in **Figure 8**, even when region 2 is very thick [18]. Like the method in Ref. [19], it does not involve a contour integration and could be extended to more complicated configurations.

The discrete complex image method (DCIM) has been shown to deteriorate sharply for distances between source and observation points larger than a few wavelengths [20]. So, the total least squares algorithm (TLSA) is applied to the determination of the proper and improper poles of spectral domain multilayered Green's functions that are closer to the branch point and to the determination of the residues at these poles [21].

The complex-plane $k\rho$ for the determination of proper and improper poles is shown in **Figure 9**. Since half the ellipse is in the proper sheet of the $k\rho$-plane and half the ellipse is in the improper sheet, the poles will not only correctly capture the information of the proper poles but will also capture the information of those improper poles that are closer to the branch point $k\rho = k0$.

For the 2-D dielectric photonic crystals as shown in **Figure 10**, the integral equation is written in terms of the unknown equivalent current sources flowing on the surfaces of the periodic

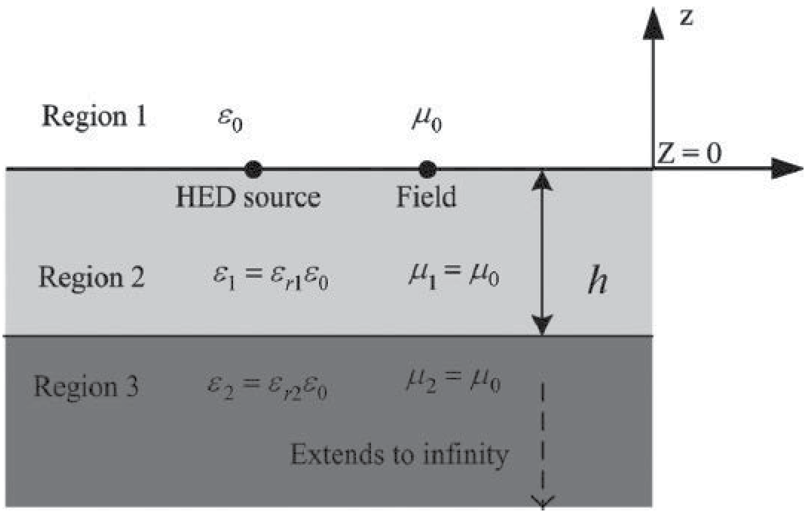

Figure 8. A general configuration with a three-layered medium: region 1 is free space, region 2 is a substrate with thickness h and relative permittivity $\varepsilon r1$, and region 3 is a half space with relative permittivity $\varepsilon r2$.

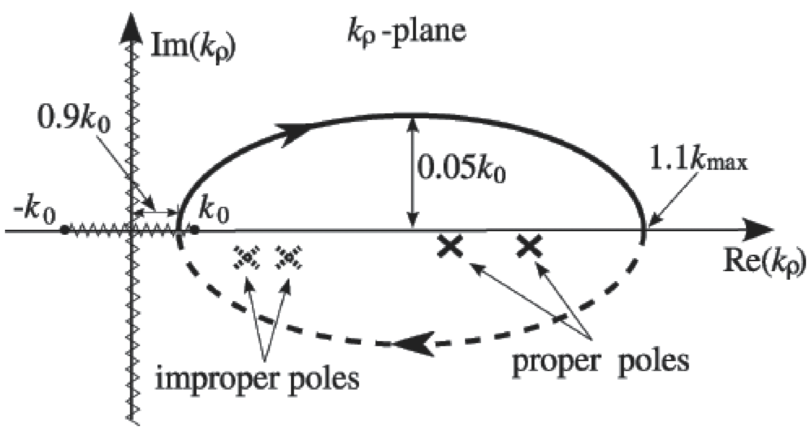

Figure 9. Elliptic path chosen in the complex $k\rho$-plane when applying the total least squares algorithm. The upper half ellipse (solid line) is located in the proper Riemman sheet, and the lower half ellipse (dashed line) is located in the improper sheet.

2-D cylinders. The method of moments is then employed to solve for the unknown current distributions. The required Green function of the problem is represented in terms of a finite summation of complex images. It is shown that when the field-point is far from the periodic sources, it is just sufficient to consider the contribution of the propagating poles in the structure [22]. This will result in a summation of plane waves that has an even smaller size compared with the conventional complex images Green function. This provides an analyzed method for the dielectric periodic structures.

http://dx.doi.org/10.5772/68028

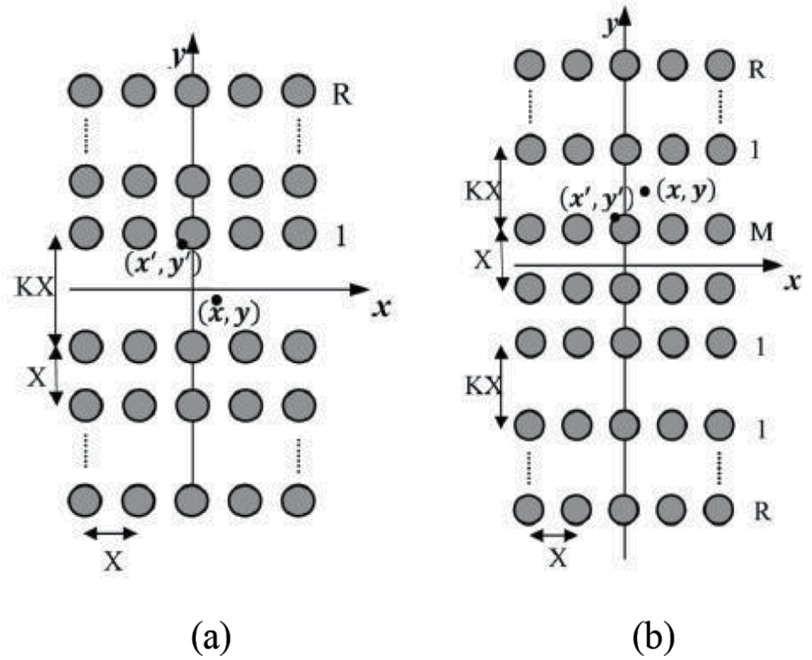

Figure 10. Typical (a) waveguide and (b) directional coupler in a rectangular lattice.

Others, since the Gaussian function is an eigenfunction of the Hankel transform operator, for the microstrip structures, the spectral Green's function can be expanded into a Gaussian series [23]. By introducing the mixed-form thin-stratified medium fast-multiple algorithm (MF-TSM-FMA), which includes the multipole expansion and the plane wave expansion in one multilevel tree, the different scales of interaction can be separated by the multilevel nature of the the fast multipole algorithm [24].

The vector wave functions, L, M, and N, are the solutions of the homogeneous vector Helmholtz equation. They can also be used for the analyses of the radiation in multilayer and this method avoids the finite integration in some cases.

7.2. Multilayer structure

The volume integral equation (VIE) can analyze electromagnetic radiation and scattering problems in inhomogeneous objects. By introducing an "impulse response" Green function, and invoking Green theorem, the Helmholtz equation can be cast into an equivalent volume integral equation including the source current or charges distribution. But the number of unknowns is typically large and the equation should be reformulated if there are in contrast both permittivity and permeability. At present, it is utilized to analyse the general scatterers in layered medium [25, 26].

When the inhomogeneity is one dimension, the Green function can be determined analytically in the spectral (Fourier) domain, and the spatial domain counterpart can be obtained by simply inverse Fourier transforming it.

Surface integral equation (SIE) method is another powerful method to handle electromagnetic problems. Similarly, by introducing the Green function, the Helmholtz equation can be cast into an equivalent surface integral equation, where the unknowns are pushed to the boundary of the scatterers [27].

Despite the convergence problem, the locations of the source and observation point may cause the change of Green function form, for example, for a source location either inside or outside the medium, the algebraic form of the Green functions changes as the receiver moves vertically in the direction of stratification from one layer to another [28].

First, we introduce the full-wave computational model [29]. A multilayer structure involving infinitely 1-D periodic chains of parallel circular cylinders in any given layer can be constructed as shown in **Figure 11**. Each layer consists of a homogeneous slab within which the circular cylinders are embedded. This is the typical aeronautic situation with fiber-reinforced four-layer pile (with fibers orientated at 0°, 45°, −45°, and 90°), but any other arrangement is manageable likewise.

In the multilayered photonic crystals, the Rayleig's method and mode-matching are combined to produce scattering matrices. An S-matrix-based recursive matrix is developed for modeling electromagnetic scattering. Field expansions and the relationship between expansion coefficients are given.

There is a mix treatment for the inhomogeneous and homogeneous multilayered structure [30]. As shown in **Figure 12**, a substrate is divided into two regions. The top region is laterally inhomogeneous and for the finite-difference method (FDM) or the finite element method (FEM), the volume integral equation, is used. The bottom region is layerwise homogeneous,

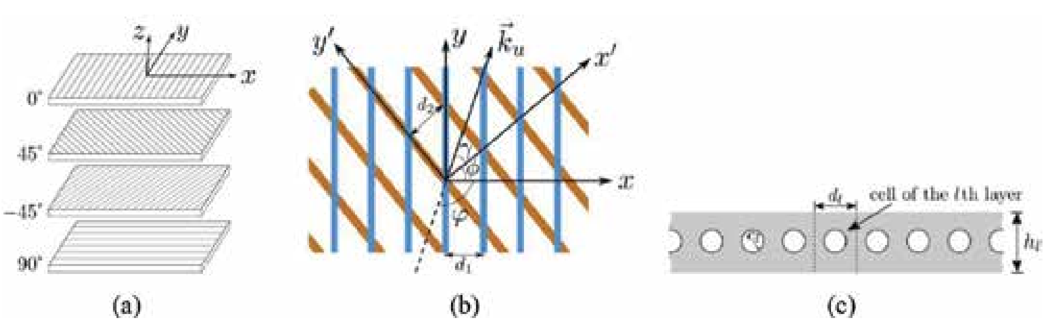

Figure 11. (a) Sketch of a standard (0, 45, −45, 90) degree, four-layer fiber-reinforced composite laminate as in aeronautics. (b) General two-layer pile of interest exhibiting two different cylinder orientations and associated coordinate systems with geometrical parameters as indicated. (c) Cell defined in the lth layer of multilayered photonic crystals.

http://dx.doi.org/10.5772/68028

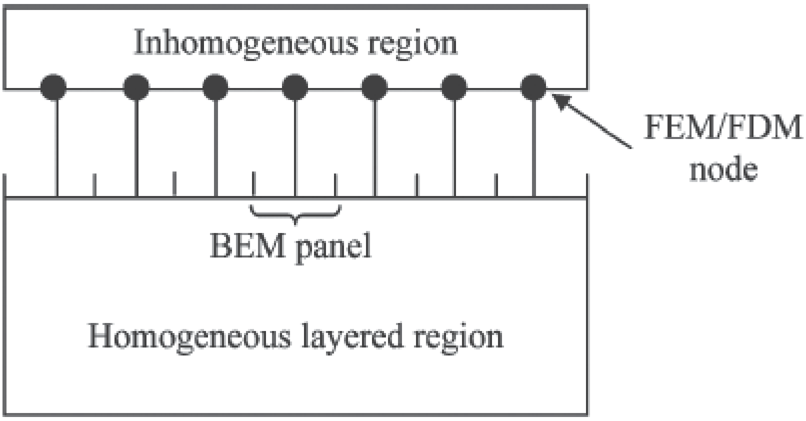

Figure 12. Substrate is divided into homogeneous and inhomogeneous regions in combined BEM/FEM and BEM/FDM methods.

and the boundary-element methods (BEM) are used. The two regions are connected such as a BEM panel is associated with an FEM node on the interface.

A Green function was derived for a layerwise uniform substrate and was then used in a layerwise nonuniform substrate with additional boundary conditions applied to the interface. Given that the lateral inhomogeneity is local, volume meshing is used only for the local inhomogeneous regions, BEM meshing is applied to the surfaces of these local regions.

For a field (observation) point in the *j*th layer and a source point in the *k*th layer, the Green function has the form:

$$G_{jk}^{u,l} = G_{jk,0}^{u,l} + \sum_{\substack{m=0 \\ m+n\neq 0}}^{\infty} \sum_{n=0}^{\infty} \frac{c_{mn}\varphi_{jk}^{u,l}}{ab\varepsilon_k\gamma_{mn}} \times \cos\frac{m\pi x_f}{a} \cos\frac{n\pi y_f}{b} \cos\frac{m\pi x_s}{a} \cos\frac{n\pi y_s}{b} \tag{138}$$

where the superscripts u and l indicate the upper and lower solutions, respectively, depending on whether the field point (or observation point) is above or below the source point. a and b are the substrate dimensions in the x- and y- directions, respectively, and more details can be found in Refs. [31, 32].

The electromagnetic field in a multilayer structure can be efficiently simplified by the assumption that the multilayer is grounded by a perfect electric conducto (PEC) plane [33, 34]. When the source and the field points are assumed to be inside the dielectric slab, in a layered medium as shown in **Figure 13**, by applying the boundary conditions, the 1-D Green functions is

$$G_x(x, x_0; \lambda_{x1}, \lambda_{x2}) = (G_x^{\mathrm{PMC}} + G_x^{\mathrm{PEC}})/2 \tag{139}$$

where PMC represents the perfect magnetic conductor. The simplified Green function form can be deduced to the cae of (b).

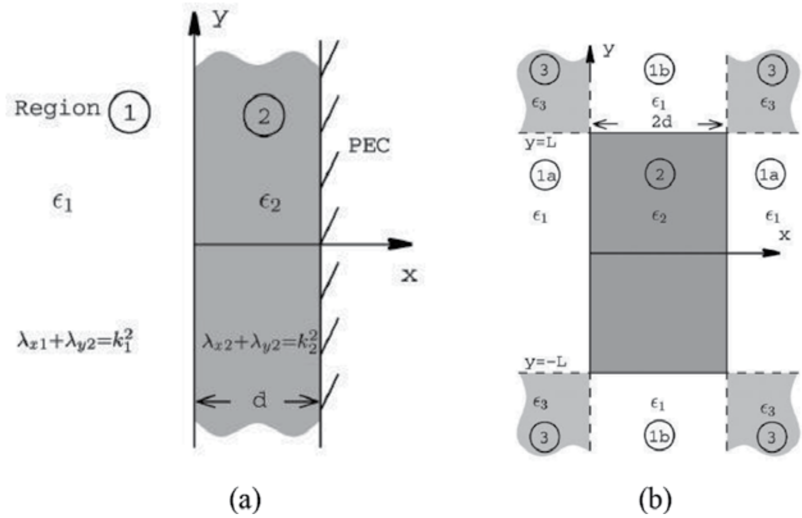

Figure 13. (a) Geometry of an infinite dielectric slab of thickness d grounded by a PEC plane at $x = d$. (b) Geometry of a finite dielectric slab of thickness $2d$ and height $2L$ surrounded by regions □ and □.

The three-dimensional (3-D) Green function for a continuous, linearly stratified planar media, backed by a PEC ground plane, can also be expressed in terms of a single contour integral involving one-dimensional (1-D) green function. The constructure is shown in **Figure 14**.

The general formulation for a single electric current element has been worked out in detail in Ref. [35] which is based on the appropriate information from Ref. [36].

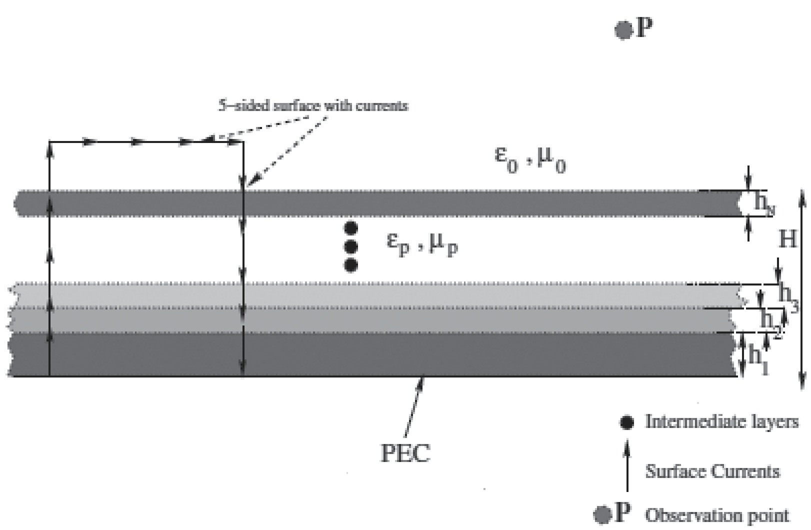

Figure 14. Representation of the continuous, linearly stratified media by discrete slabs of finite thickness and constant permittivity, εp and permeability μp for the pth layer of thickness hp. The thicknesses, permittivities and permeabilities are different for each layer.

http://dx.doi.org/10.5772/68028

Author details

Jing Huang

Address all correspondence to: jhuang@scut.edu.cn

Physics Department, South China University of Technology, Guangzhou, China

References

[1] Abramowitz M, Stegun I. Handbook of Mathematical Functions. New York: Dover Publications; 1965

[2] Chew WC. Waves and Fields in Inhomogenous Media. New York: Wiley-IEEE Press; January 1999

[3] Tai C-T. Dyadic Green Functions in Electromagnetic Theory. 2nd ed. New York: IEEE press; 1994

[4] Nussbaumer HJ. Fast Fourier Transform and Convolution Algorithms. New York: Springer Verlag; 1982

[5] Huang J, Yao J, Xu D. Green function method for the time domain simulation of pulse propagation. Applied Optics. 2014;**53:**3533–3539

[6] Tai CT. Complementary reciprocity theorems in electromagnetic theory. IEEE Transactions on Antennas and Propagation. 1992;**40:**675481

[7] Sommerfeld A. Partial Differential Equation. New York: Academic Press; 1949

[8] Kong JA. Electromagnetic Wave Theory. New York: John Wiley & Sons; 1986

[9] Tai CT. Dyadic Green functions for a rectangular waveguide filled with two dielectrics. Journal of Electromagnetic Waves and Applied. 1988;**2:**245–253

[10] Hansen WW. A new me of expansion in radiation problems. Physical Review. 1935;**47:** 139–143

[11] Hansen WW. Directional characteristics of any antenna over a plane earth. Journal of Applied Physics. 1936;**7:**460465

[12] Hansen WW. Transformations useful in certain antenna calculations. Journal of Applied Physics. 1937;**8:**282–286

[13] Di Ventra M. Electrical Transport in Nanoscale Systems. Cambridge: Cambridge University Press; 2008

[14] Ferry DK, Goodnick SM. Transport in Nanostructures. Cambridge: Cambridge University Press; 1997

[15] Michalski KA, Mosig JR. Multilayered media Green's functions in integral functions. IEEE Transactions on Antennas and Propagation. 1997;**45**:508–519

[16] Chow YL, Yang JJ, Fang DG, Howard GE. A closed-form spatial Green's function for the thick microstrip substrate. IEEE Transactions on Microwave Theory and Techniques. 1991;**39**:588–592

[17] Aksun MI. A robust approach for the derivation of closed-form Green's functions. IEEE Transactions on Microwave Theory and Techniques. 1996;**44**:651–658

[18] Hu J, Zhou HX, Song Z, Hong W. Locating all the modes of Green's function for a three-layered medium based on the path tracking algorithm. IEEE Transactions on Antennas and Propagation. 2009,**57**:2315–2322

[19] Tsang L, Wu BP. Electromagnetic fields of Hertzian dipoles in layered media of moderate thickness including the effects of all modes. IEEE Antennas and Wireless Propagation Letters. 2007;**6:**316–319

[20] Shuley NV, Boix RR, Medina F, Horno M. On the fast approximation of Green's functions in MPIE formulations for planar layered media. IEEE Transactions on Microwave Theory and Techniques. 2002;**50**:2185–2192

[21] Fructos A L, Boix RR, Raúl Rodríguez-Berral, Mesa F. Efficient determination of the poles and residues of spectral domain multilayered Green's functions that are relevant in far-field calculations. IEEE Transactions on Antennas and Propagation. 2010;**58:**218–222

[22] Ameri H, Faraji-Dana R. Green's function analysis of electromagnetic wave propagation in photonic crystal devices using complex images technique. IEEE Journal of Lightwave Technolgy. 2011;**29**:298–304

[23] Tajdini MM, Shishegar AA. A novel analysis of microstrip structures using the Gaussian Green's function method. IEEE Transactions on Antennas and Propagation. 2010;**58:**88–94

[24] Chen YP, Xiong JL, Chew WC. A mixed-form thin-stratified medium fast-multipole algorithm for both low and mid-frequency problems, IEEE Transactions on Antennas and Propagation. 2011,**59:**2341–2349

[25] Cui TJ, Chew WC. Fast algorithm for electromagnetic scattering by buried 3-D dielectric objects of large size. IEEE Transactions on Geoscience and Remote Sensing. 1999;**37:**2597–2608

[26] Millard X, Liu QH. Simulation of near-surface detection of objects in layeredmedia by the BCGS-FFTmethod, IEEE Transactions on Geoscience and Remote Sensing. 2004;**42:**327–334

[27] Chew WC. Waves and Fields in Inhomogeneous Media. Berlin, Germany: Van Nostrand Reinhold; 1990, Reprinted by New York: IEEE Press; 1995

[28] Chatterjee D. Phase-integral formulation of the single-layer microstrip Green's function. 2010 URSI International Symposium on Electromagnetic Theory. Berlin: 2010. pp. 970–973

http://dx.doi.org/10.5772/68028

[29] Li C, Lesselier D, Zhong Y. Full-wave computational model of electromagnetic scattering by arbitrarily rotated 1-D periodic multilayer structure. IEEE Transactions on Antennas and Propagation. 2016;**64:**1047–1060

[30] Xu C, Gharpurey R, Fiez TS, Mayaram K. Extraction of parasitics in inhomogeneous substrates with a new Green function-based method. IEEE Transactions on Computer-Aided Design of Integrated Circuits Systems. 2008;**27:**1595–1606

[31] Niknejad AM, Gharpurey R, Meyer RG. Numerically stable Green function for modeling and analysis of substrate coupling in integrated circuits. IEEE Transactions on Computer-Aided Design of Integrated Circuits Systems.1998;**17:**305–315

[32] Xu C, Fiez T, Mayaram K. On the numerical stability of Green's function for substrate coupling in integrated circuits. IEEE Transactions on Computer-Aided Design of Integrated Circuits Systems. 2005;**24:**653–658

[33] Parsa A, Paknys R. Interior Green's function solution for a thick and finite dielectric slab. IEEE Transactions on Antennas and Propagations. 2007;**55:**3504–3514

[34] Rogier H. New series expansions for the 3-D Green's function of multilayered media with 1-D periodicity based on perfectly matched layers. IEEE Transactions on Microwave Theory and Techniques. 2007;**55:**1730–1738

[35] Chatterjee D, Walker SD. Study of Sommerfeld and phase integral approaches for Green's functions for PEC-terminated inhomogeneous media, technical memorandum NRL/MR/5310-10-9240, January 2010, Naval Research Laboratory, Washington, DC, USA.

[36] Felsen LB, Marcuvuitz N. Radiation and Scattering of Waves, IEEE Classic Reissue. New York, USA: IEEE-Wiley Press; 1994

Chapter 4

Renormalization Group Theory of Effective Field Theory Models in Low Dimensions

Takashi Yanagisawa

Additional information is available at the end of the chapter

http://dx.doi.org/10.5772/intechopen.68214

Abstract

We discuss the renormalization group approach to fundamental field theoretic models in low dimensions. We consider the models that are universal and frequently appear in physics, both in high-energy physics and condensed matter physics. They are the non-linear sigma model, the ϕ^4 model and the sine-Gordon model. We use the dimensional regularization method to regularize the divergence and derive renormalization group equations called the beta functions. The dimensional method is described in detail.

Keywords: renormalization group theory, dimensional regularization, scalar model, non-linear sigma model, sine-Gordon model

1. Introduction

The renormalization group is a fundamental and powerful tool to investigate the property of quantum systems [1–15]. The physics of a many-body system is sometimes captured by the analysis of an effective field theory model [16–19]. Typically, effective field theory models are the ϕ^4 model, the non-linear sigma model and the sine-Gordon model. Each of these models represents universality as a representative of a universal class.

The ϕ^4 model is the model of a phase transition, which is often referred to as the Ginzburg-Landau model. The renormalization of the ϕ^4 model gives a prototype of renormalization group procedures in field theory [20–24].

The non-linear sigma model appears in various fields of physics [15, 25–27] and is the effective model of Quantum chromodynamics (QCD) [28] and also that of magnets (ferromagnetic and anti-ferromagnetic materials) [29–32]. This model exhibits an important property called the asymptotic freedom. The non-linear sigma model is generalized to a model with fields that take values in a compact Lie group G [33–42]. This is called the chiral model.

The sine-Gordon model also has universality [43–49]. The two-dimensional (2D) sine-Gordon model describes the Kosterlitz-Thouless transition of the 2D classical XY model [50, 51]. The 2D sine-Gordon model is mapped to the Coulomb gas model where particles interact with each other through a logarithmic interaction. The Kondo problem [52, 53] also belongs to the same universality class where the scaling equations are just given by those for the 2D sine-Gordon model, i.e. the equations for the Kosterlitz-Thouless transition [53–57]. The one-dimensional Hubbard model is also mapped onto the 2D sine-Gordon model on the basis of a bosonization method [58, 59]. The Hubbard model is an important model of strongly correlated electrons [60–65]. The Nambu-Goldstone (NG) modes in a multi-gap superconductor become massive due to the cosine potential, and thus the dynamical property of the NG mode can be understood by using the sine-Gordon model [66–71]. The sine-Gordon model will play an important role in layered high-temperature superconductors because the Josephson plasma oscillation is analysed on the basis of this model [72–75].

In this paper, we discuss the renormalization group theory for the ϕ4 theory, the non-linear sigma model and the sine-Gordon model. We use the dimensional regularization procedure to regularize the divergence [76].

2. ϕ^4 model

2.1. Lagrangian

The ϕ^4 model is given by the Lagrangian

$$\mathcal{L} = \frac{1}{2}(\partial_\mu \phi)^2 - \frac{1}{2}m^2\phi^2 - \frac{g}{4!}\phi^4, \tag{1}$$

where ϕ is a scalar field and g is the coupling constant. In the unit of the momentum μ, the dimension of $\mathcal{L}$ is given by d, where d is the dimension of the space-time: $[\mathcal{L}] = \mu^d$. The dimension of the field ϕ is $(d-2)/2$: $[\phi] = \mu^{(d-2)/2}$. Because $g\phi^4$ has the dimension d, the dimension of g is given by $4 - d$: $[g] = \mu^{4-d}$. Let us adopt that ϕ has N components as $\phi = (\phi_1, \phi_2, \ldots, \phi_N)$. The interaction term ϕ^4 is defined as

$$\phi^4 = \left(\sum_{i=1}^{N} \phi_i^2\right)^2. \tag{2}$$

The Green's function is defined as

$$G_i(x-y) = -i\langle 0|T\phi_i(x)\phi_i(y)|0\rangle, \tag{3}$$

where T is the time-ordering operator and $|0\rangle$ is the ground state. The Fourier transform of the Green's function is

$$G_i(p) = \int d\,^d x e^{ip\cdot x} G_i(x). \tag{4}$$

In the non-interacting case with $g = 0$, the Green's function is given by

$$G_i^{(0)}(p) = \frac{1}{p^2 - m^2}, \tag{5}$$

where $p^2 = (p_0)^2 - \vec{p}^{\,2}$ for $p = (p_0, \vec{p})$.

Let us consider the correction to the Green's function by means of the perturbation theory in terms of the interaction term $g\phi^4$. A diagram that appears in perturbative expansion contains, in general, L loops, I internal lines and V vertices. They are related by

$$L = I - V + 1. \tag{6}$$

There are L degrees of freedom for momentum integration. The degree of divergence D is given by

$$D = d \cdot L - 2I. \tag{7}$$

We have a logarithmic divergence when $D = 0$. Let E be the number of external lines. We obtain

$$4V = E + 2I. \tag{8}$$

Then, the degree of divergence is written as

$$D = d \cdot L - 2I = d + (d-4)V + \left(1 - \frac{d}{2}\right)E. \tag{9}$$

In four dimensions $d = 4$, the degree of divergence D is independent of the numbers of internal lines and vertices

$$D = 4 - E \tag{10}$$

When the diagram has four external lines, $E = 4$, we obtain $D = 0$ which indicates that we have a logarithmic (zero-order) divergence. This divergence can be renormalized.

Let us consider the Lagrangian with bare quantities

$$\mathcal{L} = \frac{1}{2}(\partial_\mu \phi_0)^2 - \frac{1}{2} m_0^2 \phi_0^2 - \frac{1}{4!} g_0 \phi_0^4, \tag{11}$$

where ϕ_0 denotes the bare field, g_0 denotes the bare coupling constant and m_0 is the bare mass. We introduce the renormalized field ϕ, the renormalized coupling constant g and the renormalized mass m. They are defined by

$$\phi_0 = \sqrt{Z_\phi}\phi, \tag{12}$$

$$g_0 = Z_g g, \tag{13}$$

$$m_0^2 = m^2 Z_2/Z_\phi, \tag{14}$$

where Z_ϕ, Z_g and Z_2 are renormalization constants. When we write Z_g as

$$Z_g = Z_4/Z_\phi^2, \tag{15}$$

we have $g_0 Z_\phi^2 = gZ_4$. Then, the Lagrangian is written by means of renormalized field and constants

$$\mathcal{L} = \frac{1}{2}Z_\phi(\partial_\mu\phi)^2 - \frac{1}{2}m^2 Z_2\phi^2 - \frac{1}{4!}gZ_4\phi^4. \tag{16}$$

2.2. Regularization of divergences

2.2.1. Two-point function

We use the perturbation theory in terms of the interaction $g\phi^4$. For a multi-component scalar field theory, it is convenient to express the interaction ϕ^4 as in **Figure 1**, where the dashed line indicates the coupling g. We first examine the massless case with $m \to 0$. Let us consider the renormalization of the two-point function $\Gamma^{(2)}(p) = iG(p)^{-1}$. The contributions to $\Gamma^{(2)}$ are shown in **Figure 1**. The first term indicates $p^2 Z_\phi$ and the contribution in the second term is represented by the integral

$$I = \int \frac{d^d q}{(2\pi)^d}\frac{1}{q^2 - m^2}. \tag{17}$$

Using the Euclidean co-ordinate $q_4 = -iq_0$, this integral is evaluated as

$$I = -i\frac{\Omega_d}{(2\pi)^d} m^{d-2}\frac{1}{2}\Gamma\left(\frac{d}{2}\right)\Gamma\left(1 - \frac{d}{2}\right), \tag{18}$$

where Ω_d is the solid angle in d dimensions. For $d > 2$, the integral I vanishes in the limit $m \to 0$. Thus, the mass remains zero in the massless case. We do not consider mass renormalization in the massless case. Let us examine the third term in **Figure 2**.

There are $4^2 \cdot 2N + 4^2 \cdot 2^2 = 32N + 64$ ways to connect lines for an N-component scalar field to form the third diagram in **Figure 2**. This is seen by noticing that this diagram is represented as a sum of two terms in **Figure 3**.

The number of ways to connect lines is $32N$ for (a) and 64 for (b). Then we have the factor from these contributions as

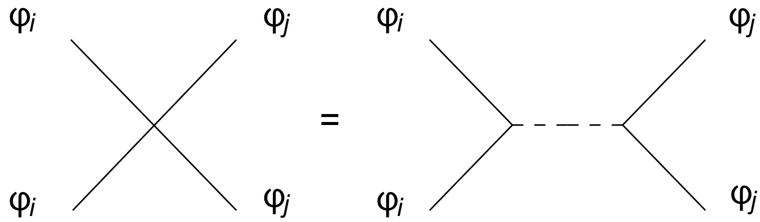

Figure 1. ϕ^4 interaction with the coupling constant g.

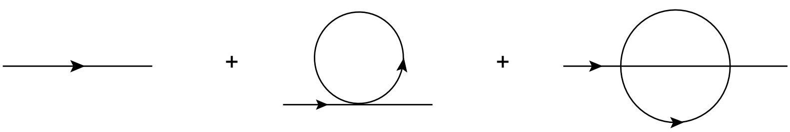

Figure 2. The contributions to the two-point function $\Gamma^{(2)}(p)$ up to the order of g^2.

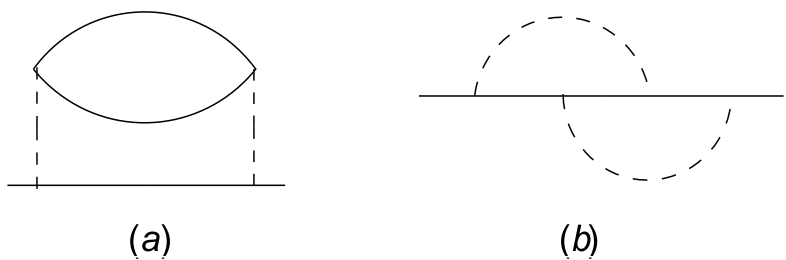

Figure 3. The third term in **Figure 2** is a sum of two configurations (a) and (b).

$$\left(\frac{1}{4!}g\right)^2(32N+64)=\frac{N+2}{18}g^2. \tag{19}$$

The momentum integral of this term is given as

$$J(k):=\int\frac{d^{\,d}p}{(2\pi)^d}\frac{d^dq}{(2\pi)^d}\frac{1}{p^2q^2(p+q+k)^2}. \tag{20}$$

The integral J exhibits a divergence in four dimensions $d = 4$. We separate the divergence as $1/\epsilon$ by adopting $d = 4 - \epsilon$. The divergent part is regularized as

$$J=-\left(\frac{1}{8\pi^2}\right)^2\frac{1}{8\epsilon}+\text{regular terms} \tag{21}$$

To obtain this, we first perform the integral with respect to q by using

$$\frac{1}{q^2(p+q+k)^2} = \int_0^1 dx \frac{1}{[q^2x+(p+q+k)^2(1-x)]^2}. \tag{22}$$

For $q' = q + (1 - x)(p + k)$, we have

$$\begin{aligned}
\int \frac{d^dq}{(2\pi)^d}\frac{1}{q^2(p+q+k)^2} &= \int \frac{d^dq'}{(2\pi)^d}\int_0^1 dx \frac{1}{[q'^2+x(1-x)(p+k)^2]^2} \\
&= \frac{\Omega_d}{(2\pi)^d}\int_0^1 dx \Big(x(1-x)\Big)^{\frac{d}{2}-2}\Big((p+k)^2\Big)^{\frac{d}{2}-2}\int_0^\infty dr r^{d-1}\frac{1}{(r^2+1)^2} \\
&= \frac{\Omega_d}{(2\pi)^d}\frac{1}{2}\Gamma\left(\frac{d}{2}\right)\Gamma\left(2-\frac{d}{2}\right)\Gamma\left(\frac{d}{2}-1\right)^2\frac{1}{\Gamma(d-2)}\Big((p+k)^2\Big)^{\frac{d}{2}-2}.
\end{aligned} \tag{23}$$

Here, the following parameter formula was used

$$\frac{1}{A^nB^m} = \frac{\Gamma(n+m)}{\Gamma(n)\Gamma(m)}\int_0^1 dx \frac{x^{n-1}(1-x)^{m-1}}{[xA+(1-x)B]^{n+m}}. \tag{24}$$

Then, we obtain

$$\begin{aligned}
\int \frac{d^dp}{(2\pi)^d}\frac{1}{p^2\Big((p+k)^2\Big)^{2-d/2}} &= \frac{\Gamma(3-d/2)}{\Gamma(2-d/2)}\int_0^1 dx(1-x)^{1-d/2}\int \frac{d^dp'}{(2\pi)^d}\frac{1}{[p'^2+x(1-x)k^2]^{3-d/2}} \\
&= \frac{\Omega_d}{(2\pi)^d}\frac{\Gamma(3-d/2))}{\Gamma(2-d/2)}B\left(d-2,\frac{d}{2}-1\right)\frac{1}{2}B\left(\frac{d}{2},3-d\right)(k^2)^{d-3}.
\end{aligned} \tag{25}$$

Here $B(p, q) = \Gamma(p)\Gamma(q)/\Gamma(p+q)$. We use the formula

$$\Gamma(\epsilon) = \frac{1}{\epsilon} + \text{finite terms} \tag{26}$$

for $\epsilon \to 0$. This results in

$$\int \frac{d^dp}{(2\pi)^d}\frac{d^dq}{(2\pi)^d}\frac{1}{p^2q^2(p+q+k)^2} = -\left(\frac{1}{8\pi^2}\right)^2\frac{1}{8\epsilon}k^2 + \text{ regular terms} \tag{27}$$

Therefore, the two-point function is evaluated as

$$\Gamma^{(2)}(p) = Z_\phi p^2 + \frac{1}{8\epsilon}\frac{N+2}{18}\left(\frac{g}{8\pi^2}\right)^2 p^2, \tag{28}$$

up to the order of $O(g^2)$. In order to cancel the divergence, we choose Z_ϕ as

$$Z_\phi = 1 - \frac{1}{8\epsilon}\frac{N+2}{18}\left(\frac{1}{8\pi^2}\right)^2 g^2. \tag{29}$$

2.2.2. Four-point function

Let us turn to the renormalization of the interaction term g^4. The perturbative expansion of the four-point function is shown in **Figure 4**. The diagram (b) in **Figure 4**, denoted as $\Delta\Gamma_b^{(4)}$, is given by for $N = 1$:

$$\Delta\Gamma_b^{(4)}(p) = g^2 \frac{1}{2} \int \frac{d^d q}{(2\pi)^d} \frac{1}{(q^2 - m^2)\Big(((p+q)^2 - m^2\Big)}. \tag{30}$$

As in the calculation of the two-point function, this is regularized as

$$\Delta\Gamma_b^{(4)}(p) = i \frac{1}{8\pi^2} \frac{1}{2\epsilon} g^2, \tag{31}$$

for $d = 4 - \epsilon$. Let us evaluate the multiplicity of this contribution for $N > 1$. For $N = 1$, we have a factor $4^2 3^2 2/4!4! = 1/2$ as shown in Eq. (30). **Figure 4c** and **d** gives the same contribution as in Eq. (31), giving the factor 3/2. For $N > 1$, there is a summation with respect to the components of ϕ. We have the multiplicity factor for the diagram in **Figure 4b** as

$$\left(\frac{1}{4!}\right)^2 2^2 2^2 2N = \frac{N}{18}. \tag{32}$$

Since we obtain the same factor for diagrams in **Figure 4c** and **d**, we have $N/6$ in total. We subtract 1/6 for $N = 1$ from 3/2 to have 8/6. Finally, the multiplicity factor is given by $(N + 8)/6$. Then, the four-point function is regularized as

$$\Delta\Gamma^{(4)}(p) = i \frac{1}{8\pi^2} \frac{N+8}{6} \frac{1}{\epsilon} g^2. \tag{33}$$

Because g has the dimension $4 - d$ such as $[g] = \mu^{4-d}$, we write g as $g\mu^{4-d}$ so that g is the dimensionless coupling constant. Now, we have

$$\Gamma^{(4)}(p) = -igZ_4\mu^\epsilon + i \frac{1}{8\pi^2} \frac{N+8}{6} \frac{1}{\epsilon} g^2. \tag{34}$$

for $d = 4 - \epsilon$ where we neglect μ^ϵ in the second term. The renormalization constant is determined as

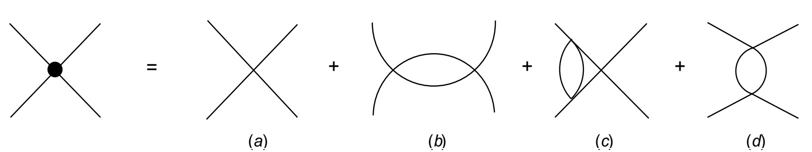

Figure 4. Diagrams for four-point function.

$$Z_4 = 1 + \frac{N+8}{6\epsilon}\frac{1}{8\pi^2}g. \tag{35}$$

As a result, the four-point function $\Gamma^{(4)}$ becomes finite.

2.3. Beta function $\beta(g)$

The bare coupling constant is written as $g_0 = Z_g g\mu^{4-d} = (Z_4/Z_\phi^2)g\mu^{4-d}$. Since g_0 is independent of the energy scale, μ, we have $\mu\partial g_0/\partial\mu = 0$. This results in

$$\mu\frac{\partial g}{\partial\mu} = (d-4)g - g\mu\frac{\partial g}{\partial\mu}\frac{\partial \ln Z_g}{\partial g}, \tag{36}$$

where $Z_g = Z_4/Z_\phi^2$. We define the beta function for g as

$$\beta(g) = \mu\frac{\partial g}{\partial\mu}, \tag{37}$$

where the derivative is evaluated under the condition that the bare g_0 is fixed. Because

$$Z_g = 1 + \frac{N+8}{6\epsilon}\frac{1}{8\pi^2}g + O(g^2), \tag{38}$$

the beta function is given as

$$\beta(g) = \frac{-\epsilon g}{1 + g\frac{\partial \ln Z_g}{\partial g}} = -\epsilon g + \frac{N+8}{6}\frac{1}{8\pi^2}g^2 + O(g^3). \tag{39}$$

$\beta(g)$ up to the order of g^2 is shown as a function of g for $d < 4$ in **Figure 5**. For $d < 4$, there is a non-trivial fixed point at

$$g_c = \epsilon\frac{48\pi^2}{N+8}. \tag{40}$$

For $d = 4$, we have only a trivial fixed point at $g = 0$.

For $d = 4$ and $N = 1$, the beta function is given by

$$\beta(g) = \frac{3}{16\pi^2}g^2 + \cdots. \tag{41}$$

In this case, the $\beta(g)$ has been calculated up to the fifth order of g [77]:

$$\beta(g) = \frac{3}{16\pi^2}g^2 - \frac{17}{3}\frac{1}{(16\pi^2)^2}g^3 + \left(\frac{145}{8} + 12\zeta(3)\right)\frac{1}{(16\pi^2)^3}g^4 + A_5\frac{1}{(16\pi^2)^4}g^5, \tag{42}$$

where

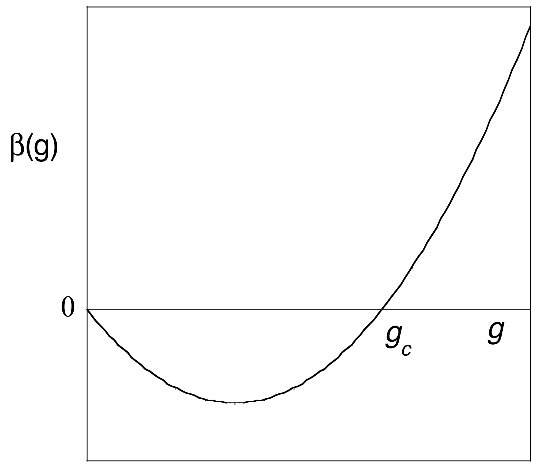

Figure 5. The beta function of g for $d < 4$. There is a finite fixed point g_c.

$$A_5 = -\left(\frac{3499}{48} + 78\zeta(3) - 18\zeta(4) + 120\zeta(5)\right), \tag{43}$$

and $\zeta(n)$ is the Riemann zeta function. The renormalization constant Z_g and the beta function $\beta(g)$ are obtained as a power series of g. We express Z_g as

$$Z_g = 1 + \frac{N+8}{6\epsilon} g + \left(\frac{b_1}{\epsilon^2} + \frac{b_2}{\epsilon}\right) g^2 + \left(\frac{c_1}{\epsilon^3} + \frac{c_2}{\epsilon^2} + \frac{c_3}{\epsilon}\right) g^3 + \cdots, \tag{44}$$

and then $\beta(g)$ is written as

$$\begin{aligned} \beta(g) =& -\epsilon g + \epsilon g^2 \left[\frac{N+8}{6\epsilon} + 2\left(\frac{b_1}{\epsilon^2} + \frac{b_2}{\epsilon}\right) g + \frac{(N+8)^2}{36\epsilon^2} g + \cdots\right] \\ =& -\epsilon g + \frac{N+8}{6} g^2 - \frac{9N+42}{36} g^3 + \cdots \end{aligned} \tag{45}$$

Here, the factor $1/8\pi^2$ is included in g. The terms of order $1/\epsilon^2$ are cancelled because of

$$b_1 = -\frac{(N+8)^2}{72}. \tag{46}$$

In general, the nth order term in $\beta(g)$ is given by $n!g^n$. The function $\beta(g)$ is expected to have the form

$$\beta(g) = -\epsilon g + \frac{N+8}{6} g^2 + \cdots + n! a^n n^b c g^n + \cdots, \tag{47}$$

where a, b and c are constants.

2.4. *n*-point function and anomalous dimension

Let us consider the n-point function $\Gamma^{(n)}$. The bare and renormalized n-point functions are denoted as $\Gamma_B^{(n)}(p_i, g_0, m_0, \mu)$ and $\Gamma_R^{(n)}(p_i, g, m, \mu)$, respectively, where p_i (i = 1,…, n) indicate momenta. The energy scale μ indicates the renormalization point. $\Gamma_R^{(n)}$ has the mass dimension $n + d - nd/2$: $[\Gamma_R^{(n)}] = \mu^{n+d-nd/2}$. These quantities are related by the renormalization constant Z_ϕ as

$$\Gamma_R^{(n)}(p_i, g, m^2, \mu) \ = \ Z_\phi^{n/2}\Gamma_B^{(n)}(p_i, g_0, m_0^2, \mu). \tag{48}$$

Here, we consider the massless case and omit the mass. Because the bare quantity $\Gamma_B^{(n)}$ is independent of μ, we have

$$\frac{d}{d\mu}\Gamma_B^{(n)} = 0. \tag{49}$$

This leads to

$$\mu\frac{d}{d\mu}\left(Z_\phi^{-n/2}\Gamma_R^{(n)}\right) = 0. \tag{50}$$

Then we obtain the equation for $\Gamma_R^{(n)}$:

$$\left(\mu\frac{\partial}{\partial\mu} + \mu\frac{\partial g}{\partial\mu}\frac{\partial}{\partial g} - \frac{n}{2}\gamma_\phi\right)\Gamma_R^{(n)}(p_i, g, \mu) = 0, \tag{51}$$

where γ_ϕ is defined as

$$\gamma_\phi = \ \mu\frac{\partial}{\partial\mu}\ln Z_\phi. \tag{52}$$

A general solution of the renormalization equation is written as

$$\Gamma_R^{(n)}(p_i, g, \mu) = \ \exp\left(\frac{n}{2}\int_{g_1}^{g}\frac{\gamma_\phi(g')}{\beta(g')}dg'\right)f^{(n)}(p_i, g, \mu), \tag{53}$$

where

$$f^{(n)}(p_i, g, \mu) = F\left(p_i, \ln\mu - \int_{g_1}^{g}\frac{1}{\beta(g')}dg'\right), \tag{54}$$

for a function F and a constant g_1. We suppose that $\beta(g)$ has a zero at $g = g_c$. Near the fixed point g_c, by approximating $\gamma_\phi(g')$ by $\gamma_\phi(g_c)$, $\Gamma_R^{(n)}$ is expressed as

$$\Gamma_R^{(n)}(p_i, g_c, \mu) = \mu^{\frac{n}{2}\gamma_\phi(g_c)} f^{(n)}(p_i, g_c, \mu). \tag{55}$$

In general, we define $\gamma(g)$ as

$$\gamma(g)\ln\mu = \int_{g_1}^{g} \frac{\gamma_\phi(g')}{\beta(g')} dg', \tag{56}$$

Then, we obtain

$$\Gamma_R^{(n)}(p_i, g, \mu) = \mu^{\frac{n}{2}\gamma(g)} f^{(n)}(p_i, g, \mu). \tag{57}$$

Under a scaling $p_i \to \rho p_i$, $\Gamma_R^{(n)}$ is expected to behave as

$$\Gamma_R^{(n)}(\rho p_i,\ g_c,\ \mu) = \rho^{n+d-nd/2}\Gamma_R^{(n)}(p_i,\ g_c,\ \mu/\rho), \tag{58}$$

because $\Gamma_R^{(n)}$ has the mass dimension $n + d - nd/2$. In fact, **Figure 4b** gives a contribution being proportional to

$$\begin{aligned} g^2(\mu^{4-d})^2 \int d^d q \frac{1}{q^2(\rho p + q)^2} &= g^2(\mu^{4-d})^2 \rho^{d-4} \int d^d q \frac{1}{q^2(p+q)^2} \\ &= \rho^{4-d} g^2 \left(\frac{\mu}{\rho}\right)^{2(4-d)} \int d^d q \frac{1}{q^2(p+q)^2}, \end{aligned} \tag{59}$$

after the scaling $p_i \to \rho p_i$ for $n = 4$. We employ Eq. (58) for $n = 2$

$$\begin{aligned} \Gamma_R^{(2)}(\rho p_i,\ g_c,\ \mu) &= \rho^2 \Gamma_R^{(2)}(p_i,\ g_c,\ \mu/\rho) = \rho^2 \left(\frac{\mu}{\rho}\right)^{\gamma} f^{(2)}(p_i,\ g_c,\ \mu/\rho) \\ &= \rho^{2-\gamma}\mu^{\gamma} f^{(2)}(p_i,\ g_c,\ \mu/\rho) = \rho^{2-\gamma}\Gamma_R^{(2)}(p_i,\ g_c,\ \mu/\rho). \end{aligned} \tag{60}$$

This indicates

$$\Gamma^{(2)}(p) = p^{2-\eta} = p^{2-\gamma} = (p^2)^{1-\gamma/2}. \tag{61}$$

Thus, the anomalous dimension η is given by $\eta = \gamma$. From the definition of $\gamma(g)$ in Eq. (56), we have

$$\gamma_\phi(g) = \gamma(g) + \beta(g)\frac{\partial\gamma(g)}{\partial g}\ln\ \mu. \tag{62}$$

At the fixed point $g = g_c$, this leads to

$$\eta = \gamma = \gamma(g_c) = \gamma_\phi(g_c). \tag{63}$$

The exponent η shows the fluctuation effect near the critical point.

The Green's function $G(p) = \Gamma^{(2)}(p)^{-1}$ is given by

$$G(p) = \frac{1}{p^{2-\eta}}. \tag{64}$$

The Fourier transform of $G(p)$ in d dimensions is evaluated as

$$G(r) = \int \frac{1}{p^{2-\eta}} e^{ip\cdot r} d^d p = \Omega_d \frac{1}{r^{d-2+\eta}} \frac{\pi}{2\Gamma(4-\eta-d)\sin\left((4-\eta-d)\pi/2\right)}. \tag{65}$$

When $4 - \eta - d$ is small near four dimensions, $G(r)$ is approximated as

$$G(r) \approx \Omega_d \frac{1}{r^{d-2+\eta}}. \tag{66}$$

The definition of γ_ϕ in Eq. (52) results in

$$\gamma_\phi(g) = \mu \frac{\partial g}{\partial \mu} \frac{\partial}{\partial g} \ln Z_\phi = \beta(g) \frac{\partial}{\partial g} \ln Z_\phi. \tag{67}$$

Up to the lowest order of g, γ_ϕ is given by

$$\begin{aligned} \gamma_\phi &= \left(-\frac{1}{8\epsilon} \frac{N+1}{9} \frac{1}{(8\pi^2)^2} g \right) \beta(g) + O(g^3) \\ &= \frac{N+2}{72} \frac{1}{(8\pi^2)^2} g^2 + O(g^3). \end{aligned} \tag{68}$$

At the critical point $g = g_c$, where

$$\frac{1}{8\pi^2} g_c = \frac{6\in}{N+8}, \tag{69}$$

the anomalous dimension is given as

$$\eta = \gamma_\phi(g_c) = \frac{N+2}{2(N+8)^2} \epsilon^2 + O(\epsilon^3). \tag{70}$$

For $N = 1$ and $\epsilon = 1$, we have $\eta = 1/54$.

2.5. Mass renormalization

Let us consider the massive case $m \neq 0$. This corresponds to the case with $T > T_c$ in a phase transition. The bare mass m_0 m and renormalized mass m are related through the relation $m^2 = m_0^2 Z_\phi / Z_2$. The condition $\mu \partial m_0 / \partial \mu = 0$ leads to

$$\mu \frac{\partial \ln m}{\partial \mu} = \mu \frac{\partial}{\partial \mu} \ln \frac{Z_\phi}{Z_2}. \tag{71}$$

From Eq. (50), the equation for $\Gamma_R^{(n)}$ is

$$\left[\mu \frac{\partial}{\partial \mu} + \beta(g) \frac{\partial}{\partial g} - \frac{n}{2}\gamma_\phi + \mu \frac{\partial}{\partial \mu} \ln\left(\frac{Z_\phi}{Z_2}\right) \cdot m^2 \frac{\partial}{\partial m^2}\right] \Gamma_R^{(n)}(p_i,\ g,\ \mu,\ m^2) = 0. \tag{72}$$

We define the exponent ν by

$$\frac{1}{\nu} - 2 = \mu \frac{\partial}{\partial \mu} \ln\left(\frac{Z_2}{Z_\phi}\right), \tag{73}$$

then

$$\left[\mu \frac{\partial}{\partial \mu} + \beta(g) \frac{\partial}{\partial g} - \frac{n}{2}\gamma_\phi - \left(\frac{1}{\nu} - 2\right) m^2 \frac{\partial}{\partial m^2}\right] \Gamma_R^{(n)}(p_i,\ g,\ \mu,\ m^2) = 0. \tag{74}$$

At the critical point $g = g_c$, we obtain

$$\left[\mu \frac{\partial}{\partial \mu} - \frac{n}{2}\eta - \zeta m^2 \frac{\partial}{\partial m^2}\right] \Gamma_R^{(n)}(p_i,\ g_c,\ \mu,\ m^2) = 0, \tag{75}$$

where $\gamma_\phi = \eta$ and we set

$$\zeta = \frac{1}{\nu} - 2. \tag{76}$$

At $g = g_c$, $\Gamma_R^{(n)}$ has the form

$$\Gamma_R^{(n)}(p_i,\ g_c,\ \mu,\ m^2) = \mu^{\frac{n}{2}} F^{(n)}(p_i,\ \mu m^{2/\zeta}). \tag{77}$$

because this satisfies Eq. (75).

In the scaling $p_i \to \rho p_i$, we adopt

$$\Gamma_R^{(n)}(\rho p_i,\ g_c,\ \mu,\ m^2) = \rho^{n+d-nd/2} \Gamma_R^{(n)}(p_i,\ g_c,\ \mu/\rho,\ m^2/\rho^2). \tag{78}$$

From Eq. (77), we have

$$\Gamma_R^{(n)}(k_i,\ g_c,\ \mu,\ m^2) = \rho^{n+d-nd/2-n\eta/2} \mu^{\frac{n}{2}\eta} F^{(n)}\left(\rho^{-1} k_i,\ \rho^{-1}\mu(\rho^{-2}m^2)^{1/\zeta}\right), \tag{79}$$

where we put $\rho p_i = k_i$. We assume that $F^{(n)}$ depends only on $\rho{-}1k_i$. We choose ρ as

$$\rho = (\mu m^{2/\zeta})^{\zeta/(\zeta+2)} = \mu\left(\frac{m^2}{\mu^2}\right)^{1/(\zeta+2)}. \tag{80}$$

This satisfies $\rho^{-1}\mu(\rho^{-2}m^2)^{1/\varsigma} = 1$ and results in

$$\Gamma_R^{(n)}(k_i,\ g_c,\ \mu,\ m^2) = \mu^{d+\frac{n}{2}(2-d-\eta)} \left(\frac{m^2}{\mu^2}\right)^{\{d+\frac{n}{2}(2-d-\eta)\}\frac{1}{\zeta+2}} \mu^{\frac{n}{2}\eta} F^{(n)}\left(\mu^{-1}\left(\frac{m^2}{\mu^2}\right)^{-\frac{1}{\zeta+2}} k_i\right). \tag{81}$$

We take μ as a unit by setting $\mu = 1$, so that $\Gamma_R^{(n)}$ is written as

$$\Gamma_R^{(n)}(k_i,\ g_c,\ 1,\ m^2) = m^{2\nu\left\{d+\frac{n}{2}(2-d+\eta)\right\}} F^{(n)}(k_i m^{-2\nu}), \tag{82}$$

because $\varsigma + 2 = 1/\nu$. We can define the correlation length ξ by

$$(m^2)^{-\nu} = \xi. \tag{83}$$

The two-point function is written as

$$\Gamma_R^{(2)}(k, m^2) = m^{2\nu(2-\eta)} F^{(2)}(km^{-2\nu}). \tag{84}$$

Now let us turn to the evaluation of ν. Since $\gamma_\phi = \mu\,\partial \ln Z_\phi/\partial\mu$, from Eq. (73) ν is given by

$$\frac{1}{\nu} = 2 + \mu\frac{\partial}{\partial\mu}\ln\left(\frac{Z_2}{Z_\phi}\right) = 2 + \beta(g)\frac{\partial}{\partial g}\ln Z_2 - \gamma_\phi(g). \tag{85}$$

The renormalization constant Z_2 is determined from the corrections to the bare mass m_0. The one-loop correction, shown in **Figure 6**, is given by

$$\Sigma(p^2) = i\frac{N+2}{6}g\int\frac{d^dk}{(2\pi)^d}\frac{1}{k^2 - m_0^2}, \tag{86}$$

where the multiplicity factor is (8 + 4N)/4!. This is regularized as

$$\Sigma(p^2) = \frac{N+2}{6}g\int\frac{d^dk}{(2\pi)^d}\frac{1}{k_E^2 + m_0^2} = -\frac{N+2}{6}g\frac{1}{8\pi^2}m_0^2\frac{1}{\epsilon}, \tag{87}$$

for $d = 4 - \epsilon$. Therefore the renormalized mass is

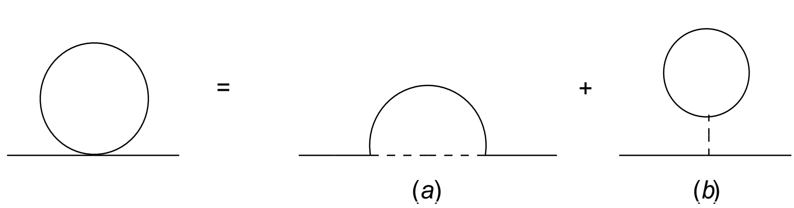

Figure 6. Corrections to the mass term. Multiplicity weights are 8 for (a) and 2N for (b).

$$m^2 = m_0^2 + \Sigma(p^2) = m_0^2\left(1 - \frac{N+2}{6\epsilon}\frac{1}{8\pi^2}g\right) \tag{88}$$

Z_2 is determined to cancel the divergence in the form m^2Z_2/Z_ϕ. The result is

$$Z_2 = 1 + \frac{N+2}{6\epsilon}\frac{1}{8\pi^2}g. \tag{89}$$

Then, we have

$$\beta(g)\frac{\partial}{\partial g}\ln Z_2 = -\frac{N+2}{6}\frac{1}{8\pi^2}g + O(g^2). \tag{90}$$

Eq. (85) is written as

$$\frac{1}{\nu} = 2 - \frac{N+2}{6}\frac{1}{8\pi^2}g_c - \eta = 2 - \frac{N+2}{N+8}\epsilon + O(\epsilon^2), \tag{91}$$

where we put $g = g_c$ and used $\eta = \gamma_\phi(g) = (N+2)/\left(2(N+8)^2\right)\cdot\epsilon$. Now the exponent ν is

$$\nu = \frac{1}{2}\left(1 + \frac{N+2}{2(N+8)}\epsilon\right) + O(\epsilon^2). \tag{92}$$

In the mean-field approximation, $\nu = 1/2$. This formula of ν contains the fluctuation effect near the critical point. For $N = 1$ and $\epsilon = 1$, we have $\nu = 1/2 + 1/12 = 7/12$.

3. Non-linear sigma model

3.1. Lagrangian

The Lagrangian of the non-linear sigma model is

$$\mathcal{L} = \frac{1}{2g}(\partial_\mu\phi)^2, \tag{93}$$

where ϕ is a real N-component field $\phi = (\phi_1,\ldots,\phi_N)$ with the constraint $\phi^2 = 1$. This model has an O(N) invariance. The field ϕ is represented as

$$\phi = (\sigma,\ \pi_1,\ \pi_2,\ \cdots,\ \pi_{N-1}) \tag{94}$$

with the condition $o^2 + \pi_1^2 + \cdots + \pi_{N-1}^2 = 1$. The fields π_i ($i = 1, \ldots, N - 1$) are regarded as representing fluctuations. The Lagrangian is given by

$$\mathcal{L} = \frac{1}{2g}\{(\partial_\mu \sigma)^2 + (\partial_\mu \pi_i)^2\}, \tag{95}$$

where summation is assumed for index i. In this Section we consider the Euclidean Lagrangian from the beginning. Using the constraint $\sigma^2 + \pi_i^2 = 1$, the Lagrangian is written in the form

$$\mathcal{L} = \frac{1}{2g}(\partial_\mu \pi_i)^2 + \frac{1}{2g}\frac{1}{1-\pi_i^2}(\pi_i \partial_\mu \pi_i)^2 \tag{96}$$

$$= \frac{1}{2g}(\partial_\mu \pi_i)^2 + \frac{1}{2g}(\pi_i \partial_\mu \pi_i)^2 + \cdots \tag{97}$$

The second term in the right-hand side indicates the interaction between π_i fields. The diagram for this interaction is shown in **Figure 7**.

Here, let us check the dimension of the field and coupling constant. Since $[\mathcal{L}] = \mu^d$, we obtain $[\pi] = \mu^0$ (dimensionless) and $[g] = \mu^{2-d}$. g_0 and g are used to denote the bare coupling constant and renormalized coupling constant, respectively. The bare and renormalized fields are indicated by π_{Bi} and π_{Ri}, respectively. We define the renormalization constants Z_g and Z by

$$g_0 = g\mu^{2-d} Z_g, \tag{98}$$

$$\pi_{Bi} = \sqrt{Z}\,\pi_{Ri} \tag{99}$$

where g is the dimensionless coupling constant. Then, the Lagrangian is expressed in terms of renormalized quantities:

$$\mathcal{L} = \frac{\mu^{d-2} Z}{2gZ_g}\left\{(\partial_\mu \pi_{Ri})^2 + \frac{1}{4}(\partial_\mu \pi_{Ri}^2)^2 + \cdots\right\}. \tag{100}$$

In order to avoid the infrared divergence at d = 2, we add the Zeeman term to the Lagrangian which is written as

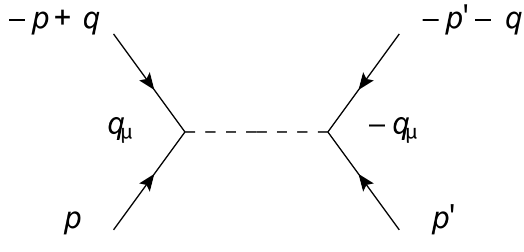

Figure 7. Lowest order interaction for π_i.

http://dx.doi.org/10.5772/intechopen.68214

$$\mathcal{L}_Z = \frac{H_B}{g_0}\sigma = \frac{H_B}{g_0}\left(1 - \frac{Z}{2}\pi_{Ri}^2 - \frac{Z^2}{8}\pi_{Ri}^4 + \cdots\right) \tag{101}$$

$$= const. \; - \; H_B\frac{Z}{2gZ_g}\mu^{d-2}\pi_{Ri}^2 - \; H_B\frac{Z^2}{8gZ_g}\mu^{d-2}(\pi_{Ri}^2)^2. \tag{102}$$

Here, H_B is the bare magnetic field and the renormalized magnetic field H is defined as

$$H = \frac{\sqrt{Z}}{Z_g}H_B \tag{103}$$

Then, the Zeeman term is given by

$$\mathcal{L}_z = const. \; - \frac{\sqrt{Z}}{2g}H\mu^{d-2}\pi_{Ri}^2 - \frac{Z^{\frac{3}{2}}}{8g}H\mu^{d-2}(\pi_{Ri}^2)^2 + \cdots. \tag{104}$$

3.2. Two-point function

The diagrams for the two-point function $\Gamma^{(2)}(p) = G^{(2)}(p)^{-1}$ are shown in **Figure 8**. The contributions in **Figure 8c** and **d** come from the magnetic field. **Figure 8b** presents

$$I_b = \int \frac{d^dk}{(2\pi)^d}\frac{(k+p)^2}{k^2+H} = (p^2 - H)\int \frac{d^dk}{(2\pi)^d}\frac{1}{k^2+H'} \tag{105}$$

where we used the formula in the dimensional regularization given as

$$\int d^dk = 0. \tag{106}$$

Near two dimensions, $d = 2 + \epsilon$, the integral is regularized as

$$I_b = (p^2 - H)\frac{\Omega_d}{(2\pi)^d}H^{\frac{d}{2}-1}\Gamma\left(\frac{d}{2}\right)\Gamma\left(1-\frac{d}{2}\right) = -(p^2 - H)\frac{\Omega_d}{(2\pi)^d}\frac{1}{\epsilon}. \tag{107}$$

The H-term I_c in **Figure 8c** just cancels with $-H$ in I_b. The contribution I_d in **Figure 8d** has the multiplicity $2 \cdot 2 \cdot (N-1)$ because (π_i) has $N-1$ components. I_d is evaluated as

$$I_c = \frac{1}{8}\cdot 4(N-1)\int \frac{d^dk}{(2\pi)^d}\frac{1}{k^2+H} = -\frac{\Omega_d}{(2\pi)^d}\frac{N-1}{2}\frac{1}{\epsilon}. \tag{108}$$

As a result, up to the one-loop-order the two-point function is

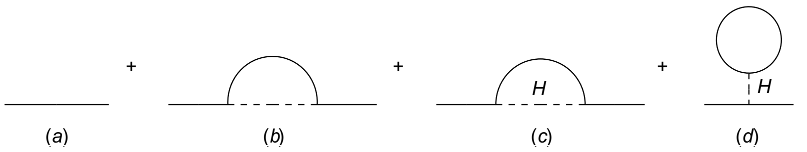

Figure 8. Diagrams for the two-point function. The diagrams (c) and (d) come from the Zeeman term.

$$\Gamma^{(2)}(p) = \frac{Z}{Z_g g}p^2 + \frac{\sqrt{Z}}{g}H - \frac{1}{\epsilon}\left(p^2 + \frac{N-1}{2}H\right), \tag{109}$$

where the factor $\Omega_d/(2\pi)^d$ is included in g for simplicity. To remove the divergence, we choose

$$\frac{Z}{Z_g} = 1 + \frac{g}{\epsilon}, \tag{110}$$

$$\sqrt{Z} = 1 + \frac{N-1}{2\epsilon}g. \tag{111}$$

This set of equations indicates

$$Z_g = 1 + \frac{N-1}{\epsilon}g + O(g^2), \tag{112}$$

$$Z = 1 + \frac{N-1}{\epsilon}g + O(g^2). \tag{113}$$

The case $N = 2$ is s special case, where we have $Z_g = 1$. This will hold even when including higher order corrections. For $N = 2$, we have one π field satisfying

$$\sigma_2 + \pi_2 = 1 \tag{114}$$

When we represent σ and π as $\sigma = \cos\theta$ and $\pi = \sin\theta$, the Lagrangian is

$$\mathcal{L} = \frac{1}{2g}\{(\partial_\mu\sigma)^2 + (\partial_\mu\pi)^2\} = \frac{1}{2g}(\partial_\mu\theta)^2. \tag{115}$$

If we disregard the region of θ, $0 \le \theta \le 2\pi$, the field θ is a free field suggesting that $Z_g = 1$.

3.3. Renormalization group equations

The beta function $\beta(g)$ of the coupling constant g is defined by

$$\beta(g) = \mu\frac{\partial g}{\partial\mu}, \tag{116}$$

where the bare quantities are fixed in calculating the derivative. Since $\mu\,\partial g_0/\partial\mu = 0$, the beta function is derived as

http://dx.doi.org/10.5772/intechopen.68214

$$\beta(g) = \frac{\epsilon g}{1 + g\frac{\partial}{\partial g}\ln Z_g} = \epsilon g - (N-2)g^2 + O(g^3), \tag{117}$$

for $d = 2 + \epsilon$. The beta function is shown in **Figure 9** as a function of g. We mention here that the coefficient $N - 2$ of g^2 term is related with the Casimir invariant of the symmetry group O(N) [34, 49].

In the case of $N = 2$ and $d = 2$, $\beta(g)$ vanishes. This case corresponds to the classical XY model as mentioned above and there may be a Kosterlitz-Thouless transition. The Kosterlitz-Thouless transition point cannot be obtained by a perturbation expansion in g.

In two dimensions $d = 2$, $\beta(g)$ shows asymptotic freedom for $N > 2$. The coupling constant g approaches zero in high-energy limit $\mu \to \infty$ in a similar way to QCD. For $N = 1$, g increases as $\mu \to \infty$ as in the case of QED. When $d > 2$, there is a fixed point g_c:

$$g_c = \frac{\epsilon}{N-2}, \tag{118}$$

for $N > 2$. There is a phase transition for $N > 2$ and $d > 2$.

Let us consider the n-point function $\Gamma^{(n)}(k_i, g, \mu, H)$. The bare and renormalized n-point functions are introduced similarly and they are related by the renormalization constant Z

$$\Gamma_R^{(n)}(k_i, g, \mu, H) = Z^{n/2}\Gamma_B^{(n)}(k_i, g, \mu, H). \tag{119}$$

From the condition that the bare function $\Gamma_B^{(n)}$ is independent of μ, $\mu\, d\Gamma_B^{(n)}/d\mu = 0$, the renormalization group equation is followed

$$\left[\mu\frac{\partial}{\partial\mu} + \mu\frac{\partial g}{\partial\mu}\frac{\partial}{\partial g} - \frac{n}{2}\zeta(g) + \left(\frac{1}{2}\zeta(g) + \frac{1}{g}\beta(g) - (d-2)\right)H\frac{\partial}{\partial H}\right]\Gamma_R^{(n)}(k_i, g, \mu, H) = 0, \tag{120}$$

where we defined

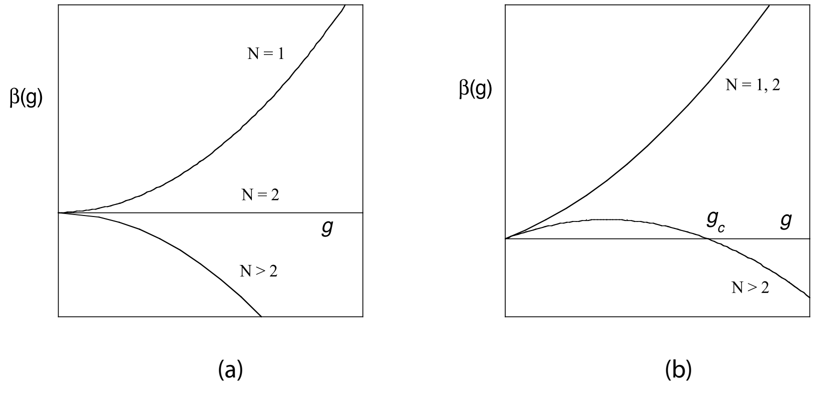

Figure 9. The beta function $\beta(g)$ as a function of g for $d = 2$ (a) and $d > 2$ (b). There is a fixed point for $N > 2$ and $d > 2$. $\beta(g)$ is negative for $d = 2$ and $N > 2$, which indicates that the model exhibits an asymptotic freedom.

$$\zeta(g) = \mu \frac{\partial}{\partial \mu} \ln Z = \beta(g) \frac{\partial}{\partial g} \ln Z. \tag{121}$$

From Eq. (113), $\zeta(g)$ is given by

$$\zeta(g) = (N-1)g + O(g^2). \tag{122}$$

Let us define the correlation length $\xi = \xi(g, \mu)$. Because the correlation length near the transition point will not depend on the energy scale, it should satisfy

$$\mu \frac{d}{d\mu} \xi(g, \mu) = \left(\mu \frac{\partial}{\partial \mu} + \beta(g) \frac{\partial}{\partial g} \right) \xi(g, \mu) = 0. \tag{123}$$

We adopt the form $\xi = \mu^{-1} f(g)$ for a function $f(g)$, so that we have

$$\beta(g) \frac{df(g)}{dg} = f(g). \tag{124}$$

This indicates

$$f(g) = C \exp\left(\int_{g_*}^{g} \frac{1}{\beta(g')} dg' \right), \tag{125}$$

where C and g_* are constants. In two dimensions ($\epsilon = 0$), the beta function in Eq. (117) gives

$$\xi = C\mu^{-1} \exp\left(\frac{1}{N-2} \left(\frac{1}{g} - \frac{1}{g_*} \right) \right). \tag{126}$$

When $N > 2$, ξ diverges as $g \to 0$, namely, the mass proportional to ξ^{-1} vanishes in this limit. When $d > 2$ ($\epsilon > 0$), there is a finite-fixed point g_c. We approximate $\beta(g)$ near $g = g_c$ as

$$\beta(g) \approx a(g - g_c), \tag{127}$$

with $a < 0$, ξ is

$$\xi = \mu^{-1} \exp\left(\frac{1}{a} \ln \left\lfloor \frac{g - g_c}{g_* - g_c} \right\rfloor \right). \tag{128}$$

Near the critical point $g \approx g_c$, ξ is approximated as

$$\xi^{-1} \approx \mu \lfloor g - g_c \rfloor^{1/\lfloor a \rfloor}. \tag{129}$$

This means that $\xi \to \infty$ as $g \to g_c$. We define the exponent v by

http://dx.doi.org/10.5772/intechopen.68214

$$\xi^{-1} \approx \lfloor g - g_c \rfloor^{\nu}, \tag{130}$$

then we have

$$\nu = -\frac{1}{\beta'(g_c)}. \tag{131}$$

Since $\beta'(g_c) = \epsilon - 2(N-2)g_c = -\epsilon$, this gives

$$\frac{1}{\nu} = \epsilon + O(\epsilon^2) = d - 2 + O(\epsilon^2). \tag{132}$$

Including the higher-order terms, ν is given as

$$\frac{1}{\nu} = d - 2 + \frac{(d-2)^2}{N-2} + \frac{(d-2)^3}{2(N-2)} + O(\epsilon^4). \tag{133}$$

3.4. 2D quantum gravity

A similar renormalization group equation is derived for the two-dimensional quantum gravity. The space structure is written by the metric tensor $g_{\mu\nu}$ and the curvature R. The quantum gravity Lagrangian is

$$\mathcal{L} = -\frac{1}{16\pi G}\sqrt{g}R \tag{134}$$

where g is the determinant of the matrix $(g_{\mu\nu})$ and G is the coupling constant. The beta function for G was calculated as [78–81]

$$\beta(G) = \epsilon G - bG^2, \tag{135}$$

for $d = 2 + \epsilon$ with a constant b. This has the same structure as that for the non-linear sigma model.

4. Sine-Gordon model

4.1. Lagrangian

The two-dimensional sine-Gordon model has attracted a lot of attention [43–49, 82–91]. The Lagrangian of the sine-Gordon model is given by

$$\mathcal{L} = \frac{1}{2t_0}(\partial_\mu\phi)^2 + \frac{\alpha_0}{t_0}\cos\phi, \tag{136}$$

where ϕ is a real scalar field, and t_0 and α_0 are bare coupling constants. We also use the Euclidean notation in this section. The second term is the potential energy of the scalar field.

We adopt that t and α are positive. The renormalized coupling constants are denoted as t and α, respectively. The dimensions of t and α are $[t] = \mu^{2-d}$ and $[\alpha] = \mu^2$. The scalar field ϕ is dimensionless in this representation. The renormalization constants Z_t and Z_α are defined as follows

$$t_0 = t\mu^{2-d}Z_t,\ \alpha_0 = \ \alpha\mu^2 Z_\alpha. \tag{137}$$

Here, the energy scale μ is introduced so that t and α are dimensionless. The Lagrangian is written as

$$\mathcal{L} = \frac{\mu^{d-2}}{2tZ_t}(\partial_\mu\phi)^2 + \frac{\mu^d \alpha Z_\alpha}{tZ_t}\cos\phi. \tag{138}$$

We can introduce the renormalized field $\phi_B = \sqrt{Z_\phi}\phi_R$ where Z_ϕ is the renormalization constant. Then the Lagrangian is

$$\mathcal{L} = \frac{\mu^{d-2}Z_\phi}{2tZ_t}(\partial_\mu\phi)^2 + \frac{\mu^d \alpha Z_\alpha}{tZ_t}\cos\phi. \tag{139}$$

where ϕ denotes the renormalized field ϕ_R.

4.2. Renormalization of α

We investigate the renormalization group procedure for the sine-Gordon model on the basis of the dimensional regularization method. First consider the renormalization of the potential term. The lowest-order contributions are given by diagrams with tadpole contributions. We use the expansion $\cos\phi = 1 - \frac{1}{2}\phi^2 + \frac{1}{4!}\phi^4 - \cdots$. Then the corrections to the cosine term are evaluated as follows. The constant term is renormalized as

$$1 - \frac{1}{2}\langle\phi^2\rangle + \frac{1}{4!}\langle\phi^4\rangle - \ \cdots = 1 - \frac{1}{2}\langle\phi^2\rangle + \frac{1}{2}\left(\frac{1}{2}\langle\phi^2\rangle\right)^2 - \ \cdots = \exp\left(-\frac{1}{2}\langle\phi^2\rangle\right). \tag{140}$$

Similarly, the ϕ^2 is renormalized as

$$-\frac{1}{2}\phi^2 + \frac{1}{4!}6\langle\phi^2\rangle\phi^2 - \frac{1}{6!}15\cdot 3\langle\phi^2\rangle^2\phi^2 + \ \cdots = exp\left(-\frac{1}{2}\langle\phi^2\rangle\right)\left(-\frac{1}{2}\phi^2\right). \tag{141}$$

Hence the $\alpha Z_\alpha \cos\left(\sqrt{Z_\phi}\phi\right)$ is renormalized to

$$\alpha Z_\alpha \exp\left(-\frac{1}{2}Z_\phi\langle\phi^2\rangle\right)\cos\left(\sqrt{Z_\phi}\phi\right) \approx \alpha Z_\alpha\left(1 - \frac{1}{2}Z_\phi\langle\phi^2\rangle + \cdots\right)\cos\left(\sqrt{Z_\phi}\phi\right). \tag{142}$$

The expectation value $\langle\phi^2\rangle$ is regularized as

$$Z_\phi\langle\phi^2\rangle = t\mu^{2-d}\ Z_t\int \frac{d^dk}{(2\pi)^d}\frac{1}{k^2+m_0^2} = \ -\frac{t}{\epsilon}\frac{\Omega_d}{(2\pi)^d}, \tag{143}$$

where $d = 2+\epsilon$ and we included a mass m_0 to avoid the infrared divergence and Z_t=1 to this order. The constant Z_α is determined to cancel the divergence:

$$Z_\alpha = 1-\frac{t}{2}\frac{1}{\epsilon}\frac{\Omega_d}{(2\pi)^d}. \tag{144}$$

From the equations $\mu\,\partial t_0/\partial\mu = 0$ and $\mu\,\partial\alpha_0/\partial\mu = 0$, we obtain

$$\mu\frac{\partial t}{\partial\mu} = \ (d-2)t - t\mu\frac{\partial\,\ln Z_t}{\partial\mu}, \tag{145}$$

$$\mu\frac{\partial\alpha}{\partial\mu} = \ -2\alpha - \ \alpha\mu\frac{\partial\,\ln Z_\alpha}{\partial\mu} \tag{146}$$

The beta function for α reads

$$\beta(\alpha) \equiv \ \mu\frac{\partial\alpha}{\partial\mu} = \ -2\alpha + \ t\alpha\frac{1}{2}\frac{\Omega_d}{(2\pi)^d}, \tag{147}$$

where we set $\mu\,\partial\, t/\partial\mu = (d-2)t$ with $Z_t = 1$ up to the lowest order of α. The function $\beta(\alpha)$ has a zero at $t = t_c = 8\pi$.

4.3. Renormalization of the two-point function

Let us turn to the renormalization of the coupling constant t. The renormalization of t comes from the correction to p^2 term. The lowest-order two-point function is

$$\Gamma_B^{(2)(0)}(p) = \ \frac{1}{t_0}p^2 = \ \frac{1}{t\mu^{2-d}Z_t}p^2. \tag{148}$$

The diagrams that contribute to the two-point function are shown in **Figure 10** [88]. These diagrams are obtained by expanding the cosine function as $\cos\phi = 1-(1/2)\phi^{\,2}+\cdots$. First, we consider the Green's function,

$$G_0(x) = \ Z_\phi{<}\phi(x)\phi(0){>} = t\mu^{2-d}Z_t\int\frac{d^dp}{(2\pi)^d}p\frac{e^{ip\cdot x}}{p^2+m_0^2} = t\mu^{2-d}Z_t\frac{\Omega_d}{(2\pi)^d}K_0(m_0|x|), \tag{149}$$

where K_0 is the zeroth modified Bessel function and m_0 is introduced to avoid the infrared singularity. Because $\sinh I - I = I^3/3! + \cdots$, the diagrams in **Figure 10** are summed up to give

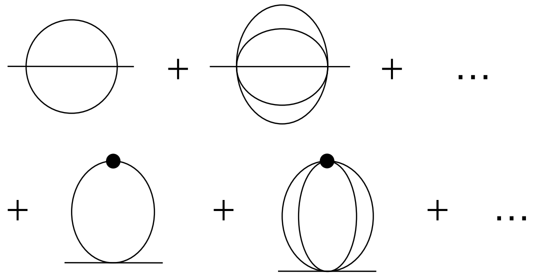

Figure 10. Diagrams that contribute to the two-point function.

$$\Sigma(p) = \int d^d x [e^{ip\cdot x}(\sinh I - I) - (\cosh I - 1)], \tag{150}$$

Where $I = G_0(x)$. Since $\sinh I - I \approx e^I/2$ and $\cosh I \approx e^I/2$, the diagrams in **Figure 10** lead to

$$\Gamma_B^{(2)c}(p) = -\frac{1}{2}\left(\frac{\alpha\mu^d Z_\alpha}{tZ_t}\right)^2 \int d^d x (e^{ip\cdot x} - 1)e^{G_0(x)}. \tag{151}$$

We use the expansion $e^{ip\cdot x} = 1 + ip\cdot x - (1/2)(p\cdot x)^2 + \cdots$, and keep the p_2 term. We denote the derivation of t from the fixed point $t_c = 8\pi$ as ν:

$$\frac{t}{8\pi} = 1 + \nu, \tag{152}$$

for $d = 2$. Using the asymptotic formula $K_0(x)^{\sim} - \gamma - \ln(x/2)$ for small x, we obtain

$$\begin{aligned}\Gamma_B^{(2)c}(p) &= \frac{1}{8}\left(\frac{\alpha\mu^d}{tZ_t}\right)^2 p^2 (c_0 m_0^2)^{-2-2\nu}\Omega_d \int_0^\infty dx x^{d+1}\frac{1}{(x^2+a^2)^{2+2\nu}} \\ &= -\frac{1}{8}p^2\left(\frac{\alpha\mu^d}{tZ_t}\right)^2 (c_0 m_0^2)^{-2}\Omega_d \frac{1}{\epsilon} + \mathrm{O}(\nu) \\ &\approx -\frac{1}{t\mu^{2-d}Z_t}p^2\frac{1}{32}\alpha^2\mu^{d+2}(c_0 m_0^2)^{-2}\frac{1}{\epsilon} + O(\nu)\end{aligned} \tag{153}$$

where c_0 is a constant and $a = 1/\mu$ is a small cut-off. The divergence of α was absorbed by Z_α. Now the two-point function up to this order is

$$\Gamma_B^{(2)}(p) = \frac{1}{t\mu^{2-d}Z_t}\left[p^2 - \frac{1}{32}\alpha^2\mu^{d+2}(c_0 m_0^2)^{-2}\frac{1}{\epsilon}\right] \tag{154}$$

The renormalized two-point function is $\Gamma_R^{(2)} = Z_\phi \Gamma_B^{(2)}$. This indicates that

$$\frac{Z_\phi}{Z_t} = 1 + \frac{1}{32}\alpha^2\mu^{d+2}(c_0 m_0^2)^{-2}\frac{1}{\epsilon}. \tag{155}$$

Then, we can choose $Z_\phi = 1$ and

$$Z_t = 1 - \frac{1}{32}\alpha^2\mu^{d+2}(c_0 m_0^2)^{-2}\frac{1}{\epsilon}. \tag{156}$$

Z_t/Z_ϕ can be regarded as the renormalization constant of t up to the order of $\alpha 2$, and thus we do not need the renormalization constant Z_ϕ of the field ϕ. This means that we can adopt the bare coupling constant as $t_0 = t\mu^{2-d}\tilde{Z}_t$ with $\tilde{Z}_t = Z_t/Z_\phi$.

The renormalization function of t is obtained from the equation $\mu\,\partial\, t_0/\partial\mu = 0$ for $t_0 = t\mu^{2-d}Z_t$:

$$\begin{aligned}\beta(t) \;&\equiv\; \mu\frac{\partial t}{\partial\mu} = \; (d-2)t + \frac{1}{32}(c_0 m_0^2)^{-2}\frac{1}{\epsilon}\left(2\alpha\mu^{d+2}\mu\frac{\partial\alpha}{\partial\mu} + (d+2)\alpha^2\mu^{d+2}\right)t \\ &= \; (d-2)t + \frac{1}{32}\mu^{d+2}(c_0 m_0^2)^{-2}t\alpha^2\end{aligned} \tag{157}$$

Because the finite part of $G_0(x \to 0)$ is given by $G_0(x \to 0) = -(1/2\pi)\ln(e^\gamma m_0/2\mu)$, we perform the finite renormalization of α as $\alpha \to \alpha c_0 m_0^2 a^2 = \alpha c_0 m_0^2 \mu^{-2}$. This results in

$$\beta(t) = \; (d-2)t + \frac{1}{32}t\alpha^2. \tag{158}$$

As a result, we obtain a set of renormalization group equations for the sine-Gordon model

$$\beta(\alpha) = \; \mu\frac{\partial\alpha}{\partial\mu} = \; -\alpha\left(2 - \frac{1}{4\pi}t\right), \tag{159}$$

$$\beta(t) = \; \mu\frac{\partial t}{\partial\mu} = \; (d-2)t + \frac{1}{32}t\alpha^2, \tag{160}$$

Since the equation for α is homogeneous in α, we can change the scale of α arbitrarily. Thus, the numerical coefficient of $t\alpha^2$ in $\beta(t)$ is not important.

4.4. Renormalization group flow

Let us investigate the renormalization group flow in two dimensions. This set of equations reduces to that of the Kosterlitz-Thouless (K-T) transition. We write $t = 8\pi(1+\nu)$, and set $x = 2\nu$ and $y = \alpha/4$. Then, the equations are

$$\mu \frac{\partial x}{\partial \mu} = y^2, \tag{161}$$

$$\mu \frac{\partial y}{\partial \mu} = xy, \tag{162}$$

These are the equations of K-T transition. We have

$$x^2 - y^2 = \text{const}. \tag{163}$$

The renormalization flow is shown in **Figure 11**. The Kosterlitz-Thouless transition is a beautiful transition that occurs in two dimensions. It was proposed that the transition was associated with the unbinding of vortices, that is, the K-T transition is a transition of the binding-unbinding transition of vortices.

The Kondo problem is also described by the same equations. In the s-d model, we put

$$x = \pi\beta J_z - 2, \; y = 2|J_\perp|\tau. \tag{164}$$

where J_z and $J_\perp(= J_x = J_y)$ are exchange coupling constants between the conduction electrons and the localized spin, and β is the inverse temperature. τ is a small cut-off with $\tau \propto 1/\mu$. The scaling equations for the s-d model are [53, 57]

$$\tau \frac{\partial x}{\partial \tau} = -\frac{1}{2}y^2, \tag{165}$$

$$\tau \frac{\partial y}{\partial \tau} = -\frac{1}{2}xy. \tag{166}$$

The Kondo effect occurs as a crossover from weakly correlated region to strongly correlated region. A crossover from weakly to strongly coupled systems is a universal and ubiquitous

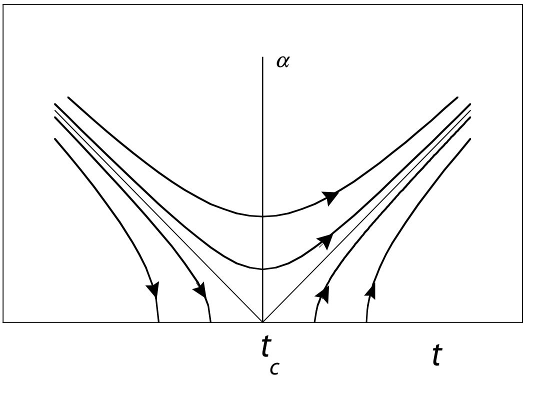

Figure 11. The renormalization group flow for the sine-Gordon model as $\mu \to \infty$.

phenomenon in the world. There appears a universal logarithmic anomaly as a result of the crossover.

5. Scalar quantum electrodynamics

We have examined the ϕ^4 theory and showed that there is a phase transition. This is a second-order transition. What will happen when a scalar field couples with the electromagnetic field? This issue concerns the theory of a complex scalar field ϕ interacting with the electromagnetic field A_μ, called the scalar quantum electrodynamics (QED). The Lagrangian is

$$\mathcal{L} = \frac{1}{2}|(D_\mu\phi)|^2 - \frac{1}{4}g(|\phi|^2)^2 - \frac{1}{4}F_{\mu\nu}^2, \tag{167}$$

where g is the coupling constant and $F_{\mu\nu} = \partial_\mu A_\nu - \partial_\nu A_\mu$. D_μ is the covariant derivative given as

$$D_\mu = \partial_\mu - ieA_\mu, \tag{168}$$

with the charge e. The scalar field ϕ is an N component complex scalar field such as $\phi = (\phi_1, \cdots, \phi_N)$. This model is actually a model of a superconductor. The renormalization group analysis shows that this model exhibits a first-order transition near four dimensions $d = 4 - \epsilon$ when $2N < 365$ [92–96]. Coleman and Weinberg first considered the scalar QED model in the case $N = 1$. They called this transition the dimensional transmutation. The result based on the ϵ-expansion predicts that a superconducting transition in a magnetic field is a first-order transition. This transition may be related to a first-order transition in a high magnetic field [97].

The bare and renormalized fields and coupling constants are defined as

$$\phi_0 = \sqrt{Z_\phi}\phi, \tag{169}$$

$$g_0 = \frac{Z_4}{Z_\phi^2}g\mu^{4-d}, \tag{170}$$

$$e_0 = \frac{Z_e}{\sqrt{Z_A Z_\phi}}e, \tag{171}$$

$$A_{\mu 0} = \sqrt{Z_A}A_\mu, \tag{172}$$

where ϕ, g, e and A_μ are renormalized quantities. We have four renormalization constants. Thanks to the Ward identity

$$Z_e = Z_A, \tag{173}$$

three renormalization constants should be determined. We show the results:

$$Z_\phi = 1 + \frac{3}{8\pi^2\epsilon}e^2, \tag{174}$$

$$Z_A = 1 - \frac{2N}{48\pi^2\epsilon}e^2, \tag{175}$$

$$Z_g = 1 + \frac{2N+8}{8\pi^2\epsilon}g + \frac{3}{8\pi^2\epsilon}\frac{1}{g}e^4. \tag{176}$$

The renormalization group equations are given by

$$\mu\frac{\partial e^2}{\partial\mu} = -\epsilon e^2 + \frac{N}{24\pi^2}e^4, \tag{177}$$

$$\mu\frac{\partial g}{\partial\mu} = -\epsilon g + \frac{N+4}{4\pi^2}g^2 + \frac{3}{8\pi^2}e^4 - \frac{3}{4\pi^2}e^2 g. \tag{178}$$

The fixed point is given by

$$e_c = \frac{24}{N}\pi^2\epsilon, \tag{179}$$

$$g_c = \epsilon\frac{2\pi^2}{N+4}\left\{1 + \frac{18}{N} \pm \frac{(n^2-360n-2160)^{1/2}}{n}\right\}, \tag{180}$$

where $n = 2N$. The square root $\delta \equiv (n^2 - 360n - 2160)^{1/2}$ is real when $2N > 365$. This indicates that the zero of a set of beta functions exists when N is sufficiently large as long as $2N > 365$. Hence there is no continuous transition when N is small, $2N \leq 365$, and the phase transition is first-order.

There are also calculations up to two-loop-order for scalar QED [98, 99]. This model is also closely related with the phase transition from a smectic-A to a nematic liquid crystal for which a second-order transition was reported [100]. When N is large as far as $2N > 365$, the transition becomes second-order. Does the renormalization group result for the scalar QED contradict with second-order transition in superconductors? This subject has not been solved yet. A possibility of second-order transition was investigated in three dimensions by using the renormalization group theory [101]. An extra parameter c was introduced in [101] to impose a relation between the external momentum p and the momentum q of the gauge field as $q = p/c$. It was shown that when $c > 5.7$, we have a second-order transition. We do not think that it is clear whether the introduction of c is justified or not.

6. Summary

We presented the renormalization group procedure for several important models in field theory on the basis of the dimensional regularization method. The dimensional method is very useful and the divergence is separated from an integral without ambiguity. We invested three fundamental models in field theory: $\phi 4$ theory, non-linear sigma model and sine-Gordon model. These models are often regarded as an effective model in understanding physical phenomena. The renormalization group equations were derived in a standard way by regularizing the ultraviolet divergence. The renormalization group theory is useful in the study of various quantum systems.

The renormalization means that the divergences, appearing in the evaluation of physical quantities, are removed by introducing the finite number of renormalization constants. If we need infinite number of constants to cancel the divergences for some model, that model is called unrenormalizable. There are many renormalizeable field theoretic models. We considered three typical models among them. The idea of renormalization group theory arises naturally from renormalization. The dependence of physical quantities on the renormalization energy scale easily leads us to the idea of renormalization group.

Author details

Takashi Yanagisawa

Address all correspondence to: t-yanagisawa@aist.go.jp

National Institute of Advanced Industrial Science and Technology, Tsukuba, Ibaraki, Japan

References

[1] Zinn-Justin J. Quantum Field Theory and Critical Phenomena. UK: Clarendon Press; 2002.

[2] Gross D. Methods in Field Theory. In: Balian R, Zinn JJ, editors. Les Houches Lecture Notes. Vol. XXVIII. North Holland, Amsterdam; 1976.

[3] Itzykson C, Zuber JB. Quantum Field Theory. New York: McGraw-Hill Book Company, 1980.

[4] Coleman S. Aspects of Symmetry. Cambridge: Cambridge University Press; 1985.

[5] Peskin ME, Schroeder DV. An Introduction to Quantum Field Theory. USA: Westview Press; 1995.

[6] Ramond P. Field Theory: A Modern Primer. Redwood City, California: Addison-Wesley; 1989.

[7] Weinberg S. The Quantum Theory of Fields. Vols. I–III. Cambridge: Cambridge University Press; 1995.

[8] Ryder LH. Quantum Field Theory. Cambridge: Cambridge University Press; 1985.

[9] Nash C. Relativistic Quantum Fields. New York: Academic Press; 1978. Mineola, New York: Dover Publications; 2011.

[10] Nishijima K. Fields and Particles. Massachusetts: Benjamin/Cummings Publishing Company; 1969.

[11] Bogoliubov NN, Shirkov DV. Introduction to the Theory of Quantized Fields. New York: John Wiley and Sons; 1980.

[12] Anderson PW. Basic Notions in Condensed Matter Physics. Menlo Park, California: Benjamin/Cummings; 1984.

[13] Parisi G. Statistical Field Theory. Menlo Park, California: Benjamin/Cummings; 1988.

[14] Amit DJ. Field Theory, the Renormalization Group, and Critical Phenomena. Singapore: World Scientific Pub; 2005.

[15] Polyakov AM. Gauge Fields and Strings. Switzerland: Harwood Academic Publishers; 1987.

[16] Abrikosov AA, Gorkov LP, Dzyaloshinskii IE. Quantum Field Theoretical Methods in Statistical Physics. Oxford: Pergamon; 1965.

[17] Tsvelik AM. Quantum Field Theory in Condensed Matter Physics. Cambridge: Cambridge University Press; 1995.

[18] Fradkin E. Field Theories of Condensed Matter Systems. Redwood City, California: Addison-Wesley; 1991.

[19] Popov VN. Functional Integrals and Collective Excitations. Cambridge: Cambridge University Press; 1987.

[20] Wilson KG, Fisher ME. Physical Review Letters. 1972;28:240

[21] Wilson KG. Physical Review Letters. 1972;28:548

[22] Wilson KG, Kogut JB. Physics Reports. 1974;12;75

[23] Brezin E, Wallace DJ, Wilson KG. Physical Review Letters. 1972;29:591

[24] Brezin E, Le GJC, Zinn JJ. Physical Review. 1982;D8:434

[25] Polyakov AM. Physical Letters. 1975;59B:79

[26] Brezin E, Zinn JJ. Physical Review Letters. 1976;36:691

[27] Zakrzewski WJ. Low Dimensional Sigma Models. Adam Hilger, Bristol: IOP Publishing; 1989.

[28] Ellis RK, Stirling WJ, Webber BR. QCD and Collider Physics. Cambridge: Cambridge University Press; 2003.

[29] Nelson DR, Pelcovits RA. Physical Review. 1977;B16:2191

[30] Chakravarty S, Halperin BI, Nelson DR. Physical Review Letters. 1988;60:1057

[31] Chakravarty S, Halperin BI, Nelson DR. Physical Review. 1989;B39:2344

[32] Yanagisawa T. Physical Review. 1992;B46:13896

[33] Perelomov AM. Physical Report. 1989;174:229

[34] Brezin E, Hikami S, Zinn JJ. Nuclear Physics. 1980;B165:528

[35] HIkami S. Progress of Theoretical Physics. 1979;64;1466

[36] Hikami S. Progress of Theoretical Physics. 1980;64:1425

[37] Hikami S. Nuclear Physics. 1983;B21:555

[38] Wess J, Zumino B. Physical Letters. 1971;B37:95

[39] Witten E. Nuclear Physics. 1983; B223:422

[40] Witten E. Communications in Mathematical Physics. 1984;92:455

[41] Novikov SP. Soviet mathematics - Doklady. 1982;24:222

[42] Golo VL, Perelomov AM. Physical Letters. 1978;B79:112

[43] Coleman S. Physical Review. 1975;D11:2088

[44] Brezin E, Itzykson C, Zinn JJ, Zuber JB. Physical Letters. 1979;B82: 442

[45] Dashen RF, Hasslacher B, Neveu A. Physical Review. 1979;D11: 3424

[46] Zamolodchikov AB, Zamolodchikov ALB. Annals of Physics. 1979;120:253

[47] Rajaraman R. Solitons and Instantons. North-Holland Publishing Co. Amsterdam, The Netherlands; 1982.

[48] Manton NS, Sutcliffe P. Topological Solitons. Cambridge: Cambridge University Press; 2004.

[49] T. Yanagisawa, Europhysics Letters 113, 41001 (2016).

[50] Kosterlitz JM, Thouless DJ. Journal of Physics. 1973;C6:1181

[51] Kosterlitz JM. Journal of Physics. 1974;C7:1046

[52] Kondo J. Progress of Theoretical Physics. 1964;32:34

[53] Kondo J. The Physics of Dilute Magnetic Alloys. Cambridge: Cambridge University Press; 2012.

[54] Anderson PW. Journal of Physics. 1970;C3:2436

[55] Anderson PW, Yuval G. Physical Review Letters. 1969;23:89

[56] Yuval G, Anderson PW. Physical Review. 1970;B1:1522

[57] Anderson PW, Yuval G Hamann DR. Physical Review. 1970;B1:4464

[58] Solyom J. Advances in Physics. 1979;28:201

[59] Haldane FDN. Journal of Physics. 1966;C14:901

[60] Hubbard J. Proceedings of the Royal Society of London. 1963;276:238

[61] Yamaji K, Yanagisawa T, Nakanishi T, Koike S. Physica. 1998;C304:225

[62] Yanagisawa T et al. Physical Review. 2001;B64:184509

[63] Yanagisawa T et al. Physical Review. 2003;B67:132408

[64] Yamaji K et al. Physica 2000;B284:415

[65] Yanagisawa T. Journal of the Physical Society of Japan. 2016;85:114707

[66] Leggett AJ. Progress of Theoretical Physics. 1966;36:901

[67] Tanaka Y and Yanagisawa T. Journal of the Physical Society of Japan. 2010;79:114706

[68] Tanaka Y, Yanagisawa T. Solid State Communications. 2010;150:1980

[69] Yanagisawa T, et al. Journal of the Physical Society of Japan. 2012;81:024712

[70] Yanagisawa T, Hase I. Journal of the Physical Society of Japan. 2013;82:124704

[71] Yanagisawa T, Tanaka Y. New Journal of Physics. 2014;16:123014

[72] Kleiner R, et al. Physical Review Letters. 2013;68:2349

[73] Tamasaku K, et al. Physical Review Letters. 1992;69:1455

[74] Matsuda Y, et al. Physical Review Letters. 1995;75:4512

[75] Koyama T, Tachiki M. Physical Review. 1996;B54:16183

[76] Hooft T, Veltman M. Nuclear Physics. 1972;B44:189

[77] Vladimirov AA, Kazanov DJ, Tarasov OV. Soviet Physics-JETP. 1979;50:521

[78] Gastmans R, Kallosh R, Truffin C. Nuclear Physics. 1978;B133:417

[79] Christensen SM, Duff MJ. Physical Letters. 1978;79B:213

[80] Smolin L. Nuclear Physics. 1982;B208:439

[81] Kawai H, Ninomiya M. Nuclear Physics. 1990;B336:115

[82] Mandelstam S. Physical Review. 1975;D11:2088

[83] José JV, Kadanoff LP, Kirkpatrick S, Nelson DR. Physical Review. 1977;B16:1217

[84] Schroer B, Truong T. Physical Review. 1977;D15:1684

[85] Samuel S. Physical Review. 1978;D18: 1916

[86] Wiegmann PB. Journal of Physics. 1978;C11:1583

[87] Kogut J. Reviews of Modern Physics. 1979;51:659

[88] Amit DJ, Goldschmidt YY, Grinstein G. Journal of Physics. A: Mathematical and General. 1980;13:585

[89] Huang K, Polonyi J. International Journal Modern Physics. 1991;A6:409

[90] Nandori I, Jentschura UD, Sailer K, Soff G. Physical Review. 2004;D69:025004

[91] Nagy S, Nandori I, Polonyi J, Sailer K. Physical Review Letters. 2009;102;241603

[92] Coleman S, Weinberg E. Physical Review. 1973;D7:1883

[93] Halperin BI, Lubensky T, Ma SK. Physical Review Letters. 1974;32:292

[94] Hikami S. Progress of Theoretical Physics. 1979;62:226

[95] Lubensk TC, Chen JH. Physical Review. 1978;B17:366

[96] Chen JH, Lubensky TC, Nelson DR. Physical Review. 1978;B17:4274

[97] Maki K, Tsuneto T. Progress of Theoretical Physics. 1964;3:945

[98] Kolnberger S, Folk R. Physical Review. 1990;B41:4083

[99] Folk R, Holovatch Y. Journal of Physics. 1996;A29:3409

[100] Davidov D et al. Physical Review. 1979;B19:1657

[101] Herbut IF and Tesanovich Z. Physical Review Letters. 1996;76:4588

Chapter 5

Relativistic Perturbation Theory Formalism to Computing Spectra and Radiation Characteristics: Application to Heavy Elements

Alexander V. Glushkov, Olga Yu. Khetselius, Andrey A. Svinarenko, Vasily V. Buyadzhi, Valentin B. Ternovsky, Anna A. Kuznetsova and Petr G. Bashkarev

Additional information is available at the end of the chapter

http://dx.doi.org/10.5772/intechopen.69102

Abstract

Fundamentals of gauge-invariant relativistic many-body perturbation theory (PT) with optimized ab initio zeroth approximation in theory of relativistic multi-electron systems are presented. The problem of construction of optimal one-electron representation is directly linked with a problem of the correct accounting for multielectron exchange-correlation effects and gauge-invariance principle fulfilling in atomic calculations. New approach to construction of optimal PT zeroth approximation is based on accurate treating the lowest order multielectron effects, in particular, the gauge-dependent radiative contribution for the certain class of photon propagator (for instance, the Coulomb, Feynman, Babushkin ones) gauge. This value is considered to be a typical representative of important multielectron exchange-correlation effects, whose minimization is a reasonable criteria in the searching for optimal PT one-electron orbital basis. This procedure derives an undoubted profit in the routine many-body calculations as it provides the way of refinement of the atomic characteristics calculations, based on the "first principles". The relativistic density-functional approximation is taken as the zeroth one. There have taken into account all exchange-correlation corrections of the second order and dominated classes of the higher orders diagrams (polarization interaction, quasiparticles screening, etc.). New form of multi-electron polarization functional is used. As illustration, the results of computing energies, transition probabilities for some heavy ions are presented.

Keywords: relativistic many-body perturbation theory, density-functional approximation, exchange-correlation effects, radiative transitions, oscillator strengths, heavy atoms

1. Introduction

Perturbation theory (PT) formalism has a long history in studying different multielectron (more generally, multifermion) systems, including different atomic, molecular, and nuclear properties. Really, one should say about formalism of the many-body PT as, a rule, usually it applies to studying different properties of the multiparticle systems, for instance, ionization and excitation energies, spectra, electron exchange-correlation energies, hyperfine structure, radiative and autoionization decay rates (transition probabilities, oscillator, and lines strengths), as well as the influence of an external electromagnetic fields. In the last few decades, the PT methods have been refined with a sophisticated and comprehensive approach of more correct treatment of the exchange-correlation effects, electron-nuclear dynamics, and so on [1–44]. Rephrasing the known interesting quote by Bartlett and Musiał [3, 4] and earlier by Wilson, one could say that *the PT methods are an emerging computational area that is sixty years ahead of lattice gauge theory… and a rich source of new ideas and new approaches to the computation of many fermion systems*. The old multibody quantum theoretical approaches often take place, which have been primarily developed in a theory of a superfluity and/or a superconductivity, and generally speaking in a theory of solids, became the powerful tools for developing new conceptions in many-body (multielectron) atomic, nuclear, and molecular calculations [1–7].

A number of the PT versions include a synthesis of cluster expansions, Brueckner's summation of ladder diagrams, the summation of ring diagrams Gell-Mann, and an infinite-order generalization of manybody PT (Kelly, 1969; Ivanov-Tolmachev, 1969–1974, Bartlett and Silver, 1974–1976, etc.; see review in Ref. [7]). Using quantum-field methods in atomic and molecular theory allowed obtaining a very powerful approach for the correct treatment of the exchange-correlation effects in many-electron systems. In this context, it is useful to remind about such sophisticated methods as a coupled-cluster theory, the Green-functions method, configuration interaction methods, and so on. Only with this property are applications to solids or the electron gas possible, and, even for small atoms and molecules, its effects are numerically quite essential. When relativistic effects became essential in the studied multielectron (fermion) system, naturally it is necessary to formulate a formalism of the relativistic many-body PT. In the first attempts, an account for the relativistic effects had been reduced to treating the Darwin, mass-velocity, and spin-orbit effects, which have to be added to the nonrelativistic solution and provide different approximations lying between the Schrödinger equation and the four-component Dirac equation [2, 6, 7]. Among recent developments in this field, special attention should be given to two very general and important computer systems for relativistic and QED calculations of atomic and molecular properties developed in the Oxford, Troitsk, and other groups (known as "GRASP," "Dirac," "BERTHA," "QED," "Superatom," etc.; Ref. [1–13] and references therein). For example, a new relativistic molecular structure theory within the QED framework with accounting of the electron correlation and higher-order QED effects has been formulated and further realized as the BERTHA program. The master system of equations includes the so-called Dirac-Hartree-Fock-Breit self-consistent field equations. The useful overview of the relativistic electronic structure theory is presented in Refs. [2, 7] from the QED point of view. The next important step is an adequate taking into account the QED corrections. This topic has been a subject of intensive theoretical and experimental interest.

Hitherto, most many-body PT studies concerned atoms with a simple electron-shell structure, namely atoms of the inert gases and atoms and ions with a single electron (or hole) above (or inside) the closed shells core. The fundamental limitation to extend the many-body procedure beyond such simple atomic systems arises from the complexity of any perturbation expansion if more than just one or two *effective* particles appear in the derivation (see detailed analysis in Ref. [5]). In order to overcome this difficulty, a number of different efficient techniques of complex expansions were developed. As a rule, the atomic PT expansions are expressed in terms of the Feynman-Goldstone diagrams in Rayleigh-Schrödinger PT formulation. Above the most popular and known versions of the PT formalism, one should mention formally exact relativistic many-body PT with the model zeroth approximation by Ivanova-Ivanov et al., relativistic PT with the Hartree-Fock (HF) or Dirac-Fock (DF) zeroth approximations by Johnson et al., Flambaum-Dzuba et al., Safronova and Safronova et al., Khetselius et al., and so on [9–38]).

The searching for the optimal one-electron zeroth representation is one of the oldest in the theory of multielectron atoms and, respectively, in the formulation of the effective PT formalism. Two decades ago, Davidson had pointed the principal disadvantages of the traditional representation based on the self-consistent field approach and suggested the optimal "natural orbitals" representation [11]. Nevertheless, there remain insurmountable computational difficulties in the realization of the Davidson program (see, e.g., Refs. [11, 12]). One of the simplified recipes represents, for example, a density functional theory (DFT) formalism [8]. Unfortunately, this approach does not provide a regular refinement procedure in the case of the complicated atom with few quasiparticles (QPs) (electrons or vacancies above a core of the closed electronic shells). The problem of construction of the optimal one-electron representation is tightly linked with the problem of the correct accounting for the multielectron exchange-correlation effects. In Refs. [47, 48], the PT lowest-order multielectron effects, in particular, the gauge-dependent radiative contribution (gauge-noninvariant) for the certain class of the photon propagator gauge is treated. This value is considered to be the typical representative of the multielectron exchange-correlation effects contribution. New fundamental idea has been proposed in Refs. [47, 48] in order to construct the optimal PT one-electron basis and is in minimization of the gauge-noninvariant contribution into a radiation width of atomic level. Such an approach allows to determine an effectiveness of accounting of the multielectron exchange-correlation effects and provides the practical way of the refinement of the atomic characteristics calculations, based on the "first principles." Really, the known standard criterion of the multielectron computing quality in atomic spectroscopy is linked with a closeness of the atomic level radiation width values, calculated using two alternative forms of the transition operator (the "length" and the "velocity" forms). It is of special interest to verify the compatibility of the new optimization principle with the other requirements conditioning a "good" one-electron representation. We suppose that this point should be obligatory in formulation of the effective, optimal PT formalism.

In this chapter, we present the theoretical fundamentals of the gauge-invariant relativistic many-body PT with using the optimized one-QP representation in the theory of relativistic multielectron systems [21–23, 47, 48]. All exchange-correlation corrections of the second-order and dominated classes of the higher-orders diagrams (polarization interaction, QPs screening, etc.) [47–67] have been taken into account. As illustration of application of the presented PT formalism, we list the results of computing energies, transition probabilities (oscillator strengths) in some heavy atoms (ion of Hg+).

2. Relativistic many-body perturbation theory with optimized one-quasiparticle zeroth representation

2.1. General remarks

Our relativistic PT version is constructed on the same principles as the known formally exact PT with model zeroth approximation by Ivanova-Ivanov et al. [33–47]; however, there a few principal points, where our formalism differs from this known theory. At first, this is another definition of the zeroth approximation, namely within the relativistic DFT one [14–17, 19–22]. Second, this is an implementation of the principally new approach to construction of the optimized one-QP representation, which allows correctly to take into account a gauge invariance principle fulfilling.

In nonrelativistic theory of multielectron atoms, a powerful field approach for computing the electron energy shift ΔE of the degenerate states is known, which are usually present in the dense spectra of the complex relativistic atomic multielectron systems **(Tolmachev-Ivanov-Ivanova, 1969–1974)**. The key algorithm of this approach includes construction of the secular matrix M using the known Gell-Mann and Low adiabatic formula and its further diagonalization. The analogous approach using the Gell-Mann and Low formula with an electrodynamic scattering matrix has been developed in a theory of the relativistic atom [33–36]; however, the M matrix elements in the relativistic representation are complex; the corresponding imaginary parts determine the values of radiation widths. According to Ref. [34], the total electron energy shift can be defined as follows:

$$\Delta E = \mathrm{Re}\,\Delta E + i\,\mathrm{Im}\Delta E \quad \mathrm{Im}\Delta E = -\Gamma/2. \tag{1}$$

Here, Γ is a radiation width of the atomic level (or a possibility **P** of the radiation decay or transition: $P = \Gamma$. Within the general framework, the corresponding energies of a nondegenerated excited states and their radiation decay amplitudes can be determined by means of the computing and further diagonalization of the matrix M. In Refs. [33–37], the $\mathrm{Re}\Delta E$ calculation procedure has been generalized for the case of nearly degenerate states, whose levels form a more or less compact group. Naturally, the matrix M reduces to one term (ΔE) in the case of well-identified and separated energy spectrum. The Gell-Mann and Low formula allow further to obtain the expansion of the M elements into PT series on interelectron interaction and apply the standard Feynman diagrammatic technique. The corresponding PT series is as follows:

$$M = M^{(0)} + M^{(1)} + M^{(2)} + M^{(3)}. \tag{2}$$

Here, $M^{(0)}$ is the contribution of the PT all-orders vacuum diagrams (in fact, this is a real matrix, which determines only the general atomic levels shift); $M^{(1)}$, $M^{(2)}$,and $M^{(3)}$ are the contributions, which correspond to the one-, two- and three-QP PT diagrams, respectively. The diagonal matrix $M^{(1)}$ can be easily calculated as it represents a sum of the one-QP contributions. Generally speaking, computing all the one-QP diagrams contributions within the PT formalism is the most simple procedure. The more complicated problem is computing the $M^{(2)}$ and $M^{(3)}$contributions. Using the Feynman diagrams technique, the authors [33–38] have in detail analyzed the $M^{(2)}$ contributions. Naturally, the fundamental point of the whole consideration is the definition of the PT zeroth approximation.

2.2. The perturbation theory zeroth approximation

We will describe an atomic multielectron system by the relativistic Dirac Hamiltonian (the atomic units are used) as follows [14, 15]:

$$H = \sum_i \{\alpha c p_i - \beta c^2 - Z/r_i\} + \sum_{i>j} \exp(i|\omega|r_{ij})(1-\alpha_i\alpha_j)/r_{ij}, \tag{3}$$

where Z is a charge of nucleus, α_i, α_j are the Dirac matrices, ω_{ij} is the transition frequency, and c, a light velocity. The interelectron interaction potential (second term in Eq. (3)) takes into account the retarding effect and magnetic interaction in the lowest order on parameter α^2 (α is the fine structure constant). Let us note that in order to account for the nuclear finite size effect (in the zeroth approximation), one could describe a charge distribution in the atomic nucleus $\rho(r)$ by the Gaussian or Fermi (another variant is relativistic mean-field theory of a nucleus) functions and write the Coulomb potential for the spherically symmetric nuclear density $\rho(r|R)$ as [14]

$$V_{nucl}(r|R) = -\Big((1/r)\int_0^r dr' r'^2 \rho(r'|R) + \int_r^\infty dr' r' \rho(r'|R). \tag{4}$$

Here, R is a nuclear radius. According to the known Ivanova-Ivanov et al. method of differential equations [33–36], computing the potential (20) can be reduced to solving the system of the differential equations. By the way, this method is used by us in further under computing the PT first- and second-order corrections. The zeroth-order Hamiltonian H_0 and perturbation operator can be presented in the standard form as follows [7, 14, 15]:

$$\begin{aligned} H_0 &= \sum_i a_i^+ a_i E_i \\ H_{\text{int}} &= \sum_{ij} a_i^+ a_j V_{ij} + \frac{1}{2}\sum_{ijkl} V_{ijkl} a_i^+ a_j^+ a_k a_l \\ V_{ij} &= \int d\vec{r} \cdot \varphi_i(\vec{r})[-V_{MF}(r)] \cdot \varphi(\vec{r}) \\ V_{ijkl} &= \iint d\vec{r}_1 d\vec{r}_2\, \varphi(\vec{r}_1)\, \varphi(\vec{r}_2)\, V(r_1 r_2)\, \varphi_k(\vec{r}_2)\, \varphi_l(\vec{r}_1), \end{aligned} \tag{5}$$

where $\varphi(\vec{r})$ are one-electron functions (Dirac bispinors), E_i , one-electron energies, and V_{MF} is the central field self-consistent potential of the Coulomb type. The latter can be taken in the form of the usual Dirac-Fock potential or even any appropriate model potential, which imitates an effect of the electron subsystem. Let us remind that in the relativistic PT by Ivanova-Ivanov et al., the consistent model (as a rule, empirical) potential was taken as $V_{\mathrm{MF.}}$ In our PT version, we use the potential

$$V_{MF} = V^{DKS}(r) = [V^{D}_{Coul}(r) + V_{X}(r) + V_{C}(r|a)] \tag{6}$$

Further as $V_X(r)$ we use the standard Kohn-Sham (KS) exchange potential as follows [8]:

$$V^{KS}_{X}(r) = -(1/\pi)[3\pi^2\rho(r)]^{1/3}. \tag{7}$$

The standard definition of the exchange potential in the density-functional theory is as follows:

$$V_X[\rho(r), r] = \frac{\delta E_X[\rho(r)]}{\delta\rho(r)}, \tag{8}$$

In the relativistic multielectron theory with a Hamiltonian having a transverse vector potential (for describing the photons), one could determine the homogeneous density $\rho(r)$, construct the corresponding exchange energy $E_X[\rho(r)]$, and introduce the following exchange potential [16]:

$$V_X[\rho(r), r] = V^{KS}_{X}(r) \cdot \left\{ \frac{3}{2} \ln \frac{[\beta + (\beta^2+1)^{1/2}]}{\beta(\beta^2+1)^{1/2}} - \frac{1}{2} \right\}, \tag{9}$$

where $\beta = [3\pi^2\rho(r)]^{1/3}/c$. The corresponding correlation functional is as follows [16, 17]:

$$V_C[\rho(r), r] = -0.0333 \cdot b \cdot \ln[1 + 18.3768 \cdot \rho(r)^{1/3}], \tag{10}$$

where b is the optimization parameter (for details, see below and Refs. [16–19, 47–49] too). Naturally, potential (6) is subtracted from the interelectron potential in Eq. (3) in the perturbation operator. The Dirac equations for F and G components can be written as [14] follows:

$$\begin{aligned} f' &= -(\chi + |\chi|)f/r - \alpha ZVg - (\alpha ZE_{n\chi} + 2/\alpha Z)g, \\ g' &= (\chi - |\chi|)g/r - \alpha ZVf + \alpha ZE_{n\chi}f. \end{aligned} \tag{11}$$

Here, $E_{n\chi}$ is one-electron energy without the rest energy. The boundary values are defined by the first terms of the Taylor expansion:

$$g = \left(V(0) - E_{n\chi}\right) r\alpha Z/(2\chi + 1); \quad f = 1 \; at \; \chi < 0, \tag{12a}$$

$$f = \left(V(0) - E_{n\chi} - 2/\alpha^2 Z^2\right)\alpha Z; \quad g = 1 \; at \; \chi > 0. \tag{12b}$$

The condition $f, g \to 0$ at $r \to \infty$ determines the quantified energies of the state $E_{n\chi}$. The system of Eq. (11) is numerically solved by the Runge-Kutta method ('Superatom" package is used [7, 13–23, 34, 36, 47–67]).

2.3. The perturbation theory first- and second-orders corrections: correlation effects

In the PT first order, one should determine the matrix elements of the PT operator with the relativistic Coulomb-Breit potential, which are the contributions of the following type [36]:

$$\begin{aligned} M_1^{(2)} &= \langle\, n_1 l_1 j_1 \quad n_2 l_2 j_2 [J]\, | V_{\text{int}} |\, n_4 l_4 j_4 \quad n_3 l_3 j_3 [J]\, \rangle \\ &= P_1 P_2 (-1)^{1+j_2+j_4+J} [(2j_1+1)(2j_2+1)(2j_3+1)(2j_4+1)]^{1/2} \\ &\times \sum_{i,k} \sum_a \begin{Bmatrix} j_i j_k J \\ j_2 j_1 a \end{Bmatrix} \left(\delta_{i,3}\delta_{k,4} + (-1)^J \delta_{i,4}\delta_{k,3} \right) \cdot Q_\lambda, \end{aligned} \tag{13}$$

where

$$P_1 = \begin{cases} 1 & \text{if} \quad n_1 l_1 j_1 \neq n_2 l_2 j_2 \\ 1/2 & \text{if} \quad n_1 l_1 j_1 = n_2 l_2 j_2 \end{cases}, \; P_2 = \begin{cases} 1 & \text{if} \quad n_3 l_3 j_3 \neq n_4 l_4 j_4 \\ 1/2 & \text{if} \quad n_3 l_3 j_3 = n_4 l_4 j_4 \end{cases}. \tag{14}$$

The value of the Q_λ can be expressed through the radial Slater-like integrals and presented as a sum of the Coulomb and Breit parts: $Q_\lambda = Q_\lambda^{Qul} + Q_\lambda^{Br}$, which corresponds to a partition of the interelectron potential into the Coulomb and Breit ones in the second term of Eq. (1). Let us remind that, for instance, the Coulomb part in Eq. (13) is expressed through the radial integrals and angle coefficients as follows:

$$\begin{aligned} Q_\lambda^{Qul} &= \frac{1}{Z} \Big\{ R_l(1243) S_\lambda(1243) + R_l(\tilde{1}24\tilde{3}) S_\lambda(\tilde{1}24\tilde{3}) + \\ &+ R_l(1\tilde{2}\tilde{4}3) S_\lambda(1\tilde{2}\tilde{4}3) + R_l(\tilde{1}\tilde{2}\tilde{4}\tilde{3}) S_\lambda(\tilde{1}\tilde{2}\tilde{4}\tilde{3}) \Big\}. \end{aligned} \tag{15}$$

In the nonrelativistic limit, there remains only the first term in Eq. (15) depending only on the large component $f(r)$ of the one-electron Dirac functions. For example, its imaginary part is as follows [36]:

$$\begin{aligned} \text{Im}\, R_\lambda(12;43) &= \frac{1}{2}(2\lambda+1)\pi X_\lambda(13) X_\lambda(24) \\ X_\lambda(12) &= \int dr\, r^{3/2} f_1(r) J^{(1)}_{\lambda+1/2}\left(r\alpha Z |\omega| f_2(r) \right) \end{aligned} \tag{16}$$

The angular coefficient has only a real part:

$$S_\lambda(12;43) = S_\lambda(13) S_\lambda(24) \qquad\qquad S_\lambda(13) = \{\lambda l_1 l_3\} \begin{pmatrix} j_1 & j_3 & \lambda \\ \frac{1}{2} & -\frac{1}{2} & 0 \end{pmatrix} \tag{17}$$

Here, $\{\lambda l_1 l_3\}$ means that λ, l_1 and l_3 must satisfy the triangle rule and the sum $\lambda + l_1 + l_3$ must be an even number. The rest terms in Eq. (16) include the small components of the Dirac functions. The tilde in Eq. (13) designates that the large radial component f must be replaced by the small one g, and instead of l_i, $\tilde{l}_i = l_i - 1$ should be taken for $j_i < l_i$ and $\tilde{l}_i = l_i + 1$ for $j_i > l_i$. The Breit (magnetic) part can be expressed by the similar way (see details in Refs. [13–16]).

Then, exchange-correlation effects can be treated within the PT formalism as effects of the second and higher PT orders. In the second order, one should especially note the polarization and ladder diagrams. In **Figures 1** and **2**, we list some important diagrams of the second order describing the effects of the polarization interaction of quasiparticles and screening of the external quasiparticles (or antiscreening in the case, say, of an electron and a vacancy).

The polarization diagrams take into account the quasiparticle interaction through the polarizable core, and the ladder diagrams account for the immediate quasiparticle interaction. An effective approach to accounting the polarization contributions is in adding the effective two-QP polarizable operator into the first-order matrix elements. The corresponding polarization operator can be taken in the following form [50]:

$$V_{\text{pol}}^{d}(r_1 r_2) = X \left\{ \int \frac{dr' \left(\rho_c^{(0)}(r')\right)^{1/3} \theta(r')}{|r_1 - r'| \cdot |r' - r_2|} - \int \frac{dr' \left(\rho_c^{(0)}(r')\right)^{1/3} \theta(r')}{|r_1 - r'|} \int \frac{dr'' \left(\rho_c^{(0)}(r'')\right)^{1/3} \theta(r'')}{|r'' - r_2|} \Big/ \left\langle \left(\rho_c^{(0)}\right)^{1/3} \right\rangle \right\} \tag{18a}$$

$$\left\langle \left(\rho_c^{(0)}\right)^{1/3} \right\rangle = \int dr \left(\rho_c^{(0)}(r)\right)^{1/3} \theta(r), \tag{18b}$$

$$\theta(r) = \left\{ 1 + [3\pi^2 \cdot \rho_c^{(0)}(r)]^{2/3} / c^2 \right\}^{1/2} \tag{18c}$$

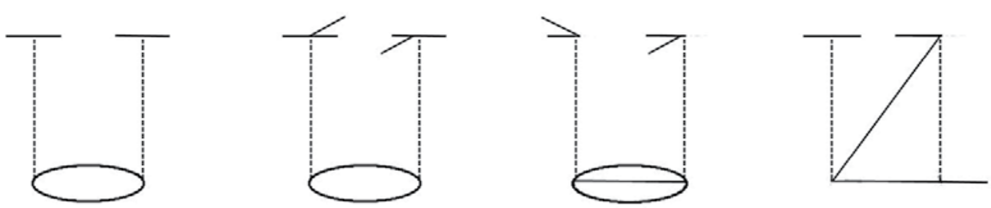

Figure 1. Some diagrams of the second order, taking into account the exchange and polarization interaction of quasiparticles and electrons of the closed shells core.

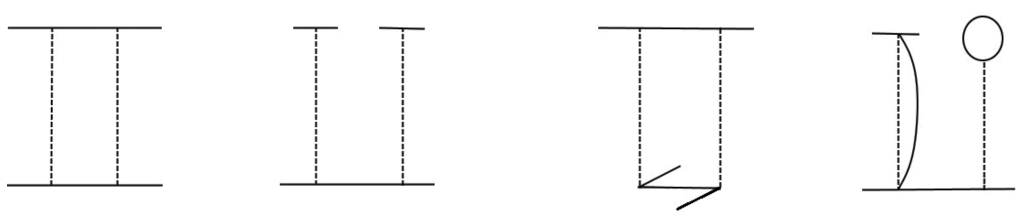

Figure 2. Some diagrams of the second order, describing a direct interaction of the two or three external quasiparticles.

where ρ_c^0 is the core electron density (without account for the quasiparticle), X is the numerical coefficient, and c is the light velocity. The similar approximate potential representation has been received for the exchange polarization interaction of quasiparticles (see details in Refs. [7, 14–19]). The polarization potential Eqs. (18a)–(18c) generalizes the corresponding nonrelativistic operator, which has been derived in Ref. [36].

In order to take into account the ladder diagrams contributions as well as some of the three-quasiparticle diagram contributions in all PT orders, we use the special procedure, which includes a modification of the mean-filled potential, which describes the effects of screening (antiscreening) of the core potential of each QP by the others (see details in Refs. [7, 14–19, 33–38]). Introduction of the additional screening potential into the Dirac equations for the large and small components changes the 1-QP energies and orbitals. It results in the corresponding modification of the diagonal 1-QP matrix $\tilde{M}^{(1)}$ and further 2-QP one too; $\tilde{M}^{(2)}$ is computed using the PT first-order formulae and the modified radial 1-QP wave functions.

2.4. Optimization of the relativistic orbitals basis

In order to obtain a precise description of the spectral characteristics of multielectron atomic systems, within the PT framework one should generate the optimized relativistic orbitals basis (see "Introduction" section) [1–7, 9–15]. The powerful ab initio approach to construction of the optimized PT basis has been developed in Ref. [48] and reduced to consistent treating gauge-dependent multielectron contributions $\mathrm{Im}\Delta E_{\mathrm{ninv}}$ of the lowest relativistic PT corrections to the atomic level radiation width and their further functional minimization.

For simplicity, let us consider now the one-quasiparticle atomic system (i.e., atomic system with one electron or vacancy above a core of the closed electronic shells). The multiquasiparticle case does not contain principally new moments. In the PT lowest, second order for the ΔE, there is only one-quasiparticle Feynman diagram B (see **Figure 3**), contributing the $\mathrm{Im}\Delta E$ (the radiation decay width).

In the fourth order of QED PT (the second order of the atomic PT), the diagrams appear, whose contribution to the $\mathrm{Im}\Delta E_{\mathrm{ninv}}$ accounts for the multielectron exchange-correlation (polarization) effects (diagrams A_d, A_{ex}; **Figure 3**). This multielectron contribution is dependent on the photon propagator gauge (the gauge-noninvariant contribution). Let us remind about the known criterion of the correctness of the atomic-computing radiation transition probabilities using the alternative forms for the transition operator ("length" and "velocity" transition operator forms). Their closeness of the "length" and "length" transition probabilities values

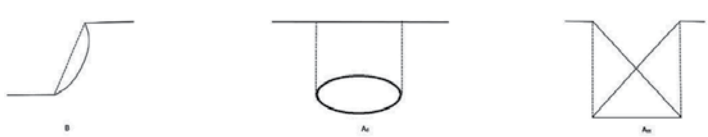

Figure 3. B: second other PT diagram contributing the imaginary energy part related to the radiation transitions; A_d and A_{ex}: QED PT fourth (atomic PT second)-order polarization diagrams.

confirms the correctness of the relativistic orbitals basis construction. Correspondingly, their noncoincidence is provided by multielectron by their nature and gauge-noninvariant terms.

In Ref. [48], the gauge-noninvariant contribution to an imaginary part of the electron energy has been calculated, which is as follows:

$$\begin{aligned}&\mathrm{Im}\Delta E_{ninv}(\alpha - s|A_d) = -C\frac{e^2}{4\pi}\iiiint dr_1 dr_2 dr_3 dr_4 \sum \Big(\frac{1}{\omega_{mn}+\omega_{\alpha_s}}+\\&\frac{1}{\omega_{mn}-\omega_{\alpha_s}}\Big)\Psi_\alpha^+(r_1)\Psi_m^+(r_2)\Psi_s^+(r_3)\Psi_n^+(r_4)(1-\alpha_1\alpha_2)/r_{12}\cdot\\&\{[(\alpha_3\alpha_4-(\alpha_3 n_{34})(\alpha_4 n_{34}))/r_{34}\cdot \sin[\omega_{\alpha_n}(r_{12}+r_{34})+\omega_{\alpha_n}\cdot\\&\cos[\omega_{\alpha_n}(r_{12}+r_{34})](1+(\alpha_3 n_{34})(\alpha_4 n_{34}))]\}\Psi_m(r_3)\Psi_\alpha(r_4)\Psi_n(r_2)\Psi_s(r_1)\end{aligned} \tag{19}$$

where C is the gauge constant, and f is the boundary of the closed shells.

Realizing a principle of minimization of the functional $\mathrm{Im}\Delta E_{\mathrm{ninv},}$ one could obtain the Dirac-Kohn-Sham (DKS)-like equations for an electron density. Their numerical solution allows to obtain the optimized basis of the one-QP relativistic orbitals. The corresponding procedure is described in detail, for example, in Refs. [18–23]. All details of the presented PT formalism can be found in Refs. [7, 14–20, 47–49].

2.5. Radiation decay probability as an imaginary part of the electron energy shift. Method of calculation

The method of computing the radiation decay (transition probabilities, oscillator strengths) probabilities within the relativistic energy approach is presented in, for instance, Refs. [16–19, 33–35, 47, 48]. Here, we only note that a probability is directly linked with the imaginary part of electron energy shift, which is defined in the PT lowest order as follows:

$$\mathrm{Im}\Delta E = -\frac{e^2}{4\pi}\sum_{\substack{\alpha>n>f\\ [\alpha<n\le f]}} V_{\alpha n\alpha n}^{|\omega_{\alpha n}|}, \tag{20}$$

where $\sum_{\alpha>n>f}$ is for electron and $\sum_{\alpha<n\le f}$ for vacancy, and $V_{\alpha n\alpha n}^{|\omega_{\alpha n}|}$ is determined as follows:

$$V_{ijkl}^{|\omega|} = \iint dr_1 dr_2 \Psi_i^*(r_1)\Psi_j^*(r_2)\frac{\sin|\omega|r_{12}}{r_{12}}(1-\alpha_1\alpha_2)\Psi_k^*(r_2)\Psi_l^*(r_1) \tag{21}$$

The individual terms of the sum Eq. (21) represent the contributions of different channels and probability, for instance, of the dipole α-n transition as $P_{\alpha n}\sim\frac{1}{4\pi}V_{\alpha n\alpha n}^{|\omega_{\alpha_n}|}$; the probability with accounting for the core polarization correction is $P_{\alpha_n}\sim\frac{1}{4\pi}\cdot\{V_{\alpha n\alpha n}^{|\omega_{\alpha_n}|}+(V_{pol}^{d+ex})_{\alpha n\alpha n}\}$. The total probability of a λ-pole transition is usually represented as a sum of the electric P_λ^E and magnetic P_λ^M

parts. The electric (or magnetic) λ-pole transition $\gamma \to \delta$ connects two states with parities which by λ (or $\lambda + 1$) units. In our designations,

$$\begin{aligned} &P_\lambda^E(\gamma \to \delta) = 2(2j+1)Q_\lambda^E(\gamma\delta;\gamma\delta) \qquad Q_\lambda^E = Q_\lambda^{Cul} + Q_{\lambda,\ \lambda-1}^{Br} + Q_{\lambda,\ \lambda+1}^{Br} \\ &P_\lambda^M(\gamma \to \delta) = 2(2j+1)Q_\lambda^M(\gamma\delta;\gamma\delta) \qquad Q_\lambda^M = Q_{\lambda,\ \lambda}^{Br}. \end{aligned} \tag{22}$$

In a case of the two-quasiparticle states (for instance, the excited atomic state is treated as a state with the two QP: electron and vacancy above the closed shells core), the corresponding probability has the following form (say, transition: $j_1 j_2 [J] \to \bar{j}_1 j_2 [\bar{J}]$):

$$P(\lambda | j_1 j_2 [J], \bar{j}_1 j_2 [\bar{J}]) = (\bar{J}) \begin{Bmatrix} \lambda \ldots J \ldots \bar{J} \\ j_2 \cdots \bar{j}_1 \cdots j_1 \end{Bmatrix} P(\lambda | 1\bar{1})(\bar{j}_1), \tag{23}$$

It is worth noting that all relativistic atomic calculations are usually carried out in the *jj*-coupling scheme. The transition to the intermediate-coupling scheme is realized by diagonalization of the M matrix, but usually only ReM should be diagonalized. The important simplified moment of the procedure is connected with converting the imaginary part by means of the matrix of eigenvectors $\{C_{mk}\}$, obtained by diagonalization of ReM:

$$\mathrm{Im}\, M_{mk} = \sum_{ij} C_{mi}^{*}\, M_{ij}\, C_{jk} \tag{24}$$

where M_{ij} are the matrix elements in the *jj*-coupling scheme, and M_{mk} in the intermediate-coupling scheme representation. The procedure is correct to terms of the order of Im M/Re M.

In conclusion, let us also underline that the tedious procedure of phase convention in calculating the matrix elements of different operators is avoided in the energy approach, although the final formulae, certainly, must coincide with the formulae obtained using the traditional amplitude quantum-mechanical method. All other details can be found in Refs. [7, 16–19, 33–36, 47–50].

3. Some results and conclusions

As illustration of the application of the above presented formalism, we present the results of computing energies, transition probabilities (oscillator strengths) in the heavy multielectron ion of Hg^+. A great interest to studying similar systems (Hg) is explained by the importance of the corresponding data, for instance, for laser effect studying. The collision of atoms of the Mendeleev table second raw with ions of helium (other inert gases) leads to creating ions in the excited states which is important for creating the inverse populations and laser effect. The available literature data on radiative characteristics are definitely insufficient. An account of the relativistic and correlation effects has a critical role in the cited systems as the studied transitions occur in the external shells in a strong field of atom with large Z. Within the relativistic PT, the Hg^+ states can be treated one- and three-QP states of electrons (6s) and vacancy ($5d^{-1}$) above the core of the closed shells $5d^{10}6s^2$. The interaction "quasiparticle core" is described by the potential (6). The polarization interaction of the quasiparticles through the core is described by the two-particle effective potential Eqs. (18a)–(18c). All calculations are performed using the modified atomic code "Superatom-ISAN."

In **Tables 1–3**, we present the experimental (NIST) [32] and theoretical energies, electric E1 ($5d^{10}7p(P_{1/2},P_{3/2})$-$5d^{10}6s(S_{1/2})$, $5d^{10}7p(P_{1/2},P_{3/2})$-$5d^{10}7s(S_{1/2})$), and E2 ($5d^9 6s^2$ ($D_{5/2}$, $D_{3/2}$)-$5d^{10}6s$ ($S_{1/2}$)) probabilities of the transitions in the spectrum of Hg^+. The theoretical results are obtained within the Hartree-Fock, Dirac-Fock methods by Ostrovsky-Sheynerman, relativistic PT theory with the empirical model potential zeroth approximation (RPT-MP) [18, 31], and our optimized RPT using relativistic energy approach (RPT-EA).

The standard HF and DF approaches in the single-configuration approximations do not allow to obtain very accurate results. Using the empirical transition energies significantly improve the theoretical results as in fact it means an account for very important interparticle correlations effects. In our approach, the corresponding exchange-correlation effects (the polarization

Method	E_{6s}	$7P_{1/2}$-$6S_{1/2}$	$7P_{3/2}$-$6S_{1/2}$	$7P_{1/2}$-$7S_{1/2}$	$7P_{3/2}$-$7S_{1/2}$	$D_{3/2}$-$S_{1/2}$
HF	−1.07	0.721	0.721	0.095	0.095	0.863
DF	−1.277	0.904	0.922	0.109	0.127	0.608
RPT-MP	−1.377	0.986	1.019	0.114	0.147	0.462
RPT-EA	−1.378	0.987	1.020	0.115	0.148	0.462
Exp.	−1.378	0.987	1.020	0.115	0.148	0.461

Theoretical data—Hartree-Fock (HF), Dirac-Fock (DF) [31]; relativistic PT with the empirical model potential approximation (RPT-MP) [18]; relativistic PT-RPT-EA (this work); experimental data—Moore (NBS, Washington) [32] (see text).

Table 1. The energies of the $5d^9 6s^2(D_{5/2},D_{3/2})$-$5d^{10}6s$ ($S_{1/2}$), $5d^{10}7p(P_{1/2},P_{3/2})$-$5d^{10}6s(S_{1/2})$, $5d^{10}7p(P_{1/2},P_{3/2})$-$5d^{10}7s(S_{1/2})$, $5d^9 6s^2(D_{5/2},D_{3/2})$-$5d^{10}6s$ ($S_{1/2}$) transitions in Hg^+ (Ry).

Method	$7P_{3/2}$-$6S_{1/2}$	$7P_{1/2}$-$6S_{1/2}$	$7P_{3/2}$-$7S_{1/2}$	$7P_{1/2}$-$7S_{1/2}$	$7P_{3/2}$-$6S_{1/2}$
HF	4.75×10^6	4.75×10^6	3.65×10^7	3.65×10^7	3.65×10^7
DF	8.45×10^7	1.67×10^7	6.89×10^7	6.89×10^7	4.71×10^7
DF (E_{exp})	1.17×10^8	2.04×10^7	1.10×10^8	1.10×10^8	5.52×10^7
RPT-MP	1.49×10^8	2.31×10^7	1.41×10^8	1.41×10^8	6.33×10^7
RPT-EA	1.51×10^8	2.33×10^7	1.43×10^8	1.43×10^8	6.35×10^7
Exp.	1.53×10^8	2.35×10^7	1.44×10^8	1.44×10^8	6.37×10^7

HF, Hartree-Fock data; DF, Dirac-Fock data; DF (E_{exp}), DF data using the experimental transitions energies [31]; relativistic perturbation theory with the empirical model potential approximation RPT-MP [18]; relativistic PT-RPT-EA (this work); experimental data—Moore (NBS, Washington) [32] (see text).

Table 2. Probabilities of the transitions $5d^{10}7p(P_{1/2},P_{3/2})$-$5d^{10}6s(S_{1/2})$, $5d^{10}7p(P_{1/2},P_{3/2})$-$5d^{10}7s(S_{1/2})$ in Hg^+ (in s^{-1}).

http://dx.doi.org/10.5772/intechopen.69102

Method	$D_{3/2}$-$S_{1/2}$	$D_{5/2}$-$S_{1/2}$
HF	1360	1360
DF	257.0	77.4
DF (E_{exp})	63.9	13.3
RPT-MP	54.54	11.8
RPT-EA	54.52 (0.2%)	11.7 (0.2%)
Exp.	53.5 ± 2.0	11.6 ± 0.4

HF, Hartree-Fock data; DF, Dirac-Fock data; DF (E_{exp}), DF data using the experimental transitions energies [31]; relativistic perturbation theory with the empirical model potential approximation (RPT-MP) [18]; relativistic PT-RPT-EA (this work); experimental data—Moore (NBS, Washington) [32] (see text).

Table 3. The E2 probabilities of the $5d^96s^2(D_{5/2},D_{3/2})$-$5d^{10}6s$ ($S_{1/2}$) transition in Hg^+ (in s^{-1}).

interaction of the QPs, mutual screening and anti-screening corrections, etc.) are taken into account more accurately. The core polarization correction to the transition probability is of great importance as it changes significantly the probability value (~15–40%). It should be also noted that the gauge-noninvariant contribution to radiation width is very small (0.2%; see **Table 2** in the line "EA") that means equivalence of the calculation results in the standard amplitude approach with using the length and velocity forms for transition operator. From the other side, this is an evidence of the successful choice of the PT zeroth approximation and accurate account of the multi-particle correlation effects.

We have presented the fundamentals of the new relativistic many-body PT formalism with construction of the optimized one-QP representation in the theory of relativistic multielectron systems. The relativistic density-functional approximation with the Kohn-Sham potential is taken as the zeroth one and all exchange-correlation corrections of the second-order and dominated classes of the higher-orders diagrams (polarization interaction, QPs screening, etc.) have been taken into account. In order to reach the corresponding optimization, we have used a procedure of the accurate treating of the PT lowest-order multielectron effects, in particular, the gauge-dependent radiative contribution for the certain class of the photon propagator gauge. The corresponding contribution is considered to be the typical representative of the important multielectron exchange-correlation effects, whose minimization is reasonable criteria in the searching for the optimal PT one-electron basis. This procedure derives an undoubted profit in the routine many-body calculations as it provides the way of the refinement of the atomic (molecular) characteristics calculations, based on the "first principles." The presented relativistic PT formalism can be further generalized, in particular, by the way of accounting for the radiation, QED (the Lamb shift self-energy and vacuum polarization corrections, for instance in the effective Uhling-Serber approximation with account for the Källen-Sabry and Wichmann-Kroll corrections), and nuclear (the Bohr-Weisskopf and Breit-Rosenthal-Crawford-Schawlow effects, nuclear finite size correction, magnetic moment distribution, etc.) effects [13–23].

Author details

Alexander V. Glushkov*, Olga Yu. Khetselius, Andrey A. Svinarenko, Vasily V. Buyadzhi, Valentin B. Ternovsky, Anna A. Kuznetsova and Petr G. Bashkarev

*Address all correspondence to: glushkovav@gmail.com

Odessa State Environmental University, Odessa, Ukraine

References

[1] Wilson S. Handbook on Molecular Physics and Quantum Chemistry. Chichester: Wiley; 2003. p. 680

[2] Dyall KG, Faegri R, Jr. Introduction to Relativistic Quantum Theory. Oxford: Oxford University Press; 2007. p. 780

[3] Bartlett RJ, Musiał MN. Coupled-cluster theory in quantum chemistry. Review of Modern Physics. 2007;**79**:291–328

[4] Shavitt I, Bartlett RJ. Many-Body Methods in Chemistry and Physics: MBPT and Coupled-Cluster Theory. New York, NY: Cambridge University Press; 2009. p. 390

[5] Fritzsche S, Fricke B, Sepp W-D. Computer-algebraic derivation of atomic Feynman–Goldstone expansions. In: Schweizer W, Schmelcher P, editors. Atoms and Molecules in Strong External Fields. Vol. 1. New York, NY: Kluwer; 1997. pp. 101–108

[6] Parpia FA, Froese-Fischer C, Grant IP. Generalized relativistic atomic structure package: GRASP. Computer Physics Communications. 1996;**94**(2):249–270

[7] Glushkov AV. Relativistic Quantum Theory. Relativistic Quantum Mechanics of Atomic Systems. Odessa: Astroprint; 2008. p. 700

[8] Kohn W, Sham S. Quantum density oscillations in an inhomogeneous electron gas. Physical Review A. 1965;**137**:1697–1710

[9] Johnson WR, Sapistein J, Blundell SA. Atomic structure calculations associated with PNC experiments in atomic Cs. Physica Scripta T. 1993;**46**:184–192

[10] Desclaux JP. A multiconfiguration relativistic DIRAC-FOCK program. Computer Physics Communications. 1975;**9**(1):31–45

[11] Feller D, Davidson ER. An approximation to frozen natural orbitals through use of Hartree-Fock exchange potential. Journal of Chemical Physics. 1981;**74**(7):3977–3989

[12] Dietz K, Hess BA. Single particle orbitals for configuration interaction derived from quantum electrodynamics. Physica Scripta. 1989;**39**:682–688

[13] Glushkov AV, Khetselius OYu, Malinovskaya SV. New laser-electron nuclear effects in the nuclear γ transition spectra in atomic and molecular systems. In: Wilson S, Grout PJ, Maruani J, Delgado-Barrio G, Piecuch P, editors. Frontiers in Quantum Systems in Chemistry and Physics. Series: Progress in Theoretical Chemistry and Physics. Vol. 18. Berlin: Springer; 2008. pp. 523–542

[14] Glushkov AV, Ambrosov SV, Loboda AV, Gurnitskaya EP, Khetselius OYu. QED calculation of heavy multicharged ions with account for the correlation, radiative and nuclear effects. In: Julien J-P, Maruani J, Mayou D, Wilson S, Delgado-Barrio G, editors. Recent Advances in Theoretical Physics and Chemistry Systems. Series: Progress in Theoretical Chemistry and Physics. Vol. 15. Berlin: Springer; 2006. pp. 285–300

[15] Glushkov AV, Khetselius OYu, Gurnitskaya EP, Loboda AV, Florko TA, Sukharev DE, Lovett L. Gauge-invariant QED perturbation theory approach to calculating nuclear electric quadrupole moments, hyperfine structure constants for heavy atoms and ions. In: Wilson S, Grout PJ, Maruani J, Delgado-Barrio G, Piecuch P, editors. Frontiers in Quantum Systems in Chemistry and Physics. Series: Progress in Theoretical Chemistry and Physics. Vol. 18. Berlin: Springer; 2008. pp. 501–522

[16] Glushkov AV, Khetselius OYu, Lovett L. Electron-β-nuclear spectroscopy of atoms and molecules and chemical environment effect on the β-decay parameters. In: Piecuch P, Maruani J, Delgado-Barrio G, Wilson S, editors. In: Advances in the Theory of Atomic and Molecular Systems Dynamics, Spectroscopy, Clusters, and Nanostructures. Series: Progress in Theoretical Chemistry and Physics. Vol. 20. Berlin: Springer; 2010. pp. 125–152

[17] Glushkov AV, Khetselius OYu, Svinarenko AA. Relativistic theory of cooperative muon-gamma-nuclear processes: Negative muon capture and metastable nucleus discharge. In: Hoggan P, Brandas E, Maruani J, Delgado-Barrio G, Piecuch P, editors. Advances in the Theory of Quantum Systems in Chemistry and Physics. Series: Progress in Theoretical Chemistry and Physics. Vol. 22. Berlin: Springer; 2011. pp. 51–70

[18] Glushkov AV. Advanced relativistic energy approach to radiative decay processes in multielectron atoms and multicharged ions. In: Nishikawa K, Maruani J, Brandas E, Delgado-Barrio G, Piecuch P, editors. Quantum Systems in Chemistry and Physics: Progress in Methods and Applications. Series: Progress in Theoretical Chemistry and Physics. Vol. 26. Berlin: Springer; 2012. pp. 231–254

[19] Khetselius OYu. Relativistic energy approach to cooperative electron-gamma-nuclear processes: NEET Effect. In: Nishikawa K, Maruani J, Brandas E, Delgado-Barrio G, Piecuch P, editors. Quantum Systems in Chemistry and Physics: Progress in Methods and Applications. Series: Progress in Theoretical Chemistry and Physics. Vol. 26. Berlin: Springer; 2012. pp. 217–230

[20] Glushkov AV, Khetselius OYu, Svinarenko AA, Prepelitsa GP. Energy approach to atoms in a laser field and quantum dynamics with laser pulses of different shape. In: Duarte FJ, editor. Coherence and Ultrashort Pulsed Emission Rijeka: InTech; 2010. pp. 159–186

[21] Glushkov AV. Operator perturbation theory for atomic systems in a strong DC electric field. In: Hotokka M, Maruani J, Brandas E, Delgado-Barrio G, editors. Advances in Quantum Methods and Applications in Chemistry, Physics, and Biology. Series: Progress in Theoretical Chemistry and Physics. Vol. 27. Berlin: Springer; 2013. pp. 161–178

[22] Khetselius OYu. Optimized perturbation theory to calculating the hyperfine line shift and broadening for heavy atoms in the buffer gas. In: Nascimento M, Maruani J, Brandas E, Delgado-Barrio G, Piecuch P, editors. Frontiers in Quantum Methods and Applications in Chemistry and Physics. Series: Progress in Theoretical Chemistry and Physics. Vol. 29. Berlin: Springer; 2015. pp. 54–76

[23] Glushkov AV, Svinarenko AA, Khetselius OYu, Buyadzhi VV, Florko TA, Shakhman AN. Relativistic quantum chemistry: Advanced approach to construction of the Green's function of the Dirac equation with complex energy and mean-field nuclear potential. In: Nascimento M, Maruani J, Brandas E, Delgado-Barrio G, Piecuch P, editors. Frontiers in Quantum Methods and Applications in Chemistry and Physics. Series: Progress in Theoretical Chemistry and Physics. Vol. 29. Berlin: Springer; 2015. pp. 197–218

[24] Safronova UI, Johnson W, Derevianko A. Relativistic many-body calculations of energy levels, hyperfine constants, electric-dipole matrix elements, static polarizabilities for alkali-metal atoms. Physical Review A. 1999;**60**:4476–4486

[25] Safronova MS, Safronova UI. Critically evaluated theoretical energies, lifetimes, hyperfine constants, and multipole polarizabilities in 87Rb . Physical Review A. 2011;**83**:052508

[26] Safronova UI, Safronova MS. Third-order relativistic many-body calculations of energies, transition rates, hyperfine constants, and blackbody radiation shift in 171Yb+. Physical Review A. 2009;**79**:022512

[27] Safronova MS, Johnson WR, Safronova UI. Excitation energies, hyperfine constants, E1, E2,M1 transition rates and lifetimes of 6s2nl states in TlI and PbII . Physical Review A. 2005;**71**:052506

[28] Yerokhin V, Artemyev A, Shabaev VM. QED treatment of electron correlation in Li-like ions. Physical Review A. 2007;**75**:062501

[29] Dzuba VA, Flambaum VV, Silvestrov PG, Sushkov DE. Many-body perturbation theory calculations in atoms with open shells. Physical Reviews A. 1991;**44**:2828–2831

[30] Dzuba VA, Harabati C, Johnson WR, Safronova MS. Breit correction to the parity-nonconservation amplitude in cesium. Physical Reviews A. 2001;**63**:044103

[31] Ostrovsky VN, Sheynerman SA. Radiation transitions in external shells of the ion Hg+. Optics and Spectroscopy. 1989;**67**:16–22

[32] Martin W. NIST Spectra Database, Version 2.0 (http://physics.nist.gov.asd). Washington: NIST; 2004

[33] Ivanov LN, Ivanova EP. Extrapolation of atomic ion energies by model potential method: Na-like spectra. Atomic Data and Nuclear Data Tables. 1979;**24**(2):95–121

[34] Driker MN, Ivanova EP, Ivanov LN, Shestakov AF. Relativistic calculation of spectra of 2-2 transitions in O-and F-like atomic ions. Journal of Quantitative Spectroscopy and Radiative Transfer. 1982;**28**(6):531–535

[35] Ivanov LN, Letokhov VS. Spectroscopy of autoionization resonances in heavy elements atoms. Com.Modern Phys. D.: Atomic and Molecular Physics. 1985;**4**:169–184

[36] Ivanova EP, Ivanov LN, Glushkov AV, Kramida AE. High-order corrections in relativistic perturbation theory with model zero approximation. Physica Scripta. 1985;**32**(4):512–524

[37] Ivanova EP, Glushkov AV. Theoretical study of multicharged ions spectra of F-, Ne-isoelectronic sequences. Journal of Quantitative Spectroscopy & Radiative Transfer. 1986;**36**(N2):127–145

[38] Bekov GI, Vidolova-Angelova EP, Ivanov LN, Letokhov VS, Mishin VI. Laser spectroscopy of narrow doubly excited autoionizing states of ytterbium atoms. Soviet Physics JETP. 1981;**53**(3):441–447

[39] Vidolova-Angelova E, Ivanov LN, Ivanova EP, Angelov DA. Relativistic perturbation method for studying radiation decay of highly-excited many-electron atoms: Tm. Journal of Physics B: Atomic, Molecular and Optical Physics. 1986;**19**:2053–2069

[40] Vidolova-Angelova E, Ivanov LN, Angelov DA. Autoionization decay of excited Rydberg Tm states. Journal of Physics B: Atomic, Molecular and Optical Physics. 1988;**21**:3877–3890

[41] Ivanova EP, Ivanov LN, Aglitsky EV. Modern trends in spectroscopy of multi-charged ions. Physics Reports. 1988;**166**(N6):315–390

[42] Vidolova-Angelova E, Ivanov LN. Autoionizing Rydberg states of thulium. Re-orientation decay due to monopole interaction. Journal of Physics B: Atomic, Molecular and Optical Physics. 1991;**24**:4147–4158

[43] Ivanova EP, Gulov AV. Theoretical investigation of the neon isoelectronic sequence. Atomic Data And Nuclear Data Tables. 1991;**49**:1–64

[44] Ivanov LN, Ivanova EP, Knight L. Energy approach to consistent QED theory for calculation of electron-collision strengths. Physics Review A. 1993;**48**(9):4365–4374

[45] Ivanov LN, Ivanova EP. Sturm orbitals method in calculation of physical characteristics of radiation of the atoms. JETP. 1996;**110**(6):483–498

[46] Ivanova EP, Zinoviev NA. The possibility of X-ray lasers based on inner-shell transitions of Ne-like ions. Physics Letters A. 2001;**274**:239–246

[47] Glushkov AV, Ivanov LN, Ivanova, EP. Relativistic decay of excited atomic states. Generalized energy approach. In: Autoionization Phenomena in Atoms. Moscow: Moscow University Press; 1986. pp. 152–164

[48] Glushkov AV, Ivanov LN. Radiation decay of atomic states: Atomic residue and gauge non-invariant contributions. Physics Letters A. 1992;**170**(1):33–37

[49] Glushkov AV. Negative ions of inert gases. JETP Letters. 1992;**55**(2):97–100

[50] Glushkov AV. Relativistic polarization potential of a many-electron atom. Soviet Physics Journal. 1990;**33**(1):1–8

[51] Glushkov AV. Correction for exchange and correlation effects in multielectron system theory. Journal of Structural Chemistry. 1990;**31**(4):529–533

[52] Glushkov AV. Relativistic multiconfiguration time-dependent self-consistent-field theory for molecules. Soviet Physics Journal. 1991;**34**(10):871–876

[53] Glushkov AV, Ivanov LN, Letokhov VS. Nuclear Quantum Optics. Moscow-Troitsk: Preprint of Institute for Spectroscopy of the USSR Academy of Sciences (ISAN); 1991. **AS-N4**:1–16

[54] Glushkov AV, Ivanov LN. DC strong field Stark effect: Consistent quantum mechanical approach. Moscow-Troitsk: Preprint of Institute for Spectroscopy of the USSR Academy of Sciences (ISAN); 1992. **AS-N1**:1–16

[55] Glushkov AV, Ivanov LN. A broadening of the thulium atom autoionization resonances in a weak electric field. Moscow-Troitsk: Preprint of Institute for Spectroscopy of the USSR Academy of Sciences (ISAN); 1992. **AS-N2**:1–10

[56] Glushkov AV, Ivanov LN. Shift and deformation of radiation atomic lines in the laser emission field. Multiphoton processes. Moscow-Troitsk: Preprint of Institute for Spectroscopy of the USSR Academy of Sciences (ISAN); 1992. **AS-N3**:1–12

[57] Glushkov AV, Ivanov LN. DC strong-field Stark-effect: Consistent quantum-mechanical approach. Journal of Physics B: Atomic, Molecular and Optical Physics. 1993;**26**(16): L379-L396

[58] Glushkov AV, Ambrosov SV, Ignatenko AV, Korchevsky DA. DC strong field Stark effect for non-hydrogenic atoms: New consistent quantum mechanical approach. International Journal of Quantum Chemistry. 2004;**99**(5):936–939

[59] Glushkov AV, Malinovskaya SV, Chernyakova YuG, Svinarenko AA. Cooperative laser-electron-nuclear processes: QED calculation of electron satellites spectra for multi-charged ion in laser field. International Journal of Quantum Chemistry. 2004;**99**(5):889–893

[60] Glushkov AV, Ambrosov SV, Loboda AV, Chernyakova YuG, Svinarenko AV, Khetselius OYu. QED calculation of the superheavy elements ions: Energy levels, radiative corrections and hyperfine structure for different nuclear models. Nuclear Physics A. 2004;**734S**:21–25

[61] Glushkov AV, Khetselius OYu, Malinovskaya SV. Optics and spectroscopy of cooperative laser-electron nuclear processes in atomic and molecular systems—New trend in quantum optics. European Physics Journal. 2008;**T160**:195–204

[62] Glushkov AV, Ambrosov SV, Loboda AV, Gurnitskaya EP, Prepelitsa GP. Consistent QED approach to calculation of electron-collision excitation cross-sections and strengths: Ne-like ions. International Journal of Quantum Chemistry. 2005;**104**(1):562–569

[63] Glushkov AV, Malinovskaya SV, Loboda AV, Gurnitskaya EP, Korchevsky DA. Diagnostics of the collisionally pumped plasma and search of the optimal plasma parameters of x-ray lasing: Calculation of electron-collision strengths and rate coefficients for Ne-like plasma. Journal of Physics: Conference Series. 2005;**178**:188–198

[64] Glushkov AV, Loboda AV, Gurnitskaya EP, Svinarenko AA. QED theory of radiation emission and absorption lines for atoms in a strong laser field. Physica Scripta. 2009; **T.135**:014022

[65] Malinovskaya SV, Glushkov AV, Khetselius OY, Svinarenko AA, Mischenko EV, Florko TA. Optimized perturbation theory scheme for calculating the interatomic potentials and hyperfine lines shift for heavy atoms in the buffer inert gas. International Journal of Quantum Chemistry. 2009;**109**(14):3325–3329

[66] Malinovskaya SV, Glushkov AV, Khetselius OY, Lopatkin YM, Loboda AV, Nikola LV, Svinarenko AA, Perelygina TB. Generalized energy approach for calculating electron collision cross-sections for multicharged ions in a plasma: Debye shielding model. International Journal of Quantum Chemistry. 2011;**111**(2):288–296

[67] Glushkov AV, Malinovskaya SV, Khetselius OYu, Loboda AV, Sukharev DE, Lovett L. Green's function method in quantum chemistry: New numerical algorithm for the Dirac equation with complex energy and Fermi-model nuclear potential . International Journal of Quantum Chemistry. 2009;**109**(8):1717–1727

Chapter 6

Atoms-Photonic Field Interaction: Influence Functional and Perturbation Theory

Emmanouil G. Thrapsaniotis

Additional information is available at the end of the chapter

http://dx.doi.org/10.5772/67774

Abstract

We study the dynamics of one-electron atoms interacting with a pulsed, elliptically polarized, ultrashort, and coherent state. We use path integral methods. We path integrate the photonic part and extract the corresponding influence functional describing the interaction of the pulse with the atomic electron. Then we angularly decompose it. We keep the first-order angular terms in all but the last factor as otherwise their angular integration would contribute infinites as the number of time slices tends to infinity. Further we use the perturbative expansion of the last factor in powers of the inverse volume and integrate on time. Finally, we obtain a closed angularly decomposed expression of the whole path integral. As an application we develop a scattering theory and study the two-photon ionization of hydrogen.

Keywords: path integrals, influence functional, perturbation, coherent state, hydrogen, sign solved propagator, two photons

1. Introduction

The study of the interaction of radiation with matter is an area of major importance in physics. The production in laboratories of pulses of various durations and central frequencies has given a further boost in that study. These pulses can be used in the study of various elementary processes such as the excitation or photoionization of atoms [1–7]. This is possible due to their short time length of the order of a few femtoseconds or of a few hundreds attoseconds. Sub-100-as pulses have been generated as well. Moreover, their photons' energy may belong in the ultraviolet or extreme ultraviolet and therefore just one or two photons may be enough to cause excitation or ionization.

In the present chapter, we introduce a fully quantum mechanical field theoretical treatment, for the interaction of a pulsed, elliptically polarized ultrashort coherent state with one optically active electron atoms. We use path integral methods. So we integrate the photonic part and extract the corresponding influence functional describing the interaction of the pulse with the atomic electron.

Proceeding we use the discrete form of that influence functional and angularly decompose its expression. We keep first-order angular terms in all but the last factor as otherwise their angular integration would contribute infinites as the number of time slices tends to infinity. Further, we use the perturbative expansion of the last factor in powers of the inverse volume and integrate on time. So we generate a perturbative series describing the action of the photonic field on the electron of the atom. It includes photonic and vacuum fluctuations contributions. Moreover, we manipulate the angular parts of the atomic action via standard path integral methods to finally obtain a closed angularly decomposed expression of the whole path integral.

As an application we develop a scattering theory and we study the two-photon ionization of hydrogen from its ground state to continuum. For the same transitions and to the same order vacuum fluctuation terms contribute as well. In the present application we consider orthogonal pulses. We use the propagator that appears in its sign solved propagator (SSP) form Ref. [8]. Previously, we have considered other kinds of photonic states interacting with one-electron atoms (see Refs. [6, 7, 9, 10]).

The present chapter proceeds as follows. In Section 2, we describe the present system and integrate its photonic part. Then in Section 3, we give the angular decomposition of the propagator in the case of elliptic polarization. In Section 4, we give an application and our conclusions in Section 5. Finally, in the Appendix we give some functions necessary in the evaluation of certain integrals.

2. System Hamiltonian and path integration

In the present chapter, we consider a one-electron atom initially in its ground state under the action of a coherent state. Therefore, the system Hamiltonian H can be decomposed into a sum of three terms. The electron's one H_e, the photonic field one H_f, and an interaction term of the photonic field with the electron H_I .that is,

$$H = H_e + H_f + H_I. \tag{1}$$

H_e has the form

$$H_e = \frac{1}{2}\vec{p}^{\,2} + V(\vec{r}), \tag{2}$$

where $V(\vec{r})$ is the atomic potential. The photonic field has the Hamiltonian

$$H_f = \omega a^{+} a, \tag{3}$$

while the interaction term H_I in the Power-Zienau-Woolley formalism takes the form

http://dx.doi.org/10.5772/67774

$$H_I = -e\vec{r} \cdot \vec{E}_f(\vec{r}, \tau). \tag{4}$$

$\vec{E}_f(\vec{r}, \tau)$ is the field operator of the photonic pulse given by the expression

$$\vec{E}_f(\vec{r}, \tau) = \frac{1}{\sqrt{V}} il(\omega)\wp(\tau)\left[\hat{\varepsilon} a e^{i\vec{k}_{ph}\cdot\vec{r}} - \hat{\varepsilon}^* a^+ e^{-i\vec{k}_{ph}\cdot\vec{r}}\right]. \tag{5}$$

$\wp(\tau)$ is the pulse's envelope function. In Eq. (5) $l(\omega) = \sqrt{2\pi\omega}$ is a real frequency function, $\hat{\varepsilon}$ is the polarization vector, ω is the pulse's carrier frequency, $\vec{k}_{\mathrm{ph}}$ is the radiation wave vector and V is a large volume. Then H_I has the form

$$H_I = g(\tau)a + g^*(\tau)a^+. \tag{6}$$

We have set

$$g(\tau) = -\frac{1}{\sqrt{V}} iel(\omega)\wp(\tau)\hat{\varepsilon} \cdot \vec{r}(\tau)e^{i\vec{k}_{\mathrm{ph}}\cdot\vec{r}(\tau)}. \tag{7}$$

Now we combine the photonic field variables in the term

$$H_0(a^+, a; \tau) = H_f + H_I = \omega a^+ a + g(\tau)a + g^*(\tau)a^+. \tag{8}$$

The propagator between the initial and final states corresponding to the Hamiltonian Eq. (1) can be obtained by integrating on both the space and photonic field variables. At first we integrate the photonic field variables, which appear only in H_0 (Eq. (8)). Then we obtain the following path integral of only the spatial variables:

$$\begin{aligned} &K(\alpha_f, \vec{r}_f, t_f; \alpha_i, \vec{r}_i; t_i) = \int D\vec{r}(\tau)\frac{D\vec{p}(\tau)}{(2\pi)^3} \times \\ &\exp\left[i\int_{t_i}^{t_f} d\tau\left(\vec{p}(\tau)\cdot\dot{\vec{r}}(\tau) - \frac{\vec{p}^{\,2}(\tau)}{2} - V(\vec{r}(\tau))\right) - i\int_{t_i}^{t_f} d\tau g(\tau)Z(\tau, t_i) - \right. \\ &\left.\frac{1}{2}(|\alpha_f|^2 + |\alpha_i|^2) + Y(t_f, t_i)\alpha_f^*\alpha_i + Z(t_f, t_i)\alpha_f^* - i\alpha_i X(t_f, t_i)\right], \end{aligned} \tag{9}$$

where $Y(t_f, t_i)$, $X(t_f, t_i)$, and $Z(t_f, t_i)$ read:

$$Y(t_f, t_i) = \exp\left[-i\int_{t_i}^{t_f} d\tau\omega(\tau)\right] = \exp\Big(-i\omega(t_f - t_i)\Big), \tag{10}$$

$$X(t_f, t_i) = \int_{t_i}^{t_f} d\tau g(\tau)Y(\tau, t_i), \tag{11}$$

$$Z(t_f, t_i) = -i\int_{t_i}^{t_f} d\tau g^*(\tau) \exp\left[-i\int_{\tau}^{t_f} d\tau' \omega(\tau')\right]. \tag{12}$$

The propagator in Eq. (9) with diagonal field variables ($\alpha_i = \alpha_f = \alpha$) can be written as

$$K(\alpha, \vec{r}_f, t_f; \alpha, \vec{r}_i, t_i) = \int D\vec{r}(\tau) \frac{D\vec{p}(\tau)}{(2\pi)^3} \exp\left[i\int_{t_i}^{t_f} d\tau \left[\vec{p}(\tau) \cdot \dot{\vec{r}}(\tau) - \frac{\vec{p}^{\,2}(\tau)}{2} - V(\vec{r}(\tau))\right]\right.$$
$$\left. +A - B|\alpha|^2 + D_1\alpha + D\alpha^*\right]. \tag{13}$$

The parameters are given as follows:

$$A(t_f, t_i) = -\frac{1}{V} e^2 l^2(\omega) \int_{t_i}^{t_f} d\tau \int_{t_i}^{\tau} d\rho \wp(\tau) \widehat{\varepsilon} \cdot \vec{r}(\tau) e^{i\vec{k}_{\mathrm{ph}} \cdot \vec{r}(\tau)} \wp(\rho) \widehat{\varepsilon}^* \cdot \vec{r}(\rho) e^{-i\vec{k}_{ph} \cdot \vec{r}(\rho)} e^{-i\omega(\tau-\rho)}, \tag{14}$$

$$B(t_f - t_i) = 1 - Y(t_f, t_i) = 1 - e^{-i\omega(t_f - t_i)}, \tag{15}$$

$$D(t_f, t_i) = \frac{1}{\sqrt{V}} el(\omega) \int_{t_i}^{t_f} d\tau \wp(\tau) \widehat{\varepsilon}^* \cdot \vec{r}(\tau) e^{-i\vec{k}_{\mathrm{ph}} \cdot \vec{r}(\tau)} e^{-i\omega(t_f - \tau)}, \tag{16}$$

$$D_1(t_f, t_i) = -\frac{1}{\sqrt{V}} el(\omega) \int_{t_i}^{t_f} d\tau \wp(\tau) \widehat{\varepsilon} \cdot \vec{r}(\tau) e^{i\vec{k}_{\mathrm{ph}} \cdot \vec{r}(\tau)} e^{-i\omega(\tau - t_i)}. \tag{17}$$

In the case of a field transition between an initial photonic state $|\Phi_1\rangle$ and a final one $|\Phi_2\rangle$, the reduced propagator of finite time takes the form

$$\tilde{K}(\vec{r}_f, t_f; \vec{r}_i, t_i) = \int \frac{d^2\alpha}{\pi} e^{|\alpha|^2} \langle \Phi_2|\alpha\rangle K(\alpha, \vec{r}_f, t_f; \alpha, \vec{r}_i, t_i) \langle \alpha|\Phi_1\rangle. \tag{18}$$

Here we consider that we have a field transition from an initial coherent state $|\beta\rangle$ to a final one $|\gamma\rangle$. So we can integrate to obtain the following reduced propagator for the motion of the electron,

$$\begin{aligned} \tilde{K}(\vec{r}_f, t_f; \vec{r}_i, t_i) &= C(t_f - t_i) K_0(\vec{r}_f, t_f; \vec{r}_i, t_i) \\ &= C(t_f - t_i) \int\int D\vec{r}(\tau) \frac{D\vec{p}(\tau)}{(2\pi)^3} \exp\{iS_{\mathrm{tot}}[\vec{p}, \vec{r}, \tau]\}, \end{aligned} \tag{19}$$

where

http://dx.doi.org/10.5772/67774

$$C(t) = \frac{\exp\left(\frac{\beta\gamma^*}{B(t)} - \frac{1}{2}|\beta|^2 - \frac{1}{2}|\gamma|^2\right)}{B(t)}. \tag{20}$$

The action is

$$\begin{aligned}
S_{\text{tot}}[\vec{p}, \vec{r}, \tau] &= \int_{t_i}^{t_f} \left[\vec{p}(\tau)\cdot\dot{\vec{r}}(\tau) - \frac{\vec{p}^{\,2}(\tau)}{2} - V(\vec{r}(\tau))\right] d\tau \\
&+ i\frac{1}{\sqrt{V}} e l(\omega) \int_{t_i}^{t_f} d\tau \left(\beta\chi(\tau)\hat{\varepsilon}\cdot\vec{r}(\tau)e^{i\vec{k}_{\text{ph}}\cdot\vec{r}(\tau)} + \gamma^*\chi^*(\tau)\hat{\varepsilon}^*\cdot\vec{r}(\tau)e^{-i\vec{k}_{ph}\cdot\vec{r}(\tau)}\right) \\
&+ \frac{1}{V}e^2 l^2(\omega)\int_{t_i}^{t_f} d\tau\wp(\tau)\int_{t_i}^{\tau} d\rho\wp(\rho)\left[i\frac{e^{i\omega(\tau-\rho)}}{e^{i\omega(t_f-t_i)}-1}\left(\hat{\varepsilon}^*\cdot\vec{r}(\tau)e^{-i\vec{k}_{ph}\cdot\vec{r}(\tau)}\right)\left(\hat{\varepsilon}\cdot\vec{r}(\rho)e^{i\vec{k}_{ph}\cdot\vec{r}(\rho)}\right) + c.c.\right],
\end{aligned} \tag{21}$$

where $\chi(\tau)$ has the form

$$\chi(\tau) = \wp(\tau)\frac{e^{-i\omega\tau}}{e^{-i\omega t_i} - e^{-i\omega t_f}}. \tag{22}$$

We notice the following identities:

$$\frac{1}{B(t)} = \frac{1}{2} - \frac{1}{2}i\cot\left(\frac{\omega t}{2}\right) = \frac{1}{2} - \frac{i}{\omega}\sum_{m=-\infty}^{\infty}\frac{1}{t - \frac{2\pi m}{\omega}}. \tag{23}$$

On using them and for arbitrary $A(t)$ we can obtain the following formula after a direct Fourier transform,

$$\int_{-\infty}^{\infty}\frac{A(t)}{B(t)}e^{ift}dt = \frac{1}{2}\int_{-\infty}^{\infty}A(t)e^{ift}dt + \frac{\pi}{\omega}\sum_{m=-\infty}^{\infty}A\left(\frac{2\pi m}{\omega}\right)\exp\left(if\frac{2\pi m}{\omega}\right). \tag{24}$$

Finally, upon using an inverse Fourier transform we obtain the following functional identities

$$\frac{A(t)}{B(t)} = A(t)\left[\frac{1}{2} + \frac{\pi}{\omega}\sum_{m=-\infty}^{\infty}\delta\left(\frac{2m\pi}{\omega} - t\right)\right] = A(t)\left[\frac{1}{2} + \frac{1}{2}\sum_{m=-\infty}^{\infty}\delta\left(m - \frac{\omega t}{2\pi}\right)\right]. \tag{25}$$

In the above expressions, the summation is to be performed symmetrically. Identity in Eq. (25) is to be used in Eqs. (19) and (20). The delta functions do not contribute in the final expressions of Section 4 at the specific times introduced by them the photonic influence functional becomes zero. Moreover, the measure of all those times is zero. Further to handle the exponential in Eq. (20) within the scattering theory of Section 4 we use the limit

$$\lim_{t\to\infty}\frac{1}{B(t)}=\lim_{t\to\infty}\frac{1}{1-\exp\left(-i(\omega-i0)t\right)}=1. \tag{26}$$

Now due to the large volume V, we shall approximate the exact action (21) by neglecting in the Taylor expansions

$$\vec{r}(\rho)=\vec{r}(\tau)+(\rho-\tau)\dot{\vec{r}}(\tau)+\dots, \tag{27}$$

higher terms than the first one, as they are going to involve powers of higher order in V in the denominator. To demonstrate this we consider the action in Eq. (21) and we derive the equation of motion of the electron by using Lagrange's equation and the action's Lagrangian in the absence of $V(\vec{r})$. So the part of the Lagrangian that interests us reads

$$L=\frac{\dot{\vec{r}}^{2}(\tau)}{2}+\frac{1}{\sqrt{V}}el(\omega)\left(\beta\chi(\tau)\hat{\varepsilon}\cdot\vec{r}(\tau)e^{i\vec{k}_{\text{ph}}\cdot\vec{r}(\tau)}+\gamma^{*}\chi^{*}(\tau)\hat{\varepsilon}^{*}\cdot\vec{r}(\tau)e^{-i\vec{k}_{\text{ph}}\cdot\vec{r}(\tau)}\right)$$
$$+\frac{1}{V}e^{2}l^{2}(\omega)\wp(\tau)\int_{t_i}^{\tau}d\rho\wp(\rho)\left[i\frac{e^{i\omega(\tau-\rho)}}{e^{i\omega(t_f-t_i)}-1}\left(\hat{\varepsilon}^{*}\cdot\vec{r}(\tau)e^{-i\vec{k}_{\text{ph}}\cdot\vec{r}(\tau)}\right)\left(\hat{\varepsilon}\cdot\vec{r}(\rho)e^{i\vec{k}_{\text{ph}}\cdot\vec{r}(\rho)}\right)+c.c.\right], \tag{28}$$

and has equation of motion

$$\ddot{\vec{r}}(\tau)=O\left(\frac{1}{\sqrt{V}}\right). \tag{29}$$

Therefore we can set,

$$\vec{r}(\rho)=\vec{r}(\tau)+O\left(\frac{1}{\sqrt{V}}\right). \tag{30}$$

In the case of the presence of $V(\vec{r})$ we perform a full order perturbation expansion of the full propagator in Eq. (19) with respect to the potential term. That is,

$$K_0=T+TVT+TVTVT+\dots. \tag{31}$$

Then the propagator T, in the expansion, will be the one of the electron in the photonic field for which the approximation of Eq. (30) as discussed above is valid. Then, we sum back to obtain the final full propagator, thus maintaining the same approximation for the total propagator as well. Notice that the expansion (31) may converge very slowly but since it is a full order expansion it does not matter. Eventually in the large volume limit we get the action

$$S_{\text{tot}}\left[\vec{p},\vec{r},\tau\right]=\int_{t_i}^{t_f}\left[\vec{p}(\tau)\cdot\dot{\vec{r}}(\tau)-\frac{\vec{p}^{\,2}(\tau)}{2}-V(\vec{r}(\tau))\right]d\tau$$
$$+i\frac{1}{\sqrt{V}}el(\omega)\int_{t_i}^{t_f}d\tau\left(\beta\chi(\tau)\widehat{\varepsilon}\cdot\vec{r}(\tau)e^{i\vec{k}_{\text{ph}}\cdot\vec{r}(\tau)}+\gamma^{*}\chi^{*}(\tau)\widehat{\varepsilon}^{*}\cdot\vec{r}(\tau)e^{-i\vec{k}_{\text{ph}}\cdot\vec{r}(\tau)}\right) \tag{32}$$
$$+\frac{1}{V}e^{2}l^{2}(\omega)\int_{t_i}^{t_f}d\tau\nu(\tau)\left|\widehat{\varepsilon}\cdot\vec{r}(\tau)\right|^{2},$$

where

$$\nu(\tau)=\wp(\tau)\int_{t_i}^{\tau}\wp(\rho)\xi(\tau-\rho)d\rho, \tag{33}$$

$$\xi(\tau-\rho)=\csc\left[\frac{\omega(t_f-t_i)}{2}\right]\cos\left[\omega(\tau-\rho)-\frac{\omega(t_f-t_i)}{2}\right]. \tag{34}$$

Finally, we notice that in the long wavelength approximation we can set $e^{i\vec{k}_{\text{ph}}\cdot\vec{r}}\cong 1$. So we obtain the following expression

$$S_{\text{tot}}\left[\vec{p},\vec{r},\tau\right]=\int_{t_i}^{t_f}\left[\vec{p}(\tau)\cdot\dot{\vec{r}}(\tau)-\frac{\vec{p}^{\,2}(\tau)}{2}-V(\vec{r}(\tau))\right]d\tau+$$
$$i\frac{1}{\sqrt{V}}el(\omega)\int_{t_i}^{t_f}d\tau\left[\beta\chi(\tau)\widehat{\varepsilon}\cdot\vec{r}(\tau)+\gamma^{*}\chi^{*}(\tau)\widehat{\varepsilon}^{*}\cdot\vec{r}(\tau)\right]+ \tag{35}$$
$$\frac{1}{V}e^{2}l^{2}(\omega)\int_{t_i}^{t_f}d\tau\nu(\tau)\left|\widehat{\varepsilon}\cdot\vec{r}(\tau)\right|^{2}.$$

Now we proceed to the angular decomposition of the above expressions.

3. Angular decomposition

We intend to perform angular decomposition and evaluate the SSP corresponding to the propagator of Eq. (19) in the long wavelength approximation.

Here we consider elliptic polarization so that the polarization vector takes the form

$$\widehat{\varepsilon}=\widehat{\varepsilon}_{x}\cos\left(\frac{\xi}{2}\right)\pm i\widehat{\varepsilon}_{y}\sin\left(\frac{\xi}{2}\right), \tag{36}$$

where $\widehat{\varepsilon}_x$ and $\widehat{\varepsilon}_y$ are the unit vectors along the x- and y-axis. The upper sign corresponds to left polarization while the lower one to right one.

The propagator $K_0^{\xi}(\vec{r}_f, t_f; \vec{r}_i, t_i)$ of Eq. (19) with the above polarization vector $\widehat{\varepsilon}$ has the discrete form

$$K_0^{\xi}(\vec{r}_f, t_f; \vec{r}_i, t_i) = \prod_{n=1}^{N}\left[\int_{-\infty}^{\infty} d\vec{r}_n\right]\prod_{n=1}^{N+1}\left[\int_{-\infty}^{\infty}\frac{d\vec{p}_n}{(2\pi)^3}\right]$$
$$\times \exp\left\{ i\sum_{n=1}^{N+1}\left[\vec{p}_n\cdot(\vec{r}_n-\vec{r}_{n-1})-\varepsilon\left(\frac{\vec{p}_n^{\,2}(\tau)}{2}+V(\vec{r}_n)\right)\right.\right. \tag{37}$$
$$\left.\left.+i\sqrt{\frac{2\pi\omega}{V}}\varepsilon(\beta\chi_n\widehat{\varepsilon}\cdot\vec{r}_n+\gamma^*\chi_n^*\widehat{\varepsilon}^*\cdot\vec{r}_n)+\frac{2\pi\omega}{V}\varepsilon\nu_n\left|\widehat{\varepsilon}\cdot\vec{r}_n\right|^2\right]\right\}.$$

All the functions with index n are evaluated at time $\tau_n = n\varepsilon + t_i$ where $\varepsilon = \frac{t_f - t_i}{N+1}$. χ_n and ν_n have the form (see Eqs. (22) and (33))

$$\chi_n = \wp(\tau_n)\frac{e^{-i\omega\tau_n}}{e^{-i\omega t_i}-e^{-i\omega t_f}}, \tag{38}$$

$$\nu_n = \nu(\tau_n). \tag{39}$$

Additionally, we note that we have set $\vec{r}_0 = \vec{r}_i$ and $\vec{r}_{N+1} = \vec{r}_f$.

Now we insert delta functions in Eq. (37) to get the expression

$$K_0^{\xi}(\vec{r}_f, t_f; \vec{r}_i, t_i) =$$
$$\prod_{n=1}^{N}\left[\int_{-\infty}^{\infty} d\vec{r}_n\right]\prod_{n=1}^{N+1}\left[\int_{-\infty}^{\infty}\frac{d\vec{p}_n}{(2\pi)^3}\right]\prod_{n=1}^{N+1}\left[\int_{-\infty}^{\infty} d^2w_n\right]\prod_{n=1}^{N+1}\left[\delta^{(2)}\left(w_n-\widehat{\varepsilon}\cdot\vec{r}_n\right)\right]$$
$$\times \exp\left\{ i\sum_{n=1}^{N+1}\left[\vec{p}_n\cdot\left(\vec{r}_n-\vec{r}_{n-1}\right)-\varepsilon\left(\frac{\vec{p}_n^{\,2}(\tau)}{2}+V(\vec{r}_n)\right)\right.\right. \tag{40}$$
$$\left.\left.+i\sqrt{\frac{2\pi\omega}{V}}\varepsilon\left(\beta\chi_n w_n+\gamma^*\chi_n^* w_n^*\right)+\frac{2\pi\omega}{V}\varepsilon\nu_n\left|w_n\right|^2\right]\right\}.$$

We have defined $\delta^{(2)}(z) = \delta(z)\delta(z^*)$. Moreover $w_n = w_{xn} + iw_{yn}$. The delta functions have the representation

$$\delta^{(2)}\left(w_n - \hat{\varepsilon}\cdot\vec{r}_n\right) =$$
$$\delta^{(2)}\left(w_n - r_n\left[\sin\vartheta_n\left(\cos\left(\frac{\xi}{2}\right)\cos\varphi_n \pm i\sin\left(\frac{\xi}{2}\right)\sin\varphi_n\right)\right]\right) = \frac{1}{(2\pi)^2}$$
$$\times\int_{-\infty}^{\infty}\int_{-\infty}^{\infty} d^2\lambda_n \exp\left[i\frac{1}{2}\left(\lambda_n w_n + \lambda_n^* w_n^*\right) - i\frac{1}{2}\lambda_n\left(\hat{\varepsilon}_x\cos\left(\frac{\xi}{2}\right) \pm i\hat{\varepsilon}_y\sin\left(\frac{\xi}{2}\right)\right)\cdot\vec{r}_n\right. \tag{41}$$
$$\left.-i\frac{1}{2}\lambda_n^*\left(\hat{\varepsilon}_x\cos\left(\frac{\xi}{2}\right) \mp i\hat{\varepsilon}_y\sin\left(\frac{\xi}{2}\right)\right)\cdot\vec{r}_n\right] = \frac{1}{(2\pi)^2}\int_{-\infty}^{\infty}\int_{-\infty}^{\infty} d^2\lambda_n$$
$$\times\exp\left[i\lambda_{\text{xn}}w_{\text{xn}} - i\lambda_{\text{yn}}w_{\text{yn}} - i\lambda_{\text{xn}}\cos\left(\frac{\xi}{2}\right)\hat{\varepsilon}_x\cdot\vec{r}_n \pm i\lambda_{\text{yn}}\sin\left(\frac{\xi}{2}\right)\hat{\varepsilon}_y\cdot\vec{r}_n\right].$$

We have set $\lambda_n = \lambda_{\text{xn}} + i\lambda_{\text{yn}}$. Now we perform the change of variables $\lambda_{\text{xn}} \to \frac{\lambda_{\text{xn}}}{\cos\left(\frac{\xi}{2}\right)}$, $\lambda_{\text{yn}} \to \frac{\lambda_{\text{yn}}}{\sin\left(\frac{\xi}{2}\right)}$, $w_{\text{xn}} \to \cos\left(\frac{\xi}{2}\right)w_{\text{xn}}$, $w_{\text{yn}} \to \sin\left(\frac{\xi}{2}\right)w_{\text{yn}}$. The factor due to the integration on λ_n is cancelled with the factor due to the integration on w_n. Further we expand angularly according to the identity,

$$e^{i\vec{\kappa}\cdot\vec{r}} = 4\pi\sum_{l=0}^{\infty}\sum_{m=-l}^{l} i^l j_l(|\vec{\kappa}|r)Y^*_{\text{lm}}(\vartheta_\kappa,\varphi_\kappa)Y_{\text{lm}}(\vartheta,\varphi), \tag{42}$$

where j_l are spherical Bessel functions, and Y_{lm} are spherical harmonics. So for right elliptic polarization we get

$$\delta^{(2)}(w_n - \hat{\varepsilon}\cdot\vec{r}_n) = \sum_{l_n=0}^{\infty}\sum_{m_n=-l_n}^{l_n} g_{l_n m_n}(w'_n, r_n)\sqrt{4\pi}Y_{l_n m_n}(\vartheta_n,\varphi_n), \tag{43}$$

where

$$g_{l_n m_n}(w'_n, r_n) = (-i)^{l_n}\frac{O_{l_n m_n}}{(2\pi)^2}\int_{-\infty}^{\infty}\int_{-\infty}^{\infty} d^2\lambda_n \exp\left[i\lambda_{\text{xn}}w'_{\text{xn}} - i\lambda_{\text{yn}}w'_{\text{yn}}\right] \tag{44}$$
$$\times j_{l_n}(|\lambda_n|r_n)\exp\left(-im_n\varphi_{\lambda n}\right),$$

$$O_{l_n m_n} = \sqrt{(2l_n+1)\frac{(l_n-m_n)!}{(l_n+m_n)!}}P_{l_n}^{m_n}(0)$$
$$= \sqrt{(2l_n+1)\frac{(l_n-m_n)!}{(l_n+m_n)!}}\frac{\sqrt{\pi}2^{m_n}}{\Gamma\left(\frac{l_n-m_n}{2}+1\right)\Gamma\left(\frac{-l_n-m_n+1}{2}\right)}. \tag{45}$$

We notice that if $l_n + m_n$ is odd then $O_{l_n m_n}$ is zero. Moreover $|\lambda_n|$, $\varphi_{\lambda n}$ are the polar coordinates of λ_n on the x-y plane. We have set

$$w_{\mathrm{xn}} = w'_{\mathrm{xn}} \cos\left(\frac{\xi}{2}\right) = |w'_n| \cos\left(\varphi_{w'n}\right) \cos\left(\frac{\xi}{2}\right), \tag{46}$$

$$w_{\mathrm{yn}} = w'_{\mathrm{yn}} \sin\left(\frac{\xi}{2}\right) = |w'_n| \sin\left(\varphi_{w'n}\right) \sin\left(\frac{\xi}{2}\right), \tag{47}$$

and

$$w'_n = w'_{\mathrm{xn}} + i w'_{\mathrm{yn}} = |w'_n| e^{i\varphi_{w'n}}. \tag{48}$$

On integrating over $\varphi_{\lambda n}$ we get

$$\begin{aligned} g_{l_n m_n}(w'_n, r_n) = (-i)^{l_n} \frac{O_{l_n m_n}}{2\pi} \exp\left(i m_n \left(\varphi_{w'n} + \frac{\pi}{2}\right)\right) \\ \times \int_0^\infty d\rho_{\lambda_n} \rho_{\lambda_n} j_{l_n}(\rho_{\lambda_n} r_n) J_{m_n}(\rho_{\lambda_n} |w'_n|). \end{aligned} \tag{49}$$

$\rho_{\lambda_n} = |\lambda_n|$ and J_{m_n} are Bessel functions. In the appendix we give results for the expression in Eq. (49).

Finally, we replace the delta functions in Eq. (40) with the above angularly decomposed expressions. As $N \to \infty$ and within the range from $n = 0$ to N we keep first-order angular terms. Higher order angular parts would contribute infinites. Finally, the propagator takes the form

$$\begin{aligned} K_0^\xi(\vec{r}_f, t_f; \vec{r}_i, t_i) = \\ \frac{1}{r_f r_i} \sum_{l=0}^{\infty} \sum_{m=-l}^{l} \sum_{q=0}^{\infty} \sum_{p=-q}^{q} K_{\mathrm{lmq}}^\xi(r_f, t_f; r_i, t_i) \sqrt{4\pi} Y_{\mathrm{lm}}(\vartheta_f, \varphi_f) Y_{\mathrm{qp}}(\vartheta_f, \varphi_f) Y_{\mathrm{qp}}^*(\vartheta_i, \varphi_i), \end{aligned} \tag{50}$$

where after standard manipulations [11] on the angular parts of the atomic system $K_{\mathrm{lmq}}^\xi(r_f, t_f; r_i, t_i)$ takes the form

$$\begin{aligned} K_{\mathrm{lmq}}^\xi(r_f, t_f; r_i, t_i) = \prod_{n=1}^{N} \left[\int_0^\infty dr_n\right] \prod_{n=1}^{N+1} \left[\int_{-\infty}^{\infty} \frac{dp_n}{2\pi}\right] \prod_{n=1}^{N+1} \left[\iint_{|w'_n|<r_n} d^2 w'_n\right] \prod_{n=1}^{N} [g_{00}(w'_n, r_n)] \\ \times g_{\mathrm{lm}}(w'_{N+1}, r_{N+1}) \exp\left\{ i \sum_{n=1}^{N+1} \left[p_n(r_n - r_{n-1}) - \varepsilon\left(\frac{p_n^2}{2} + \frac{q(q+1)}{2r_n^2} + V(r_n)\right) \right.\right. \\ \left.\left. + i\sqrt{\frac{2\pi\omega}{V}} \varepsilon(\beta \chi_n w_n + \gamma^* \chi_n^* w_n^*) + \frac{2\pi\omega}{V} \varepsilon v_n |w_n|^2 \right] \right\}. \end{aligned} \tag{51}$$

Further we observe that

http://dx.doi.org/10.5772/67774

$$\lim_{N\to\infty}\prod_{n=1}^{N}\left[\iint\limits_{|w'_n|<r_n} d^2w'_n\right]\prod_{n=1}^{N}\left[g_{00}(w'_n, r_n)\right]$$
$$\times\exp\left\{i\frac{t_f-t_i}{N+1}\sum_{n=1}^{N}\left[i\sqrt{\frac{2\pi\omega}{V}}(\beta\chi_n w_n+\gamma^*\chi_n^* w_n^*)+\frac{2\pi\omega}{V}\nu_n|w_n|^2\right]\right\} \tag{52}$$
$$=\exp\left\{i\frac{2\pi\omega}{3V}\int\limits_{t_i}^{t_f^-}d\tau\left[\nu(\tau)r^2(\tau)\right]\right\}.$$

So Eq. (51) becomes

$$K^{\xi}_{\mathrm{lmq}}(r_f, t_f; r_i, t_i)=F_{\mathrm{lm}}(r_f)\iint Dr(\tau)\frac{Dp(\tau)}{2\pi}$$
$$\times\exp\left\{i\int\limits_{t_i}^{t_f}d\tau\left[p\dot{r}-\left(\frac{p^2}{2}+\frac{q(q+1)}{2r^2}+V(r)\right)\right]+i\frac{2\pi\omega}{3V}\int\limits_{t_i}^{t_f^-}\nu(\tau)r^2(\tau)d\tau\right\}, \tag{53}$$

where

$$F_{\mathrm{lm}}(r_f)=\iint\limits_{|w'_f|<r_f}d^2w'_f g_{\mathrm{lm}}(w'_f, r_f)\times$$
$$\exp\left\{-\sqrt{\frac{2\pi\omega}{V}}\varepsilon(\beta\chi w_f+\gamma^*\chi^* w_f^*)+i\frac{2\pi\omega}{V}\varepsilon\nu|w_f|^2\right\}. \tag{54}$$

We notice that to evaluate the integrals in Eq. (54) we have to take into account the expressions of Eqs. (46) and (47). Then we expand it on parameters of interest and integrate on time.

In the next section, we use the present propagator in its SSP form which appears after the solution of the sign problem. It is

$$K^{\xi}_{1}(\vec{r}_f, t; \vec{r}_i, 0)=\frac{1}{r_f r_i}\delta(r_f-r_i)\sum_{l=0}^{\infty}\sum_{m=-l}^{l}\sum_{q=0}^{\infty}\sum_{p=-q}^{q}Y_{\mathrm{qp}}(\vartheta_f, \varphi_f)Y^*_{\mathrm{qp}}(\vartheta_i, \varphi_i)$$
$$\times\sqrt{4\pi}Y_{\mathrm{lm}}(\vartheta_f, \varphi_f)F_{\mathrm{lm}}(r_f)\exp\left[i\frac{2\pi\omega}{3V}r_f^2\int\limits_0^t\nu(\tau)d\tau\right]. \tag{55}$$

We have dropped the phase due to the atomic Hamiltonian because in the subsequent application of the present chapter, it eventually cancels.

4. Application and results

Proceeding to an application of the present theory we apply the above formalism to the case of the ionization of hydrogen. In that case the potential is given as

$$V(\vec{r}) = -\frac{1}{r}. \tag{56}$$

We use as an initial state, the hydrogen's ground one with wavefuction,

$$\Psi_i(\vec{r},t) = \Psi_i(\vec{r})e^{-i\varepsilon_i t} = R_{1s}(r)Y_{00}(\vartheta,\phi)e^{-i\varepsilon_i t} = 2e^{-r}Y_{00}(\vartheta,\phi)e^{-i\varepsilon_i t}, \tag{57}$$

where $\varepsilon_i = -1/2$ is the energy of the ground $H(1s)$ state.

The final state of the ionized electron with wave vector $\vec{k} = k(\sin\vartheta_k \cos\varphi_k, \sin\vartheta_k \sin\varphi_k, \cos\vartheta_k)$ is

$$\begin{aligned}&\Psi_f^{\vec{k}}(\vec{r},t) =\\ &\Psi_f^{\vec{k}}(\vec{r})e^{-i\varepsilon t} = \exp\left(\frac{\pi}{2k}\right)\Gamma\left(1+\frac{i}{k}\right)e^{i\vec{k}\cdot\vec{r}}{}_1F_1\left(-\frac{i}{k};1;-ikr-i\vec{k}\cdot\vec{r}\right)e^{-i\varepsilon t}.\end{aligned} \tag{58}$$

It has energy

$$\varepsilon = {}^{k^2}/_2, \tag{59}$$

and partial wave expansion

$$\Psi_f^{\vec{k}}(\vec{r}) = \frac{2\pi}{k}\sum_{s=0}^{\infty} i^s e^{-i\delta_s} R_s^k(r) \sum_{t=-s}^{s} Y_{\mathrm{st}}^*(\vartheta,\phi)Y_{\mathrm{st}}(\vartheta_k,\phi_k). \tag{60}$$

$$\begin{aligned}R_s^k(r) = &\frac{\sqrt{8\pi k}}{\sqrt{1-\exp(-2\pi/k)}}\prod_{y=1}^{s}\left(\sqrt{y^2+\frac{1}{k^2}}\right)\frac{1}{(2s+1)!}\\ &\times(2kr)^s e^{-ikr}{}_1F_1\left(\frac{i}{k}+s+1, 2s+2, 2ikr\right)\end{aligned} \tag{61}$$

is the radial function and $\delta_s = \arg\Gamma\left(1-\frac{i}{k}+s\right)$ a phase. Then the transition amplitude from the initial state i at $t \to -\infty$ to the final continuum state f at $t \to +\infty$ may be evaluated at any time t; it is

$$A_{\mathrm{fi}} = \langle\Phi_f^-(t)|\Phi_i^+(t)\rangle, \tag{62}$$

where $\Phi_f^-(\vec{r},t)$ and $\Phi_i^+(\vec{r},t)$ are exact solutions of the present system's time-dependent Schrodinger equation subject to the asymptotic conditions

$$\Phi_f^-(\vec{r},t) \underset{t\to+\infty}{\to} \Psi_f^{\vec{k}}(\vec{r},t), \tag{63}$$

$$\Phi_i^+(\vec{r},t) \underset{t\to-\infty}{\to} \Psi_i(\vec{r},t). \tag{64}$$

According to standard scattering theory we obtain the following form of the transition amplitude

$$A_{\rm fi} = \frac{1}{2} \lim_{\substack{t_1\to-\infty \\ t_2\to\infty}} \left\langle \Psi_f^{\vec{k}} \middle| U^0(t_2)^+ \exp\left(-i\int_0^{t_2} H_{eff}(t_2,\rho)d\rho + i\int_0^{t_1} H_{\rm eff}(t_1,\rho)d\rho \right) U^0(t_1) \middle| \Psi_i \right\rangle. \tag{65}$$

The effective Hamiltonian $H_{\rm eff}$, appearing above and corresponding to the action of Eq. (35) has the form (see Eq. (2))

$$H_{\rm eff} = H_e - i\frac{1}{\sqrt{V}} el(\omega)(\beta\chi\hat{\varepsilon}\cdot\vec{r} + \beta^*\chi^*\hat{\varepsilon}^*\cdot\vec{r}) - \frac{1}{V}e^2 l^2(\omega)\nu|\hat{\varepsilon}\cdot\vec{r}|^2. \tag{66}$$

Moreover

$$U^0(t) = e^{-iH_e t}. \tag{67}$$

We set $\beta = \gamma$. This appears to be a requirement in order the Hamiltonian to be PT (parity–time reversal) symmetric. The one-half factor in Eq. (65) appears due to the initial $\frac{1}{B(t)}$ factor in Eq. (20) and the identity in Eq. (25). At the times introduced by the delta functions the propagator $K_1^{\xi}(\vec{r}_f, \tau; \vec{r}_i, 0)$(see below) becomes zero. Moreover the exponential in Eq. (20) is one as $\lim_{t\to\infty}\frac{1}{B(t)} = 1$ and $\beta = \gamma$.

Now to proceed we set $t_2 = -t_1 = t$ and take into account the PT invariance of the whole system as the Hamiltonian Eq. (66) is PT invariant. So we reverse the time sign of the terms involving the time t_1 something that equivalently implies for the position $\vec{r} \to -\vec{r}$, for the momentum $\vec{p} \to \vec{p}$ and for the imaginary unit $i \to -i$. Then we differentiate the operators between the bra and the ket in Eq. (65), with respect to the variable t. Finally, after certain standard manipulations and a subsequent integration we obtain the result

$$\begin{aligned} A_{\rm fi} = {} & \left\langle \Psi_f^{\vec{k}} | \Psi_i \right\rangle + \\ & + \int_0^{\varsigma} d\tau \left\langle \Psi_f^{\vec{k}} | U^0(\tau)^+ \exp\left(-i\int_0^{\tau} H_{\rm eff}(\tau,\rho)d\rho + i\int_{-\tau}^{0} H_e(\rho)d\rho \right)\right. \\ & \left. \times \left(-\frac{1}{\sqrt{V}} el(\omega)(\beta\chi\hat{\varepsilon}\cdot\vec{r} + \beta^*\chi^*\hat{\varepsilon}^*\cdot\vec{r}) + i\frac{1}{V}e^2 l^2(\omega)\nu|\hat{\varepsilon}\cdot\vec{r}|^2 \right) U^0(\tau) \middle| \Psi_i \right\rangle. \end{aligned} \tag{68}$$

We have supposed that the duration of the pulse is ς, as well as that it begins at time zero. Now in order to proceed we take into account that the asymptotic initial and final states are orthogonal. Further we make use of the path-integral representation of the exponential in Eq. (68) and angularly decompose it. So on making use of the results of the previous section and solving the sign problem [8], Eq. (68) becomes

$$\begin{aligned} A_{\text{fi}} = &\int_0^{\zeta} d\tau \iint d\vec{r}_f d\vec{r}_i \frac{1}{r_i^2} e^{i(\varepsilon-\varepsilon_i)\tau} \left(\Psi_f^{\vec{k}}(\vec{r}_f)\right)^* K_1^{\xi}(\vec{r}_f,\tau;\vec{r}_i,0) \\ &\times \left(-\sqrt{\frac{2\pi\omega}{V}}\left(\beta\chi(\tau)\widehat{\varepsilon}\cdot\vec{r}_i + c.c.\right) + i\frac{2\pi\omega}{V}|\widehat{\varepsilon}\cdot\vec{r}_i|^2\nu(\tau)\right)\Psi_i(\vec{r}_i). \end{aligned} \tag{69}$$

We have used the prior form of the transition amplitude. $K_1^{\xi}(\vec{r}_f,\tau;\vec{r}_i,0)$ is given by Eq. (55). The phase which appears after the solution of the sign problem has cancelled.

As the present theory is PT symmetric we have to use PT symmetric quantum mechanics. So our equations take their final form according to the fact that $\left(\Psi_f^{\vec{k}}(\vec{r})\right)^{PT} = \left(\Psi_f^{\vec{k}}(\vec{r})\right)^*$.

Here we want to study two-photon ionization processes. They are of order $\frac{1}{V}$ or higher. For the same transitions the vacuum fluctuations term contributes to the same order. So we take it into account. The amplitude takes the form

$$\begin{aligned} A = &\int_0^{\zeta} d\tau \iint d\vec{r}_f d\vec{r}_i \frac{1}{r_i^2} e^{i(\varepsilon-\varepsilon_i)\tau} \left(\Psi_f^{\vec{k}}(\vec{r}_f)\right)^* \\ &\times \left(-\sqrt{\frac{2\pi\omega}{V}} S_{l=1}^{\xi}(\vec{r}_f,\tau;\vec{r}_i,0)\left(\beta\chi(\tau)\widehat{\varepsilon}\cdot\vec{r}_i + c.c.\right) + i\frac{2\pi\omega}{V} S_{l=0}^{\xi}(\vec{r}_f,\tau;\vec{r}_i,0)|\widehat{\varepsilon}\cdot\vec{r}_i|^2\nu(\tau)\right)\Psi_i(\vec{r}_i). \end{aligned} \tag{70}$$

Upon expanding to powers of volume the sign solved propagators appearing in Eq. (70) take the form

$$\begin{aligned} S_{l=1}^{\xi}(\vec{r}_f,\tau;\vec{r}_i,0) = &\frac{1}{r_f r_i}\delta(r_f - r_i)\sum_{q=0}^{\infty}\sum_{p=-q}^{q} Y_{\text{qp}}(\vartheta_f,\varphi_f) Y_{\text{qp}}^*(\vartheta_i,\varphi_i) \\ &\times \left[-\sqrt{\frac{2\pi\omega}{V}}\left(\widehat{\varepsilon}\cdot\vec{r}_f\beta\int_0^{\tau} d\rho\chi(\rho) + c.c.\right)\right] \exp\left[i\frac{2\pi\omega}{3V} r_f^2 \int_0^{\tau}\nu(\rho)d\rho\right], \end{aligned} \tag{71}$$

and

$$S^{\xi}_{l=0}(\vec{r}_f,\tau;\vec{r}_i,0)=\frac{1}{r_f r_i}\delta(r_f-r_i)\sum_{q=0}^{\infty}\sum_{p=-q}^{q}Y_{\text{qp}}(\vartheta_f,\varphi_f)Y^*_{\text{qp}}(\vartheta_i,\varphi_i)$$
$$\times\left\{1+\frac{2\pi\omega}{3V}r_f^2\left(i\int_0^\tau\nu(\rho)d\rho+\left|\beta\int_0^\tau d\rho\chi(\rho)\right|^2+\cos\xi\,\mathrm{Re}\left[\left(\beta\int_0^\tau d\rho\chi(\rho)\right)^2\right]\right)\right\} \tag{72}$$
$$\times\exp\left[i\frac{2\pi\omega}{3V}r_f^2\int_0^\tau\nu(\rho)d\rho\right].$$

Finally, we obtain the second-order transition probability

$$\frac{\partial P}{\partial\varepsilon}=\frac{1}{4\pi^2}k\int|A|^2 d\Omega_{\vec{k}}. \tag{73}$$

Here we consider the case of an orthogonal pulse of duration ζ. Then

$$\wp(\tau)=\begin{cases}1 & 0\le\tau\le\zeta\\ 0 & \text{otherwise}\end{cases}. \tag{74}$$

In **Figure 1**, we plot the second-order term $\frac{\partial P}{\partial\varepsilon}$ as a function of the energy of the injected electron ε for ζ = 100 as and various values of the elliptic polarization parameter ξ. We use

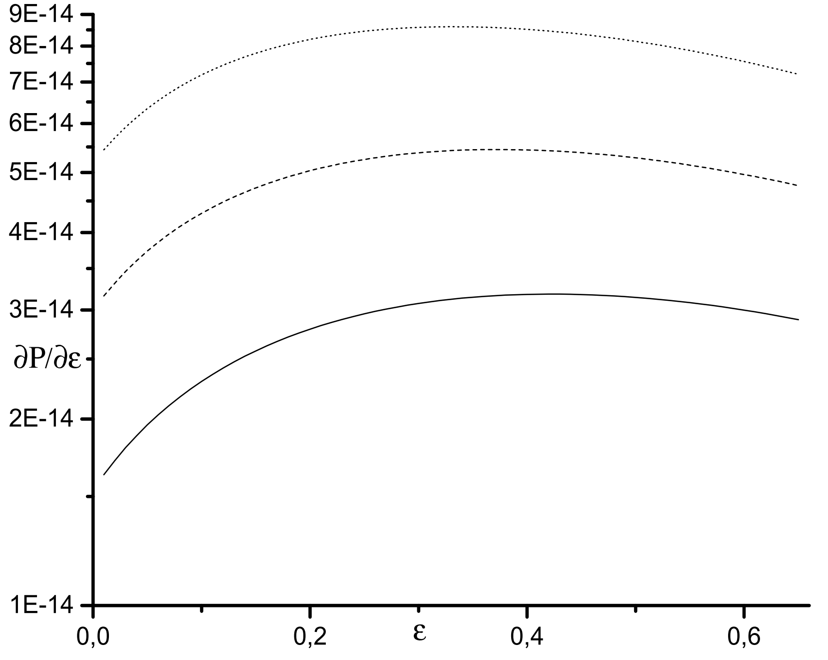

Figure 1. Second-order probability $\frac{\partial P}{\partial\varepsilon}$ of ionization as a function of the ε. We set ζ = 100 as. We give curves corresponding to $\xi=\frac{\pi}{2}$ (solid) $\xi=\frac{\pi}{3}$ (dashed) $\xi=\frac{\pi}{20}$ (dotted). We use $\omega=0.4275$a.u., β = 1 and $V=10^7$.

$2\omega = 0.855$ a.u. Within the range $0 \le \xi \le \frac{\pi}{2}$ the larger the ξ the smaller the transition probability. $\xi = \frac{\pi}{2}$ corresponds to circular polarization. We give another approach of this case in [10]. $\xi = 0$ corresponds to linear polarization. In that case the present approach is degenerate. We give other approaches in [6, 7, 9].

5. Conclusions

In the present chapter we have used path-integral methods in the study of the interaction of electrons with photonic states. We have integrated the photonic field and then angularly decomposed the electron—photonic field influence functional. Within those manipulations there have appeared terms due to the electromagnetic vacuum fluctuations.

As an application we have developed a scattering theory and used it in the two-photon ionization of hydrogen. For those transitions, the electromagnetic vacuum fluctuations contribute to the same order. Moreover to handle the path integrals that appear, we have used the relevant propagators in their sign solved propagator (SSP) form. The SSP theory appears in Ref. [8].

Concluding the present method is tractable and can be used in many problems involving the quantum mechanics of one-electron atoms interacting with radiation.

Appendix

In Eq. (49), we have the expression (here we drop the n indices)

$$\begin{aligned}
g_{\mathrm{lm}}(w', r) &= (-i)^l \frac{O_{\mathrm{lm}}}{2\pi} \exp\left(im\left(\varphi_{w'} + \frac{\pi}{2}\right)\right) \int_0^\infty d\rho_\lambda \rho_\lambda j_l(\rho_\lambda r) J_m(\rho_\lambda |w'|) \\
&= \frac{O_{\mathrm{lm}}}{2\pi} (-i)^l i^m e^{im\varphi_{w'}} \sqrt{\frac{\pi}{2r}} \int_0^\infty d\rho_\lambda \sqrt{\rho_\lambda} J_{l+\frac{1}{2}}(\rho_\lambda r) J_m(\rho_\lambda |w'|) \\
&= \frac{O_{\mathrm{lm}}}{2\pi} i^m (-i)^l e^{im\varphi_{w'}} \frac{\sqrt{\pi} |w'|^m \Gamma\left(\frac{l+m}{2} + 1\right)}{r^{m+2} \Gamma\left(\frac{l-m+1}{2}\right) \Gamma(m+1)} \\
&\times F\left(\frac{l+m}{2} + 1, \frac{m-l+1}{2}; m+1; \frac{|w'|^2}{r^2}\right) \Theta(r - |w'|) \\
&= \frac{O_{\mathrm{lm}}}{2\pi} i^m (-i)^l e^{im\varphi_{w'}} \frac{2^m \sqrt{\pi} \Gamma\left(\frac{l+m}{2} + 1\right)}{r \Gamma\left(\frac{l-m+1}{2}\right)} \frac{1}{\sqrt{r^2 - |w'|^2}} \\
&\times P_l^{-m}\left(\frac{\sqrt{r^2 - |w'|^2}}{r}\right) \Theta(r - |w'|),
\end{aligned} \tag{75}$$

where $\Theta(x)$ is the step function

$$\Theta(x) = \begin{cases} 1, & x > 0 \\ 0, & x < 0 \end{cases}. \tag{76}$$

We give the following cases:

$$g_{00}(w', r) = \frac{1}{2\pi} \frac{1}{r\sqrt{r^2 - |w'|^2}} \Theta(r - |w'|), \tag{77}$$

$$g_{1\pm1}(w', r) = \mp\sqrt{\frac{3}{2}} \frac{e^{\pm i\varphi_{w'}}}{2\pi} \frac{|w'|}{r^2} \frac{1}{\sqrt{r^2 - |w'|^2}} \Theta(r - |w'|). \tag{78}$$

Author details

Emmanouil G. Thrapsaniotis

Address all correspondence to: egthra@hotmail.com

Athens, Greece

References

[1] Chin CL, Lambropoulos P. Multiphoton Ionization of Atoms. Orlando: Academic Press; 1984

[2] Joachain C, Kylstra N, Potvliege R. Atoms in Intense Laser Fields. Cambridge: CUP; 2012

[3] Cohen-Tannoudji C. Atoms in Electromagnetic Fields. 2nd ed. Singapore: World Scientific; 2004

[4] Delone NB,. Krainov VP. Multiphoton Processes in Atoms. 2nd ed. Berlin: Springer Verlag; 2000

[5] Krainov VP, Reiss HR, Smirnov BM. Radiative Processes in Atomic Physics. New York: Wiley; 1997

[6] Thrapsaniotis EG. Chapter 12. In: Nilsson VP, editor. Photonic Research Developments. New York: Nova Science Publishers; 2008

[7] Thrapsaniotis EG. Chapter 19. In: George TF, Letfullin RR, Zhang G, editors. Perspectives in Theoretical Physics. New York: Nova Science Publishers; 2011

[8] Thrapsaniotis EG. Path integral methods via the use of the central limit theorem and application. Journal of Physics A: Mathematical and Theoretical. 2008;**41:**205202

[9] Thrapsaniotis EG. Path-integral approach of ionization by ultrashort laser pulses. Physics Review A. 2004;**70:**033410

[10] Thrapsaniotis EG, Path Integral Approach to the Interaction of One Electron Atoms with Pulsed Coherent States. Far East Journal of Dynamical Systems. 2013;**22**:87

[11] Kleinert H. Path Integrals in Quantum Mechanics, Statistics, Polymer Physics and Financial Markets. Singapore: World Scientific; 2004

Chapter 7

Detection and Measurement of Quantum Gravity by a Curvature Energy Sensor: H-States of Curvature Energy

Francisco Bulnes

Additional information is available at the end of the chapter

http://dx.doi.org/10.5772/68026

Abstract

The curvature energy as spectra of a field observable that is resulted of the variation of energy due to the speed of direction change in the space, is measured and detected by a sensor designed and developed through H-fields of energy that are superposes, obtaining strong variations in the fermion state to the H-torsion (second curvature energy) of the space-time via the gravitational covariant derivative having that the actions can be consigned to these H-fields as Majorana states with a corresponding action of gauge field. Likewise, in this chapter, some geometrical models of these H-states and their spectra of curvature are generated and discussed, which are extrapolated to the design of curvature energy sensors to quantum gravity.

Keywords: curvature energy, curvature energy sensor H-states, H-torsion, quantum gravity, spectral curvature, torsion

1. Introduction

The study of the field theory in physics establishes that the field actions can be measurable through their observables such as curvature or torsion of the space, which represent forms in how the field affects the space giving it a geometrical shape that depends directly on the field sources and their localization in the space. From the viewpoint of the topological field theory (TFT), these relations between the sources localizing in the space, where born the actions of the field, are born and the proper geometry engendered in the space by the actions of field to deform the space establish to the curvature and their second version; the torsion, as the geometrical invariant most important to characterize to a space and their geometry as implicit part of the field acting in the space through their energy. Physically, the detection of the field presence, without causing its extension in the space, is realized through its energy. This makes us think that curvature measurements can be realized using the energy concept that considers the curvature as an energy perturbation in the space, which can be measured through its spectra.

Likewise, a new concept developed above through new measurement methods and new technology prototypes to measure curvature as field observable [1, 2], or as microscopic deforming of the space-time associated to the gauge fields that enter in action with the quantum gluing of the matter and the constructing of the electric charge of the particles, is the curvature energy [1, 2], which is determined as a variation of energy perceived by a change in speed rate of direction in the space detected by the energy condition or censorship condition designed by certain integrals of energy born of the curvature integral transforms [3, 4] applied on certain cycles of the signal space acting on the space, to obtain certain energy co-cycles that are curvature data of the space and which represent in an energy space the curvature energy (see **Figure 1**).

This raises the need to design a sensor and also the space perception of a device (censorship condition), which must use a modulation space with a domineering energy condition given by [2, 3] as follows:

$$[V]^2 \int_C hk^2 ds \geq \left(\int_C h^2 - k \right)^2 ds \geq \frac{1}{2} AV^2 \int_0^{2\pi} k d\theta \tag{1}$$

Here voltages V are factored by mean and principal curvatures along the curved part of curved surface, having an inequality of Hilbert type, which establishes the energy range in which the curvature energy exists.

Then the measure of curvature can be obtained as an extrinsic curvature from a space classes (cycles) with a curvature measure well defined and which represent the interacting of the rate of direction changes of the space with pulses of energy (Fourier analysis) that go sensing these direction variations and consigned in their energy spectrum through of their co-cycles. Some measurements realized have been the obtained applying energy Gaussian pulses $\pi(x, y)$, [2] that determine, in the infinitum the measure of curvature through of this spectra (see the **Figure 2**).

Thus from the perturbation theory viewpoint, the curvature energy can be defined as the energy perturbing product of the interaction of the electrical field of the curvature sensor (with their censorship) with the surface curvature in accordance with the metrology study realized in [5], where the curvature energy is given by the units as Voltage m^{-3} and is proved with the experiments (see **Figure 3**) introducing the curvature integral transform as follows:

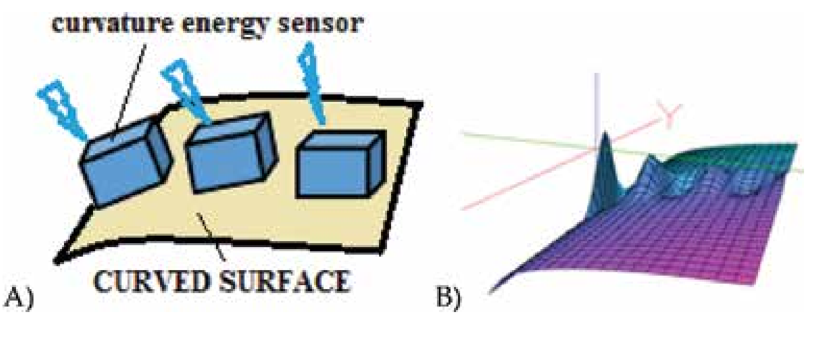

Figure 1. (A) Curvature energy sensor advancing on curved surface. (B) Curvature energy perturbation due to the surface curvature.

http://dx.doi.org/10.5772/68026

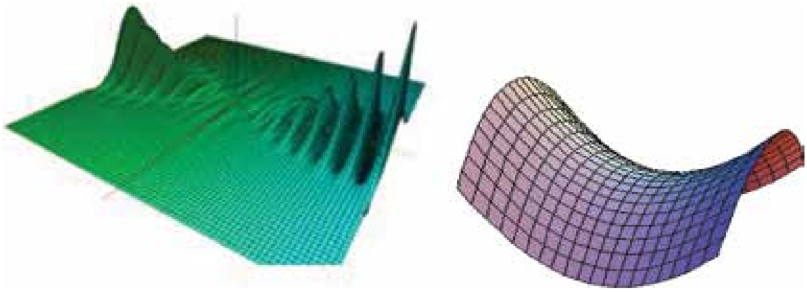

Figure 2. Curvature energy spectra of hyperbolic paraboloid z = xy.

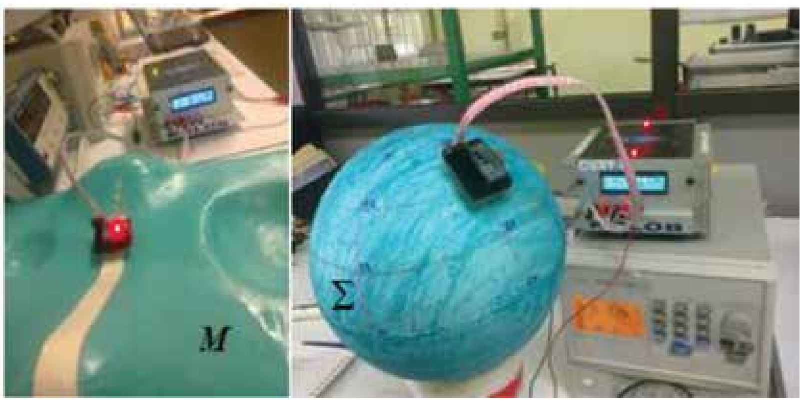

Figure 3. Curvature gauged in curvature energy on an arbitrary surface M, using a spherical surface Σ, [5].

$$O_E = d_\gamma \mathrm{Hom}_K(M, S^2)\int \Omega, \tag{2}$$

But this obeys to the field condition given by gravity in their more fine aspects, since gravity acts as subjacent energy in the geometrical aspect of any space (all the objects in the space are always affected by gravity) using the universal gravitation in the modality of field theory given by Einstein equations.[1] Likewise, the scaled gravitational energy is used in the process of gauging of sensor device whose advances correspond to that measured and gauged by the proper universal gravitation and considered by the spherizer operator O_E , [2, 6, 7]. Then using the result enounced in [8], and considering the scaled gravitational constant $\chi = \frac{8\pi}{c^4}G = 2.071 \times 10^{-43}\,\mathrm{sec}^2\mathrm{meter}^{-1}\mathrm{kg}^{-1}$, which is the proportionality between space-time curvature and energy (as shown in **Figure 3** in [8]), and using Eq. (2) and the field Einstein equations, we have the following:

$$O_E = d_\gamma \mathrm{Hom}_K(M, S^2)\int_M e(-1)^n d\Sigma(f(x)) = 8\pi^2, \tag{3}$$

[1] $R_{\mu\nu} - \frac{1}{2}Rg_{\mu\nu} = \chi T_{\mu\nu}$.

which is the energy quantity measured per determined curvature. Similarly, using this measure of net energy, gravitational waves can be detected by the device that involves this energy to measure curvature energy through electromagnetic fields as gauge fields. This idea is and will be fundamental to determine conditions of energy [Hilbert inequations as given in Eq. (1)] to any censorship required to design a curvature sensor in field theory, including the microscopic theory to QFT. Similarly, in this respect arises the possibility of using the torsion field as the second curvature to measure curvature in field theory considering certain modifications that can be used in field quantum equations as Dirac equation. But far of want the unification of the gravitational and electromagnetic forces to construct a unique field (which is failured reheresal considering only the Einstein equations) is necessary involves the Dirac equation and their solutions in their first integral given by the field actions to curvature in a homogeneous space [3, 7] as described in [7] and using the field theory on the homogeneous space $G[[z]]/\mathbf{X}$, [9] whose curvature energy measures can be constructed by co-cycles in this space.

Other studies followed in the search of curvature measure through light waves were realized in [6] under the same philosophy of the energy integral value on curved spaces (more specific Riemannian manifolds), considering integral transforms defined in homogeneous spaces or cycle spaces (whose cycles are invariant under translations and rotations on the proper manifold). Similarly, the curvature was obtained initially (using the units of volts on cubic meter, mentioned before) as measure through the corresponding co-cycles as integral transform [2, 10]:

$$\kappa(\omega_1, \omega_2) = \int_M \kappa(p, \phi) e^{-j(\omega_1 t_1 + \omega_2 t_2)} dp d\phi, \tag{4}$$

which are our spectra of curvature to a measure realized by our curvature device in an instant t In the case of light waves, the censorship condition is given in [6] as follows:

Theorem (F. Bulnes) 1. 1. [6, 11]. The Radon transform of the Gaussian curvature whose detection condition is the inequality (*censorship*[2]) is as follows:

$$[\log\varphi(\xi(t))]^2 \left[\int \log\sigma(t)\right]^2 \geq \left(\int \Omega(1 - \nabla^2 \log\Omega)\right)^2 \geq 4\pi \int \Omega, \tag{5}$$

and using the signals, the curvature measured by light beam is

$$\iint |K\varphi, L_{\zeta}, \bullet)|_{L^1} = \frac{2}{R} \iint_{D^2} |K_h(\sigma(t))| dxdy, \tag{6}$$

Proof. [6, 11].

Likewise, considering the representation of curvature in a Hilbert space (energy space) that is to say, given by $\Lambda_{\tilde{g}}(f),\ \forall v \in V_{\zeta}, \forall \zeta \in K^{\wedge},$ and $f \in C_c^{\infty}(G/K)$,[3] (*theorem* (*F. Bulnes*) [12, 13]), we have the following:

---

[2]Theoretical sensor of curvature by a wave of light [6, 10, 11]

[3]$\tilde{g}$, is the pseudo-Riemannian metric in G/K, induced by the pseudo-Riemannian metric of the manifold M.

http://dx.doi.org/10.5772/68026

$$< \Lambda_{\tilde{g}}(V), f \geq \oplus_{\zeta \in K^{\wedge}} < \Lambda_{\tilde{g}}(V(\zeta)), f > , \tag{7}$$

which is an "energy" representation of curvature. This permit generalizes the idea of the curvature as field observable to a level of its energy, having the concept of *curvature energy to quantum level*, that is to say, the domineering energy in the action of a quantum field on a curved space [14] to displace a particle on said space (see **Figure 2**). The next step is that it can interpret these energy observables as field observables, which are born of the deformations obtained on space-time background. Remember that the representations of curvature determined in Eq. (7) obey a fine structure with weak topological conditions from a point of view of global analysis. Each isotopic component is a co-cycle in the spectral space or spectrum of curvature.

But how to design a field gauge to measure the gravity observables through curvature energy to a quantum level?

Re-writing the symmetric tensor of the metric, it stays as $o^{\mu\nu(S)}$. This tensor is analogue to the usual metric tensor"g" but refers to lengths (as is usual) where the distance is symmetric as functional. The super fix that is represented as "*S*" refers to symmetric state [15]. The asymmetric tensor that could be the case of more general metric tensor (*which could consider electromagnetic fields as field gauges to measurements of other fields as gravitational field*) is defined through the external product between tetrads as follows [9, 15]:

$$o^{ab}_{\mu\nu} = o^{a}_{\mu} o^{b}_{\nu} = o^{ab\,(S)}_{\mu\nu} + o^{ab\,(A)}_{\mu\nu}, \tag{8}$$

The anti-symmetric form involves the symmetry and anti-symmetry parts. The anti-symmetric component from Eq. (8) is $o^{ab\,(A)}_{\mu\nu}$. The anti-symmetric tensor of the metric is defined through the wedge product of two tetrads [9, 15]:

$$o^{ab\,(A)}_{\mu\nu} = o^{a}_{\mu} \wedge o^{b}_{\nu}, \tag{9}$$

The action of the product of the tensors of curvatures $R^{\alpha\beta}$ and o^{α}_{μ} will establish "torsion effect on the action of gravity", which is measurable and representable *as distortions produced from the gravity*, in the presenece of a gauge field (see (**Figure 4**)). In this point, the spectrum of the searched curvature can be constructed. Then with the application of the quantum mechanics, more specifically, the QFT, and their interrelation with the gravitation is searched and the cause of the field through the quantum interactions that generate this is established. Then in this new "exhibition of gravity", the Einstein field equations can be re-written as follows:

$$R^{a}_{\mu} - \frac{1}{2} R o^{a}_{\mu} = \chi T^{a}_{\mu}, \tag{10}$$

and using this fact, the new metric tensor can be expressed as[4]:

[4]The new metric tensor is anti-symmetric.

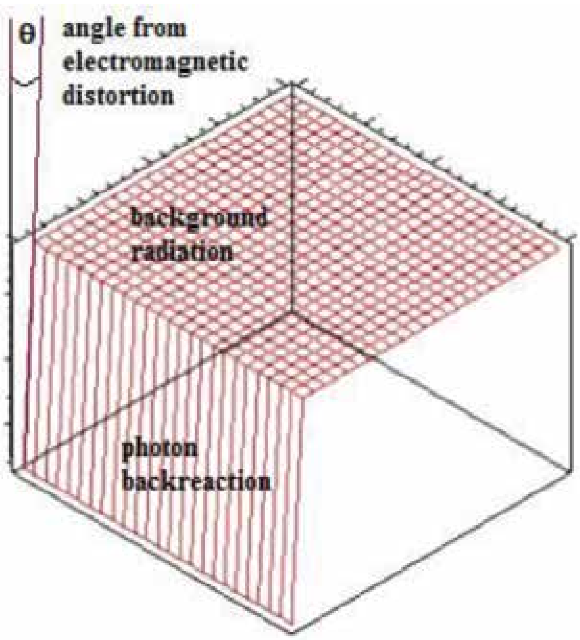

Figure 4. Flat-$\mathbb{R}^4$-Worldsheet of distortion angle obtained for the electromagnetic backreaction with the background radiation (gravity). The photon is the gauge field to measure quantum gravity action.

$$g_{\mu\nu}^{ab(A)} = o_\mu^a \wedge o_\nu^b, \tag{11}$$

we arrive at the new field equation to electrodynamics that is generally covariant:

$$o_\mu^a \wedge (R_\nu^b - \frac{1}{2} R o_\nu^b) = \chi o_\mu^a \wedge T_\nu^b, \tag{12}$$

which gives us the spin or torsion of the field. However, this must be accompanied with the Dirac equation to a designed boson to the start of the second curvature, which must have inherence in the microstructure of the space-time to perceive the gravity to microscopic scale. In the asymmetric space-time model are obtained field models that reflect the torsion as the central part (this is due to the field polarization to particle level) that defines field perturbations whose origins are quantum and whose operators are non-commutative [9]; for example, the asymmetric field theory given by Yang-Mills where this theory provides an extension of Maxwell theory to the case of non-Abelian fields. In these dimensions raise the wrappings and the loop contributions that will contribute to the energy micro-states used to define electromagnetic signal effects of power that can be consigned in a harmonic analyzer with polynomial enters in a non-harmonic interphase of Legendre polynomials.

2. Curvature from quantum gravity: a curvature sensor in field theory

How measure curvature of the space-time from the concept of quantum gravity interpreting their observables as light-field deformations obtained on space-time background with the action of a gauge field?

To this measurement, we use a hypothetical particle graviton that is modelled as dilaton, being a gauge graviton (gauge boson) [1, 15]. According to our curvature, studies come from a theoretical sensor of curvature in the presence of the incurve and detected by a wave of light [1, 6]. This was mentioned in the previous section. The curvature quantum perception in the space is associated as a little distortion of the fine micro-local structure of the space-time due to the interaction of particles of the matter and energy with diverse field manifestations [1]. The matter is shaped by hypothetical particles that take as base the background radiation of the space, which in last studies due to QFT [16] and brane theory are organized and tacked to shape spaces of major dimensions. These spaces are represented by diverse particles of the matter, such as gravitons, barions, fermions of three generations, etc. [1, 9]. These particles are shaping gravity to quantum level, obtaining representations of the same for classes of cohomology of the QFT, for example, the FRW-cohomology (which is a Floer Wrapped Cohomology [16]), which brings exact solutions to the Einstein field equations. This last affirmation considers diverse symmetries of cylindrical and spherical type for the gravity modelled like a wave of gravitational energy "quasi-locally" (see **Figure 5**) [1, 9].

We can determine action integrals of the gravitational energy density (Hamiltonian) given for [1, 9, 18] as follows:

$$\mathrm{H}_{\mathrm{TOTAL}} = \frac{1}{G8\pi}\int_{M} \Gamma + \frac{1}{2}L^{\alpha}T_{\alpha\beta}X^{\beta}, \tag{13}$$

where L^{α} is the Lagrangian, $T_{\alpha\beta}$ is the corresponding tensor of matter and energy, Γ is a Hamiltonian density and X^{β} is the corresponding field of displacement of the particles in the space moving for action of L^{α} influenced by the matter and energy tensor $T_{\alpha\beta}$ [1, 9].

In the study of the microscopic space-time exist the group representations of SU(2), where one of these considers that the super-symmetry is given for S^3 (sphere of dimension 3) [15]. In it, the topological invariant of their 2–form ω_3, and given in the cohomology group $H^3(SU(2), \mathbb{R}) \neq 0,$ [9, 17, 19] will show clearly the gravity presence.

This registry, at least, is realized on the surface of this ball S^3, which is a mini-twister surface in the presence of gravity [9], having as ambitwistor space the set of field couples (Z^{α}, W_{α}), to the microscopic space-time. Here, Z^{α} is the field of gauge nature (in this case electromagnetic fields) and W^{α}, the field of particles of the gravity (gravitons, that in this case is the background) [1, 9].

Similarly, it was mentioned and considered that the curvature value can be understood as the deformation contour on a surface (initial idea created and developed relative to the understanding of curvature in a space-time [10, 15]).

Also the curvature can be understood to the field distortion as undulating in the space-time for the back-reaction due to the photon propagation in the presence of gravity [see **Figure 5 (a)** and **(b)** (using string theory)].

We can extrapolate this idea to design a type of accelerometer that can be connected to the devices of navigation of a travelling satellite by space. In said accelerometer, a sensor of ultra-sensitive gravity based on a solid sphere S^3, whose material can be similar to a colloid, could be involved in their interior, capturing the changes of the weight of a liquid that is also of colloid type (perhaps of major density that of the ball S^3) due to the universal factor G [1, 17].

A censorship[5] device in the earth's gravity can be designed to construct a fine curvature sensor to detect energy for the matter inflow in the space occupied by matter. This brings to collation the perception of the matter-energy tensor $T_{\alpha\beta}$, which influences the movement of the sensor device.[6]

The measured curvature will be a Gaussian curvature expressed through spherical harmonics given by Legendre polynomials.

---

[5]This censorship can be understood as electromagnetic detectors of curvature, which can design the cosmic sensors of curvature with the Penrose censor [1].

[6]Considering M, a four – dimensional space is necessary to consider the spherical map $\partial M \rightarrow S^3$, where for this case the electromagnetic fields can be used as gauges, remembering that $SU(2) \cong S^3$. Then the cohomology group of the Cartan forms ω_1, and ω_2 are annulled [17], that is to say $H^1(SU(2), \mathbb{R}) = 0$, *that is the case of the integrals* $\oint\omega_1 = 0$ $(\oint\delta A^i = \delta(\oint A^i) = 0)$. To the non-null case, as was mentioned earlier, the unique unique 2-form to the determination of curvature is ω_3. Thus, the value of the integral of this group of cohomology is [1, 9] as follows:

$$\frac{1}{8\pi^2}\int_{SU(2)\cong S^3} \omega_3 = 2 < F, \overline{F} > ,$$

But by the background radiation of a Minkowski space M (as four-dimensional model of the space-time), where the energy of the matter is given by the tensor $T^{\alpha\beta}$, , is that $J^\alpha = k^\alpha T^{\alpha\beta}$, where k^α, is the density of background radiation that establishes for the curved part of the space (*that in this case has spherical symmetry*) the variation of energy together with the energy and matter tensor that comes given as [1, 17] follows:

$$\frac{1}{4G\pi}\int_{S^2} T_{\alpha\beta}k^\alpha d\sigma^\beta \geq \int_{S^2} J^\alpha d\sigma^\beta \geq 2\pi\chi,$$

But conserved current in whole space is

$$J^\alpha = E^{\alpha\beta}k_\beta + \frac{1}{2}S^{\alpha\beta\gamma}\nabla_\beta k_\gamma,$$

Then the energy inside the sphere satisfies [7, 27]

$$\frac{1}{16\pi^2}\frac{1}{(2-2g)}\int_{SU(2)\cong S^3} \omega_3 \leq 1,$$

since the electromagnetic energy with respect to the energy of background radiation can fulfill that

$$4\pi\int \Omega^2 \geq 8\pi\int < F_{ij}, F^{ij} >.$$

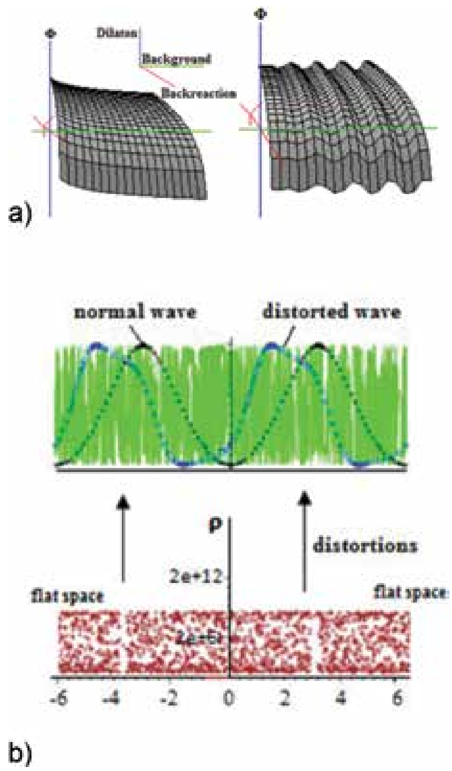

Figure 5. (a) Dilaton measuring distortion due to quantum gravity, according to the model computational magnetic. (b) The case is when there is not photon back-reaction [1, 14].

These Legendre polynomials can be measured by harmonics that can be consigned in a wave with an algebraic frequency. The device is a sensor of free fall that can register different force G, according to its position in the Cosmos [1]. The difference is consigned by the Hall Effect obtained by the scattering difference of fermions detected in each case by particles/anti-particles [1, 17].

Inside the device, considering the Lagrangian action given for [1], the actions of change registered by the free little falls can be reprogrammed. The distortions detected on the 3-sphere can be identified with these harmonics and thereafter consigned as spectral curvature (**Figure 6**) [17].

With our ideas and precise goal, we can consider some useful concepts and create other.

Def. 3. 1 (F. Bulnes, M. Ramírez, L. Ramirez, O. Ramírez). *broson* is a hypothetical particle that is a fermion that comes from D – Branes, being the hypothetical particle wrapped by gauge bosons in the space-time [15].

Being a field solution, the *broson* will be our solution of the Dirac equation to distortions of field [1, 9, 15] that are perturbations in the space-time created by reaction of this particle with background. Likewise the broson will be solution of the field equation:

$$(\square + \chi T)o_{\mu}^{a} = 0, \tag{14}$$

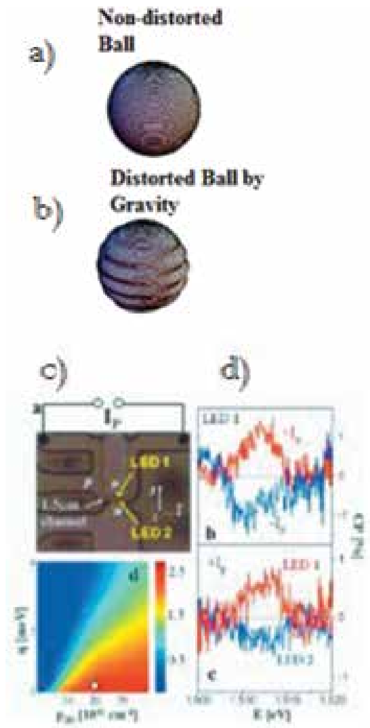

Figure 6. (a) Sensor device to consignee the little variations in free fall for gravity of the sensitive material ball in the space-time. (b) Deformed ball due gravity sensing. (c) The device is designed to be used in a traveler satellite. (d) Gravity spectra.

If we have the term χT, this must be imagined as spherical density. The term R is the curvature of the space-time, which is a deformation of the spatial scenery due to the presence of matter in space. The exact values are not important in this last description, but their implications in the geometrical scenery and their invariants [15] hold significance because these describe the shape of the space-time, at least, locally.

The torsion is produced by the gauge bosons in the microscopic space due to the electromagnetic characteristics of these bosons that are photons [15], realizing back-reaction [1, 17] with the space covered or affected by gravity.

Indeed, in the non-Abelian electromagnetic theory "ghosts" are produced that are states of negative norm or fields with the wrong sign of the kinetic term linked to every particle whose effect is predicted by Faddaev-Popov [19, 20, 21].

Every ghost is associated to a gauge field where the gauge field acquires a mass via a Higgs mechanism (mechanism that creates matter and charge, although each one takes its proper way in the particle decomposition).

The associated ghost field acquires the same mass (in the *Feynman-'t Hooft gauge* only, not true for other gauges) where the gauge must be designed or proposed in accordance to the Feynman-t'Hooft theory) [1, 9].

http://dx.doi.org/10.5772/68026

In the QFT, and particle physics frame, the existence of a weak field has been established that helps to define the unification to the neutron. The weak field, whose nature is electromagnetic, is associated with the gauge boson as of the type W boson. Similarly, when the neutron exists outside the atomic nucleus, it is transformed after 10 minutes into an electron, anti-neutrino and one proton. This establishes the condition to create matter and anti-matter in the required proportion that is needed in the Universe [14].

We consider the algebraic object assigned as a set of rules of a chain complex (as a graded module equipped with degree d, such that $d^2 = 0$) that permits to understand the movement as a continuous transformation whose image in a quantum space is a deformation of the space-time to microscopic level given by little changes in energy. Their macroscopic image of such quantization can be consigned inside a Poisson manifolds family that under certain quasi-equivalence [9, 15, 20, 21] and through homotopies can be carried to a macroscopic reality [9, 15]. Through the duality of Koszul complexes on microstate spaces can be demonstrated that the entropy is an aspect of the evolution of the energy that can be considered as an inverted image in a mirror space of the equivalences. Gravity in this case is consigned under torsion (and defined as pressure on a body or particles) in a *Drinfeld space* with *twisted loops*, where these loops and strings could be our "brosons" according to definition 3. 1., given [1, 15].

Taking into consideration the optimal design of the censorship condition, using the microscopic torsion theory and involving the field solution to Eqs. (10) and (14) from the QFT (considering that the artificial particle is defined before, because remember that *the broson must be a fermion to be consistent with the different helicities of strings*), we have the movement ramification as macroscopic effect of the following field action[7] [15]:

$$\Im_{\text{Total}} = \Im_{G} + \Im_{\text{QED}-\text{fermions}}, \tag{15}$$

3. H-fields in a generalized curvature tensor and some boson-fermion measurements

Through the integration formalism applied to the total action integral of $g_{\mu\nu}^{ab(A)}$, which comes from the actions of two tensors, the partial action due to the curvature tensor and the electromagnetic tensor, including in this last, along with the fermion self-interactions induced by the quantum second curvature, we can establish the following total action as second integral of Eq. (12):

$$\begin{aligned}\Im_{\text{TOTAL}} = \frac{1}{2\kappa}\int d^4xoo_\mu^a o_\nu^b R(\varpi) + \frac{i}{2}\int d^4xo\times \\ \times(o_\mu^a(\overline{\psi}\overline{\gamma}^a D_\mu(\varpi,A)\psi - \overline{D_\mu(\varpi,A)\psi}\gamma^a\psi)) - \\ -\int d^4xo\frac{3}{10}\kappa J_{(A)}^{\mu} J_{(A)\mu},\end{aligned} \tag{16}$$

where $\{\gamma^\mu, \gamma^\nu\} = 2g^{\mu\nu}$, is Dirac matrix and $R^{\mu\nu} = d\omega^{\mu\nu} + \omega_\sigma^\mu \wedge \omega^{\nu\varsigma}$, is the 2-form of curvature.

[7]This is viewed as energy curvature stated using the perturbative method.

Here, $\chi = 8\pi G_N$, is the gravitational constant mentioned in the introduction section, which we know, is intimately related with the production of matter by the tensor of matter-energy-momentum in the Universe estimated inside the Einstein field equations.

However, the studies in [15, 22, 23] need to explain the mechanism of the gravitational energy with the torsion. Similarly, through the QED and QFT, (see **Figure 7**) using perhaps the *spinor frame* (because it is a wave superposing many trajectories taken by the dilaton interacting with the space-time), we have within the Dirac equation as was given in Eq. (14) the fermion interactions [14] that give the different matter particle, which is a space-time torsion, where finally is a second curvature.

Finally, this global action defined in Eq. (16) can be re-written to fermions in gravity with torsion [23, 24], with a specific scalar field of torsion (*Kalb-Ramond field strength* [25]) inspirited from the string theory [26] (UV- complete) and that can do the job of providing a constant, axial background in a local frame of FRW-cosmology. The additional fermion-piece of the form is stated as follows:

$$\Im = \frac{\alpha}{2}\int d^4xo(\overline{\psi}\overline{\gamma}^a D_\mu(\varpi, A)\psi - \overline{D_\mu(\varpi, A)\psi}\gamma^a\psi), \alpha = \mathrm{cte}, \tag{17}$$

Using the Dirac kinetic terms, the fermion action reads:

$$\Im_{\mathrm{Dirac-Holst-Fermi}} = \frac{\alpha}{2}\int d^4xo(\overline{\Psi}\overline{\gamma}^a(1 - i\alpha\gamma_5)\mathcal{D}_\mu\Psi - \overline{\mathcal{D}_\mu\Psi}\gamma^a(1 - i\alpha\gamma_5)\Psi), \tag{18}$$

where inside the integrand the Dirac equations to the differentiating fermions are involved in the non-Harmonic analysis that appears in the anti-symmetric behaviour of the curvature field measured for quantum interactions (see **Figure 8**).

This establishes the conjecture in [15], which we enounce.

Conjecture (F. Bulnes) 3. 1. The curvature from the quantum gravity is the measure through the link-wave or perturbation wave (see **Figure 9a**) between a hypothetical graviton particle

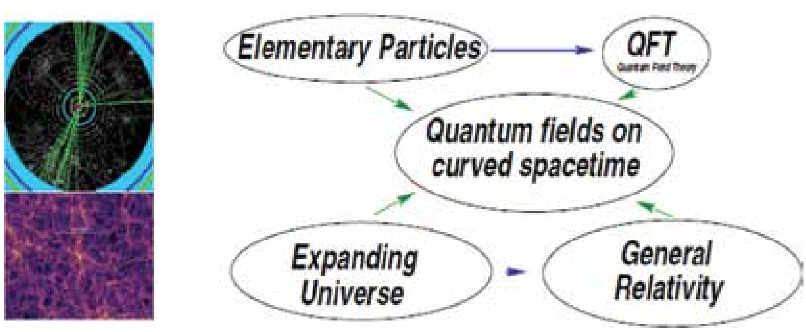

Figure 7. Construction of string energy curvature through the study areas to quantum fields on curved space. To obtain the curvature energy, we consider QFT and general relativity on expanding Universe, and to initial conditions we consider elemental particle behaviour in the early Universe. The curvature energy model in quantum level is necessary to consider fields that are solutions of the Cartan-Einstein equations and Dirac equation. This has been mentioned in the Introduction section I.

modelled as dilaton (gauge graviton) and the trace of any particle in the space-time, whose relativistic Feynman diagram followed to a quantum field [15].

Theorem (F. Bulnes). *The quantum curvature is the set of curvature energy states from the perturbative method of their Hamiltonian* [15].

The perturbation method consider a Hamiltonian $H = H_1 + \varepsilon H_2$, which determines first, energy spectra and after on the base of an action as the given through a field broson action [15], obtain curvature as torsion or second curvature. Similarly, the electro-gravitational energy

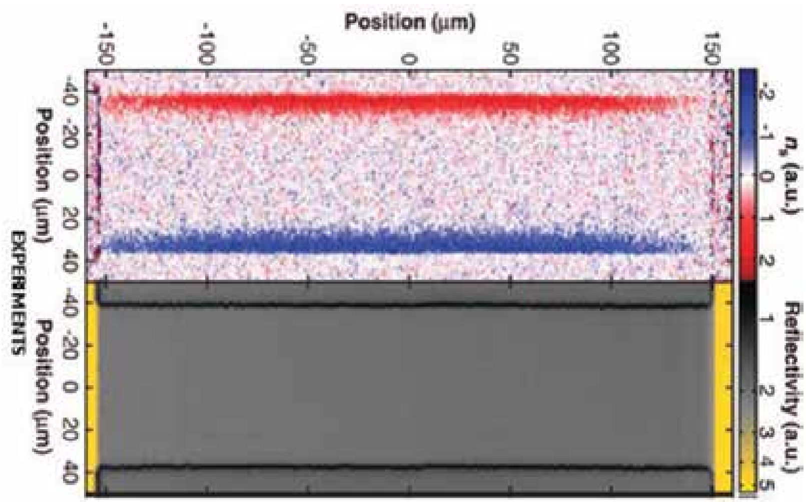

Figure 8. Refs. [14, 26] Separation of fermions due to their spin ½ in the non-Harmonic analysis that appear in the anti-symmetric behaviour of the curvature in a gravitational field measured for quantum interactions. This is realized in a spintronic simulation.

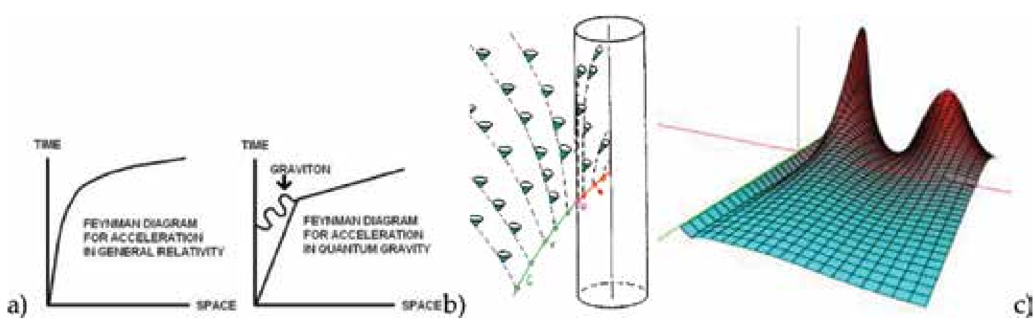

Figure 9. (a) Curvature measured to quantum level as the little quantum distortion given by the link-wave between a hypothetical particle as graviton modelled as dilaton (gauged graviton) and the trace on relativistic Feynman diagram followed in quantum gravity [15]. (b) The quantum curvature can be considered as different times in the causality and conformal structure of the the space-time [15]. The different deviations to the world lines in each case show the curvature. (c) The microscopic perturbation on a cylindrical surface is retaken [15]. Also it is considered the causal structure given by light cones. The red segment in Figure 9b corresponds to the surface model given in **Figure 9c**.

produced can be consigned to torsion energy and its detection can be obtained by back-reaction on background space-time as energy perturbation expressed as perturbation wave.

In microscopic UV-radiation frame, the underlying theory of quantum gravity takes different tensors with a corresponding particle spin involved in the interaction. Likewise, we consider the Kalb-Ramond field $B_{\mu\nu} = -B_{\nu\mu}$, [27] with the massless gravitational multiplets of *"closed" strings* such as scalar or *dilaton* (spin 0), traceless symmetric rank (spin 2), 2-tensor or the *graviton (*spin 1), anti-symmetric rank 2-tensor or *electromagnetic tensor.*

A gauge invariant to effective field theories (in low-energy scale $E << M_s$) given for $B_{\mu\nu} \rightarrow B_{\mu\nu} + \partial_{[\mu}\theta(x)_{\nu]}$, is feasible, which depends only on the field strength $H_{\mu\nu\varrho} = \partial_{[\mu}B_{\nu\varrho]}$, [27]. Then we give the Bianchi identity as follows:

$$\partial_{[\sigma}H_{\mu\nu\varrho]} = 0, \tag{19}$$

However, the detected anomalies by gravitational field interacting with gauge field cancellations of strings (*necessary to the perceiving of the gravitational waves letting only the gravitational strings*) require a re-definition of the H-fields given in Eq. (19) considering the extension due to the Majorana neutrinos masses from (three loop) anomalous terms with axion-neutrino couplings [27]. The corresponding extended Bianchi identity to these anomalous terms is stated as follows:

$$H_{\mu\nu\varrho} = \partial_{[\mu}B_{\nu\varrho]} + \frac{\alpha'}{2\kappa}(\Omega_L - \Omega_V), \tag{20}$$

Thus interesting results from the study of the phase-space density are derived from the difference between the Chern-Simons 3-forms [28] Ω_L, and Ω_V, where Lorentz-Chern-Simons 3-form Ω_L defined to neutrinos is considered and the electro-gravitational formalism in gauge theory is considered in the case of the gauge Chern-Simons 3-form[27].

In quantum gravity, a theoretical study related to the propagation of photons shows that a region of space-time with a singularity is supported by an energy that decreases asymptotically to the infinite. This hypothetical energy can be constructed with the expression of a Lagrangian-type given in **Table 1** [1, 29], with cylindrical gravitational wave given by the *dilaton* (gauge particle) [27] as follows:

$$\Phi = (1/10000(\exp(-4\xi)J_{\nu,x}(3\xi, 1) + \exp(-4\xi)Y_{\nu,x}(2\xi, 1)) \tag{21}$$

where the equation expresses a wave model for energy of gravitational waves (see Eqs. (1), (9), (17)) [1]. Also see **Figure 10a** [1, 9].

Now, considering the effective gravitational action (that is to say, the action whose Lagrangian is effective) in string low-energy and in terms of a generalized curvature Riemannian tensor (where the Christoffel connection includes the H-fields, that is to say, $\overline{\Gamma}^{\mu}_{\nu\varrho} = \Gamma^{\mu}_{\nu\varrho} + \frac{\kappa}{\sqrt{3}}H^{\mu}_{\nu\varrho} \neq \overline{\Gamma}^{\mu}_{\varrho\nu}$, defined in Eq. (20)), we can give the four-dimensional action as follows:

http://dx.doi.org/10.5772/68026

Electromagnetic Lagrangian action	Electromagnetic interaction
$\Im(x(s)) = \int_M L_{MAX}(x(s))d(x(s)),$	Classic electromagnetism
$\mathring{\Im} = \int R_{ij} \wedge \Sigma^{ij} - \frac{1}{2} < F_{ij}, F^{ij} >_{\tilde{M}} \text{Vol}(g),$	Quantized electromagnetism
$\Im = \frac{1}{2\pi}\int d^2z(G_{\mu\nu} + B_{\gamma\nu})\partial x^{\mu}\bar{\partial}x^{\mu} + \frac{1}{4\pi}\int \sqrt{g}R\Phi(x^L),$	Electromagnetic string photons (Bosons)
$\Im = \frac{k}{4}I_{SO(3)}(\lambda, \theta, \omega) + \frac{1}{2\pi}\int d^2z[\partial x^0\bar{\partial}x^0 + \psi^0\partial\psi^0 + \sum_{l=1}^{3}\psi^l\partial\psi^l] + \frac{Q}{4\pi}\int \sqrt{g}Rx^L,$	Gravitational heterotic string (gravitons)
$\Im = \int d^4x\sqrt{G}e^{-2\Phi}[R + 4(\nabla\Phi)^2 - \frac{1}{12}H^2 - \frac{1}{4g^2}F^{\mu}_{\alpha\beta}F^{\mu,\alpha\beta} + \frac{C}{3}],$	Electro-gravitational heterotic string dilaton-graviton
$\delta\Im = \frac{\sqrt{kk_gH}}{2\pi}\int d^2z[\partial\omega + \cos\theta\partial\lambda],$	Magnetic distortion (back-reaction)

Table 1. Lagrangian actions to electromagnetic interactions [1, 9, 17].

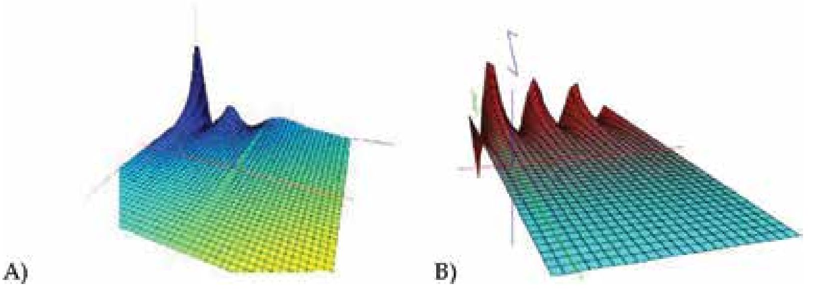

Figure 10. (A) Gravitational alteration perceived by the censor is designed by Eq. (20) when it is obtained as a great alteration of energy near the singularity of the space-time. (B) Spinor waves superposing due to the curvature energy due to singularity. These are created as small quantum field fluctuations in the post-limit of Newtonian gravity. The singularity is not combing thus the unique admissible representation is through spinor waves which can be superposed to shape a perturbing measurable in energy space.

$$\begin{aligned} S^{(4)} &= \int d^4x\sqrt{-g}\left(\frac{1}{2\kappa^2}R - \frac{1}{6}H_{\mu\nu\varrho}H^{\mu\nu\varrho}\right) \\ &= \int d^4x\sqrt{-g}\left(\frac{1}{2\kappa^2}\overline{R} - \frac{1}{3}\kappa^2H_{\mu\nu\varrho}H^{\mu\nu\varrho}\right), \end{aligned} \tag{22}$$

where the dual of H, in four dimensions, is given by the differential equation:

$$-3\sqrt{2}\partial_\sigma b = \sqrt{-g} \in_{\mu\nu\varrho\sigma} H^{\mu\nu\varrho}, \tag{23}$$

where b(x) is a pseudo-scalar that defines the Kalb-Ramond axion. Then to a dilaton Φ, that satisfies Eq. (23) has the properties described in Eq. (14) as gravitational wave, the field equation is as follows:

$$H^{\mu\nu\varrho} = o^{2\Phi} \in_{\mu\nu\varrho\sigma} \partial^{\sigma} b(x), \tag{24}$$

The linear dilaton solution in string frame (or logarithmic in FRW-time in Einstein frame) with conformally flat Einstein-frame target space-time [see **Figure 11a**] is exact in all orders of a parameter that appears in Eq. (17) [27].

Then considering the principles dictated in Eqs. (18)–(20) and the differentiated fermions in the non-Harmonic analysis that appears in the anti-symmetric behaviour of the curvature field measured by quantum interactions (**Figure 8**), we can give the following action that comes from the Majorana states in fermionic field theories with H-torsion [9, 27]:

$$S_{\psi} = -\frac{3}{4}\int d^4\sqrt{-g} S_{\mu}\overline{\psi}\gamma^{\mu}\gamma^{5}\psi, \tag{25}$$

Then considering the extra-charge created by the fermion interaction (central charge underlying in the world-sheet conformal field theory [16]), we can define the scalar field:

$$b(x) = \sqrt{2} e^{-\phi_0}\sqrt{Q^2}\frac{M_s}{\sqrt{n}} t, \forall n \in Z, \tag{26}$$

which is a field model with fine electromagnetic terms, where this can be used to create a basic charge in a component of g-cell [27].

Also we use the theorem on curvature given in [3], which must consider an isotopic component of Gaussian *factor* to lectures of curvature, then we can define a sensor whose 3-ball of non-Newtonian fluid can receive these signals and re-interpret through voltage-curvature energy, such as said by *theorem III. 1* [1, 14, 17].

These data as little electrical voltages that come from the surface of the 3-ball can be censored (and sensored) as little changes in the background (that are perturbations) due to the dilaton interaction with this [14, 27].

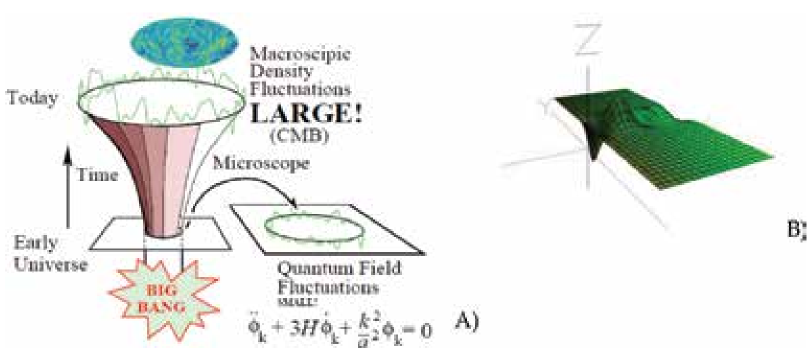

Figure 11. (A) Macroscopic Fluctuations density detected by CMB in the Newtonian limit, which can be consigned in microwave map realized by the SWAP Universe. The quantum field fluctuations that generate the macroscopic fluctuations can be modelled by a dilaton ϕ, that enters in back-reaction with the background radiation. (B) Perturbation surface in the Newtonian limit (in beginning of the flatness of the space-time supported by the neutrinos/anti-neutrinos totality).

http://dx.doi.org/10.5772/68026

Likewise, realizing some experiments with little accelerometers in curvature sensor performance, we can include a charged ball whose charge variation in time is given by the energy spectra [1, 27]. Then the position variation of the accelerometer in respect to their horizontal frame (Ecuador) registered in their g-cell change (see **Figure 8**) will measure the falls by gravity, these being consigned in curvature energy. We can use two leads to determine the polarization effect created in natural way by the fermionic behaviour [27] (see **Figures 6** and **8**).

Then we can define an accelerometer in a classic sense in the earth's gravity. The curvature will be expressed as a Gaussian curvature according to spherical harmonics given by Legendre polynomials [14, 27]. These polynomials carry the information of ball variations. Likewise, the sensor is a sensor of free fall that can register different force factors G. This difference is consigned by the Hall Effect obtained by the scattering difference of fermions detected in each case, particles/anti-particles. The proper device considering these as a Lagrangian action given can reprogram the actions of the changes [1, 9, 27].

Then extrapolating this experiment in the ambit of the photonics, the folds or "creases" in a deformable sphere (**Figure 6**) are oscillations in the Universe, which are given by the mixture of neutrinos/anti-neutrinos for the eco of the Early Universe [27], which will arrive until our days.

The Universe will maintain its basic non-spherical symmetry until our days, which can be expressed through its Lagrangian as follows:

$$\mathcal{L} = \mathcal{L}_f + \mathcal{L}_I = \sqrt{-g}\overline{\psi}[i\gamma^a\partial_a - m) + \gamma^a\gamma^5 B_a]\psi, \tag{27}$$

where $\overline{\psi}$, and ψ, are component of the field spinor Ψ. The oscillations are received as spherical auto-modes of the alteration of central charge Q, obtained by the differentiated fermionic process (see **Figure 9**) (extension of the model the axion b(x), using total derivatives of the gravitational $cR^{\mu\nu\varrho\sigma}\tilde{R}_{\mu\nu\varrho\sigma}$, and electromagnetic $cF^{\mu\nu}\tilde{F}_{\mu\nu}$, terms [18] of the fields o^a_μ, translated to H-fields).

In the Universe, the neutrinos and anti-neutrinos conform to the asymmetry around the black holes or space-time singularities [25]. Inside singularities, the gravitational field is dementia. Then their particles and anti-particles (by the same polarization process) can be generated from the torsion. Likewise, using a plane wave approximation, different dispersion relations between particles and anti-particles to finite densities assuming constant background torsion can be obtained (see Ref. [27]).

Finally, through a magnetic dilaton Φ, we can give a model of magnetic distortion, that is to say, the energy curvature in the gravitational media can be translated as magnetic deformation of thefour-dimensional part of the string of background radiation (see **Figure 11**) [9, 27].

The gravitational energy is the curvature energy obtained through components of Bessel functions or harmonic polynomials (see **Figure 12**).

Finally, we can conclude that the curvature energy expressed through the H-states can be written using the superposing principle to each connection $\omega_C^{\otimes j}$, (with C, a curve) that

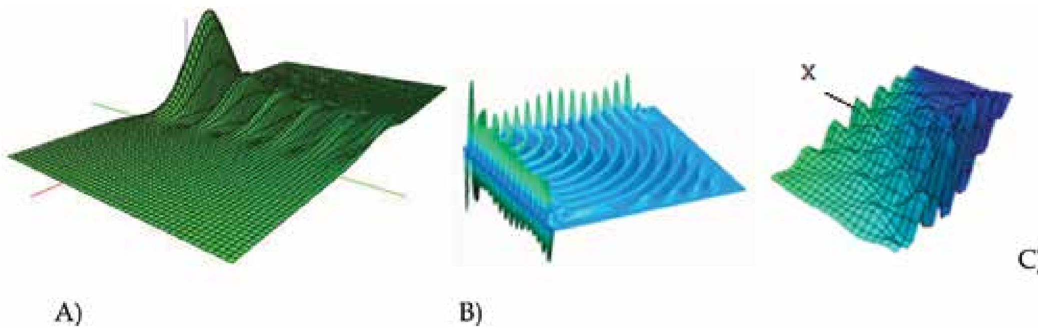

Figure 12. (A) Direct sum of H-states to establish the curvature measure by field ramification. (B) The waves that are *spinor waves* can be consigned in oscillations in the *space-time* in the presence of *curvature* to the change of particles spin. (C) Gravitational waves produced by quantum gravity due to H-states on cylindrical surface. Their propagation is realized on axis X. These gravitational waves are originated for the oscillations in the space-time-curvature/spin (that is to say using causal fermions systems).

describes the corresponding dilaton. Likewise, in a Hamiltonian densities space [9], we have **Figure 12(a)** considering a Hitchin base that is stated as follows:

$$H^0(\omega_C) \oplus H^0(\omega_C^{\otimes 2}) \oplus \ldots \oplus H^0(\omega_C^{\otimes n}), \tag{28}$$

In the case of spinor representation, the corresponding H-states can be given as spinor waves [see **Figure 12b**], which can be consigned in oscillations in the space-time-curvature/spin, to a microscopic deformation measured in $\mathcal{H}$.

4. Conclusions

The curvature as field observable can be detected by back-reaction of a gauge field considering that the quantum gravity is the quantum effect produced by interaction of particles that conform to the matter (that is to say, particles of matter) with gauge particles, which in most cases are of boson type. However, we can consider an underlying causal fermion system or fundamental causal fermion system from which effects (from their energy states) as geometrical invariants to the space-time can be observed, which can be described to the space-time as discretized by H-states of Majorana states (as given in 28 to a space-time modelled initially as complex Riemannian manifold and transformed later to be a discrete manifold).

Then we can establish quantum geometry of the space-time, and using the concept of curvature energy associated to the particle/wave, we can give a representation as perturbation $H = H_1 + \varepsilon H_0$, generated by the interaction of particles mentioned. Likewise, geometrical models of quantum gravity can be given to show the quantum behaviour of observables obtained for photons that act on the background radiation (or microwave radiation) such that a second curvature as torsion can be induced for fields as dilatons or gauge bosons, which can exhibit observable of gravitational field that is curvature in all cases. As this process is realized in quantum level, results remain curvature to quantum gravity, which is curvature energy or gravitational energy (as defined in the introduction of this chapter from the energy-matter tensor $T_{\alpha\beta}$) that will exist until our days as an echo of the times of the creation of the gravity in the transit of the Early Universe. Then a censorship condition can be used to sensing and gauging of curvature, which can give characteristics to construct and design a sensor device, using the curvature energy to measure and detect quantum gravity as such [29].

Author details

Francisco Bulnes

Address all correspondence to: francisco.bulnes@tesch.edu.mx

Research Department in Mathematics and Engineering, Tecnológico de Estudios Superiores de Chalco, Mexico

References

[1] Bulnes F. Electromagnetic gauges and maxwell lagrangians applied to the determination of curvature in the space-time and their applications. Journal of Electromagnetic Analysis and Applications. 2012;**4**(6);252–266. DOI: 10.4236/jemaa.2012.46035

[2] Bulnes F, Martínez I, Mendoza A, Landa M. Design and development of an electronic sensor to detect and measure curvature of spaces using curvature energy. Journal of Sensor Technology. 2012;**2**(3):116–126. DOI: 10.4236/jst.2012.23017

[3] Bulnes F. Research on Curvature of Homogeneous Spaces. 1st ed. State of Mexico, Mexico: Tescha; 2010. pp. 44–66

[4] Bulnes F. Orbital Integrals on Reductive Lie Groups and Their Algebras, Orbital Integrals on Reductive Lie Groups and Their Algebras. Croatia: Intech; 2013. ISBN: 978-953-51-1007-1. Available from: http://www.intechopen.com/books/orbital-integrals-on-reductive-liegroups-and-their-algebras/orbital-integrals-on-reductive-lie-groups-andtheir-algebrasB

[5] Bulnes F, Martínez I, Zamudio O. Fine curvature measurements through curvature energy and their gauging and sensoring in the space. Sergey Y. Yueish, editor. Book of Sensors and Applications in Measuring and Automation Control Systems Advances in Sensors: Reviews. Vol. 4. Barcelona Spain: IFSA Publishing; (2017). Chapter 20

[6] Bulnes F, Hernandez E, Maya J. Design of measurement and detection devices of curvature through of the synergic integral operators of the mechanics on light waves. In Proceedings of International Mechanics Engineering Conference and Exposition (ASME-IMECE'09); 2009; Orlando Florida. USA: ASME; 16 November 2009. pp. 91–102. DOI: 10.1115/IMECE2009-10038

[7] Bulnes F. "Curvature spectrum to 2-dimensional flat and hyperbolic spaces through integral transforms," Journal of Mathematics, 2015;**1**(1):17–24

[8] Bulnes F, Martínez I, Cayetano R, Zamudio O, Gutierrez C, Martínez I. Autonomous and mobile prototype of curvature sensor with remote reliable communication of spectral curvature. Journal of Sensor Technology. 2016;**6**:159–179. http://dx.doi.org/10.4236/jst.2016.64012

[9] Bulnes F. Integral Geometry Methods in the Geometrical Langlands Program. USA: SCIRP; 2016

[10] Bulnes F, Martínez I, Zamudio O, Negrete G. Electronic sensor prototype to detect and measure curvature through their curvature energy. Science Journal of Circuits, Systems and Signal Processing. 2015;**4**(5):41–54. DOI: 10.11648/j.cssp.20150405.12

[11] Bulnes F. Radon transform and curvature of an universe, Postgraduate [thesis]. UNAM; 2001, Mexico

[12] Kaajakari V. Closed form expressions for RF MEMS switch actuation and release time. Electronics Letters. 2009;**43**(3):149–150

[13] Kobayashi K, Nomizu K. Foundations of Differential Geometry. New York: Wiley and Sons; 1969

[14] Bulnes F. Design of Quantum Gravity Sensor by Curvature Energy and their Encoding. London, UK: IEEE Processing, SAI; 2014. pp. 855–861

[15] Ramirez M, Ramírez L, Ramírez O, Bulnes F. Field Ramifications: The energy-vacuum interaction that produces movement. Journal on Photonics and Spintronics. November. 2013;**2**(4):4–11

[16] Prezas N, Sfetsos K. Supersymmetric moduli of the $SU(2) \times R_{\phi}$ linear dilaton background and NS5-branes. Journal of High Energy Physics. 2008;**06**:80

[17] Bulnes F, Hernández E, Sánchez A. Measurements of quantum curvature: New measurements of curvature based in concepts of gravitational waves measured by electromagnetic waves. Journal on Photonics and Spintronics. **1**(1):1–13

[18] Mason LJ, Frauendiener J. Sparling 3-form, Ashtekar Variables and Quasi-Local Mass. Twistor, Twistor in Mathematics and Physics. Cambridge Press, Cambrindge, UK: 1990.

[19] Yang CN, Mills R. Conservation of isotopic Spin and isotopic gauge invariance. Physical Review. 1954;**96**:191–195

[20] Popov VN, Faddeev LD. English translation: Perturbation theory for gauge-invariant fields. Kiev Institute of Theoretical of the Physics Academy Science. 1967;preprint ITP **67**:36

[21] Kontsevich M. Deformation quantization of poisson manifolds. Lettersin Mathematical Physics. 2003;**66**(3):157–216.

[22] Guivenchy E. Torsion field matther and Neutrinos: CPT violation in torsionful geometries of the early Universe (K-R Axions). Journal on Photonics and Spintronics. **4**(4):9–15

[23] Wilson FL. Fermi's theory of beta deacay. American Journal of Physics. 1968;**36**(12):1150

[24] Guivenchy E. Torsion matter and their corresponding dirac equations on neutrinos and matter/anti-matter asymmetries (Part I: Scattering difference between neutrinos/anti-neutrinos). Journal on Photonics and Spintronics. **3**(4):9–18

[25] Kontsevich M. Homological algebra of mirror symmetry. Proceedings of the International Congress of Mathematicians; 1995. pp. 120–139. DOI: arXiv:alg-geom/9411018

[26] Bulnes F. Quantum gravity sensor by curvature energy: Their encoding and computational models. IJACSA 2014, Extended Papers of London Conference, UK; 2014. pp. 65-73. DOI: 10.14569/SpecialIssue.2014.040308

[27] Chern S-S, Simons J. Characteristic forms and geometric invariants. The Annals of Mathematics. Second Series. 1974;**99**(1):48–69

[28] Król J. Quantum Gravity Insights from Smooth 4-Geometries on Trivial R4, Quantum Gravity. Croatia: Intech; 2012. pp. 53–78. Chapter IV

[29] Salamon D, Wehrheim K. Instanton floer homology with Lagrangian boundary conditions. Geometry & Topology. 2008;**12**(2):747–918

Edited by Dimo I. Uzunov

The book contains seven chapters written by noted experts and young researchers who present their recent studies of both pure mathematical problems of perturbation theories and application of perturbation methods to the study of the important topic in physics, for example, renormalization group theory and applications to basic models in theoretical physics (Y. Takashi), the quantum gravity and its detection and measurement (F. Bulnes), atom-photon interactions (E. G. Thrapsaniotis), treatment of spectra and radiation characteristics by relativistic perturbation theory (A. V. Glushkov et al), and Green's function theory and some applications (Jing Huang). The pure mathematical issues are related to the problem of generalization of the boundary layer function method for bisingularly perturbed differential equations (K. Alymkulov and D. A. Torsunov) and to the development of new homotopy asymptotic methods and some of their applications (Baojian Hong).

Photo by liulolo / iStock

IntechOpen

ISBN 978-953-51-4789-3